ELUCIDATION OF THE MOLECULAR MECHANISMS OF FOODBORNE HUMAN PATHOGEN INACTIVATION BY COLD ATMOSPHERIC PLASMA THROUGH RNA-SEQ ANALYSIS

By

CHRISTOPHER TIMMONS

Bachelor of Science in Biology
University of Texas at Tyler
Tyler, Texas
2010

Master of Science in Entomology and Plant Pathology
Oklahoma State University
Stillwater, Oklahoma
2012

Submitted to the Faculty of the
Graduate College of the
Oklahoma State University
in partial fulfillment of
the requirements for
the Degree of
DOCTOR OF PHILOSOPHY
July, 2016

ELUCIDATION OF THE MOLECULAR MECHANISMS

OF FOODBORNE HUMAN PATHOGEN

INACTIVATION BY COLD ATMOSPHERIC PLASMA

THROUGH RNA-SEQ ANALYSIS

Dissertation Approved:

Li Maria Ma, Ph.D.

Dissertation Adviser

Jacqueline Fletcher, Ph.D.

William Schneider, Ph.D.

Udaya DeSilva, Ph.D.

Name: CHRISTOPHER TIMMONS

Date of Degree: JULY, 2016

Title of Study: ELUCIDATION OF THE MOLECULAR MECHANISMS OF FOODBORNE HUMAN PATHOGEN INACTIVATION BY COLD ATMOSPHERIC PLASMA THROUGH RNA-SEQ ANALYSIS

Major Field: PLANT PATHOLOGY

Abstract:

Foodborne human illness caused by pathogenic bacteria is a significant health and economic burden worldwide. Efficient food decontamination methods that do not alter food quality can greatly alleviate this burden. Cold atmospheric plasma, which is ionized gas generated at room temperature and atmospheric pressure, is an emerging technology that offers a dry, non-thermal, rapid decontamination process with minimal damage to food products. Surface dielectric barrier discharge (SDBD) is an open-air cold plasma generation technology with low power requirements that is more flexible, portable, and scalable than current cold plasma generation methods. Although the bactericidal effects of cold plasma are well documented, the specific mechanism by which bacterial inactivation occurs is not well understood. In this research, a novel SDBD design was used to evaluate 1) induced airflow dynamics and bacterial foodborne pathogen inactivation, 2) morphological and transcriptomic responses of *Salmonella* to cold plasma treatment, and 3) the potential for bacterial resistance development to cold plasma. The novel SDBD actuator designs were found to induce a localized airflow that pushes reactive species to distant surfaces, allowing inactivation of common bacterial pathogens on biotic and abiotic surfaces. The transcriptomic response of surviving *Salmonella* cells to SDBD revealed a general decrease in stress responses thought to be a result of rapid lipid peroxidation, cytosolic leakage, and cell lysis, as revealed by transmission electron microscopy and RNA sequencing. In contrast, DNA and protein damage by plasma-produced RONS were found to have a minor role in SDBD-induced inactivation of *Salmonella*. Furthermore, after treating a population of plasma-injured cells in succession, no significant differences in bacterial inactivation rates or differential gene expression were identified that could potentially lead to resistance development. These results confirm that the novel SDBD cold plasma actuators have potential applications in food surface decontamination and that the physical process of lipid peroxidation is a major cause of bacterial inactivation. Following further optimization and delineation of treatment parameters and plasma generation characteristics of the novel SDBD actuators, cold plasma will be a viable alternative to help alleviate the global burden of foodborne illness and continued antibiotic resistance development among bacterial pathogens.

TABLE OF CONTENTS

Chapter Page

LIST OF TABLES

Table Page

CHAPTER III

CHAPTER IV

CHAPTER V

Table Page

LIST OF FIGURES

Figure Page

CHAPTER III

CHAPTER IV

Figure Page

CHAPTER V

APPENDIX

CHAPTER I

INTRODUCTION

Foodborne human illness caused by pathogenic bacteria is a significant health and economic burden worldwide. *Salmonella enterica* subspecies *enterica* (*Se*), Shiga toxin-producing *Escherichia coli* (STEC), and *Listeria monocytogenes* (*Lm*) are among the most commonly isolated bacterial foodborne pathogens and cause more hospitalizations and deaths than all other known bacterial pathogens (Scallan *et al.,* 2011). Contamination of food products by pathogens such as these can occur at any point throughout food production, distribution, and preparation processes, necessitating effective and efficient decontamination methods prior to consumption (Aruscavage *et al.,* 2006; Abadias *et al.,* 2006). However, few effective and minimally damaging decontamination methods are available for foods that are consumed raw or minimally processed (Goodburn and Wallace, 2013). Consumers are becoming increasingly conscious of the nutritional benefits of some minimally processed foods, especially fresh produce, and an increased consumption of these products has been documented in recent years (Barth *et al.,* 2010). Unfortunately, concomitant with this trend, an increased incidence of foodborne illness associated with fresh produce has also been documented (Sivapalasingam *et al.,* 2004; Painter *et al.,* 2013; CDC, 2013).

Foods consumed raw or minimally processed pose notable challenges for decontamination. The nutritional, structural, and aesthetic properties of such foods are important to consumers and need to be maintained. However, few of the major decontamination methods currently used for fresh produce, including chlorine washes, chlorine dioxide treatments, ozone fumigation, and irradiation, are ideally cost effective, versatile, and efficient while maintaining the physical and nutritional traits desired by consumers (Goodburn and Wallace, 2013; Gil *et al.*, 2015). Therefore, new decontamination methodologies are continually being developed and tested (Foong-Cunningham and Verkaar, 2012; Stopforth *et al.*, 2008). The use of cold atmospheric plasma, which is ionized gas generated at ambient temperature and atmospheric pressure, is one such method.

UV light, charged particles, and reactive species are the cold plasma products most often cited for causing bacterial inactivation (Misra *et al.*, 2011; Mai-Prochnow *et al.*, 2014). UV light and charged particles play minor roles in bacterial inactivation, whereas reactive oxygen and nitrogen species (RONS) are the primary plasma products that damage bacterial cells when the plasma is generated in air. RONS are components or by-products of several essential cellular processes and bacteria have well established pathways for reducing these reactive species before they can cause cellular damage. However, in times of high oxidative stress, such as during cold plasma treatment, cells are not able to keep up with the accumulation of reactive species and damage to lipids, proteins, and DNA can occur, resulting in cell death. Ozone (O_3) is a neutral reactive oxygen species of special note that has received increased interest in recent years for food decontamination applications. This relatively long-lived ROS that naturally converts back

to harmless molecular oxygen is a well-known and powerful antimicrobial agent that is produced in high amounts by cold plasma generation in air (Khadre *et al.,* 2001; Sakiyama *et al.,* 2012) and is generally recognized as safe (GRAS) by the FDA when used for food decontamination. It is likely that ozone itself is not a major contributor to bacterial inactivation but it serves as a precursor to other, more reactive species (such as hydrogen peroxide, superoxide, and hydroxyl radical) when it rapidly interacts with free water on the surface of bacterial cells (Sakiyama *et al.,* 2012). The detrimental effects to bacterial cells can occur in a matter of seconds when they are exposed directly to cold plasma.

There are multiple approaches to generate cold plasma with air at atmospheric pressure, only a few of which are practically suitable for food decontamination applications in a scalable format (Misra *et al.*, 2011; Niemira, 2012). Therefore, the main challenge in cold plasma treatment of complex food surfaces has to do with the means of reactive species delivery to the treated surface. Accordingly, the major differences in the various plasma-generation methods relate to the modes by which charged particles, photons, and reactive species are allowed to interact with target cells on contaminated substrates. The major plasma-generation approaches currently used include plasma pens, jets, torches, the use of high-energy deep-UV light, and microwave excitation (Misra *et al.*, 2011). All of these approaches require complex apparatuses, high input powers, and a supplied flow of inert gas, resulting in high operational costs and limited practical applications. Dielectric barrier discharge (DBD), in contrast, is one of the simplest approaches for cold plasma generation (Kogelschatz *et al.*, 1999). Using this format, plasma can be generated with air at room temperature and atmospheric pressure,

requiring no enclosures or supplied gas flow. In its most basic form, termed surface dielectric barrier discharge (SDBD), plasma is generated as a result of charge accumulation on one side of a dielectric barrier placed between two electrodes. The electric potential accumulates to a point until the air between the electrodes is ionized, forming plasma (Gibalov and Pietsch, 2000).

One of the results of the SDBD process is the production of an induced localized airflow. Accordingly, SDBD has been extensively researched and developed for applications in the aerospace industry, in which it is used to induce or modify airflow over the surfaces of aircraft wings. It is a novel low-power, active flow control technique used to improve the aerodynamic characteristics and propulsion efficiency of aircraft (Li *et al.,* 2011). The self-induced localized airflow of SDBD is therefore hypothesized to carry with it the generated reactive species and charged particles for a short distance until they revert back to their normal, stable state. The electrodes can be arranged in such a way as to increase the amount of induced airflow and therefore maximize the distance that reactive species can travel before reverting back to their unreactive state. For food decontamination applications, the induced airflow allows delivery of RONS, and particularly ozone, to surfaces that are some distance from SDBD actuators themselves. As a result of these characteristics, SDBD has the potential to overcome many of the limitations of current plasma generation approaches for food decontamination applications. Surface DBD cold plasma actuators are relatively simple and flexible apparatuses, require less energy input than other methods, induce a localized airflow and thus diffusion of reactive species into hard-to-reach surface crevices without any additional inputs, and are easily scalable.

Previous researchers investigating the effectiveness of cold plasma as a decontamination method have identified several aspects of treatment that are common to multiple types of plasma generation methods and apparatuses. These findings include that initial cell concentration influences bacterial inactivation rates (Fernandez and Thompson, 2012; Gaunt *et al.,* 2006), bacterial inactivation is independent of growth phase and temperature (Fernandez *et al.,* 2013), increased treatment time is required for decontamination of complex food surfaces (Fernandez *et al.,* 2013; Ziuzina *et al.,* 2014), and cold plasma treatment does not detrimentally affect fresh produce quality (Misra *et al.,* 2014a; Misra *et al.,* 2014b; Lacombe *et al.,* 2014; Fernandez *et al.,* 2013). What is not well understood, despite the commonalities for all plasma generation apparatuses, is the specific mechanisms by which plasma or plasma-generated species inactivate bacterial pathogens. The key distinctive feature of SDBD, when compared to other plasma generation apparatuses, is that the former induces a localized airflow that may allow delivery of reactive species and charged particles to distant surfaces.

Therefore, it was the goal of this research to evaluate the potential of SDBD to inactivate bacterial pathogens on biotic and abiotic surfaces and to contribute to the growing understanding of the mechanistic effects of cold plasma generation has on bacterial cells. Rather than simply repeat similar assays that have been done by other groups to evaluate novel cold plasma generation apparatuses, an approach was chosen for this research that would allow evaluation of the bacterial inactivation potential of SDBD in a way that has not been done before while still allowing comparison to previous findings in the literature. Thus, the bacterial inactivation potential and induced airflow dynamics of SDBD were evaluated, the transcriptomic response of *Salmonella* to SDBD

treatment was analyzed using RNA-sequencing, and the potential for resistance development was evaluated preliminarily for *Salmonella* by successively treating plasma-injured cells and comparing any genotypic changes to before the successive treatments. This research report contains the first known data correlating bacterial inactivation rates with induced airflow by SDBD (Chapter 3), evaluating the transcriptomic response of a bacterial pathogen to cold plasma treatment using RNA-sequencing (Chapter 4), and preliminarily evaluating the potential for bacterial development of resistance by successive treatments of plasma injured cells (Chapter 5). The results of this study will aid in design optimization of SDBD devices for increased pathogen inactivation efficiency and add to the growing body of literature delineating the mechanistic effects of cold plasma treatments on bacterial pathogens.

LITERATURE CITED

Abadias, M., Cañamas, T.P., Asensio, A., Angueram, M., & Viñas, I. (2006). Microbial quality of commercial 'Golden Delicious' apples throughout production and shelf-life in Lleida (Catalonia, Spain). *International Journal of Food Microbiology*. 108:404-409.

Aruscavage, D., Lee, K., Miller, S., & Lejeune, J.T. (2006). Interactions affecting the proliferation and control of human pathogens on edible plants. *Journal of Food Science.* 71:R89-R99.

Barth, M., Hankinson, T., Zhuang, H., & Breidt, F. (2010). Microbiological Spoilage of Fruits and Vegetables. In W. H. Sperber & M. P. Doyle (Eds.), *Compendium of the Microbiological Spoilage of Foods and Beverages* (pp. 135-183): Springer New York.

Centers for Disease Control and Prevention. (2013). Multistate Outbreak of Shiga toxin-producing *Escherichia coli* O157:H7 Infections Linked to Ready-to-Eat Salads (Final Update). Available at: http://www.cdc.gov/ecoli/2013/O157H7-11-13/

Fernández, A., & Thompson, A. (2012). The inactivation of *Salmonella* by cold atmospheric plasma treatment. *Food Research International*, 45(2): 678-684.

Fernández, A., Noriega, E., & Thompson, A. (2013). Inactivation of Salmonella enterica serovar Typhimurium on fresh produce by cold atmospheric gas plasma technology. *Food Microbiology*, 33(1): 24-29.

Foong-Cunningham, S., & Verkaar, E.L.C.. (2012). Microbial decontamination of fresh produce. In Demirci, A., and M.O. Ngadi (Eds.) Microbial decontamination in the food industry: Novel methods and applications. Woodhead Publishing, Cambridge, UK.

Gaunt, L. F., Beggs, C. B., & Georghiou, G. E. (2006). Bactericidal Action of the Reactive Species Produced by Gas-Discharge Nonthermal Plasma at Atmospheric Pressure: A Review. *Plasma Science, IEEE Transactions on*, 34(4):1257-1269.

Gibalov, V.I., & G.J. Pietsch. (2000). The development of dielectric barrier discharges in gas gaps and on surfaces. *J.Phys.D:Appl. Phys.* 33:2618-2636.

Gil, M. I., Selma, M. V., Suslow, T., Jacxsens, L., Uyttendaele, M., & Allende, A. (2015). Pre- and Postharvest Preventive Measures and Intervention Strategies to Control Microbial Food Safety Hazards of Fresh Leafy Vegetables. *Critical Reviews in Food Science and Nutrition*, 55(4): 453-468.

Goodburn, C., & C.A. Wallace. (2013). The microbiological efficacy of decontamination methodologies for fresh produce: A review. *Food Control. 32*(2):418-427.

Khadre, M., Yousef, A., & Kim, J. (2001). Microbiological aspects of ozone applications in food: a review. *Journal of food science-Chicago-*, 66(9): 1242-1253.

Kogelschatz, U., B. Eliasson, & W. Egli. (1999). From ozone generators to flat television screens: history and future potential of dielectric-barrier discharges. *Pure and Applied Chemistry.* 71:1819.

Lacombe, A., Niemira, B. A., Gurtler, J. B., Fan, X., Sites, J., Boyd, G., & Chen, H. (2015). Atmospheric cold plasma inactivation of aerobic microorganisms on blueberries and effects on quality attributes. *Food Microbiol,* 46, 479-484.

Li, Y.H., Y. Wu, H.M. Song, H. Liang & M. Jia . (2011). Plasma Flow control. *In* M. Mulder (Ed.). Aeronautics and Astronautics. InTech publishing, Rijeka, Croatia

Mai-Prochnow, A., A.B. Murphy, K.M. McLean, M.G. Kong, & K. Ostrikov. (2014). Atmospheric pressure plasmas: Infection control and bacterial responses. *International Journal of Antimicrobial Agents*. 43(6): 508-517.

Misra, N.N., B.K. Tiwari, K.S.M.S. Raghavarao, & P.J. Cullen. (2011). Nonthermal plasma inactivation of food-borne pathogens. *Food Engineering Reviews.* 3(3-4):159-170.

Misra, N. N., Pankaj, S. K., Walsh, T., O'Regan, F., Bourke, P., & Cullen, P. J. (2014a). In-package nonthermal plasma degradation of pesticides on fresh produce. *Journal of Hazardous Materials,* 271(0):33-40.

Misra, N. N., Patil, S., Moiseev, T., Bourke, P., Mosnier, J. P., Keener, K. M., & Cullen, P. J. (2014b). In-package atmospheric pressure cold plasma treatment of strawberries. *Journal of Food Engineering,* 125(0): 131-138.

Niemira, B.A. (2012). Cold Plasma Decontamination of Foods. *Annual Review of Food Science and Technology.* 3(1):125-142.

Painter, J. A., Hoekstra, R. M., Ayers, T., Tauxe, R. V., Braden, C. R., Angulo, F. J., & Griffin, P. M. (2013). Attribution of foodborne illnesses, hospitalizations, and deaths to food commodities by using outbreak data, United States, 1998-2008. *Emerging Infectious Disease,* 19(3): 407-415.

Sakiyama, Y., David, B. G., Hung-Wen, C., Tetsuji, S., & Gregor, E. M. (2012). Plasma chemistry model of surface microdischarge in humid air and dynamics of reactive neutral species. *Journal of Physics D: Applied Physics*, 45(42):425201.

Scallan, E., Hoekstra, R. M., Angulo, F. J., Tauxe, R. V., Widdowson, M. A., Roy, S. L., & Griffin, P. M. (2011). Foodborne illness acquired in the United States--major pathogens. *Emerging Infectious Disease,* 17(1): 7-15.

Sivapalasingam, S., Friedman, C.R., Cohen, L., & Tauxe, R.V. (2004). Fresh produce: A growing cause of outbreaks of foodborne illness in the United States, 1973 through 1997. *Journal of Food Protection.* 67(10):2342-2353.

Stopforth, J. D., Mai, T., Kottapalli, B., & Samadpour, M. (2008). Effect of Acidified Sodium Chlorite, Chlorine, and Acidic Electrolyzed Water on Escherichia coliO157:H7, Salmonella, and Listeria monocytogenesInoculated onto Leafy Greens. *Journal of Food Protection,* 71(3): 625-628.

Ziuzina, D., S. Patil, P.J. Cullen, K.M. Keener, & P. Bourke. (2014). Atmospheric cold plasma inactivation of *Escherichia coli, Salmonella enterica* serovar Typhimurium *and Listeria monocytogenes* inoculated on fresh produce. *Food Microbiology.* 42(0):109-116.

CHAPTER II

LITERATURE REVIEW

Foodborne Illness

Global awareness of the importance of food safety and food security is at an all-time high (Yiannas, 2009). Increased globalization of the food supply, changing consumer habits, intentional food adulteration, the threat of agroterrorism, and growing concerns about the sustainability of current food production systems with a rapidly increasing population each brings new challenges for developing and/or maintaining a safe and secure food supply. As defined by the Food and Agriculture Organization (FAO) of the United Nations, food security is a national responsibility enjoyed by individuals that "exists when all people, at all times, have physical and economic access to sufficient, safe and nutritious food to meet their dietary needs and food preferences for an active and healthy life (FAO, 1996)." The 4 pillars of food security, availability, access, utilization, and stability, are built upon a foundation of food safety (FAO, 2006). If a food supply is not safe, it is probably not secure. Although great progress has been made in promoting food safety and reducing foodborne illnesses through good agricultural practices (GAPs), robust hazard analysis and critical control point (HACCP) plans during

food processing, and increasingly sensitive and rapid outbreak detection methods, foodborne illness are still major public health issues worldwide (WHO 2007).

Foodborne illness is defined as disease caused by an infectious or toxic agent that enters the body through contaminated food (WHO, 2007). It can be caused by bacteria, parasites, viruses, or toxins as a result of the pathogens themselves, pathogen-produced toxins, or toxic chemicals (Hird *et al.,* 2009). While more than 250 distinct foodborne diseases have been described, the majority are caused by foodborne pathogens rather than by harmful chemicals (CDC, 2011). Approximately 9.4 million illnesses, 55,961 hospitalizations and 1,351 deaths occur each year in the United States, attributed to 31 major foodborne pathogens (Scallan *et al.,* 2011). One in 6 Americans experience foodborne illness every year, but the illness incidence in other parts of the world can be much higher (Havelaar *et al.,* 2013).

Reducing the burden of foodborne illness requires identification of commonly contaminated food sources and implementation of appropriate and effective control strategies (WHO 2007). Control strategies can be divided into 2 broad categories: 1) prevention of contamination and 2) decontamination (Thorns, 2000). While preventing contamination should be the first priority and would eliminate the need for subsequent decontamination, it is not feasible or practical for many food products. As a result, decontamination strategies are heavily relied upon in many food production, processing, and preparation systems prior to consumption (Goodburn and Wallace, 2013). Decontamination is especially important for foods that are consumed without a dedicated pathogen killing step before consumption (e.g. cooking), such as fresh fruits and vegetables. An approximately 30% increase in fresh produce consumption has been

observed in the United States over the past few decades (Barth *et al.*, 2010). Unfortunately, fresh produce has also been increasingly associated with outbreaks of foodborne illness (Sivapalasingam *et al.,* 2004; Painter *et al.,* 2013).

Identification and characterization of the primary source of contamination associated with foodborne illness allows greater insight into the natural history, epidemiology, and evolution of foodborne pathogens, all of which facilitate efforts to improve public health (Foley *et al.,* 2007). However, attributing a specific illness to a specific source is a difficult task due to the variety of potential disease-causing agents, transmission through nonfood mechanisms, variable pathogen virulence and chemical toxicity, and extensive under diagnosis and under reporting (Painter *et al.,* 2013; Scallan *et al.,* 2011). While most foodborne illnesses are sporadic, linking an illness to a particular food is rarely possible except during an outbreak, in which more than one illness can be attributed to the same source (Painter *et al.,* 2013). Outbreak investigations are the foundation of foodborne illness source attribution (Cole *et al.,* 2014).

In a comprehensive review on foodborne illness outbreaks occurring in the United States, Painter *et al.* (2013) provide critical data about the foods and pathogens most commonly associated with foodborne illness. Using 4,589 foodborne disease outbreaks attributed to known sources reported to the Centers for Disease Control and Prevention (CDC) over an 11-year span from 1998 to 2008, illnesses were attributed to 17 different food categories composed of both simple and complex foods made up of plant and animal products. One of the key findings of the study was that produce (composed of 6 plant food categories) accounted for almost half (46%) of the outbreaks (Painter *et al.,* 2013). Among the 6 plant food categories, vegetables contributed to more illnesses (34%) than

fruits and nuts (12%), with leafy vegetables accounting for the most illnesses (22%). The percentage of yearly outbreaks associated with leafy vegetables has increased from 6% in 1998-1999 to 11% in 2006-2008 (CDC, 2013). Although this increase may be an artifact of improved pathogen detection methods, it may also represent an emerging association of virulent foodborne pathogens with fresh produce (Brooks et al., 2005; Johnson *et al.*, 2006; Bettelheim, 2007; CDC, 2012, Brandl and Sundin, 2013). Pathogen-contaminated produce has been found to be a top contributor to outbreak-associated illnesses, hospitalizations, and deaths in the United States (CDC, 2013; Cole *et al.*, 2014).

Microbial contamination of fresh produce

Major sources of contamination

Contamination of fresh produce with human pathogens can occur at any point along the "farm to fork" chain, consisting of field production, packaging, distribution, and preparation processes (Aruscavage *et al.,* 2006). Since most foodborne pathogens are transmitted through the fecal-oral route, contamination of produce is often ultimately caused by direct and indirect contact with the feces of reservoir animals or previously infected humans. Survival of enteric bacterial pathogens on or within plants represents an important life cycle stage allowing environmental persistence (Barak and Schroeder, 2012). Although produce surfaces are harsh environments for enteric bacteria and enteric bacterial populations often decline over time on produce surfaces, they can still survive and persist for extended periods of time; in some instances their populations can increase (Barak and Schroeder, 2012). Fecal contamination of fresh produce most commonly occurs through soil, irrigation water, flood water, pesticide application, fertilizer

application, animal activity, harvesting and processing equipment, and human contact (Matthews, 2009; Gil *et al.,* 2013).

Produce contamination events are often classified as occurring either pre-harvest or post-harvest (Gil *et al.,* 2013). Pre-harvest contamination is arguably more difficult to control due to variations in weather, animal access, and available water sources in most fresh produce production environments. Good agricultural practices (GAP) are essentially prevention measures that are critical for reducing the likelihood of contamination and helping to ensure new pathogens are not introduced into a production system (Gil *et al.,* 2013). GAPs are not universally applicable to all commodities but are general guidelines that must be tailored to specific produce types and production systems (Codex Alimentarious, 2003; ICMSF, 2005, 2011).

Post-harvest production practices can also be major contributors to contamination. Improper food processing and storage can allow contamination, recontamination, or cross contamination, or allow pathogens present in low numbers to proliferate to an infectious titer (Gil *et al.,* 2013). Post-harvest sources of contamination often include contaminated equipment or storage facilities, contaminated wash water, and human contact. In contrast to pre-harvest contamination, post-harvest contamination can be controlled largely by proper practices that can effectively eliminate introduction of pathogens into the production process (Gil *et al.,* 2013; Goodburn and Wallace, 2013).

Major foodborne pathogens

The major pathogens associated with foodborne illness in the United States include viruses, bacteria, and parasites. Each year, noroviruses cause the most illnesses

and outbreaks among adults but bacteria cause the most hospitalizations and deaths (Scallan *et al.,* 2011; Painter *et al.,* 2013). Compared to bacteria and viruses, parasites are relatively minor contributors to foodborne illness. Bacterial foodborne pathogens are of the greatest concern due to their higher virulence and environmental persistence. The major bacterial pathogens monitored by CDC surveillance systems include *Campylobacter jejuni*, *Salmonella enterica*, Shiga toxin-producing *Escherichia coli* (STEC*), Listeria monocytogenes, Yersinia pestis*, *Shigella* spp., *Vibrio* spp., and *Clostridium* spp. While all of these pathogens can be associated with meat and animal products, *Salmonella*, STEC, and *Listeria* are commonly associated with plant-based products (Painter *et al.,* 2013).

Salmonella enterica is a rod-shaped, Gram-negative, non-spore forming, facultative anaerobic species of bacteria in the family *Enterobacteriaceae*. This fairly ubiquitous and hardy species of bacteria has a complex nomenclature system composed of 6 subspecies and over 2500 different serological variants (or serovars) (Brenner, 1998; Popoff and Le Minor, 1997; 2001). The vast majority of human infections are caused by *Salmonella enterica* subspecies *enterica*, a group of over 1500 different serovars, each of which is thought to be capable of causing human illness (Popoff *et al.,* 2004). However, different serovars can have different modes of pathogenesis in humans and are categorized as typhoidal or non-typhoidal. *Salmonella* Typhi and Paratyphi (*Salmonella enterica* subsp. *enterica* serovar Typhi) are the typhoidal serovars that, when infecting humans, can result in typhoid fever. Non-typhoidal infections are less severe, resulting in gastroenteritis, and are by far the most predominant, especially in the developed world. Non-typhoidal *Salmonella* serovars cause more hospitalizations and deaths than any other

bacterial pathogen in the United States (Scallan *et al.,* 2011) and are associated with a broad range of both animal and plant-based food products (Painter *et al.,* 2013; Cole *et al.,* 2014).

Shiga toxin-producing *Escherichia coli* (STEC) are also rod-shaped, Gram-negative, non-spore forming, facultative anaerobic bacteria in the family *Enterobacteriaceae*. This group of pathogenic bacteria, once dominated by a single serotype (*E. coli* O157:H7), seems to be ever expanding as more strains with the required virulence characteristics are being identified and isolated (Luna-Gierke et al., 2014; Johnson *et al.,* 2006). It is currently debated as to whether these pathogens are truly emerging or if their increased isolation rates are simply an artifact of increasingly sensitive detection methods and a heightened awareness of their potential presence (Brooks et al., 2005; Johnson *et al.,* 2006). Nevertheless, they remain an important public health concern and have been associated with several major national and multinational foodborne illness outbreaks (Sodha *et al.,* 2014; Luna-Gierke *et al.,* 2014). While most STEC infections result in mild diseases with symptoms common to gastroenteritis, a much more severe and life threatening complication is possible: hemolytic uremic syndrome (HUS), a form of kidney failure (Karmali, 1989). STEC are usually associated with meat products (especially beef) but have also been implicated in several major outbreaks involving produce, including spinach in 2006 (CDC, 2006), fenugreek sprouts in 2011 (CDC, 2011b), raw clover sprouts in 2012 (CDC, 2012b), and ready-to-eat salad in 2013 (CDC, 2013). STEC seem to be increasingly associated with leafy greens, possibly as a result of specific interactions that allow their survival on these products (Leff and Fierer, 2013).

Listeria monocytogenes is a species of rod-shaped, Gram-positive, non-spore forming, facultative anaerobic bacteria in the family *Listeriaceae*. The genus *Listeria* contains 6 species but only *L. monocytogenes* is known to cause human illness. Only 3 of 13 *L. monocytogenes* serotypes are commonly associated with foodborne illness. Serotypes 1/2a and 1/2b are commonly associated with sporadic cases of foodborne illness while serotype 4b has been associated with most known *Listeria* outbreaks in Europe and the United States (Ward *et al.,* 2004; Painter *et al.,* 2013). *Listeria* is the most virulent bacterial foodborne pathogen in the United States with mortality occurring in 20 to 30 percent of cases (Ramaswamy *et al.,* 2007). Although fewer illnesses are caused by *Listeria* than several other bacterial pathogens (Scallan *et al.,* 2011), the high virulence makes this pathogen of special concern. In addition to gastroenteritis, *Listeria* infections can result in several other serious clinical manifestations including septicemia, meningitis, encephalitis, pneumonia, and spontaneous abortions or stillbirths (Ramaswamy *et al.,* 2007). *Listeria* is often associated with aged cheeses and deli meats but can also be associated with fresh produce (Bae *et al.,* 2013; Kovacevic *et al.,* 2013; Painter *et al.,* 2014). One of the most deadly foodborne illness outbreaks in United States history was caused by consumption of cantaloupes contaminated with *Listeria monocytogenes* (CDC, 2012).

Decontamination of produce

Proper decontamination methods are critical for ensuring the safety of fresh fruits and vegetables (Abadias *et al.,* 2006). Although avoiding contamination during field production by implementing appropriate GAPs reduces the risks of fresh produce

contamination, decontamination methods are heavily relied upon by the food processing industry (Goodburn and Wallace, 2013). Many factors can influence the efficacy of decontamination techniques, including initial bacterial load on produce surfaces, treatment type, the nature of the surface to be treated, the type of disinfectant, andwhether pathogens are internalized within the tissues (Erickson, 2012). The ideal decontamination method for fresh produce should greatly reduce or eliminate the number of pathogens while having little to no effect on the nutritional value or sensory characteristics of the product. However, these goals are not always achievable with currently used methodologies.

The major methods currently used for decontamination of fresh produce make use of antimicrobial chemicals in either an aqueous or gaseous solution (Foong-Cunningham and Verkaar, 2012). The most commonly used antimicrobial chemicals are chlorine, chlorine dioxide, organic peroxides, and ozone (Goodburn and Wallace, 2013). Each of these chemicals has been thoroughly evaluated for their effectiveness (usually measured in log reductions) at reducing pathogen concentrations on fresh produce surfaces (Stopforth *et al.*, 2008). However, not all antimicrobial chemicals can be used in all processing systems. National and local regulations dictate which antimicrobials can be used for specific products and which cannot, depending on health and environmental concerns (Foong-Cunningham and Verkaar, 2012). Each decontaminant has its respective pros and cons and performs better with some types of produce than others (WHO, 1998; Goodburn and Wallace, 2013). As a result, several novel decontamination strategies are being developed to overcome some of the limitations of current methods (Foong-Cunningham and Verkaar, 2012).

Chlorine. Chlorine treatment, usually as a diluted sodium hypochlorite solution at 50 to 200 ppm and pH 6.5, is perhaps the most common decontamination technique used currently for produce (Shen *et al.,* 2012). It is a cost effective treatment that can be used for many different types of produce and usually has minimal effects on the produce itself. Chlorine is present in 3 different forms when added to water; elemental chlorine (Cl_2), hypochlorous acid (HOCl), and hypochlorite ion (OCl-). HOCl is the most bactericidal form, inactivating bacteria by damaging the respiratory and electron transport processes in cell membranes (Foong-Cunningham and Verkaar, 2012). HOCl is more effective against planktonic bacterial cells in the wash solution than against those on produce surfaces (Erkmen, 2010). Chlorine is commonly added to wash water during initial post-harvest processing with a contact time of 1 to 2 minutes to wash field debris from produce and to decontaminate the surface (Gil *et al.,* 2013). However, despite variations in chlorine concentration, pH, and immersion times, only up to a 2 log reduction in bacterial populations can usually be achieved (De Giusti *et al.,* 2010). Chlorine washes are effective at reducing bacterial concentrations, but not at a level high enough to ensure thorough decontamination (Goodburn and Wallace, 2013). Additionally, chlorine washes may not be possible for some types of produce due to the reduction of marketability through physical damage or reducing shelf-life. However, the greatest concern limiting the more widespread use of chlorine washes is the ability to form potentially carcinogenic organochlorine compounds such as chloramines, trihalomethanes (THMs), and semicarbizides (Foong-Cunningham and Verkaar, 2012). If a washing step is necessary, the addition of chlorine to the wash water may be a good way to reduce further

contamination but is a less than ideal method for decontamination and requires careful monitoring for acceptable performance (Goodburn and Wallace, 2013).

Chlorine dioxide. Chlorine dioxide (ClO_2) can be used as a decontaminant in either aqueous or gaseous states, depending on the type of produce (Wu and Kim, 2007). Chlorine dioxide is a highly water soluble and unstable gas; therefore it is usually dissolved in water (Foong-Cunningham and Verkaar, 2012). Although less cost effective, chlorine dioxide is a more efficient decontaminant than chlorine and is also more versatile. ClO_2 is a stronger oxidizing agent than HOCl, inactivating bacteria through oxidative stress and membrane damage more efficiently. Compared to chlorine washes, chlorine dioxide treatment is approximately 2.5 times more effective at reducing microorganism populations and also is less reactive to organic compounds (Beuchat *et al.*, 2004). As a result, chlorine dioxide does not form potentially carcinogenic chlorinated organic compounds as easily as chlorine does (Nei *et al.*, 2010). A 4 to 6 log reduction in common bacterial pathogen populations is often possible with chlorine dioxide treatment (Lee *et al.*, 2004) and the aesthetic characteristics of produce are usually not adversely affected (Stopforth *et al.*, 2008). The major drawback of chlorine dioxide is that it is unstable; it must be generated on site and can be explosive when concentrated (Goodburn and Wallace, 2013). Also, long treatment times from 10 minutes to 2 hours are usually necessary.

Organic peroxides. Organic peroxides currently used in food decontamination washes include peroxyacetic acid (PAA), peroxyoctanoic acid, cumene peroxide, hydroperoxides, diacyl peroxides, and perocyesters ((Foong-Cunningham and Verkaar, 2012). PAA is the most commonly used and inactivates bacterial cells, similar to chlorine

and chlorine dioxide, by disrupting cellular respiration through oxidation reactions (Davidson *et al.,* 2005). PAA is less affected by the organic load of produce washes than chlorine, maintaining its effectiveness for a longer period of time. Additionally, PAA is not known to be able to form potentially carcinogenic organic compounds (Foong-Cunningham and Verkaar, 2012).

Ozone. Ozone is a powerful oxidizer that can be used in either an aqueous or gaseous form for decontamination of produce (Khadre *et al.,* 2001). Ozone also inactivates bacterial pathogens by causing oxidative damage of cellular structures and results in oxidative stress, even at very low concentrations (ppb). The gaseous form is most commonly used for food decontamination applications and has also been used for decades to extend the shelf-life of food products by inactivating various food spoiling microorganisms (Xu, 1999; Khadre *et al.,* 2001; Foong-Cunningham and Verkaar, 2012). However, the strong oxidizing effects can also damage the sensory and aesthetic properties of some types of produce. Ozone treatments often result in up to a 2 log reduction in the populations of pathogenic bacteria on fresh produce surfaces despite variation in temperature and treatment times (Olmez 2010). Although similar in bacterial inactivation rates to chlorine, the short life of ozone by-products and potential of gaseous treatments are advantages over chlorine (Perry and Yousef, 2011). Ozone decomposes to molecular oxygen (O_2) in a matter of minutes in air at atmospheric pressure and room temperature, leaving no harmful residues (Khadre *et al.,* 2001). These characteristics result few non-target effects of the decontaminant. However, the treatment times and temperatures associated with ozone treatments are not optimally suited for some types of

fresh produce, greatly limiting its industrial use. Ozone is also unstable and must be generated on site.

Novel and emerging decontamination methods. Since none of the currently used decontamination methods are ideally cost effective, versatile, and efficient while not resulting in other harmful effects, new decontamination methodologies are continually being developed and tested (Gil *et al.,* 2013). A few of the promising new and emerging decontamination technologies having applications in the produce industry include irradiation, electrostatic sprays, silver and hydrogen peroxide treatment, pulsed light, electrolyzed water, biological controls, essential oils, and non-thermal plasma treatment (Goodburn and Wallace, 2013). Each of these methods show promise as effective decontamination methods for certain applications, but more research is necessary to more fully evaluate how they affect both the food product being treated and any pathogenic contaminants that may be present (Gil *et al.,* 2013; Goodburn and Wallace, 2013).

Irradiation treatments have emerged among the most effective decontamination methods for fresh produce with up to 6.5 log reductions in bacterial concentrations possible (Foley *et al.,* 2004). Irradiation treatments are dry, low temperature decontamination methods that are efficient, cost effective, and versatile. The use of gamma radiation to extend the shelf life of some produce products has also been extensively studied and represents another major benefit of this method (WHO 1998; FDA 2008). However, irradiation treatments have also been shown to reduce the sensory characteristics and shelf-life of other produce products, limiting their marketability (Roberts, 2014). Despite the effectiveness and broad applicability of this safe and efficient method, irradiation has not become a major decontamination method (Roberts,

2014). Production scale adoption of this method has been hampered largely as a result of negative consumer perception of irradiated produce (Junquiera-Goncalves *et al.,* 2010; Roberts, 2014).

Non-thermal atmospheric plasma (or cold plasma) is one of the most promising of the emerging decontamination methods for fresh produce. It has been the subject of increased research in recent years, and has been used in a variety of configurations (Niemira, 2012). Cold plasma is generated at room temperature and atmospheric pressure from air using electricity. Therefore, it overcomes many of the limitations of chlorine, chlorine dioxide, ozone, and irradiation in that it is a low temperature, dry process that is efficient, cost effective, scalable, and potentially very versatile. Currently it has no negative consumer perception (Niemira, 2012). However, there is much room for improvement in this technology and there is very little currently known about the specific mechanisms by which bacteria are inactivated by this method and if there are any potentially negative non-target effects on produce products or consumers.

Cold plasma

The term "plasma" generally refers to a partially or wholly ionized gas having a net neutral charge composed essentially of photons, ions and free electrons in addition to atoms in their fundamental or excited states (Misra *et al.,* 2011). Plasma is the fourth state of matter, with characteristics distinctly different from those of solids, liquids, and gases. In contrast to particles in a gaseous state, which have random paths, plasma particles have a defined path that aligns with surrounding electrochemical fields. Plasma is the most abundant form of matter in the universe and an essential part of our everyday lives. The

activated “species” of which plasma is composed are classified as either light or heavy; photons and electrons are light species while ions and excited atoms are heavy species. Depending on the relative energy levels of light and heavy species, plasma can be divided into two broad classes: thermal plasma and non-thermal plasma (Misra *et al.*, 2011). Thermal plasma, generated at high pressures with high energy inputs, is characterized by thermal equilibrium between light and heavy species. The Sun, for example, is primarily composed of thermal plasma. In contrast, non-thermal plasma, commonly referred to as cold plasma, is usually generated at ambient temperature at atmospheric pressure and requires less energy input than thermal plasma. It is generated by electric discharge in a gas at low pressure or by using microwaves. Since electron and photon temperatures are much higher than that of the surrounding gas and ions produced, non-thermal plasma is characterized by thermodynamic non-equilibrium between light and heavy species. Fluorescent light bulbs are common examples of cold plasma.

Although plasma is the most abundant form of matter in the universe, it is not commonly or directly experienced by living cells in concentrations high enough to have detrimental effects. Prokaryotic cells, having fewer surface protective structures and less efficient nucleic acid, lipid, and protein repair mechanisms compared to eukaryotic cells, seem to be particularly vulnerable to the reactive species and charged particles generated by cold plasma (Guzel-Seydim *et al.*, 2004). The cellular effects of cold plasma treatment can be selective, depending on cell type, resulting in a tunable feature such that pathogenic organisms can be inactivated with minimal effects on host cells or durable background surfaces (Dobrynin *et al.*, 2009; Pai *et al.*, 2015). As a result, cold plasma recently has been the focus of much research as a sterilization or decontamination method

for several different applications (Misra *et al.,* 2011; Niemira, 2012). The interaction of plasma with cells has been investigated for bacteria (Lu *et al.,* 2014; Ziuzina *et al.,* 2014), bacterial spores (Klampfl *et al.,* 2012), biofilms (Ziuzina *et al.,* 2014a; Niemira *et al.,* 2014), plant cells (Puac *et al.,* 2006; Zhang *et al.,* 2014), and animal cells (Weiss *et al.,* 2015; Ma *et al.,* 2014). The results of these investigations underscore the fact that plasma inactivation of cells is a complex process that depends upon the type of plasma generation method, the type of cells targeted, and the substrate on which cells are treated (Stoffels *et al.,* 2008). Despite these complexities and mechanistic uncertainties, cold atmospheric plasma seems to be particularly attractive for food decontamination, especially fresh produce, because it is a low temperature, low energy input, dry process that has minimal effects on the food product itself (Critzer *et al.,* 2007; Niemira, 2012; Ziuzina *et al.,* 2014).

Cold plasma generation

There are multiple approaches to generate cold plasma at atmospheric pressure (Yoon and Ryu, 2007), only a few of which are practically suitable for food product decontamination in a scalable format (Misra *et al.,* 2011; Niemira, 2012). The cell-inactivating properties of plasma can be a result of either direct or indirect contact with plasma. Direct contact with plasma results in optimal inactivation efficiency since even the most short-lived reactive species can contact cell surfaces (Stoffels *et al.,* 2004; Kieft *et al.,* 2005). However, the effects of direct plasma treatment can be quite drastic on both the treated cells and the substrate. When used for decontaminating delicate surfaces, such as fresh produce, direct plasma treatment may not be ideal, damaging the sensory and

aesthetic properties of the product (Stoffels *et al.*, 2008). Indirect plasma treatments result in cellular inactivation due to the charged particles, photons, and reactive species that are by-products of plasma generation rather than contact with the plasma *per se*. Although this is a more gentle approach, the most reactive and most short-lived species generated by cold plasma are unlikely to interact with the surface being treated (Stoffels *et al.*, 2008). Therefore, the main challenge in cold plasma treatment of delicate or complex surfaces (requiring indirect treatment) has to do with the means of reactive species delivery to the treated surface, which may be at some distance from the plasma itself. Accordingly, the major differences in the various plasma generation methods relate to the modes by which charged particles, photons, and reactive species are allowed to interact with target cells. The major plasma generation approaches currently used include plasma pens, jets, or torches, the use of high-energy deep-UV light, microwave excitation, and dielectric barrier discharge (Misra *et al.*, 2011).

Plasma pens, jets, and torches use a stream of gas that is excited with an electric charge as it passes through a nozzle directed at the object being treated (Misra *et al.*, 2011). This indirect plasma-cell interaction method represents a very successful approach for localized plasma generation in medical settings for wound and medical instrument sterilization (Hoffmann *et al.*, 2013; Klampfl *et al.*, 2012; von Woedtke *et al.*, 2014). However, plasma torches are not well suited for food decontamination due to the small effective treatment areas, high energy inputs, and complicated apparatus requirements (Niemira, 2012). Using high-energy deep-UV light and microwaves to generate cold plasma have potential applications in the food industry and can be scaled up for production purposes. However, the high amount of required energy input is a major

detractor. Also, production of microwaves and/or UV light tends to have negative effects on food quality or appearance, and therefore on marketability. Dielectric barrier discharge approaches are much more practical for the food industry, allowing more configuration options, lower energy inputs, less complicated configurations, and more scalability (Misra *et al.*, 2011; Niemira, 2012).

Dielectric barrier discharge

Cold plasma generation by dielectric barrier discharge (DBD) occurs as a result of charge accumulation on one side of a dielectric barrier placed between two electrodes. The dielectric barrier does not allow the electrical current to pass between the electrodes until the accumulation of charge on one side of the barrier results in the production of plasma, which is conductive, allowing the electric field to balance (Kogelschatz *et al.*, 1999). In this process, the migration of charge and generation of light and heavy species continues until the charge stops growing and the discharge extinguishes. Plasma generation by this method is an ephemeral process consisting of a large number of randomly distributed short-lived microdischarges (Kogelschatz *et al.*, 1999; Gibalov and Pietsch, 2000; Enloe *et al.*, 2004). DBD has traditionally been used for commercial production of ozone for water treatments since the 1930s; only relatively recently has it been investigated for surface sterilization applications (Kogelschatz *et al.*, 1999).

DBD applications for food decontamination must allow for an approximately even distribution of reactive species over the entire surface, since contamination could occur anywhere on the surface of a food product. The complex and irregular surfaces of many food products can make this goal difficult to achieve. DBD plasma generation

apparatuses can be arranged so that the treated surface either directly or indirectly contacts the plasma itself (Sysolyatina *et al.,* 2014). Direct plasma contact with food surfaces requires the food itself to be grounded, allowing the applied current to pass through the food product. This required feature would pose major challenges in production and processing facilities. As a result, DBD designs currently being investigated for food decontamination applications generate diffuse reactive species via an introduced or induced airflow within a given volume or area surrounding the food product (Niemira, 2012). The two DBD approaches used to achieve this are volumetric DBD and surface DBD.

Volumetric dielectric barrier discharge. In volumetric DBD (VDBD), a low pressure gas is passed through an enclosure between the dielectric covered electrode and the exposed electrode (Kogelschatz *et al.,* 1999). The gas is the medium used for plasma generation, forming a region of plasma between the dielectric barrier and the exposed electrode. Effective decontamination is possible with both pure and mixed gasses, even air (Pankaj *et al.,* 2014). VDBD has recently been the primary and almost exclusive cold plasma generation approach investigated for applications in food decontamination, including produce (Misra *et al.,* 2011; Niemira, 2012; Ziuzina *et al.,* 2014; Fernandez *et al.,* 2013). It has been used for decontamination of such diverse products as strawberries (Misra *et al.,* 2014), red pepper powder (Kim et al., 2014), cherry tomatoes (Misra *et al.,* 2014b), fresh corn salad leaves (Baier *et al.,* 2013), and almonds (Niemira, 2012). In most of these studies, the food product being treated was placed inside a closed chamber or a low pressure gas flow was supplied across the food surface. These characteristics impose distinct limitations on the size of potential food products for decontamination and

complicate the apparatus configuration. In-package cold plasma treatment, in which the food packaging itself serves as a dielectric barrier and the atmospheric gas inside the package serves as the plasma medium, is a practical application of this technology and has been the focus of recent research (Pankaj *et al.*, 2014). However, the complexity of the required cold plasma generation apparatus and the high energy input requirements will likely limit its commercial use.

Surface dielectric barrier discharge. Surface DBD (SDBD), in contrast, is one of the simplest approaches for cold plasma generation (Kogelschatz *et al.*, 1999). Two electrodes are placed on both sides of a dielectric barrier, usually in an asymmetrical arrangement. Using this format, plasma can be generated with air at room temperature and atmospheric pressure, requiring no enclosures or supplied gas flow. One of the electrodes (anode) is covered to prevent contact with the ambient gas while the other (cathode) is left uncovered. Plasma, formed adjacent to the uncovered cathode, consists of forms that vary from distinct streamers to diffuse discharges with low glow, based on the amplitude of supplied AC voltage and the applied frequency (Gibalov and Pietsch, 2000). This plasma actuator design has been extensively researched and developed for applications in the aerospace industry, in which it is used to induce or modify airflow over the surfaces of aircraft wings. It is a novel active flow control technique used to improve the aerodynamic characteristics and propulsion efficiency of aircraft (Li *et al.*, 2011). Additionally, less input energy per plasma generation area is required since the electrodes are much closer to each other and less charge buildup occurs before plasma generation takes place. Therefore, SDBD overcomes many of the current limitations of plasma generation approaches for applications in food decontamination in that it is a

relatively simple and flexible apparatus, it requires less energy input, it induces airflow and thus diffusion of reactive species without any additional inputs, and it is easily scalable. There are currently no published reports of food decontamination using cold plasma generated by SDBD. Using a recently developed, novel SDBD design, preliminary results indicate the possibility of a 6 log reduction of pathogenic bacteria on sterile, non-food surfaces in 2 minutes or less. Further research is necessary to delineate the optimal treatment parameters using this design and also to evaluate its inactivation efficiency and possible undesirable effects on food products.

Potential mechanisms of bacterial inactivation by cold plasma

The biocidal properties of cold plasma were recognized early (Nelson and Berger, 1989) and considerable research has been performed to elucidate the mechanisms of biological inactivation (Montie *et al.,* 2002; Misra *et al.,* 2011). Logically, the photons, electrons, ions, and other reactive molecular species that compose and are by products of cold plasma could cause mechanical and metabolic damage to cells. However, the exact cellular processes involved and the mechanisms of cellular inactivation by cold plasma treatment remain largely unknown (Mai-Prochnow *et al.,* 2014). There have been conflicting reports on the roles of some mechanisms in inactivation of different cell types, and it is likely that different types of cells respond differently to cold plasma treatments (Feng *et al.,* 2010; Niemira, 2012). Most research on plasma-induced cellular inactivation of bacterial cells shows that the process is quite complex, although not as complex as in eukaryotes (Stoffels *et al.,* 2008). Bacteria respond in a dose-dependent manner that ranges from lethal to sublethal (cell cycle arrest or induction of a viable but non-

culturable state), to nonlethal metabolic changes (Stoffels *et al.*, 2008). UV light, charged particles, and reactive species are the reasons most often cited for bacterial inactivation (Misra *et al.*, 2011; Mai-Prochnow *et al.*, 2014).

UV light. UV light, emitted when cold plasma is ignited in air, has well-characterized bactericidal properties (Gaunt *et al.*, 2006). UV photons are absorbed by bacterial chromophores and nucleic acids at discrete wavelengths ranging from 220-280 nm. The maximum bactericidal effect occurs at a wavelength of 254 nm, which is the optimal wavelength absorbed by nucleic acids, causing formation of nucleotide base (mostly pyrimidine) dimers (Beggs, 2002). Although other photoproducts and multiple combinations of nucleotide base dimers can be created by UV photons, thymine dimers are the most common (Beggs, 2002; Vleugels *et al.*, 2005; Boudam *et al.*, 2006; Roth *et al.*, 2010). However, UV photons emitted from plasma generated at atmospheric pressure are mostly reabsorbed by ozone during the plasma generation process and do not have sufficient propagation length or penetration depths to cause cellular inactivation (Gaunt *et al.*, 2006; Boudam *et al.*, 2006; Roth *et al.*, 2012; Mols *et al.*, 2013). In contrast, plasma generated under low-pressure (vacuum) conditions produces more diffuse UV radiation in the proper wavelength range to interact with treated cells and less ozone to absorb the UV photons (Gaunt *et al.*, 2006). Even if UV photons are not absorbed during plasma generation, UV radiation exposure (via UV lights) has been found to be less effective than plasma treatments of the same duration (Laroussi, 1996). Additionally, quartz filters have been used with atmospheric pressure DBD apparatuses to filter out all reactive species and charged particles, but not UV photons, from interacting with target cells and have confirmed that UV radiation is a negligible contributor to cellular inactivation

(Fridman *et al.,* 2007). Therefore, UV radiation is not considered to be an important aspect of cellular inactivation with SDBD cold plasma actuators.

Charged particles. The charged particles produced by cold plasma include ions and electrons resulting from electrical excitation of neutral atoms. Charged species are the essence of plasma and must be considered in plasma-induced cellular inactivation models (Stoffels *et al.,* 2008). Cell wall ruptures due to the accumulation of electrostatic charges at the cell surface is thought to be the major way in which charged particles contribute to cell inactivation (Mendis *et al.,* 2002; Laroussi *et al.,* 2003). Bacterial outer surfaces have a net negative charge since they are made up of mostly electronegative components such as teichoic acids linked to peptidoglycan in Gram positive bacteria and the carbohydrate ends of lipopolysaccharides in Gram negative bacteria (Stoffels et al., 2008). The accumulation of charges (either positive or negative) on the surface of bacterial cells and the production of electrochemical gradients across bacterial cell walls and membranes has been demonstrated to cause mechanical damage to a point that may result in cell death if cellular repair processes are not able to maintain structural integrity (Stoffels *et al.,* 2008; Sysolyatina *et al.,* 2014). Disturbing the surface charge equilibrium of bacterial cells may also induce cell death without actually causing mechanical damage (Wasserman and Felmy, 1998; Campanha *et al.,* 1999). Gram negative bacteria, having thinner cell walls, are often reported to be more susceptible to cell wall rupture than are Gram positive bacteria (Stoffels *et al.,* 2008); however, the double membrane of Gram negative bacteria may also allow increased resistance to surface charge accumulations (Sysolyatina *et al.,* 2014). Since the charged particles produced by cold plasma are so

short-lived and many other factors need to be considered, the precise mechanisms of cellular inactivation due to charged particles has been particularly difficult to elucidate.

Despite the potential effectiveness of surface charge accumulation for bacterial inactivation, it is important to consider that electrons, ions, and other charged particles that are produced during plasma ignition are almost exclusively limited to the confines of the plasma itself. Therefore, direct plasma interaction with cells is the primary means by which charged particles can accumulate to a level high enough to cause mechanical damage (Montie et al., 2002; Stoffels et al., 2008). Indirect plasma exposure results in minimal to no accumulation of charged particles on the surface of treated cells (Sysolyatina *et al.,* 2014). As a result, the effects of charged particles are not thought to be a major contributor to bacterial inactivation with SDBD cold plasma actuators.

Reactive species. Reactive species are formed by collisions among electrons, ions and neutral atoms as a result of the excitation and dissociation caused by cold plasma generation. Reactive species, although often charged, differ from charged particles in that they are more chemically reactive and readily participate in oxidation and reduction (redox) reactions with other molecules (Buettner *et al.,* 2013). The most reactive of the reactive species, free radicals, are atoms, ions, or molecules with unpaired valence electrons; they rapidly gain or lose an electron with other molecules with which they come into contact. Many reactive species can damage or alter all three of the major cellular constituents: lipids, nucleic acids, and amino acids (Imlay 2003). In addition to charged species and free radicals, reactive species can also include neutral species, which are less reactive but more stable, having a longer half-life. Neutral reactive species can accumulate to high local concentrations and can travel some distance from the site of

generation. As a result, neutral reactive species are thought to be the major contributors to bacterial inactivation by cold plasma generated by SDBD (Sakiyama *et al.,* 2012). Reactive neutral species themselves can have detrimental effects on bacterial cells and can also serve as precursors to other reactive species in chemical reactions that occur at the cell surface or in the cell interior (Sakiyama *et al.,* 2012). Oxygen gas plasma has been found to allow for the most efficient cellular inactivation, followed closely by air, and then by nitrogen. When plasma is ignited in air (approximately 80% nitrogen and 20% oxygen), the relatively long-lived neutral reactive species include hydrogen (H_2), hydrogen peroxide (H_2O_2), nitrous oxide (N_2O), nitrogen dioxide (NO_2), nitrous acid (HNO_2), ozone (O_3), nitrate (NO_3), nitric acid (HNO_3), and dinitrogen pentoxide (N_2O_5) (Sakiyama *et al.,* 2012).

Reactive oxygen species (ROS) and reactive nitrogen species (RNS) are essential for the normal function of all types of cells, both prokaryotic and eukaryotic, serving as cell signaling molecules, helping with cellular defense against pathogens, and being key byproducts of energy metabolism. Accordingly, cells have well-developed systems in place to alleviate the potentially negative effects of ROS and RNS by rapid enzymatic conversion of these reactive molecules to their neutral forms (Imlay 2003). However, if reactive species concentrations become too high, oxidative stress occurs through damage to cellular macromolecules. If cellular repair systems are not able to keep up with the damage, cell death may occur (Farr and Kogoma 1991; Imlay 2003). Such irreversible damage can often initiate a chain reaction of supplementary damage unrelated to the initial damage caused by exposure to reactive species (Gaunt *et al.,* 2006). Eukaryotes, having more efficient reactive species neutralization and damage repair systems, are

generally more resistant to oxidative stress than prokaryotes (Farr and Kogoma 1991; Imlay 2003). In fact, ROS are commonly used by plant and animal cells, such as during phagocytosis in mammalian cells, as a form of defense against bacterial pathogens due to the higher sensitivity of bacteria to oxidative stress (Fang 2004). In response, several bacterial species have adapted to these environments and developed multigene antioxidant defense systems to neutralize their effects (Farr and Kogoma 1991; Fang 2004; Imlay 2013). ROS and RNS produced by cold plasma mimics the oxidative stresses experienced by bacteria in these interactions (Gaunt *et al.,* 2006). Depending upon the amount of oxidative stress imposed on bacteria, the following responses can be observed: 1) alleviation of oxidative stress through increased expression of associated enzymes, 2) cell injury to macromolecules that are then repaired, and 3) cell death arising from damaged macromolecules and/or triggering of programmed cell death.

ROS and RNS generated by plasma ignited in oxygen, nitrogen, and air have been shown to effectively inactivate a wide range of microorganisms (Kelly-Wintenberg *et al.*, 1999; Feichtinger *et al.,* 2003), spores (Lee *et al.,* 2006), and viruses (Terrier *et al.,* 2009) via degradation of lipids, proteins, and nucleic acids (Mogul *et al.*, 2003; Critzer *et al.,* 2007). The major ROS include superoxide (O_2^-), peroxide (O_2^{-2}), hydrogen peroxide (H_2O_2), hydroxyl radical (·OH), and hydroxyl ion (OH^-). Superoxide and peroxide are each formed by the sequential reduction of oxygen (O_2) by the addition of electrons, whereas the formation of hydrogen peroxide, hydroxyl radical, and hydroxyl ion require the addition of hydrogen, with water (H_20) as the usual precursor (Ryan *et al.,* 2015). Several other ROS with increasing complexity can be formed depending upon the presence of other gas molecules but often have minor chemical and biological roles

(Ryan *et al.*, 2015). The major RNS are nitric oxide ($\cdot NO$), peroxynitrate ($ONOO^-$), and nitrogen dixode ($\cdot NO_2$). The interaction of nitric oxide with superoxide forms peroxynitrate, which is a precursor for many other RNS formed by the interaction with water, hydrogen ions, and carbon dioxide (CO_2). When plasma is ignited in air, superoxide and nitric oxide are the first reactive species to form as a result of the reduction/addition of electrons/oxidation of oxygen and nitrogen (Sakiyama *et al.,* 2012). Many other ROS and RNS are then able to form as these reactive species continue to interact with other molecules. If water vapor is present when plasma is ignited in humid air, over 50 different species can be formed from over 600 elementary reactions (Sakiyama *et al.,* 2012).

Superoxide, hydrogen peroxide, and hydroxyl radical are the primary precursors of other reactive species, are the most reactive species, and are continually produced during normal cell function (Fang 2004). Therefore, careful cellular management of these potentially damaging molecules is essential. No enzymes generate superoxide specifically, rather, it is formed "by accident" when oxygen adventitiously oxidizes redox enzymes that transfer electrons to other substrates or enzymes, most notably in the electron transport chain involved in cellular respiration (Imlay 2013). If superoxide produced by this process does not immediately diffuse away, a second electron transfer occurs and hydrogen peroxide is formed. Since superoxide and hydrogen peroxide can be produced relatively rapidly and can also rapidly interact with other cellular macromolecules, a large number of scavenging enzymes usually are present. These superoxide and hydrogen peroxide scavenging enzymes or proteins in bacteria include several superoxide dismutases (SODs), catalases, peroxidases, and flavoproteins. SOD

converts superoxide and hydrogen ions into hydrogen peroxide and molecular oxygen, catalases convert hydrogen peroxide into molecular oxygen and water, and peroxidases convert hydrogen peroxide, hydrogen ions, and NAD(P)H to water and NAD^+ (Imlay, 2013). Formation of hydroxyl radicals, the most reactive of the ROS (reacting with virtually all organic molecules) occurs through the Fenton reaction, in which hydrogen peroxide oxidizes Fe^{2+} as part of a small set of Fe-S dehydratases, forming a ferryl radical ($[FeO]^{2+}$) that rapidly interacts with a hydrogen ion to form Fe^{3+} and hydroxyl radical (Fang 2004). In contrast to superoxide, nitric oxide requires an enzyme for formation. In bacteria, nitric oxide synthase (iNOS) oxidizes L-arginine to nitric oxide, which can then be oxidized further to form other RNS (Crane *et al.,* 2010). If cells are not able to keep up with endogenous production of these reactive species or exogenous challenge to the cell is too much, damage to lipids, proteins, and DNA can occur.

Lipid peroxidation is one of the most well-known and substantial results of oxidative stress in eukaryotic systems (Imlay 2013). ROS, in particular, are well-known to act on fatty acids composing the lipid bilayer of cell membranes, resulting in mechanical damage and cytosolic leakage (Montie *et al.,* 2002; Critzer *et al.,* 2007). However, lipid peroxidation requires that lipids be polyunsaturated while most bacterial lipids are saturated or monounsaturated. According to the standard model of lipid peroxidation, it is unlikely that lipid damage is an initial contributor to bacterial inactivation. Yet, cell membrane leakage and structural damage to plasma-treated cells is observed commonly (Mai-Prochnow *et al.,* 2014; Guzel-Seydim *et al.,* 2004). While loss of membrane integrity of plasma treated cells is common, this characteristic may be a

feature of downstream cell death responses and not a contributor to cell death *per se* (Gaunt *et al., 2006*).

Protein damage due to oxidative stress occurs mainly via oxidative modifications to proteins with metal ion cofactors; especially iron (Fang 2004). Dehydratases with Fe-S clusters and mononuclear iron proteins are particularly vulnerable to oxidative damage (Imlay 2013). Oxidative modifications can also occur at cysteine (the most sensitive residue), methionine, tyrosine, phenylalanine, and tryptophan residues (Fang 2004). However, the affinity of cysteine to oxidation by reactive species is orders of magnitude less than that of iron. Protein carbonyls can also be formed by oxidation of arginine, proline, and lysine, but are even less likely to form than disulfide bonds at cysteine residues (Cabiscol *et al.,* 2000). Additionally, the sulfhydryl groups of thiols, present in many cofactors, such as Coenzyme A, are also sensitive to oxidative modification, but also may not be important contributors to cell inactivation (Cabiscol et al., 2000; Fang 2004; Imlay 2013). The main result of protein damage is loss of function, which can have an additive detrimental effect on normal cell function as more and more proteins are oxidized during oxidative stress events. Damaged proteins must be removed to prevent their accumulation inside the cell, and are normally degraded by proteases. Interestingly, heavily oxidized proteins can inhibit the action of proteases, preventing the degradation of these proteins (Grune et al., 1997).

DNA damage is the most important and consequential form of cellular damage that can occur by the actions of ROS and RNS (Imlay, 2013; Fang, 2004). Hydroxyl radicals, rather than superoxide or hydrogen peroxide, are the main ROS that cause DNA lesions (Imlay 2013). Hydroxyl radicals are very short lived and must be produced in

close proximity to nucleic acids to cause damage. Therefore, it is suspected that hydrogen, reacting via the Fenton reaction with unincorporated iron ions that adventitiously associate with DNA, serves as a precursor to hydroxyl radicals that can rapidly interact with nucleotide bases and sugar moieties, blocking polymerase progression and causing single or double strand breaks, respectively (Imlay 2013). Peroxynitrite (ONOO-) and nitrite ions (NO2-) can also cause DNA damage but are less reactive than hydroxyl radicals (Fang 2004). Rapid repair of DNA damaged in this way is essential to maintain proper cellular function. DNA glycosylases, exonucleases, endonucleases, and polymerases are normally expressed to facilitate DNA damage repair but may be upregulated during times of increased oxidative stress (Fang 2004). If DNA excision-repair systems are not able to keep up with the amount of damage, post-replication and recombination repair mechanisms are induced (Villani and Tanguy Le Gac, 2014). In post-replication repair, enzymes excise a stretch of damaged or newly synthesized DNA and a new strand is synthesized complementary to the old, undamaged strand. In recombination repair, double strand breaks or areas where both strands are damaged are excised by recombination enzymes (most notably RecA) that cut both strands of the damaged DNA and replace it with the same sequence from a sister molecule (Villani and Tanguy Le Gac, 2014). Expression of RecA also controls expression of the SOS system, which suspends cell separation until normal DNA replication can resume (Imlay 2013). These DNA repair systems involve a plethora of genes that are upregulated as needed and then downregulated as the cell recovers and can resume normal function. Depending upon the type of repair systems utilized and the extent of the DNA damage, it may be possible to gain a better understanding of the

specific mechanisms by which ROS and RNS from plasma generated by SDBD inactivate bacterial cells.

Genetic responses to oxidative stress can be varied depending upon the specific reactive species involved and the type and extent of macromolecule damage. However, activation of two transcription factors as a result of oxidative stress is of particular importance in *Escherichia coli* and *Salmonella enterica* (and several other gram-negative bacteria): OxyR and SoxRS (Imlay 2013; Farr and Kogoma, 1991). OxyR and SoxRS are expressed at a basal level under normal cell function but are activated when endogenous ROS or RNS concentrations rise above the normal level. Hydrogen peroxide rapidly reacts with an active site cysteine residue of OxyR, activating this transcription regulator that actively promotes a 10-fold or higher increase in transcription of a dozen or more operons and over 30 genes around the chromosome (Imlay, 2013). Many of the genes that are thus upregulated are catalases and peroxidases that can alleviate the burden of high hydrogen peroxide concentrations. Gram-positive bacteria have recently been found to have a similar peroxide-responsive regulator (PerR) that is activated by hydrogen peroxide and induces expression of many homologues of the enzymes that OxyR controls (Lee and Helmann, 2006; Imlay 2013). SoxRS, in contrast, is a homodimeric transcription regulator that has one Fe-S sensory cluster for each subunit that is oxidized by redox-cycling compounds such as phenazines and quinones, activating the regulon (Imlay 2013). Once activated, SoxRS also promotes increased expression of many genes from all over the chromosome. The SoxRS system is thought to have arisen due to the ability of some plants and other bacteria to induce increased intracellular superoxide production by excretion of phenaxines and quinones that are transported directly or

passively into target cells as a means of causing oxidative stress and potentially cell death (Imlay 2013). Therefore, in Gram-negative bacterial cells treated with SDBD cold plasma, the OxyR system is expected to be activated while the SoxRS system is not. Additionally, OxyR does not regulate any DNA repair related enzymes, its main function being to increase expression of proteins that alleviate the burden of hydrogen peroxide in the cell, possibly because the DNA repair mechanisms and SOS system need to continue even after the oxidative stress is no longer present. Therefore, it is expected that in bacterial cells challenged with reactive species from plasma treatment, the OxyR system will be induced first, followed by the SOS response if the damage is able to be repaired (Imlay 2013).

Ozone (O_3) is a neutral reactive oxygen species that is relatively long-lived, is a well-known and powerful antimicrobial agent produced in high amounts by dielectric barrier discharge in air (Khadre *et al.,* 2001; Sakiyama *et al.,* 2012). In fact, ozone generated by dielectric barrier discharge has been used for several decades for efficient industrial decontamination of water (Mizuno, 2007). Although much is known about the stability, chemical properties, and reactivity of ozone, the specific mechanisms that cause bacterial inactivation are not well characterized. Conflicting reports have been published about the importance of the role of ozone in bacterial inactivation by dielectric barrier discharge, ranging from having no effect (Gallagher et al., 2007; Gustol *et al.,* 2007) to being the major contributor to bacterial inactivation (Sakiyama *et al.,* 2012). It is likely that ozone itself is not a major contributor to bacterial inactivation but serves as a precursor to other, more reactive species (such as hydrogen peroxide, superoxide, and hydroxyl radical) when it rapidly interacts with free water on the surface of bacterial cells

(Sakiyama et al., 2012). Especially in indirect SDBD plasma treatments, the neutral and long-lived nature of ozone may allow it to travel further distances from SDBD actuators and facilitates the generation of more reactive species at the cell surface that can diffuse through the cell membrane and cause damage to vital macromolecules.

Elucidation of molecular mechanisms of bacterial inactivation by SDBD cold plasma

Almost all reports of cold plasma inactivation of cells have focused on mechanical characteristics and surface structure damage (Mai-Prochnow *et al.,* 2014). However, observing dead cells may not necessarily reveal the means of death. For example, cell lysis may be observed after cell death but membrane damage might not have played any role in inactivation (Gaunt et al., 2006). A critical look at the genetic response of cells treated with cold plasma could shed light on the specific cellular pathways and mechanisms involved in bacterial inactivation. Evaluation of genetic responses of bacterial cells to cold plasma treatment could help identify whether cell structure damage, protein damage, DNA damage, or activation of cell death related pathways are the dominant means of bacterial inactivation. Knowledge gained from such a study would help guide future development of cold plasma generation devices and help delineate the optimal cold plasma generation parameters that ensure maximal bacterial inactivation with minimal effects on background substrates. Evaluating gene expression through transcriptional changes in cells treated with cold plasma would be the ideal method of identifying the molecular mechanisms involved in bacterial inactivation. DNA microarrays and RNA-Seq are the main transcriptome analysis methods that provide the

most complete evaluation of gene expression changes resulting from a given stimulus or treatment.

DNA microarray. A DNA microarray is collection of unique oligonucleotide probe clusters spotted onto a glass slide. Tens of thousands of oligonucleotide clusters, each composed of a single, unique DNA sequence, can be covalently bound in spots to a single slide in a known arrangement. Each oligonucleotide probe sequence is designed to be complementary to a single gene. Hybridization of fluorescently labeled cDNA from one or both of two samples to a specific probe reveals that expression of that gene occurs at the time of sample mRNA isolation. Therefore, gene expression changes of a given sample can be evaluated across tens of thousands of genes at a single point in time. Microarray analysis is a powerful methodological approach that has had a major impact on advancement of molecular biology in recent years (Hoheisel, 2006). However, DNA microarrays can be limited by a lack of knowledge of specific gene expression since identification of gene expression requires a specific probe for that gene. Additionally, background noise can complicate data analysis and careful normalization is necessary to obtain quality data. While DNA microarrays can still provide extensive data for global evaluation of bacterial gene expression, they are continually becoming less common due to the advantages of next-generation sequencing based techniques.

RNA-Seq. RNA-Seq (RNA sequencing) is a powerful next-generation sequencing based technique being used with increasing frequency for both mapping and quantifying of transcriptomes (Wang *et al.,* 2009). Briefly, total mRNA from an organism is converted to cDNA and sequenced, and then resulting sequence reads are aligned to a reference genome, allowing the construction of a genome-scale transcription map that

contains the transcriptional structure as well as the level of expression for each gene. Compared to microarray analysis and a few other transcriptomic techniques, RNA-Seq usually allows higher throughput, has single base resolution, has low background noise requiring little or no normalization, can simultaneously map transcribed regions and gene expression, and has a higher dynamic range for quantifying gene expression levels. Additionally, RNA-Seq requires less starting RNA and the cost is relatively low (Wang *et al.,* 2009). RNA-Seq has also been shown to be highly accurate for expression level quantification compared to quantitative real-time PCR (qPCR) (Nagalakshmi *et al.,* 2008) and is highly reproducible (Cloonan *et al.,* 2008).

Evaluation of bacterial transcriptional changes induced by cold plasma

Evaluation of bacterial inactivation by cold plasma at the transcriptome level is in its infancy. Currently, a single study looking at transcriptional changes in a prokaryotic species (*Bacillus cereus*) resulting from nitrogen gas plasma inactivation has been published (Mols *et al.,* 2013). Transcriptional changes observed in this study were minimal, possibly a result of using the microarray approach and using only nitrogen gas. Conversely, a targeted gene expression study evaluating the effects of human cells to cold plasma treatment found noticeable transcriptional changes (Arndt *et al.,* 2013). A more complete evaluation of the transcriptome profile of pathogenic foodborne bacteria using RNA-Seq would allow a clearer understanding of the means of plasma-induced cell inactivation. Because of the reactive species and charged particles produced by cold plasma treatments, the cellular processes involving protein degradation, DNA repair, and lipid modification are of special interest. The knowledge gained from such a study would

help direct future development of cold plasma actuator designs and treatment conditions to optimize pathogen inactivation while maintaining the structural, aesthetic, and nutritional properties of commonly contaminated types of fresh produce.

LITERATURE CITED

Abadias, M., T.P. Cañamas, A. Asensio, M. Angueram, and I. Viñas. (2006). Microbial quality of commercial 'Golden Delicious' apples throughout production and shelf-life in Lleida (Catalonia, Spain). *International Journal of Food Microbiology*. 108:404-409.

Akira, M. (2007). Industrial applications of atmospheric non-thermal plasma in environmental remediation. *Plasma Physics and Controlled Fusion, 49*(5A), A1.

Arndt, S., P. Unger, E. Wacker, T. Shimizu, J. Heinlin, Y.F. Li, and S. Karrer. (2013). Cold Atmospheric Plasma (CAP) Changes Gene Expression of Key Molecules of the Wound Healing Machinery and Improves Wound Healing *In Vitro* and *In Vivo*. *PLoS ONE. 8*(11):e79325.

Aruscavage, D., K. Lee, S. Miller, and J.T. Lejeune. (2006). Interactions affecting the proliferation and control of human pathogens on edible plants. *Journal of Food Science.* 71:R89-R99.

Bae, D., K.S. Seo, T. Zhang, and C. Wang. (2013). Characterization of a potential *Listeria monocytogenes* virulence factor associated with attachment to fresh produce. *Applied and Environmental Microbiology.* 79(22):6855-6861.

Baier, M., J. Foerster, U. Schnabel, D. Knorr, J. Ehlbeck, W.B. Herppich, and O. Schlüter. (2013). Direct non-thermal plasma treatment for the sanitation of fresh corn salad leaves: Evaluation of physical and physiological effects and antimicrobial efficacy. *Postharvest Biology and Technology.* 84(0):81-87.

Barak, J.D., and B.K. Schroeder. (2012). Interrelationships of Food Safety and Plant Pathology: The Life Cycle of Human Pathogens on Plants. *Annual Review of Phytopathology.* 50(1):241-266.

Barth, M., T. Hankinson, H. Zhuang, and F. Breidt. (2010). Microbiological Spoilage of Fruits and Vegetables. In W. H. Sperber & M. P. Doyle (Eds.), *Compendium of the Microbiological Spoilage of Foods and Beverages* (pp. 135-183): Springer New York.

Beggs, C. B. (2002). A quantitative method for evaluating the photoreactivation of ultraviolet damaged microorganisms. *Photochem Photobiol Sci, 1*(6), 431-437.

Bettelheim, K.A. (2007). The Non-O157 Shiga-Toxigenic (Verocytotoxigenic) Escherichia coli; Under-Rated Pathogens. *Critical Reviews in Microbiology/ 33*(1):67-87.

Beuchat, L R., B.A. Adler, and M.M. Lang. (2004). Efficacy of chlorine and a peroxy-acetic acid sanitizer in killing Listeria monocytogenes on iceberg and romaine lettuce using simulated commercial processing conditions. *Journal of Food Protection*. 67:1238-1242.

Brandl, M., and G.W. Sundin. (2013). Focus on food safety: Human pathogens on plants. *Phytopathology*. 103:304-305.

Brooks, J.T., E.G. Sowers, J.G. Wells, K.D. Greene, P.M. Griffin, R.M. Hoekstra, and N.A. Strockbine. (2005). Non-O157 Shiga Toxin–Producing Escherichia coli Infections in the United States, 1983–2002. *Journal of Infectious Diseases.* 192(8):1422-1429.

Boudam, M., M. Moisan, B. Saoudi, C. Popovici, N. Gherardi, and F. Massines. (2006). Bacterial spore inactivation by atmospheric-pressure plasmas in the presence or absence of UV photons as obtained with the same gas mixture. *J Phys D Appl Phys.* 39:3494.

Buettner, G., B. Wagner, and V.J. Rodgers. (2013). Quantitative Redox Biology: An Approach to Understand the Role of Reactive Species in Defining the Cellular Redox Environment. *Cell Biochemistry and Biophysics.* 67(2):477-483.

Campanha, M.T., E.M. Mamizuka, and A.M. Carmona-Ribeiro. (1999). Interactions between cationic liposomes and bacteria: the physical-chemistry of the bactericidal action. *Journal of Lipid Research.* 40(8):1495-1500.

Centers for Disease Control and Prevention. (2006). Update on multi-state outbreak of *E. coli* O157:H7 infections from fresh spinach, October 6, 2006. Available at: http://www.cdc.gov/ecoli/2006/september/updates/100606.htm

Centers for Disease Control and Prevention. (2011). Food safety facts. Available at: http://www.cdc.gov/foodsafety/facts.html#what

Centers for Disease Control and Prevention. (2011b). Investigation update: Outbreak of Shiga toxin-producing *E. coli* O104 (STEC O104:H4) infections associated with travel to Germany. Available at: http://www.cdc.gov/ecoli/2011/ecoliO104/

Centers for Disease Control and Prevention. (2012). Multistate outbreak of listeriosis linked to whole cantaloupes from Jensen Farms, Colorado. Available at: http://www.cdc.gov/listeria/outbreaks/cantaloupes-jensen-farms/082712/index.html

Centers for Disease Control and Prevention (CDC). (2012). National Shiga toxin-producing *Escherichia coli* (STEC) Surveillance Overview. Atlanta, Georgia: US Department of Health and Human Services.

Centers for Disease Control and Prevention. (2012b). Multistate outbreak of Shiga toxin-producing *Escherichia coli* O26 infections linked to raw clover sprouts at Jimmy John's Restaurants (Final Update). Available at: http://www.cdc.gov/ecoli/2012/O26-02-12/

Centers for Disease Control and Prevention. (2013). Multistate outbreak of Shiga toxin-producing *Escherichia coli* O157:H7 infections linked to ready-to-eat salads (final update). Available at: http://www.cdc.gov/ecoli/2013/O157H7-11-13/

Cloonan, N., A.R.R. Forrest, G. Kolle, B.B.A. Gardiner, G.J. Faulkner, M.K. Brown, and S.M. Grimmond. (2008). Stem cell transcriptome profiling via massive-scale mRNA sequencing. *Nature Methods.* 5(7):613-619.

Cole, D., P.M. Griffin, K.E. Fullerton, T. Ayers, K. Smith, L.A. Ingram, and R.M. Hoekstra. (2014). Attributing sporadic and outbreak-associated infections to sources: blending epidemiological data. *Epidemiology & Infection.* 142(02):295-302.

Cooper, T.F., D.E. Rozen, and R.E. Lenski. (2003). Parallel changes in gene expression after 20,000 generations of evolution in Escherichia coli. *Proceedings of the National Academy of Sciences.* 100(3):1072-1077.

Crane, B.R., J. Sudhamsu, J., and B.A. Patel. (2010). Bacterial nitric oxide synthases. *Annu Rev Biochem.* 79:445-470.

Critzer, F., K. Kelly-Wintenberg, S. South, and D. Golden. (2007). Atmospheric plasma inactivation of foodborne pathogens on fresh produce surfaces. *J Food Protect.* 70(10):2290.

Davidson, P.M., J.N. Sofos, and A.L. Branen. (2005). *Antimicrobials in food*: CRC press.

De Giusti, M., C. Aurigemma, L. Marinelli, L., Tu, D. De Medici, and S. Di Pasquale. (2010). The evaluation of the microbial safety of fresh ready-to-eat vegetables produced by different technologies in Italy. *Journal of Applied Microbiology*. 109: 996-1006.

Dobrynin, D., G. Fridman, G. Friedman, and A. Fridman. (2009). Physical and biological mechanisms of direct plasma interaction with living tissue. *New J Phys.* 11:115020.

Enloe, C.L., T.E. McLaghlin, R.D. Vandyken, and K.D. Kachner. (2004). Mecahnisms and Response of a Single Dielectric Barrier Plasma Actuator: Plasma Morphology. *AIAA paper.* 42(3):589-594.

Erickson, M.C. (2012). Internalization of fresh produce by foodborne pathogens. *Annual Review of Food Science and Technology*. 3:283-319.

Erkmen, O. (2010). Antimicrobial Effects of Hypochlorite on Escherichia coli in Water and Selected Vegetables. *Foodborne Pathogens and Disease, 7*(8), 953-958.

Fang, F. C. (2004). Antimicrobial reactive oxygen and nitrogen species: concepts and controversies. *Nat Rev Microbiol, 2*(10), 820-832.

Farr, S.B., and T. Kogoma. (1991). Oxidative stress responses in Escherichia coli and Salmonella typhimurium. *Microbiological Reviews.* 55(4):561-585.

Feichtinger, J., A. Schulz, M. Walker, and U. Schumacher. (2003). Sterilization with low-pressure microwave plasmas. *Surf Coat Technol.* 174:564–569.

Fernández, A., E. Noriega, and A. Thompson. (2013). Inactivation of *Salmonella enterica* serovar Typhimurium on fresh produce by cold atmospheric gas plasma technology. *Food Microbiology*. 33(1):24-29.

Feng, H., R. Wang, P. Sun, H. Wu, Q. Liu, J. Fang, and J. Zhang. (2010). A study of eukaryotic response mechanisms to atmospheric pressure cold plasma by using *Saccharomyces cerevisiae* single gene mutants. *Applied Physics Letters.* 97(13):131501-131501-3.

Foley, D., M. Euper, F. Caporaso, and A. Prakash. (2004). Irradiation and chlorination effectively reduces *Escherichia coli* 0157:H7 inoculated on cilantro (*Coriandrum sativum*) without negatively affecting quality. *Journal of Food Protection*. 67:2092-2098.

Food and Drug Administration. (2008). Irradiation in the production, processing and handling of foods. 21 CFR 179.26. Code of Federal Regulations. Available at: http://www.fda.gov/Food/FoodIngredientsPackaging/IrradiatedfoodPackaging/ucm074734.htm

Foong-Cunningham, S., and E.L.C. Verkaar. (2012). Microbial decontamination of fresh produce. In Demirci, A., and M.O. Ngadi (Eds.) Microbial decontamination in the food industry: Novel methods and applications. Woodhead Publishing, Cambridge, UK.

Fridman, G., A.D. Brooks, M. Balasubramanian, A. Fridman, A. Gutsol, V.N. Vasilets, and G. Friedman. (2007). Comparison of Direct and Indirect Effects of Non-Thermal Atmospheric-Pressure Plasma on Bacteria. *Plasma Processes and Polymers.* 4(4):370-375.

Gaunt, L.F., C.B. Beggs, and G.E. Georghiou. (2006). Bactericidal Action of the Reactive Species Produced by Gas-Discharge Nonthermal Plasma at Atmospheric Pressure: A Review. *Plasma Science, IEEE Transactions on.* 34(4):1257-1269.

Gallagher, M. J., N. Vaze, S. Gangoli, V.N. Vasilets, A.F. Gutsol, T.N. Milovanova, and A.A. Fridman. (2007). Rapid Inactivation of Airborne Bacteria Using Atmospheric Pressure Dielectric Barrier Grating Discharge. *Plasma Science, IEEE Transactions on.* 35(5):1501-1510.

Giannoukos, G., D. Ciulla, K. Huang, B. Haas, J. Izard, J. Levin, and A. Gnirke. (2012). Efficient and robust RNA-seq process for cultured bacteria and complex community transcriptomes. *Genome Biology.* 13(3):r23.

Gibalov, V.I., and G.J. Pietsch. (2000). The development of dielectric barrier discharges in gas gaps and on surfaces. *J.Phys.D:Appl. Phys.* 33:2618-2636.

Goodburn, C., and C.A. Wallace. (2013). The microbiological efficacy of decontamination methodologies for fresh produce: A review. *Food Control. 32*(2):418-427.

Grune, T., Reinheckel, T., & Davies, K. J. (1997). Degradation of oxidized proteins in mammalian cells. *Faseb J, 11*(7), 526-534.

Gutsol, A., Vaze, N. D., Arjunan, K. P., Gallagher, M. J., Jr., Yang, Y., Zhu, J., & Fridman, A. (2008). Plasma for Air and Water Sterilization. *In* S. Güçeri, A. Fridman, K. Gibson & C. Haas (Eds.), Plasma Assisted Decontamination of Biological and Chemical Agents (pp. 21-39): Springer Netherlands.

Guzel-Seydim, Z.B., A.K. Greene, and A.C. Seydim. (2004). Use of ozone in the food industry. *Lebensmittel-Wissenschaft und-Technologie*. 37(4):453–460.

Harrington, C.A., C. Rosenow, and J. Retief. (2000). Monitoring gene expression using DNA microarrays. *Current Opinion in Microbiology.* 3(3):285-291.

Havelaar, A.H., A. Cawthorne, F. Angulo, D. Bellinger, T. Corrigan, A. Cravioto, and T. Kuchenmüller. (2013). WHO Initiative to Estimate the Global Burden of Foodborne Diseases. *The Lancet.* 381, S59.

Hirano, S.S., and C.D. Upper. (1983). Ecology and epidemiology of foliar bacterial plant pathogens. *Annu. Rev. Phytopathol.* 21:243–70.

Hoffmann, C., C. Berganza, and J. Zhang. (2013). Cold Atmospheric Plasma: methods of production and application in dentistry and oncology. *Medical Gas Research.* 3(1):21.

Imlay, J.A. (2003). Pathways of oxidative damage. *Annu Rev Microbiol, 57*, 395-418.

Jones, T.F., E. Scallan, and F.J. Angulo. (2007). FoodNet: Overview of a decade of achievement. Foodborne Pathogens and Disease. 4(1): 60-66.

Junquiera-Gonçalves, M.P., M.J. Galotto, X. Valenzuela, C.M. Dinten, P. Aguirre, and J. Miltz. (2010). Perception and view of consumers on food irradiation and the Radura symbol. *Radiation Physics and Chemistry*. 80:119-122.

Karmali, M.A. (1989). Infection by Verocytotoxin-producing *Escherichia coli*. *Clin. Microbiol. Rev.* 2:15-38.

Kelly-Wintenberg, K., A. Hodge, T. Montie, L. Deleanu, D. Sherman, J.R. Roth, P. Tsai, and L. Wadsworth. (1999). Use of a one atmosphere uniform glow discharge plasma to kill a broad spectrum of micro- organisms. *J Vacuum Sci Technol*.17:1539.

Khadre, M., Yousef, A., & Kim, J. (2001). Microbiological aspects of ozone applications in food: a review. *Journal of food science-Chicago-, 66*(9), 1242-1253.

Kieft, I. E., van Berkel, J. J. B. N., Kieft, E. R., & Stoffels, E. (2005). Radicals of Plasma Needle Detected with Fluorescent Probe *Plasma Processes and Polymers* (pp. 293-308): Wiley-VCH Verlag GmbH & Co. KGaA.

Kim, J.E., D. Lee, and S.C. Min. (2014). Microbial decontamination of red pepper powder by cold plasma. *Food Microbiology.* 38(0):128-136.

Klämpfl, T.G., G. Isbary, T. Shimizu, Y.F. Li, J.L. Zimmermann, W. Stolz, and J.U. Schmidt. (2012). Cold Atmospheric Air Plasma Sterilization against Spores and Other Microorganisms of Clinical Interest. *Applied and Environmental Microbiology.* 78(15):5077-5082.

Kogelschatz, U., B. Eliasson, and W. Egli. (1999). From ozone generators to flat television screens: history and future potential of dielectric-barrier discharges *Pure and Applied Chemistry*. 71:1819.

Kovačević, M., J. Burazin, H. Pavlović, M. Kopjar, and V. Piližota. (2013). Prevalence and level of *Listeria monocytogenes* and other *Listeria sp.* in ready-to-eat minimally processed and refrigerated vegetables. *World Journal of Microbiology and Biotechnology.* 29(4):707-712.

Kuzmichev, A.I., I.A. Soloshenko, V.V. Tsiolko, V. Kryzhanovsky, V.Y. Bazhenov, I.L. Mikhno, and V.A. Khomich. (2001). Feature of sterilization by different type of atmospheric pressure discharges. In Proc. Int. Symp. High Pressure Low Temperature Plasma Chemistry, Greifswald, Germany, pp. 402–406.

Laroussi, M. (1996). Sterilization of contaminated matter with an atmospheric pressure plasma. *Plasma Science, IEEE Transactions on, 24*(3), 1188-1191.

Laroussi, M., D. Mendis, and M. Rosenberg. (2003). Plasma interaction with microbes. *New J Phys* 5:41

Lee, S.,Y., M. Costello, and D.H. Kang. (2004). Efficacy of chlorine dioxide gas as a sanitizer of lettuce leaves. *Journal of Food Protection*. 67(7):1371-1376.

Lee, K., K. Paek, W.T. Ju, and Y. Lee. (2006). Sterilization of bacteria, yeast, and bacterial endospores by atmospheric-pressure cold plasma using helium and oxygen. *J Microbiol.* 44(3):269–275.

Lee, J.-W., & Helmann, J. D. (2006). The PerR transcription factor senses H2O2 by metal-catalysed histidine oxidation. *Nature, 440*(7082), 363-367.

Leff, J.W., and N. Fierer. (2013). Bacterial Communities Associated with the Surfaces of Fresh Fruits and Vegetables. *PLoS ONE.* 8(3): e59310.

Li, H., and R. Durbin. (2010). Fast and accurate long-read alignment with Burrows-Wheeler transform. *Bioinformatics*. 26:589-595.

Li, Y.H., Y. Wu, H.M. Song, H. Liang and M. Jia . (2011). Plasma Flow control. *In* M. Mulder (Ed.). Aeronautics and Astronautics. InTech publishing, Rijeka, Croatia.

Lu, H., Patil, S., Keener, K. M., Cullen, P. J., & Bourke, P. (2014). Bacterial inactivation by high-voltage atmospheric cold plasma: influence of process parameters and effects on cell leakage and DNA. *Journal of Applied Microbiology, 116*(4), 784-794.

Luna-Gierke, R.E., P.M. Griffin, L.H. Gould, K. Herman, C.A. Bopp, N. Strockbine, and R.K. Mody. (2014). Outbreaks of non-O157 Shiga toxin-producing Escherichia coli infection: USA. *Epidemiology & Infection, FirstView*, 1-11.

Ma, Y., Ha, C. S., Hwang, S. W., Lee, H. J., Kim, G. C., Lee, K.-W., & Song, K. (2014). Non-Thermal Atmospheric Pressure Plasma Preferentially Induces Apoptosis in p53-Mutated Cancer Cells by Activating ROS Stress-Response Pathways. *PLoS ONE, 9*(4), e91947.

Mai-Prochnow, A., A.B. Murphy, K.M. McLean, M.G. Kong, and K. Ostrikov. (2014). Atmospheric pressure plasmas: Infection control and bacterial responses. *International Journal of Antimicrobial Agents*. In press. doi: http://dx.doi.org/10.1016/j.ijantimicag.2014.01.025

Matthews, K.R. (2009). Leafy vegetables. *In* Sapers, G.M., E. Solomon, and K.R. Matthews (Eds.). The produce contamination problem: Causes and solutions. Elsevier, Waltham, MA.

Misra, N.N., B.K. Tiwari, K.S.M.S. Raghavarao, and P.J. Cullen. (2011). Nonthermal plasma inactivation of food-borne pathogens. *Food Engineering Reviews.* 3(3-4):159-170.

Misra, N.N., S.K. Pankaj, T. Walsh, F. O'Regan, P. Bourke, P.J. Cullen. (2014). In-package nonthermal plasma degradation of pesticides on fresh produce. *Journal of Hazardous Materials.* 271(0):33-40.

Misra, N.N., S. Patil, T. Moiseev, P. Bourke, J.P. Mosnier, K.M. Keener, and P.J. Cullen. (2014). In-package atmospheric pressure cold plasma treatment of strawberries. *Journal of Food Engineering.* 125(0):131-138.

Misra, N. N., Keener, K. M., Bourke, P., Mosnier, J. P., & Cullen, P. J. (2014b). In-package atmospheric pressure cold plasma treatment of cherry tomatoes. *J Biosci Bioeng, 118*(2), 177-182.

Mendis, D., M. Rosenberg, and F. Azam. (2002). A note on the possible electrostatic disruption of bacteria. *Plasma Sci IEEE Trans.* 28(4):1304–1306.

Mogul, R., A.A. Bol'shakov, S.L. Chan, R.M. Stevens, B.N. Khare, M. Meyyappan, and J.D. Trent. (2003). Impact of low-temperature plasmas on *Deinococcus radiodurans* and biomolecules. *Biotechnol Prog.* 19(3):776–783.

Mols, M., H. Mastwijk, M. Nierop Groot, and T. Abee. (2013). Physiological and transcriptional response of *Bacillus cereus* treated with low-temperature nitrogen gas plasma. *Journal of Applied Microbiology.* 115(3):689-702.

Montie, T.C., K. Kelly-Wintenberg, and J.R. Roth. (2002). An overview of research using the one atmosphere uniform glow discharge plasma (OAUGDP) for sterilization of surfaces and materials. *Plasma Sci IEEE Trans.* 28(1):41–50.

Nagalakshmi, U., Z. Wang, K. Waern, C. Shou, D. Raha, M. Gerstein, and M. Snyder. (2008). The transcriptional landscape of the yeast genome defined by RNA sequencing. *Science.* 320(5881):1344-1349.

Nei, D., Choi, J.-W., Bari, M. L., Kawasaki, S., Kawamoto, S., & Inatsu, Y. (2009). Efficacy of Chlorine and Acidified Sodium Chlorite on Microbial Population and Quality Changes of Spinach Leaves. *Foodborne Pathogens and Disease, 6*(5), 541-546.

Nelson, C.L., and T.J. Berger. (1989) Inactivation of microorganisms by oxygen gas plasma. *Current Microbiology.* 18(4):275–276.

Niemira, B.A. (2012). Cold plasma reduction of *Salmonella* and *Escherichia coli* O157:H7 on almonds using ambient pressure gases. *Journal of Food Science.* 77(3):M171-M175

Niemira, B.A. (2012). Cold Plasma Decontamination of Foods. *Annual Review of Food Science and Technology.* 3(1):125-142.

Niemira, B. A., Boyd, G., & Sites, J. (2014). Cold Plasma Rapid Decontamination of Food Contact Surfaces Contaminated with Salmonella Biofilms. *Journal of Food Science, 79*(5), M917-M922.

Ölmez, H. (2010). Effect of different sanitizing methods and incubation time and temperature on inactivation of *Escherichia coli* on lettuce. *Journal of Food Safety.* 30:288-299.

Pai, K. K., Singarapu, K., Jacob, J. D., & Madihally, S. V. (2015). Dose Dependent Selectivity and Response of Different Types of Mammalian Cells to Surface Dielectric Barrier Discharge (SDBD) Plasma. *Plasma Processes and Polymers, 12*(7), 666-677.

Pankaj, S.K., C. Bueno-Ferrer, M.N. Misra, V. Milosavljević, C.P. O'Donnell, P. Bourke, and P.J. Cullen. (2014). Applications of cold plasma technology in food packaging. *Trends in Food Science & Technology.* 35(1):5-17.

Perry, J.J., and A.E. Yousef. (2011). Decontamination of raw foods using ozone-based sanitization techniques. *Annual Review of Food Science and Technology*. 2:281-298.

Puac, Z. L. Petrovic, G. Malovic, A. Dordevic, S. Zivkovic, Z. Giba, & D. Grubisic. (2006). Measurements of voltage–current characteristics of a plasma needle and its effect on plant cells. *J. Phys. D, Appl. Phys.*, 39(16), 3514–3519.

Ramaswamy, V., V.M. Cresence, J.S. Rejitha, M.U. Lekshmi, K.S. Dharsana, S.P. Prasad, and H.M. Vijila. (2007). Listeria – review of epidemiology and pathogenesis. *J Microbiol Immunol Infect.* 40(1):4–13.

Roberts, P.B. (2014). Food irradiation is safe: Half a century of studies. *Radiation Physics and Chemistry*.

Roth, S., J. Feichtinger, and C. Hertel. (2010). Characterization of *Bacillus subtilis* spore inactivation in low pressure, low temperature gas plasma sterilization processes. *J Appl Microbiol.* 108(2):521–531.

Ryan, B., Lo Faro, M. L., Whiteman, M., & Winyard, P. (2015). Reactive Oxygen Species. In M. Parnham (Ed.), *Encyclopedia of Inflammatory Diseases* (pp. 1-6): Springer Basel.

Sakiyama, Y., David, B. G., Hung-Wen, C., Tetsuji, S., & Gregor, E. M. (2012). Plasma chemistry model of surface microdischarge in humid air and dynamics of reactive neutral species. *Journal of Physics D: Applied Physics*, *45*(42), 425201.

Shen, C., Y. Luo, X. Nan, G. Bauchan, B. Zhou, Q. Wang, *et al.* (2012). Enhanced inactivation of *Salmonella* and *Pseudonomas* biofilms on stainless steel by use of T-128, a fresh produce washing aid in chlorinated wash solution. *American Society of Microbiology*. 78(19):6789-98.

Sivapalasingam, S., C.R. Friedman, L. Cohen, and R.V. Tauxe. (2004). Fresh produce: A growing cause of outbreaks of foodborne illness in the united states, 1973 through 1997. *Journal of Food Protection.* 67(10):2342-2353.

Solomon, E.B., M. Brandl, and R.E. Mandrell. (2006). Behavior of human pathogens on produce. In: Matthews, K.R., (Ed.) Emerging Issues in Food Safety: Microbiology of Fresh Produce. Washington, D.C., ASM Press. p. 55-83.

Stoffels, E., Sladek, R. E. J., Kieft, I. E., Kersten, H., & Wiese, R. (2004). Power outflux from the plasma: an important parameter in surface processing. *Plasma Physics and Controlled Fusion, 46*(12B), B167. Dec. 2004.

Stopforth, J. D., Mai, T., Kottapalli, B., & Samadpour, M. (2008). Effect of Acidified Sodium Chlorite, Chlorine, and Acidic Electrolyzed Water on Escherichia coliO157:H7, Salmonella, and Listeria monocytogenesInoculated onto Leafy Greens. *Journal of Food Protection, 71*(3), 625-628.

Sysolyatina, E., Mukhachev, A., Yurova, M., Grushin, M., Karalnik, V., Petryakov, A., Akishev, Y. (2014). Role of the Charged Particles in Bacteria Inactivation by Plasma of a Positive and Negative Corona in Ambient Air. *Plasma Processes and Polymers, 11*(4), 315-334.

Terrier, O., B. Essere, M. Yver, M. Barthelemy, M. Bouscambert-Duchamp, P. Kurtz, D. VanMechelen, F. Morfin, G. Billaud, O. Ferraris, B. Lina, M. Rosa-Calatrava, and V. Moules. (2009). Cold oxygen plasma technology efficiency against different airborne respiratory viruses. *J Clin Virol.* 45(2):119–124.

Thorns, C.J. (2000). Bacterial food-borne zoonoses. *Rev Sci Tech.* 19(1):226-239.

Torres, M.A., J.D.G. Jones, and J.L. Dangl. (2006). Reactive oxygen species signaling in response to pathogens. *Plant Physiology.* 141(2):373-378.

Villani, G., & Tanguy Le Gac, N. (2014). DNA Repair Polymerases. In E. Bell (Ed.), *Molecular Life Sciences* (pp. 1-13): Springer New York.

Vleugels, M., G. Shama, X.T. Deng, E. Greenacre, T. Brocklehurst, and M.G. Kong. (2005). Atmospheric plasma inactivation of biofilm- forming bacteria for food safety control. *Plasma Sci IEEE Trans.* 33(2):824–828.

von Woedtke, T., H.R. Metelmann, and K.D. Weltmann. (2014). Clinical plasma medicine: State and perspectives of in vivo application of cold atmospheric plasma. *Contributions to Plasma Physics.* 54(2):104-117.

Wang, Z., M. Gerstein, and M. Snyder. (2009). RNA-Seq: a revolutionary tool for transcriptomics. *Nat Rev Genet.* 10(1):57-63.

Ward, T.J. L. Gorski, M.K. Borucki, R.E. Mandrell, J. Hutchins, and K. Pupedis. (2004). Intraspecific Phylogeny and Lineage Group Identification Based on the prfA Virulence Gene Cluster of Listeria monocytogenes. *Journal of Bacteriology.* 186(15):4994–5002.

Wasserman, E., & Felmy, A. R. (1998). Computation of the Electrical Double Layer Properties of Semipermeable Membranes in Multicomponent Electrolytes. *Applied and Environmental Microbiology, 64*(6), 2295-2300.

Weiss, M., Gümbel, D., Hanschmann, E.-M., Mandelkow, R., Gelbrich, N., Zimmermann, U., Stope, M. B. (2015). Cold Atmospheric Plasma Treatment Induces Anti-Proliferative Effects in Prostate Cancer Cells by Redox and Apoptotic Signaling Pathways. *PLoS ONE, 10*(7), e0130350.

World Health Organization, Food Safety Unit. (1998). Food safety issues: Surface decontamination of fruits and vegetables eaten raw: a review. Geneva: World Health Organization. WHO/FSF/FOS/98.2.

Wu, V.C.H., and B. Kim. (2007). Effect of a simple chlorine dioxide method for controlling five foodborne pathogens, yeasts and molds on blueberries. *Food Microbiology.* 24:794-800.

Yiannas, F. (2009). Food safety culture: Creating a behavior-based safety management system. Springer, New York, NY.

Yoon, Y.H., and K.H. Ryu. (2007). Atmospheric plasma surface treatment equipment. *News Inform Chem Eng.* 25:268–271.

Zhang, X., Liu, D., Zhou, R., Song, Y., Sun, Y., Zhang, Q., & Yang, S.-z. (2014). Atmospheric cold plasma jet for plant disease treatment. *Applied Physics Letters, 104*(4), 043702.

Ziuzina, D., S. Patil, P.J. Cullen, K.M. Keener, and P. Bourke. (2014). Atmospheric cold plasma inactivation of *Escherichia coli, Salmonella enterica* serovar Typhimurium *and Listeria monocytogenes* inoculated on fresh produce. *Food Microbiology.* 42(0):109-116.

Ziuzina, D., Patil, S., Cullen, P. J., Boehm, D., & Bourke, P. (2014). Dielectric Barrier Discharge Atmospheric Cold Plasma for Inactivation of Pseudomonas aeruginosa Biofilms. *4*(1-4), 137-152.

CHAPTER III

INACTIVATION OF *SALMONELLA ENTERICA*, SHIGA TOXIN-PRODUCING *ESCHERICHIA COLI*, AND *LISTERIA MONOCYTOGENES* BY A NOVEL COLD PLASMA DESIGN

ABSTRACT

Ionized gas generated at room temperature and atmospheric pressure, or cold atmospheric plasma, is an emerging technology that offers a dry, non-thermal, rapid process with minimal damage to food products, overcoming many of the limitations of current food decontamination methods. Each of the multiple means of generating cold plasma have direct impacts on the microbial inactivation efficiency. Surface dielectric barrier discharge (SDBD), an open-air, room temperature cold plasma generation technology having low power requirements, is more flexible, portable, and scalable than other cold plasma generation methods. In this study, a novel SDBD design that induces a localized airflow was evaluated for bacterial foodborne pathogen inactivation. Particle image velocimetry (PIV) was used to evaluate induced airflow dynamics. Bacterial inactivation was evaluated on sterile glass coverslips and on the surfaces of in-shell pecans and cherry tomatoes that were spot inoculated with multiple-strain suspensions of *Salmonella enterica* (*Se*), Shiga toxin-producing *Escherichia coli* (STEC), or *Listeria monocytogenes*

(*Lm*) (10^7 CFU/sample), air dried, and treated by cold plasma for 2 and 4 min at1, 3, 5, and 7 cm. PIV data revealed that the SDBD electrode arrangement influences the induced localized airflow due to the coupling of the electric field into the neighboring fluid (air). Inactivation of bacterial cells was observed at all distances and at all treatment times but with decreasing efficiency at increasing distance and shorter treatment times. Average log CFU/mL reductions for 4 min treatments at 1cm were 3.0 for *Se*, 3.6 for STEC, and 4.0 for *Lm.* Decimal reducition times in minutes (D-values) at 1 cm were 1.3 for *Se*, 0.9 for STEC, and 1.0 for *Lm*. An approximately 1 and 2 log CFU/mL reduction was observed on pecans and cherry tomatoes at 4 and 10 min, respectively. These results confirm that the novel SDBD actuator design induces a localized airflow that propels reactive species to distant surfaces. SDBD cold plasma actuators have potential applications in food decontamination, wound healing, and medical instrument sterilization.

INTRODUCTION

Foodborne human illness caused by pathogenic microorganisms is a significant health and economic burden worldwide. *Salmonella enterica* subspecies *enterica* (*Se*), Shiga toxin-producing *Escherichia coli* (STEC), and *Listeria monocytogenes* (*Lm*) are among the most commonly isolated bacterial foodborne pathogens and cause more hospitalizations and deaths than all other known bacterial pathogens (Scallan *et al.*, 2011). Contamination of food can occur at multiple points throughout the food production, distribution, and preparation processes, necessitating effective and efficient decontamination methods prior to consumption (Aruscavage *et al.,* 2006; Abadias *et al.,* 2006). However, few effective and minimally damaging decontamination methods are

available for foods that are consumed raw or minimally processed (Goodburn and Wallace, 2013). Consumers are becoming increasingly conscious of the nutritional benefits of some minimally processed foods, especially fresh produce, and an increased consumption of these products has been documented in recent years (Barth *et al.*, 2010). Unfortunately, concomitant with increased consumption of these higher risk foods, an increased incidence of foodborne illness associated with fresh produce has also been documented (Sivapalasingam *et al.*, 2004; Painter *et al.*, 2013; CDC, 2013).

Foods that are consumed raw or minimally processed pose notable challenges for decontamination. The nutritional, structural, and aesthetic properties of such foods are important to consumers and need to be maintained. However, few of the major decontamination methods currently used for fresh produce, such as chlorine washes, chlorine dioxide treatments, ozone fumigation, and irradiation, are ideally cost effective, versatile, and efficient while maintaining the physical and nutritional traits desired by consumers (Goodburn and Wallace, 2013; Gil *et al.*, 2015). Therefore, new decontamination methodologies are continually being developed and tested (Foong-Cunningham and Verkaar, 2012; Stopforth *et al.*, 2008). Non-thermal atmospheric ionized gas, or cold plasma, has been the focus of increased research in recent years since it is a dry process that occurs at room temperature and atmospheric pressure (Niemira, 2012). Bacterial inactivation from cold plasma treatments is a result of the reactive species, charged particles, and photons that are constituents of cold plasma (Stoffels *et al.*, 2008). Much of the recent research evaluating cold plasma as a decontamination method has been in regard to different plasma generation methods and the ways in which

reactive species produced by these methods interact with microbial pathogens on contaminated surfaces (Stoffels *et al.,* 2008; Misra *et al.,* 2011; Niemira, 2012).

Surface dielectric barrier discharge (SDBD) is an open-air, low power input plasma generation method that has the potential to overcome many of the limitations of current cold plasma apparatuses. The basic SDBD apparatus is relatively simple, consisting of a power supply and two electrodes placed on either side of a dielectric barrier. One of the electrodes is covered to prevent contact with atmospheric gas while the other electrode is left uncovered. Plasma, which is formed adjacent to the uncovered electrode, consists of forms that vary from distinct streamers to diffuse discharges with low glow based on the amplitude of supplied AC voltage and the applied frequency (Gibalov and Pietsch, 2000). SDBD was developed initially for applications in the aerospace industry, in which it is used to induce or modify airflow over the surfaces of aircraft wings, improving the aerodynamic characteristics and propulsion efficiency of aircraft (Li *et al.,* 2011). The self-induced localized airflow of SDBD is therefore hypothesized to carry with it the generated reactive species and charged particles for a short distance until they revert back to their normal, stable state. The electrodes can be arranged so as to increase the amount of induced airflow and therefore maximize the distance that reactive species can travel before reverting back to their unreactive state. Accordingly, SDBD has the potential to be versatile and particularly attractive for decontamination applications. This form of cold plasma generation requires no enclosures or supplied gas flow and has a broad treatment area, making it more flexible and scalable than other cold plasma-based decontamination apparatuses. Additionally, a minimal amount of supplied power is necessary: just enough to ignite the plasma over the

entire surface of the desired electrode arrangement (6.75 W for the actuators used in this study).

SDBD actuator design and treatment parameters have direct effects on the pathogen inactivation effectiveness of cold plasma generated by SDBD. Based on previous studies with other cold plasma generation apparatuses, treatment duration, treatment distance, initial cell concentration, and treated surface structure are the variables that are likely to alter the effectiveness of SDBD devices and these factors must be thoroughly investigated and defined (Misra *et al.*, 2011; Niemira, 2012). The purpose of this study was to evaluate the effects of treatment time and treatment distance on inactivation efficiency of SDBD plasma actuators on *Se,* STEC, and *Lm* and to evaluate the induced airflow dynamics of the SDBD design for decontamination applications. Two designs for electrode arrangement in relation to the dielectric barrier used for SDBD actuators, a key consideration for optimal airflow induction, were compared. Additionally, the effects of different contaminated surfaces were evaluated by comparing bacterial inactivation on artificially contaminated sterile glass, cherry tomatoes, and in-shell pecans. The results of this study will aid in design optimization of SDBD devices for increased pathogen inactivation efficiency.

MATERIALS AND METHODS

Plasma actuator construction. Surface dielectric barrier discharge (SDBD) actuators were constructed using 3.6 cm x 0.5 cm x 0.5 mm (*l* x *w* x *h*) copper electrodes (McMaster-Carr Supply Company, GA, USA) placed on both sides of 5 cm^2 x 0.127 mm Teflon dielectric barrier sheets (McMaster-Carr Supply Company, GA). Two different

electrode arrangements, referred to as symmetric and asymmetric, were used to evaluate their differential effects on airflow induction through particle image velocimetry (PIV) and bacterial inactivation. In the symmetric design, electrodes were placed in line with each other on each side of the dielectric material, whereas the asymmetric design had the electrodes staggered in relation to the dielectric material (Figure 1). The grounded electrodes were insulated to prevent plasma ignition. SDBD actuators were operated with an input power of 6.75 W and 13.5 V with a 50% duty cycle using a high voltage transformer (Information Unlimited, NH). Pulse width modulation (PWM), using an Arduino Uno microcontroller setup (Arduino LLC, Italy), was used to allow actuators to be on for 800 ms and off for 300 ms. Pulsing the power was found to reduce heat buildup, extending actuator lifespans (data not shown).

Particle image velocimetry. Particle image velocimetry (PIV) was used to determine the flow rate of air induced by the SDBD actuators as previously described (Pai and Jacob, 2013). In this setup, a 100 mW, 532 nm EVO laser (Wicked Lasers, Hong Kong, China) was used to generate a sheet of light with which individual particle paths could be visualized. A MotionPro X3 high speed CCD camera (IDT, FL, USA) was used to capture images at 100 frames per second using the software MotionStudio (IDT, FL, USA). The images were analyzed using ISSIPIV software (Innovative Scientific Solutions Inc., OH, USA). Smoke particles of approximately 1 μm were used as seed particles for tracking of induced fluid motion. Image analysis was carried out by comparing the procured images and generating composite images to show the motion of bulk fluid in 240 ms.

Bacterial strains and culture conditions. Multiple-strain mixtures of *Salmonella enterica* subspecies *enterica* (serovars Enteritidis, Typhimurium, Javiana, Seftenburg, and Poona), Shiga toxin-producing *Escherichia coli* (serotypes O157:H7, O111:H2, O26:H11, O103:H2, O121:H19, O145:H28, and O45:NM), and *Listeria monocytogenes* (strains F6854, 12433, G3982, J0161, and Scott A) were used for inoculation of sterile glass coverslips, cherry tomatoes, and pecans. Multiple-strain mixtures were used to more accurately represent environmental contamination of inoculated surfaces. Each bacterial strain was separately grown aerobically overnight with shaking (250 rpm) at 37°C in 5 mL tryptic soy broth (TSB, Difco, Sparks, MD). The bacterial concentration of each overnight liquid culture was determined by serially diluting the culture in 0.1% (w/v) sterile peptone (Difco, Sparks, MD) and plating in duplicate on tryptic soy agar (TSA, Difco, Sparks, MD), incubated overnight at 37°C.

Preparation of inoculum. To prepare the inocula, 1 mL of each liquid culture was centrifuged at 12,000 rpm for 3 minutes and re-suspended in 1 mL of 0.1% (w/v) sterile peptone before being combined with all other strains of the same species. The multiple-strain bacterial mixtures were then diluted to approximately 10^8 CFU/mL and 100 µL of the bacterial suspensions were used as inocula (approximately 10^7 CFU/inoculated surface), spotted in 20-25 spots (between 10^5 and 10^6 CFU/spot) onto single sterile 22 x 22 mm glass coverslips, whole unshelled pecans, or cherry tomatoes. Pecans and cherry tomatoes were obtained from a local native pecan orchard and local grocery store, respectively, and stored at 4°C until inoculated. Glass coverslips were inoculated with *Se,* STEC, and *Lm* whereas pecans and cherry tomatoes were inoculated only with *Se*. Inocula spots were spaced evenly over the entire surface of the coverslips or

within a 2 cm^2 region on the upper surface of pecans and cherry tomatoes. Inoculation spots were dried in a biosafety cabinet for 60 minutes prior to cold plasma treatment.

Cold plasma treatment by SDBD. The bacterial inactivation difference between symmetric and asymmetric electrode arrangements with SDBD actuators was evaluated only with 4 min treatments with *Lm*. Coverslips inoculated with STEC, *Se*, and *Lm* were placed in sterile 35 mm plastic petri dishes and treated with asymmetric SDBD actuators for 2 and 4 min from a distance of 1, 3, 5, and 7 cm (Figure 2). Three replicates of each culture were treated in duplicate (2 coverslips) at each distance and time at room temperature (~25°C) and atmospheric pressure. Inoculated pecans and cherry tomatoes were also placed in sterile 35 mm petri dishes but were treated for 4 and 10 min at 1cm.

Assessment of bacterial inactivation. Immediately after cold plasma treatment, treated and untreated control inoculated coverslips, pecans, and cherry tomatoes were washed by vortexing for 30 s in 10 mL 0.1% (w/v) sterile peptone in 50 mL conical tubes. The wash fluid was 10-fold serially diluted in 0.1% peptone and 100 µL of appropriate dilutions were plated in duplicate on TSA and incubated overnight at 37 °C. Pecans and cherry tomatoes, which were inoculated with *Se*, were plated on xylose lysine deoxycholate (XLD, Difco, Sparks, MD) agar overlaid with TSA. XLD, selective for *Salmonella*, was used to differentiate inoculated bacteria from background bacteria already present on the produce surfaces. Bacterial inactivation was assessed by comparing plate counts of each treatment with untreated controls.

Statistical analysis. Three biological repeats containing two replicates of each treatment were conducted. The plate counts of cells recovered from wash fluids for each replicate were transformed to log CFU/mL. Log reductions due to plasma treatment were

calculated by comparing the numbers of recovered cells from treated and untreated controls. Analysis of variance (ANOVA) was used to calculate statistical differences between samples from plate counts using SAS (Statistical Analysis System. Inst. Inc., Cary, NC, USA). Significant difference was defined at $P \leq 0.05$. Decimal reduction time (D-value) in minutes was calculated for the inoculated coverslips at each treatment distance according to the equation $D = t/(\log N_0 - \log N_u)$, where t is treatment time, N_0 is the bacterial concentration recovered from untreated controls, and N_u is the bacterial concentration recovered from plasma treated samples. Since bacterial survival curves with increasing treatment times were not calculated in this study and bacterial inactivation at single treatment times (2 and 4 min) were used for D-value calculations, the reported D-values are only estimates that may differ from actual values depending upon specific inactivation kinetics for different pathogens, initial cell concentrations, and treatment conditions. These calculations are beyond the scope of this study and will be thoroughly evaluated in future studies.

RESULTS

SDBD-induced airflow dynamics. PIV was used to evaluate the induced airflow characteristics of symmetric and asymmetric electrode arrangements with SDBD actuators. Smoke particles, following the airflow, were pulled in from the sides of the actuators and pushed towards the sample in a direction perpendicular to the actuators (Figure 3). The flow was pulled through the plasma generating region and then pushed towards the sample, allowing the air to act as a carrier for the generated reactive species. The asymmetric arrangement resulted in higher particle velocities and increased flow

turbulence than did the symmetric arrangement (Figure 3**)**. Analysis of the direction and magnitude of the particle movement revealed that particle velocities were 3 to 4 orders of magnitude higher with the asymmetric electrode arrangement than with the symmetric arrangement (Figure 3). The symmetric arrangement produced a fluid motion that was slower and more streamlined. The more turbulent flow of the asymmetric design is thought to result in better mixing of generated plasma species.

SDBD electrode arrangement effects on bacterial inactivation. Comparing the use of the symmetric and asymmetric electrode arrangements of SDBD actuators, both designs reduced *L. moncytogenes* populations on the inoculated coverslips (Table 1, Figure 4). Following 4 minute treatments at 1 cm, the asymmetric arrangement reduced the number of recovered viable cells on the coverslips from an average of 5.33 log CFU/mL to 1.34 log CFU/mL (a 3.99 log CFU reduction), whereas the symmetric arrangement reduced the number of viable cells to an average of 2.99 log CFU/mL (a 2.34 log CFU reduction) (Table 1). A decrease in bacterial inactivation efficiency, measured by averge log reduction, for both of the arrangements was observed as the sample distance from the actuators was increased (Table 1, Figure 4). At 1 and 3 cm treatment distances, the asymmetric arrangement allowed for significantly higher bacterial inactivation ($P \leq 0.05$) compared to symmetric arrangements. At 5 and 7 cm treatment distances, the differences between symmetric and asymmetric arrangements were not significantly different (Table 1, Figure 4). These data confirm that SDBD actuators with asymmetric electrode arrangements allow significantly increased bacterial inactivation efficiency compared to symmetric arrangements at distances up to 3 cm, suggesting that increased airflow induction allows reactive species to be pushed further

distances. However, there is a limit to the distance at which the reactive species are detrimental to living cells, probably a result of their relatively short half-lives.

Bacterial pathogen inactivation on sterile glass and fresh produce surfaces. Using SDBD actuators having asymmetrically-arranged electrodes, inactivation of STEC, *Se*, and *Lm* inoculated onto glass coverslips was observed at treatment times of both 2 and 4 min and at all distances, 1, 3, 5, and 7 cm (Table 2). Inactivation efficiency decreased with increasing distance and with shorter treatment times. When treated for 4 min, bacterial inactivation, measured by log reduction, was not statistically different among all 3 pathogens at each of the 4 distances ($P \leq 0.05$). Additionally, bacterial log reductions were significantly different from each other at 1, 3, and 7 cm. Results from treatment at 5 cm were significantly different from those of 1 cm treatments but not from 3 and 7 cm treatments (Table 2, Figure 5). The differences between individual pathogens and treatment distances were less pronounced when 2 min treatments were used (Table 2). Average log CFU/mL reductions for 4 min treatments at 1cm were 3.0 for *Se*, 3.6 for STEC, and 2.6 for *Lm*. D-value (min) estimates using 4 min treatments at 1 cm were 1.3 for *Se*, 0.9 for STEC, and 1.0 for *Lm* (Figure 5, Table 2). The highest log reduction, 4.90 CFU/mL, was observed with STEC at 1 cm after 4 min of cold plasma treatment. D-value (min) estimates using 2 and 4 min treatments at 1 cm ranged between 0.96 and 1.43 for all three pathogens (Table 2).

On both pecans and cherry tomatoes, an approximately 1 and 2 log CFU/mL reduction of *Se* was observed at 4 and 10 min, respectively. For each type of produce, the inoculated populations of Se were significantly decreased, compared to controls, by cold plasma treatment after both 4 and 10 min treatments ($P \leq 0.05$). However, the observed

log reductions on pecans and cherry tomatoes were substantially less than those observed in similar treatments of inoculated coverslips. Four min treatments at 1 cm reduced *Se* populations on pecans and cherry tomatoes by 1.16 and 0.7 log CFU/mL (Table 3), whereas the same treatment of *Se* populations on coverslips allowed a 3.02 log CFU/mL reduction (Table 2).

DISCUSSION

Cold atmospheric plasma, which is simply ionized air generated at ambient temperature and atmospheric pressure, is rapidly becoming one of the most talked about technologies of our day. Potential applications of cold plasma include medical instrument sterilization (Popelka *et al.,* 2012), more rapid wound healing (Isbary *et al.,* 2013), potential cancer therapies (Weiss *et al.,* 2015), pesticide degradation (Misra *et al.,* 2014), and food decontamination (Niemira, 2012). The interaction of plasma with cells has been investigated for bacteria (Lu *et al.,* 2014; Ziuzina *et al.,* 2014), bacterial spores (Klampfl *et al.,* 2012), biofilms (Ziuzina *et al.,* 2014b; Niemira *et al.,* 2014), plant cells (Puac *et al.,* 2006; Zhang *et al.,* 2014), and animal cells (Weiss *et al.,* 2015; Ma *et al.,* 2014). The results of these investigations underscore the fact that plasma inactivation of cells is a complex process that depends upon the type of plasma generation method, the type of cells used, and the substrate on which cells are treated (Stoffels *et al.,* 2004). UV light, charged particles, and reactive species, the cold plasma products most often cited for causing bacterial inactivation, are generated in a range of relative concentrations depending upon the specific type of plasma generation process used (Misra *et al.,* 2011; Gaunt *et al.,* 2006).

Although multiple approaches have been reported for generating cold plasma with air at atmospheric pressure for food decontamination applications, few are economically practical in a scalable format (Niemira, 2012). Therefore, the main challenge in cold plasma treatment of sensitive or complex surfaces (such as food surfaces) relates to the means of reactive species delivery to the treated surface. Accordingly, the major differences in the various plasma-generation methods are the modes by which charged particles, photons, and reactive species are allowed to interact with target cells on contaminated substrates. The major plasma-generation approaches currently used include plasma pens, jets, torches, high-energy deep-UV light, and microwave excitation (Misra *et al.,* 2011). All of these approaches require complex apparatuses, high input powers, and a supplied flow of inert gas, resulting in high operational costs and limited practical applications.

Surface dielectric barrier discharge (SDBD), in contrast, is one of the simplest approaches for cold plasma generation (Kogelschatz *et al.*, 1999). Using this format, plasma can be generated in air at room temperature and atmospheric pressure, requiring no enclosures or supplied gas flow. In its most basic form, plasma is generated by SDBD as a result of charge accumulation on one side of a dielectric barrier placed between two electrodes. The electric potential accumulates to a point at which the air between the electrodes is ionized, forming plasma (Gibalov and Pietsch, 2000). As a low-power, active flow control technique, SDBD has been used to improve the aerodynamic characteristics and propulsion efficiency of aircraft (Li *et al.*, 2011). For food decontamination applications, the induced airflow may allow delivery of reactive species, particularly ozone, to surfaces that are some distance from DBD actuators themselves.

Ozone (O_3) is a neutral reactive oxygen species of special note that has received increased interest in recent years for medical instrument sterilization. This relatively long-lived reactive oxygen species (ROS) that naturally converts back to harmless molecular oxygen is a well-known and powerful antimicrobial agent that is produced in high amounts by cold plasma generation in air (Khadre *et al.,* 2001; Sakiyama *et al.,* 2012) and is generally recognized as safe (GRAS) by the FDA when used for food decontamination (Khadre *et al.,* 2001). It is likely that ozone itself is not a major contributor to bacterial inactivation but it serves as a precursor to other, more reactive species (such as hydrogen peroxide, superoxide, and hydroxyl radical) when it rapidly interacts with free water on the surface of bacterial cells (Khadre *et al.,* 2001).

Previous studies investigating the effectiveness of cold plasma as a decontamination method have identified several features of such treatment in common, despite differences in plasma generation methods. These finding include that initial cell concentration influences bacterial inactivation rates (Fernandez and Thompson, 2012; Deng *et al.,* 2005; Gaunt *et al.,* 2006), bacterial inactivation is independent of growth phase and temperature (Fernandez *et al.,* 2013), increased treatment time is required for decontamination of complex food surfaces (Vannini *et al.,* 2009; Fernandez *et al.,* 2013; Ziuzina *et al.,* 2014), and that cold plasma treatment does not drastically affect fresh produce quality (Misra *et al.,* 2014a; Misra *et al.,* 2014b; Lacombe *et al.,* 2014; Fernandez *et al.,* 2013). The key distinctive feature of SDBD when compared to other plasma generation apparatuses is that SDBD induces a localized airflow that may allow delivery of reactive species and charged particles to distant surfaces. Therefore, it was the goal of this research to evaluate the induced airflow characteristics of SDBD actuators

and to evaluate bacterial pathogen inactivation at various distances on abiotic (glass) and biotic (fresh produce) surfaces. Based on the size of the SDBD actuators, glass coverslips, pecans, and cherry tomatoes were inoculated with Shiga toxin-producing *Escherichia coli*, *Salmonella enterica*, and *Listeria monocytogenes* to evaluate these effects. Differences in initial cell concentration, rates of inactivation, and effects of produce quality as a result of SDBD cold plasma treatment will be evaluated in future studies. Confirmation of the airflow-inducing properties of this design and an understanding of the design parameters that influence bacterial inactivation so as to allow design optimization is required prior to such studies using specific pathogens and specific substrates.

Particle image velocimetry (PIV) was used in this study to evaluate airflow induction of SDBD actuators with two different electrode arrangements, visualized by tracking smoke particles over time. Although both the asymmetric and symmetric electrode arrangements (Figure 1) induced a localized airflow (Figure 3), the asymmetric arrangement resulted in a significantly increased airflow velocity and turbulence. This characteristic was hypothesized to influence bacterial inactivation at increased distances due to the potential ability of the fluid motion to carry reactive species further, which was confirmed in this study (Figure 4). However, there is a limit to the distance at which the asymmetric arrangement out-performed the symmetric arrangement (5 cm), likely a result of the short lifespan of the reactive species generated from air. Accordingly, it may be possible to further increase the effective treatment distance by SDBD actuator design modifications that increase the velocity of induced airflow. The effects of actuator design on bacterial inactivation, although for a different basic design, has also been noted in

other studies (Schwabedissen *et al.*, 2007; Leipold *et al.*, 2011). Input power, electrode arrangement, electrode density, electrode material, and dielectric material have direct effects on induced airflow characteristics and may be tailored to develop SDBD actuators for specific food decontamination applications.

In this study, Shiga toxin-producing *Escherichia coli* (STEC), *Salmonella enterica* (*Se*), and *Listeria monocytogenes* (*Lm*), three of the most common bacterial foodborne pathogens, were shown to be inactivated by SDBD cold plasma actuators at distances up to 7 cm. After 4 minutes of cold plasma treatment, pathogen populations on glass coverslips were decreased by 3.6, 3.0, and 4.0 log CFU/mL for STEC, *Se*, and *Lm*, respectively. In corroboration with other cold plasma studies using different apparatuses, bacterial inactivation efficiency was reduced when complex biotic surfaces such as fresh produce were treated (Vannini *et al.*, 2009; Fernandez *et al.*, 2013; Ziuzina *et al.*, 2014). Similar to the higher chlorine concentration requirment observed in chlorine washes used for fresh produce, this observation may be a result of a decreased concentration of ROS present due to the ROS-scavenging ability of the organic surfaces being treated. Since complete bacterial inactivation curves were not evaluated in this study, D-values (min), estimated using 2 and 4 min treatments at 1 cm, ranged between 0.96 and 1.43 for all three pathogens. These levels of bacterial reduction and rates of bacterial inactivation are similar to or slightly less than previous findings using different cold plasma apparatuses (Niemira, 2012). Although volumetric dielectric barrier discharge and atmospheric pressure plasma jet apparatuses may show faster bacterial inactivation rates, they incur the disadvantages of significantly increased power requirements, more moving parts, small effective treatment areas, and increased setup and scaling costs (Niemira, 2012).

Because of these limitations, such apparatuses may be too expensive, bulky, and inconvenient for food production applications. Using a SDBD-based design similar to that described herein, Yong *et al.* (2015) observed a 4.75 log CFU/mL reduction of *Lm*. As in this study, decreased distance from actuators and increased treatment time resulted in increased bacterial inactivation (Yong *et al.*, 2015). Although a lower level of *Lm* inactivation was observed in this study (3.99 compared to 4.75 CFU/mL for Yong *et al.*), only 6.75 W were required to power the SDBD actuators compared to 250 W for similar treatment areas (Yong *et al.*, 2015).

Based on the results of this study, SDBD has the potential to overcome many of the limitations of other investigated cold plasma generation apparatuses for food decontamination applications. This plasma generation method is likely to be flexible, scalable, and cost-effective for large scale food production applications after the treatment and design parameters of this technology are more fully defined. Ample research has been conducted on how various SDBD scaling parameters, such as input power and frequency, influence the physical plasma characteristics and induction of airflow, as well as documentation of the biocidal effects of cold plasma. However, the relationships between induced airflow and bacterial inactivation have not been previously correlated. Additionally, the aspects of food quality, shelf life, nutritional characteristics, and by-product generation as a result of SDBD-treated foods must be thoroughly investigated. This study confirmed the ability to inactivate bacterial pathogens with cold plasma by SDBD and that induced airflow is the means of reactive species delivery to contaminated surfaces. In addition to food decontamination, SDBD has potential

applications in wound care, medical instrument sterilization, and consumer product decontamination.

LITERATURE CITED

Abadias, M., T.P. Cañamas, A. Asensio, M. Angueram, and I. Viñas. (2006). Microbial quality of commercial 'Golden Delicious' apples throughout production and shelf-life in Lleida (Catalonia, Spain). *International Journal of Food Microbiology*. 108:404-409.

Aruscavage, D., K. Lee, S. Miller, and J.T. Lejeune. (2006). Interactions affecting the proliferation and control of human pathogens on edible plants. *Journal of Food Science.* 71:R89-R99.

Barth, M., Hankinson, T., Zhuang, H., & Breidt, F. (2010). Microbiological Spoilage of Fruits and Vegetables. In W. H. Sperber & M. P. Doyle (Eds.), *Compendium of the Microbiological Spoilage of Foods and Beverages* (pp. 135-183): Springer New York.

Centers for Disease Control and Prevention. (2013). Multistate Outbreak of Shiga toxin-producing *Escherichia coli* O157:H7 Infections Linked to Ready-to-Eat Salads (Final Update). Available at: http://www.cdc.gov/ecoli/2013/O157H7-11-13/

Fernández, A., & Thompson, A. (2012). The inactivation of Salmonella by cold atmospheric plasma treatment. *Food Research International, 45*(2), 678-684.

Fernández, A., Noriega, E., & Thompson, A. (2013). Inactivation of Salmonella enterica serovar Typhimurium on fresh produce by cold atmospheric gas plasma technology. *Food Microbiology, 33*(1), 24-29.

Foong-Cunningham, S., and E.L.C. Verkaar. (2012). Microbial decontamination of fresh produce. In Demirci, A., and M.O. Ngadi (Eds.) Microbial decontamination in the food industry: Novel methods and applications. Woodhead Publishing, Cambridge, UK.

Gaunt, L. F., Beggs, C. B., & Georghiou, G. E. (2006). Bactericidal Action of the Reactive Species Produced by Gas-Discharge Nonthermal Plasma at Atmospheric Pressure: A Review. *Plasma Science, IEEE Transactions on, 34*(4), 1257-1269.

Gibalov, V.I., and G.J. Pietsch. (2000). The development of dielectric barrier discharges in gas gaps and on surfaces. *J.Phys.D:Appl. Phys.* 33:2618-2636.

Gil, M. I., Selma, M. V., Suslow, T., Jacxsens, L., Uyttendaele, M., & Allende, A. (2015). Pre- and Postharvest Preventive Measures and Intervention Strategies to Control Microbial Food Safety Hazards of Fresh Leafy Vegetables. *Critical Reviews in Food Science and Nutrition, 55*(4), 453-468. doi: 10.1080/10408398.2012.657808

Goodburn, C., and C.A. Wallace. (2013). The microbiological efficacy of decontamination methodologies for fresh produce: A review. *Food Control. 32*(2):418-427.
Niemira, B.A. (2012). Cold Plasma Decontamination of Foods. *Annual Review of Food Science and Technology.* 3(1):125-142.

Isbary, G., Stolz, W., Shimizu, T., Monetti, R., Bunk, W., Schmidt, H. U., Zimmermann, J. L. (2013). Cold atmospheric argon plasma treatment may accelerate wound healing in chronic wounds: Results of an open retrospective randomized controlled study in vivo. *Clinical Plasma Medicine, 1*(2), 25-30.

Khadre, M., Yousef, A., & Kim, J. (2001). Microbiological aspects of ozone applications in food: a review. *Journal of food science-Chicago-, 66*(9), 1242-1253.

Klämpfl, T.G., G. Isbary, T. Shimizu, Y.F. Li, J.L. Zimmermann, W. Stolz, & J.U. Schmidt. (2012). Cold Atmospheric Air Plasma Sterilization against Spores and Other Microorganisms of Clinical Interest. *Applied and Environmental Microbiology.* 78(15):5077-5082.

Kogelschatz, U., B. Eliasson, & W. Egli. (1999). From ozone generators to flat television screens: history and future potential of dielectric-barrier discharges *Pure and Applied Chemistry.* 71:1819.

Lacombe, A., Niemira, B. A., Gurtler, J. B., Fan, X., Sites, J., Boyd, G., & Chen, H. (2015). Atmospheric cold plasma inactivation of aerobic microorganisms on blueberries and effects on quality attributes. *Food Microbiol, 46*, 479-484.

Leipold, F., N. Schultz-Jensen, Y. Kusano, H. Bindslev, and T. Jacobsen. (2011). Decontamination of objects in a sealed container by means of atmospheric pressure plasmas. *Food Control.* 22, 1296.

Li, Y.H., Y. Wu, H.M. Song, H. Liang and M. Jia . (2011). Plasma Flow control. *In* M. Mulder (Ed.). Aeronautics and Astronautics. InTech publishing, Rijeka, Croatia.

Lu, H., Patil, S., Keener, K. M., Cullen, P. J., & Bourke, P. (2014). Bacterial inactivation by high-voltage atmospheric cold plasma: influence of process parameters and effects on cell leakage and DNA. *Journal of Applied Microbiology, 116*(4), 784-794.

Ma, Y., Ha, C. S., Hwang, S. W., Lee, H. J., Kim, G. C., Lee, K.-W., & Song, K. (2014). Non-Thermal Atmospheric Pressure Plasma Preferentially Induces Apoptosis in p53-Mutated Cancer Cells by Activating ROS Stress-Response Pathways. *PLoS ONE, 9*(4), e91947.

Misra, N.N., B.K. Tiwari, K.S.M.S. Raghavarao, and P.J. Cullen. (2011). Nonthermal plasma inactivation of food-borne pathogens. *Food Engineering Reviews.* 3(3-4):159-170.

Misra, N. N., Pankaj, S. K., Walsh, T., O'Regan, F., Bourke, P., & Cullen, P. J. (2014a). In-package nonthermal plasma degradation of pesticides on fresh produce. *Journal of Hazardous Materials, 271*(0), 33-40.

Misra, N. N., Patil, S., Moiseev, T., Bourke, P., Mosnier, J. P., Keener, K. M., & Cullen, P. J. (2014b). In-package atmospheric pressure cold plasma treatment of strawberries. *Journal of Food Engineering, 125*(0), 131-138.

Niemira, B.A. (2012). Cold Plasma Decontamination of Foods. *Annual Review of Food Science and Technology.* 3(1):125-142.

Niemira, B. A., Boyd, G., & Sites, J. (2014). Cold Plasma Rapid Decontamination of Food Contact Surfaces Contaminated with Salmonella Biofilms. *Journal of Food Science, 79*(5), M917-M922.

Pai, K,. and J. Jacob. (2013). Evaluation of Dielectric Barrier Discharge Configurations for Biological Decontamination. Proc. 51st AIAA Aerosp. Sci. Meeting Dallas, TX.

Painter, J. A., Hoekstra, R. M., Ayers, T., Tauxe, R. V., Braden, C. R., Angulo, F. J., & Griffin, P. M. (2013). Attribution of foodborne illnesses, hospitalizations, and deaths to food commodities by using outbreak data, United States, 1998-2008. *Emerg Infect Dis, 19*(3), 407-415.

Popelka, A., Novák, I., Lehocký, M., Chodák, I., Sedliačik, J., Gajtanska, M., . . . Bílek, F. (2012). Anti-bacterial Treatment of Polyethylene by Cold Plasma for Medical Purposes. *Molecules, 17*(1), 762.

Puac, Z. L. Petrovic, G. Malovic, A. Dordevic, S. Zivkovic, Z. Giba, & D. Grubisic. (2006). Measurements of voltage–current characteristics of a plasma needle and its effect on plant cells. *J. Phys. D, Appl. Phys.*, 39(16), 3514–3519.

Sakiyama, Y., David, B. G., Hung-Wen, C., Tetsuji, S., & Gregor, E. M. (2012). Plasma chemistry model of surface microdischarge in humid air and dynamics of reactive neutral species. *Journal of Physics D: Applied Physics, 45*(42), 425201.

Scallan, E., R.M. Hoekstra, F.J. Angulo, R.V. Tauxe, M.-A. Widdowson, S.L. Roy, J.L. Jones, and P.M. Griffin. (2011). Foodborne illness acquired in the United States—major pathogens. *Emerg. Infect. Dis.* 17:7-15

Schwabedissen, A., P. Łaciński, X. Chen, and J. Engemann. (2007). PlasmaLabel–a new method to disinfect goods inside a closed package using dielectric barrier discharges. *Contributions to Plasma Physics.* 47, 551.

Sivapalasingam, S., C.R. Friedman, L. Cohen, and R.V. Tauxe. (2004). Fresh produce: A growing cause of outbreaks of foodborne illness in the united states, 1973 through 1997. *Journal of Food Protection.* 67(10):2342-2353.

Stoffels, E., Sladek, R. E. J., Kieft, I. E., Kersten, H., & Wiese, R. (2004). Power outflux from the plasma: an important parameter in surface processing. *Plasma Physics and Controlled Fusion, 46*(12B), B167. Dec. 2004.

Stoffels, E., Sakiyama, Y., & Graves, D. B. (2008). Cold Atmospheric Plasma: Charged Species and Their Interactions With Cells and Tissues. *IEEE Transactions on Plasma Science, 36*(4), 1441-1457. doi: 10.1109/tps.2008.2001084.

Stopforth, J. D., Mai, T., Kottapalli, B., & Samadpour, M. (2008). Effect of Acidified Sodium Chlorite, Chlorine, and Acidic Electrolyzed Water on Escherichia coliO157:H7, Salmonella, and Listeria monocytogenesInoculated onto Leafy Greens. *Journal of Food Protection, 71*(3), 625-628.

Weiss, M., Gümbel, D., Hanschmann, E.-M., Mandelkow, R., Gelbrich, N., Zimmermann, U., Stope, M. B. (2015). Cold Atmospheric Plasma Treatment Induces Anti-Proliferative Effects in Prostate Cancer Cells by Redox and Apoptotic Signaling Pathways. *PLoS ONE, 10*(7), e0130350.

Yong, H. I., Kim, H.-J., Park, S., Alahakoon, A. U., Kim, K., Choe, W., & Jo, C. (2015). Evaluation of pathogen inactivation on sliced cheese induced by encapsulated atmospheric pressure dielectric barrier discharge plasma. *Food Microbiology, 46*, 46-50.

Zhang, X., Liu, D., Zhou, R., Song, Y., Sun, Y., Zhang, Q., & Yang, S.-Z. (2014). Atmospheric cold plasma jet for plant disease treatment. *Applied Physics Letters, 104*(4), 043702.

Ziuzina, D., S. Patil, P.J. Cullen, K.M. Keener, & P. Bourke. (2013). Atmospheric cold plasma inactivation of Escherichia coli in liquid media inside a sealed package. *Journal of Applied Microbiology*, 114 (3): 778–787.

Ziuzina, D., S. Patil, P.J. Cullen, K.M. Keener, & P. Bourke. (2014). Atmospheric cold plasma inactivation of *Escherichia coli, Salmonella enterica* serovar Typhimurium *and Listeria monocytogenes* inoculated on fresh produce. *Food Microbiology.* 42(0):109-116.

Ziuzina, D., Patil, S., Cullen, P. J., Boehm, D., & Bourke, P. (2014b). Dielectric Barrier Discharge Atmospheric Cold Plasma for Inactivation of Pseudomonas aeruginosa Biofilms. *4*(1-4), 137-152.

TABLES

Table 1. Average log reduction of *Listeria monocytogenes* (*Lm*) populations on inoculated glass coverslips after 4 min treatments with SDBD actuators having either asymmetric or symmetric electrode arrangements.

Treatment distance (cm)	Log reduction of *Lm* (CFU/mL) ± SD	
	Asymmetric	Symmetric
1	3.99 ± 0.86 [a]	2.34 ± 0.46 [b]
3	2.00 ± 0.59 [b]	1.16 ± 0.18 [c]
5	0.83 ± 0.28 [cd]	1.12 ± 0.25 [c]
7	0.35 ± 0.34 [d]	0.42 ± 0.2 [d]

Table 2. Average log reductions and D-values for *Salmonella*, STEC, and *Listeria monocytogenes* populations on inoculated glass coverslips treated using asymmetric SDBD actuators for 2 and 4 min at distances of 1, 3, 5, and 7 cm.

Treatment time	Treatment distance (cm)	Log reduction (CFU/mL) ± SD			D-value (min) ± SD		
		Salmonella	STEC	*Listeria*	*Salmonella*	STEC	*Listeria*
2 min	1	1.56 ± 0.37 [a]	2.10 ± 0.23 [a]	2.01 ± 0.50 [a]	1.32 ± 0.28	0.96 ± 0.1	1.04 ± 0.24
	3	1.16 ± 0.44 [ab]	1.41 ± 0.25 [ab]	1.31 ± 0.45 [b]	1.88 ± 0.62	1.45 ± 0.24	1.65 ± 0.54
	5	0.62 ± 0.41 [ab]	0.80 ± 0.24 [ab]	0.63 ± 0.31 [bc]	5.38 ± 5.14	2.64 ± 0.7	4.06 ± 2.74
	7	0.42 ± 0.33 [b]	0.42 ± 0.1 [b]	0.14 ± 0.07 [c]	8.54± 7.96	4.97 ± 1.34	16.59 ± 6.71
4 min	1	3.02 ± 0.91 [a]	3.61 ± 1.15 [a]	3.99 ± 0.86 [a]	1.43 ± 0.52	1.18 ± 0.35	1.13 ± 0.35
	3	1.65 ± 0.46 [b]	2.13 ± 0.73 [b]	2.00 ± 0.59 [b]	2.55 ± 0.62	2.01 ± 0.58	2.11 ± 0.56
	5	1.15 ± 0.50 [c]	1.11 ± 0.09 [bc]	0.83 ± 0.28 [bc]	3.86 ± 1.37	3.61 ± 0.3	5.17 ± 1.61
	7	0.64 ± 0.27 [c]	0.49 ± 0.16 [c]	0.35 ± 0.34 [c]	7.15 ± 3.1	8.68 ± 2.54	108.75 ± 173.38

Table 3. Average log reduction of *Salmonella* populations after inoculation onto pecans and cherry tomatoes, treated with asymmetric SDBD actuators for 4 and 10 min at 1 cm.

Treatment time (min)	Log reduction of *Se* (CFU/mL) ± SD	
	Pecans	**Cherry tomatoes**
4	1.16 ± 0.51 [a]	0.70 ± 0.03 [ab]
10	2.33 ± 0.01 [b]	1.66 ± 0.08 [c]

FIGURES

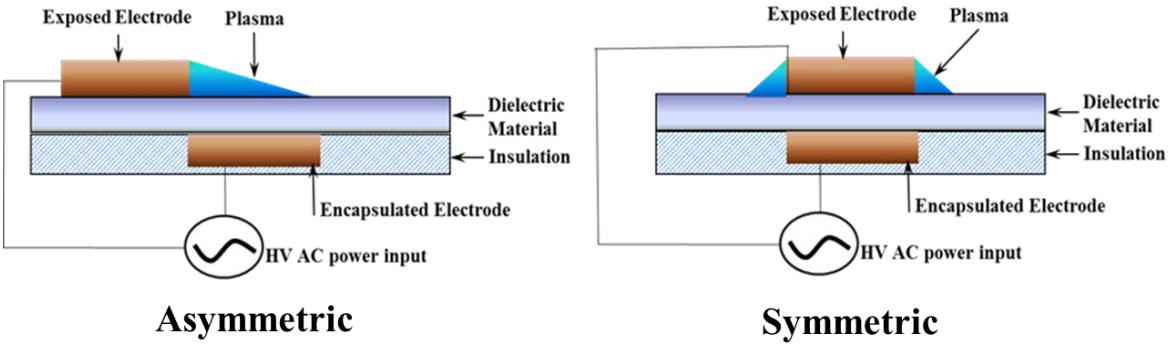

Figure 1. Asymmetric and symmetric electrode arrangements for novel surface dielectric barrier discharge (SDBD) actuators.

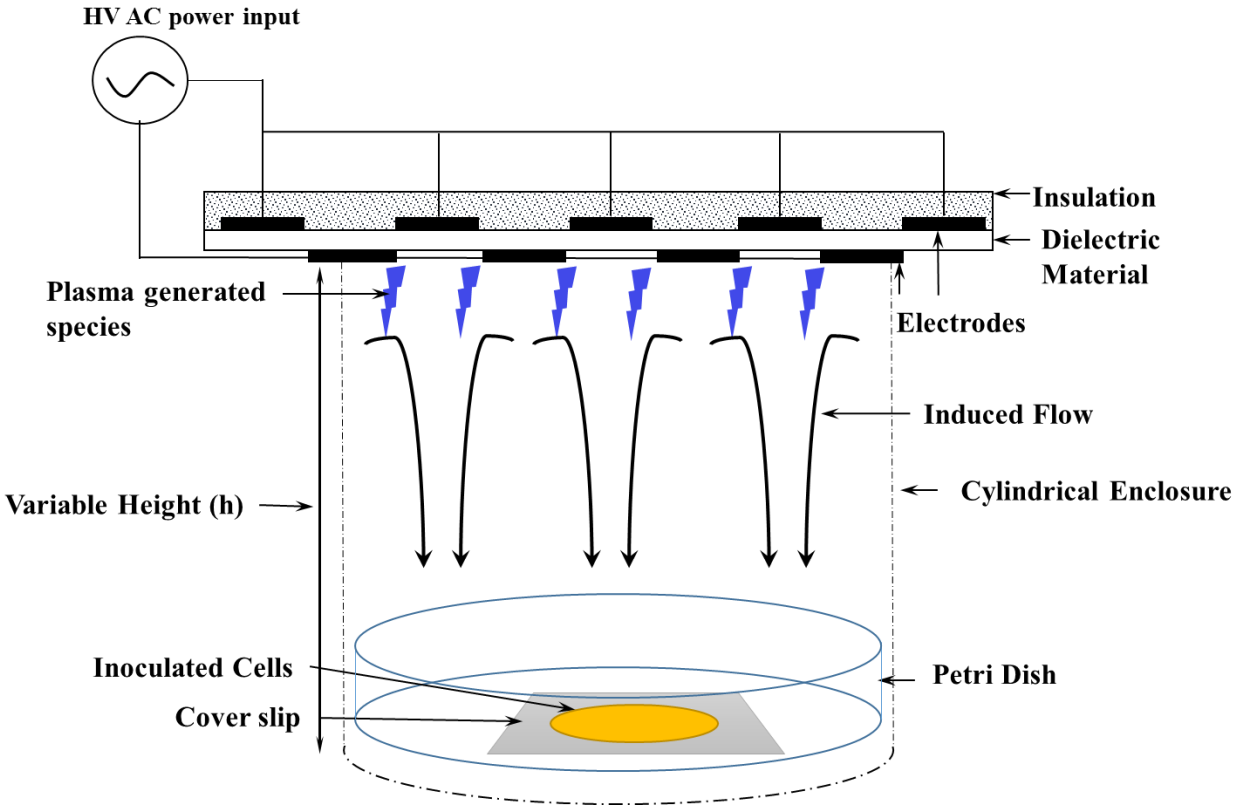

Figure 2. Schematic representation of the asymmetric SDBD set up for treating pathogen-inoculated coverslips, cherry tomatoes, and pecans at variable distances ranging from 1 to 7 cm.

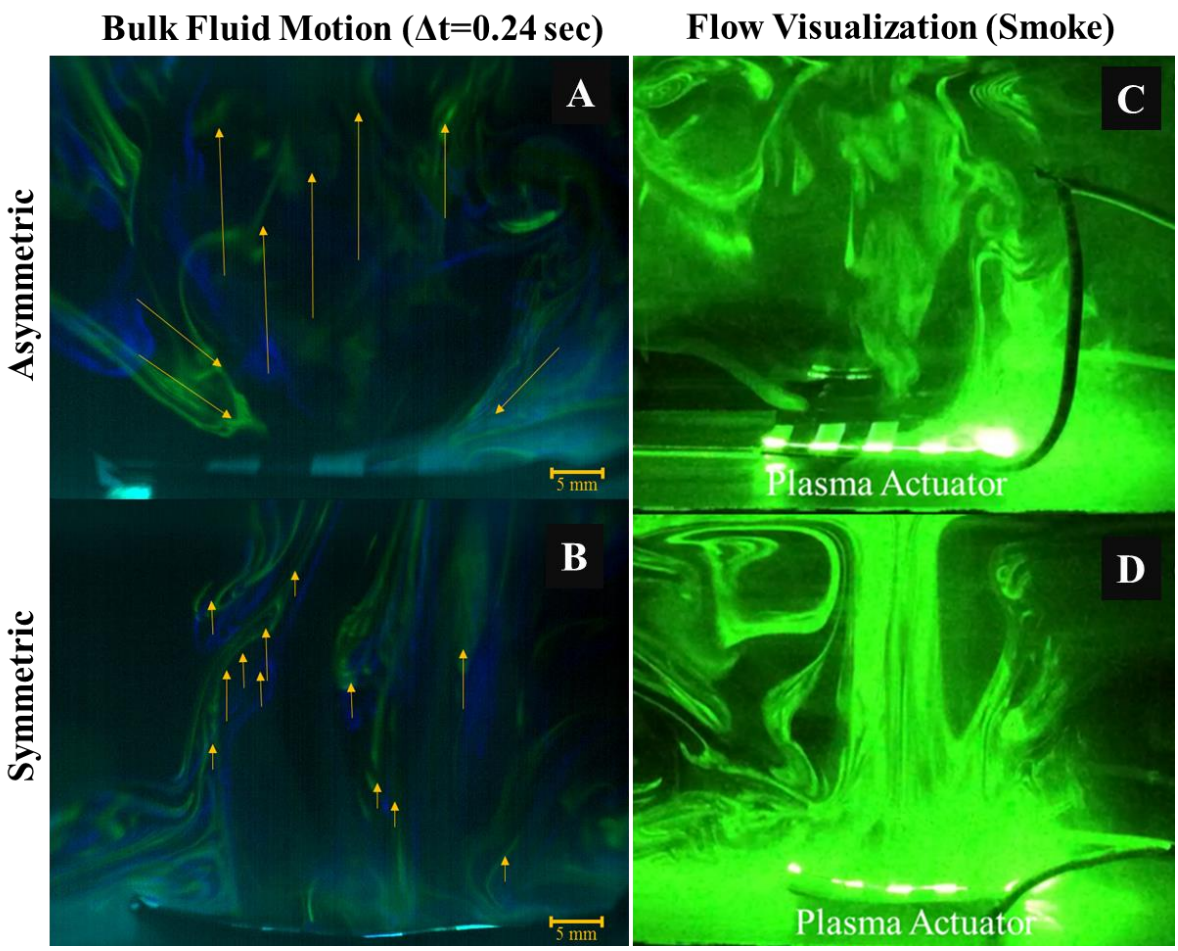

Figure 3. PIV images comparing the bulk fluid flow induction at time T=0 (blue) and T=0.24s (green) with vectors representing particle movement for asymmetric (A) and symmetric (B) electrode arrangements. Asymmetric electrode arrangements also caused a more turbulent airflow (C) compared to symmetric electrode arrangements (D) when visualized using smoke.

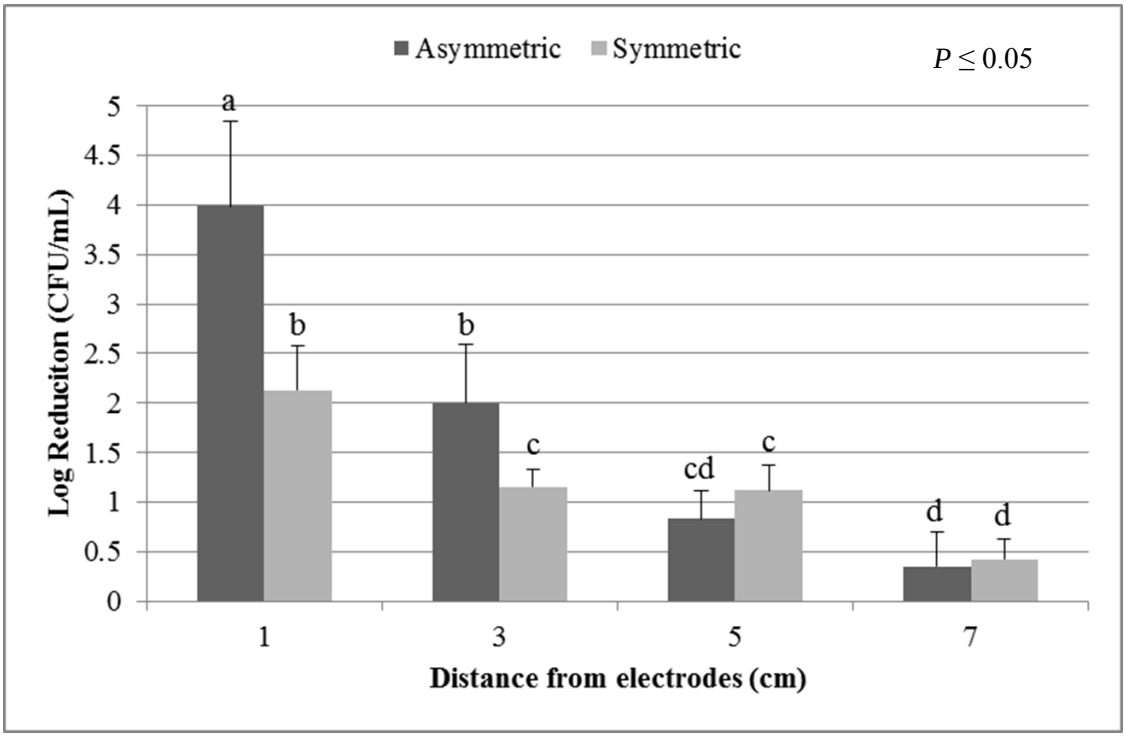

Figure 4. Average log reductions in CFU/mL of *Listeria monocytogenes* inoculated onto sterile glass coverslips treated for 4 min at 1, 3, 5, and 7 cm with SDBD actuators having asymmetric and symmetric electrode arrangements.

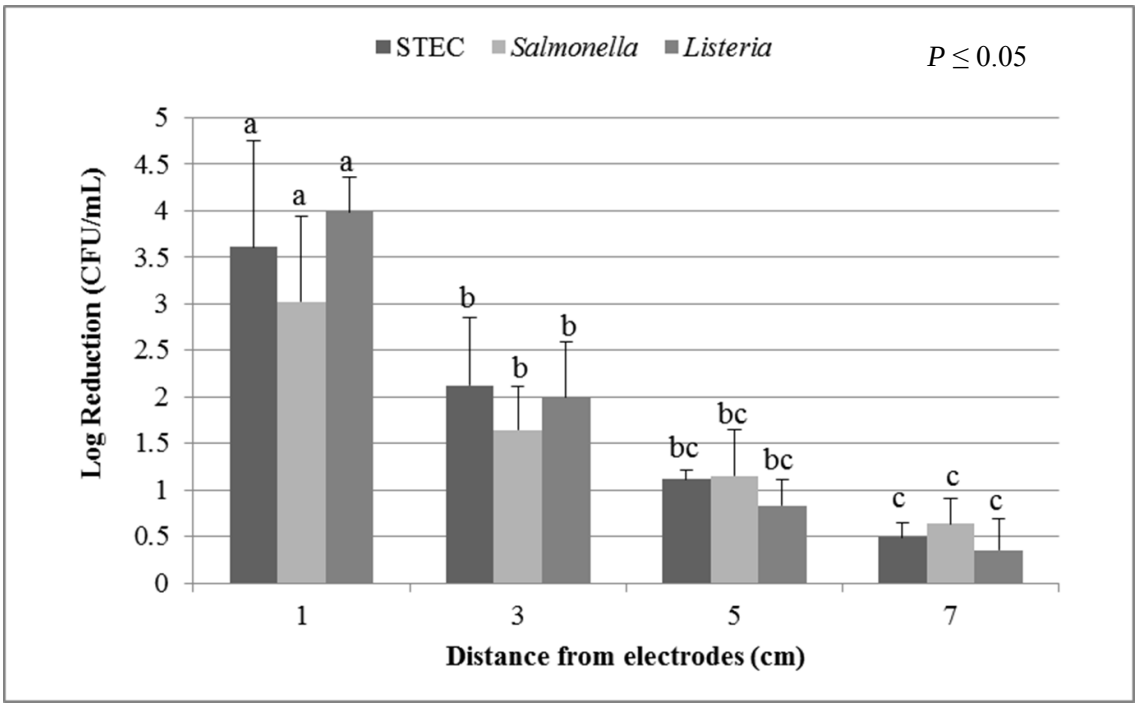

Figure 5. Average log reductions in CFU/mL of STEC, *Se*, and *Lm* inoculated onto sterile glass coverslips treated for 4 min at 1, 3, 5, and 7 cm with SDBD actuators having asymmetric electrodes.

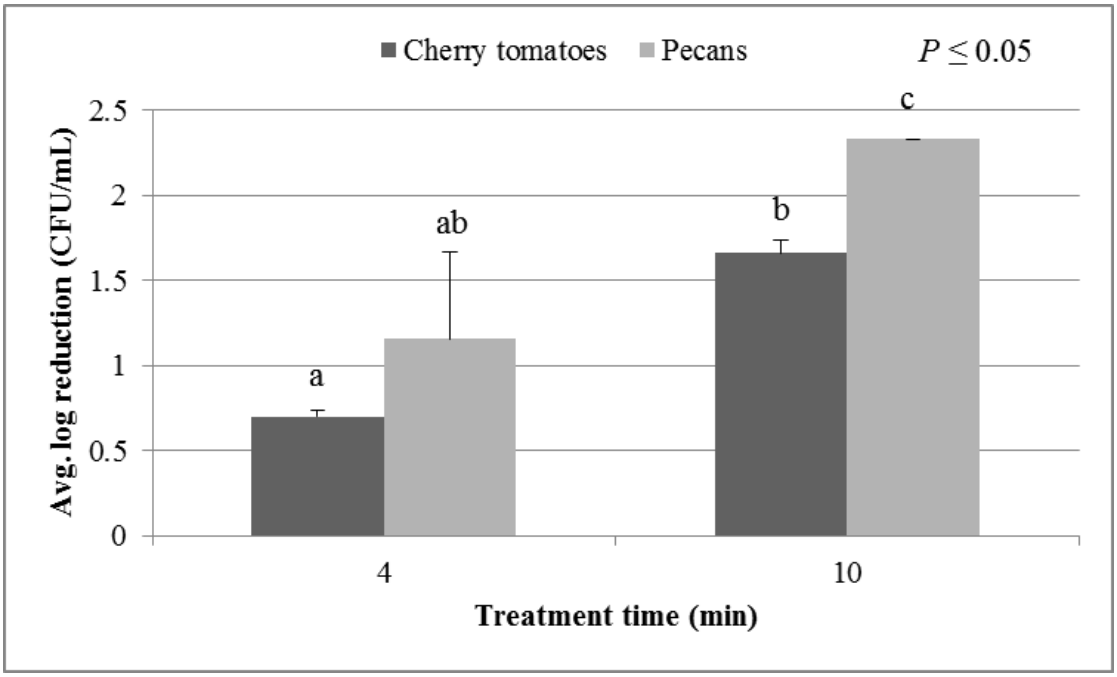

Figure 6. Average log reduction in CFU/mL of *Salmonella enterica* inoculated onto cherry tomatoes and pecans treated for 4 and 10 min at 1 cm with SDBD actuators having asymmetric electrodes.

CHAPTER IV

MORPHOLOGICAL AND TRANSCRIPTOMIC RESPONSE OF *SALMONELLA* ENTERITIDIS TO SURFACE DIELECTRIC BARRIER DISCHARGE COLD PLASMA TREATMENT

ABSTRACT

As an emerging technology, cold atmospheric plasma offers a dry, non-thermal, and rapid bacterial inactivation process that has multiple potential applications in surface and food decontamination. Although the bactericidal effects of cold plasma are well documented, the specific mechanisms and modes of interaction that result in bacterial inactivation are not well understood. The purpose of this study was to evaluate the morphological and transcriptomic response of *Salmonella* Enteritidis to surface dielectric barrier discharge (SDBD) cold plasma treatment and to identify the mechanisms of inactivation through transmission electron microscopy (TEM) and RNA sequencing (RNA-Seq). Among 764 differentially expressed genes with fold changes greater than 1.50 ($P \leq 0.01$, $FDR \leq 0.05$), 255 were up-regulated (1.50 to 3.23-fold) and 509 were downregulated (-1.50 top -120.67-fold) after plasma treatment. Genes associated with phosphate uptake, cation uptake, osmoregulation, tetrathionate utilization, phage-shock

proteins, and DNA damage repair were significantly downregulated after plasma treatment. Differentially expressed metabolic pathways included upregulation of ethanolamine utilization and downregulation of colonic acid and enterobactin biosynthesis. The observed general decrease in stress responses by SDBD plasma-treated *Salmonella* cells is thought to be a result of rapid lipid peroxidation, cytosolic leakage, and cell lysis, as revealed by TEM, of cells adjacent to those from which RNA was isolated, resulting in a nutrient rich and osmotically balanced microenvironment for surviving cells. Accordingly, DNA and protein damage by plasma-produced reactive oxygen and nitrogen species were found to have a minor role when dried Gram-negative bacteria were treated with SDBD. These results emphasize the importance of lipid peroxidation as a major mechanism by which bacterial cells are inactivated by treatment with cold plasma. SDBD plasma actuators are more flexible, scalable, versatile, and less expensive than many other cold plasma generation apparatuses and have multiple potential applications for surface sterilization or decontamination.

INTRODUCTION

Cold atmospheric plasma, ionized gas generated at ambient temperature and atmospheric pressure, has gained intense interest in recent years for a variety of surface sterilization and decontamination applications (Laroussi, 2005; Kong *et al.*, 2009; Niemira 2012). UV radiation, charged particles, and reactive oxygen and nitrogen species (RONS) are the cold plasma components or by-products most often cited for causing

cellular inactivation when generated in air, with RONS playing a dominant role (Misra *et al.,* 2011; Mai-Prochnow *et al.,* 2014; Han *et al.,* 2016). The interaction of cold plasma with cells has been investigated for bacteria (Lu *et al.,* 2014; Ziuzina *et al.,* 2014), bacterial spores (Klampfl *et al.,* 2012), biofilms (Ziuzina *et al.,* 2014b; Niemira *et al.,* 2014), viruses (Ahlfeld *et al.,* 2015), plant cells (Puac *et al.,* 2006; Zhang *et al.,* 2014), and animal cells (Weiss *et al.,* 2015; Ma *et al.,* 2014). These studies have shown that inactivation of cells by cold plasma is a complex process influenced by the type of plasma generation method, the type of treated cells, and the substrate on which cells are treated (Stoffels *et al.,* 2004; Han *et al.,* 2016; Lunov *et al.,* 2016). Recent literature suggests that prokaryotes are more sensitive than eukaryotes to plasma treatment and inactivation of bacterial pathogens on contaminated surfaces is one of the primary potential applications of this technology (Mai-Prochnow *et al.,* 2015; Pai *et al.,* 2015; Chapter 3). However, despite the rapidly growing body of literature on cold atmospheric plasma and its effects on living bacterial cells, the specific mechanisms that cause cellular inactivation are still not well understood.

Lipid peroxidation and oxidative DNA damage by plasma-produced RONS are emerging as the major contributors to bacterial inactivation (Joshi *et al.,* 2011; Mai-Prochnow *et al.,* 2014; Lunov *et al.,* 2016). High local concentrations of RONS result in membrane or cell wall damage and intracellular ROS accumulation, potentially inducing programmed cell death (Lunov *et al.,* 2016). Gram-negative bacteria are usually more sensitive to plasma treatment, have more rapid inactivation rates, and are inactivated by cell leakage and low-level DNA damage (Joshi *et al.,* 2011; Mai-Prochnow *et al.,* 2014; Han *et al.,* 2016), than the more robust, thicker cell walled Gram-positive bacteria.

Plasma treatment of Gram-positive bacteria, on the other hand, often results in minimal cell envelope damage but significantly higher intracellular DNA damage (Kvam *et al.,* 2012; Han *et al.,* 2016). Cell concentration and growth phase also affect bacterial inactivation rates, likely a result of a shadowing effect, in which some cells are shielded from the plasma produced species by other cells, and differing metabolic rates, respectively (Mai-Prochnow *et al.,* 2014). Although these findings are similar for multiple types of plasma generation methods, bacterial inactivation rates can vary from seconds to minutes when different plasma generation apparatuses are used (Mai-Prochnow *et al.,* 2014).

More complete elucidation of the specific mechanisms of bacterial inactivation caused by cold plasma is thought to be limited by the methodological difficulty associated with separating the effects of plasma-generated reactive species on bacterial cells themselves from the indirect effects of the reactive species on the medium or solution in which bacteria are growing or suspended (Kvam *et al.,* 2012). Additionally, the relatively short half-lives and high reactivity of RONS makes identifying their individual effects on cells a challenge (Lunov *et al.,* 2016). Although most practical applications of cold plasma treatment are for surface decontamination applications, almost all studies investigating the mechanistic effects of cold plasma treatment on bacteria have been evaluated using bacterial suspensions and bacteria growing on agar or growth-supporting membrane filters rather than dried cells on a given substrate. Thus, evaluation of the genotypic and phenotypic responses of dried bacterial cells exposed to plasma-produced reactive species is needed to ascertain the real-world applicability of cold plasma treatments for surface sterilization or decontamination applications.

Therefore, the goal of this study was to evaluate the genotypic and phenotypic responses of dried *Salmonella* cells to surface dielectric barrier discharge (SDBD), a novel semidirect cold plasma treatment method, using RNA sequencing (RNA-seq) and transmission electron microscopy (TEM), respectively. *Salmonella* was chosen for this study because it is a robust and common bacterial foodborne pathogen that has a high tolerance to desiccation stress (Li *et al.,* 2012). Compared to other plasma generation methods, SDBD is a relatively inexpensive, simple, scalable, and flexible apparatus that has multiple potential applications for surface sterilization (Pai *et al.*, 2015; Chapter 3). RNA-seq is ideally suited for evaluating genotypic responses to cold plasma treatment due to its high resolution with limited background noise and high dynamic range, allowing identification of even relatively subtle differential gene expression changes resulting from the treatment (Wang *et al.*, 2009). This study allowed comparison of the genotypic and phenotypic cellular effects of SDBD cold plasma on bacterial cells to other studies using different plasma generation apparatuses and helped identify the major mechanisms of bacterial inactivation on dried surfaces.

MATERIALS AND METHODS

Bacterial strain and culture conditions. *Salmonella enterica* subspecies *enterica* serovar Enteritidis strain H4639 was used to evaluate SDBD-induced inactivation and for RNA-seq analysis. An attenuated strain of *Salmonella enterica* subspecies *enterica* serovar Typhimurium, in which the major virulence genes had been knocked out, was used for transmission electron microscopy. For all experiments the

strains were grown aerobically for 18-20 hours with shaking (250 rpm) at 37°C in 5 mL tryptic soy broth (TSB, Difco, Sparks, MD). The bacterial concentration of each liquid culture was determined by serially diluting the culture in 0.1% (w/v) sterile peptone (Difco, Sparks, MD) and plating in duplicate on tryptic soy agar (TSA, Difco, Sparks, MD), incubated overnight at 37°C.

Plasma actuator construction. Surface dielectric barrier discharge (SDBD) actuators were constructed using 3.6 cm x 0.5 cm x 0.5 mm (*l* x *w* x *h*) copper electrodes (McMaster-Carr Supply Company, GA, USA) placed on both sides of 5 cm^2 x 0.127 mm Teflon dielectric barrier sheets (McMaster-Carr Supply Company, GA). Electrodes were staggered in relation to the dielectric material and grounded electrodes were insulated to prevent plasma ignition (Figure 1). SDBD actuators were operated with an input power of 13.5 V with a 50% duty cycle using a high voltage transformer (Information Unlimited, NH) and pulse width modulation (PWM) with an Arduino Uno microcontroller setup (Arduino LLC, Italy) was used to allow actuators to be on for 800 ms and off for 300 ms.

Plasma treatment conditions for RNA-seq analysis. To prepare the bacterial inoculum, 1 mL of liquid culture was centrifuged at 9,000 x g for 3 minutes and the cell pellet was re-suspended in 1 mL of 0.1% (w/v) sterile peptone. One hundred µL of the bacterial suspensions were spotted in 20-25 evenly spaced spots onto sterile 22 x 22 mm glass coverslips (approximately 10^8 CFU/coverslip, between 10^6 and 10^7 CFU/spot). Three replicates, each consisting of 10 inoculated coverslips placed in sterile 35 mm plastic petri dishes, were treated with SDBD cold plasma for 2 minutes at a distance of 1 cm from the actuators at room temperature (~25°C) and atmospheric pressure (Figure 1).

Plasma-treated and untreated control inoculated coverslips were washed by vortexing for 30 s in 10 mL 0.1% (w/v) sterile peptone in 50 mL conical tubes. The 10 coverslips of each replicate were washed individually in the same wash fluid in immediate succession following treatment of all coverslips for each replicate. The 10 untreated control coverslips for each of 3 replicates were washed in the same way after drying for 60 minutes. For enumeration, wash fluids were serially diluted 10-fold in 0.1% peptone and 100 µL of each dilution was plated in duplicate on TSA and incubated overnight at 37 °C. Bacterial inactivation due to cold plasma treatment was assessed by comparing the bacterial recovery rates from plasma-treated samples to those from untreated controls.

Isolation of bacterial RNA. Bacterial RNA was isolated from each10 mL volume of 0.1% peptone used to wash the 10 coverslips of each of 3 replicates of plasma-treated and untreated control samples. Wash fluids for each replicate were centrifuged at 9,000 x g for 3 minutes and the pellet was re-suspended in 400 µL of 0.1% peptone and then added to 800 µL of Qiagen RNA Protect Bacteria Reagent according to the manufacturer's protocol. RNA was then isolated using the Qiagen RNeasy minikit with an on-column RNase-free DNase treatment according to the manufacturer's protocol. The quantity and quality of isolated RNA was assessed using a NanoDrop ND-2000 spectrophotometer (Thermo Fisher Scientific) and an Agilent 2100 Bioanalyzer (Agilent Technologies). Since fragmented 23S rRNA is characteristically high in Enterobacteriaceae (Bhagwat *et al.,* 2013) and since the plasma treatment itself was suspected to contribute further to RNA degradation (Joshi *et al.,* 2011), DV_{200} values were used as a measure of RNA quality rather than the traditional RNA integrity number

(RIN). The DV_{200} value, a metric developed by Illumina that correlates to the percentage of RNA transcripts of at least 200 nucleotides in length, has been found to be more reliable than RIN for high quality RNA-sequencing (Illumina, 2014). Only samples with a DV_{200} value of 40 or higher were used for cDNA library preparation and sequencing.

Library preparation and sequencing. Enrichment of mRNA by rRNA depletion, fragmentation of mRNA, cDNA synthesis, and cDNA library preparation were done using the ScriptSeq Complete Kit (Bacteria) (Illumina), a kit designed specifically for low input concentrations and partially degraded RNA samples. Some RNA degradation was expected as a result of the plasma treatment and was confirmed by relatively low RIN numbers. Library quality was assessed using an Agilent 2100 Bioanalyzer and subsequently normalized and diluted according to Illumina protocols. All sample libraries were sequenced in a multiplexed manner on an Illumina HiSeq flow cell. Library preparation and sequencing was performed by Cofactor Genomics (St. Louis, MO).

Read mapping and differential gene expression analysis. Mapping and analysis of FastQ-files were performed using the CLC Genomics Workbench version 9 (Qiagen) using default mapping parameters. Although *Salmonella* Enteritidis strain H4639 was used in this study, sequence reads were mapped against *Salmonella enterica* subspecies *enterica* serovar Typhimurium strain LT2 (accession number NC_003197) rather than *Salmonella enterica* subspecies *enterica* serovar Enteritidis strain P125109 (accession number NC_011294) since strain LT2 is more fully annotated than strain P125109. When comparing read mapping against LT2 and P125109, mapping was almost identical for the annotations in common (data not shown). The average percentage of

reads mapped to the reference sequence was 84.44% (Table 1). Reproducibility of the read mapping was confirmed by comparing 3 replicates of each treatment and 3 replicates of each untreated control. Average gene fold changes were calculated from the combined replicates of each condition and genes were considered to be differentially expressed if the average fold change was greater than 1.5 or less than -1.5 with a false discovery rate (FDR) ≤ 0.05 and P value ≤ 0.01.

qRT-PCR analysis. Six genes (*pstA, phoR, phnU, fimA, eutD, invA*) differentially expressed ($P < 0.01$) by RNA-seq were selected for analysis by quantitative real-time reverse transcriptase-PCR (qRT-PCR). Primer3 software (Untergasser *et al.*, 2012) was used to design PCR primers, producing amplicon sizes between 100 and 200 bp (Table 2). The gene encoding GyrB was used as a reference for relative expression normalization using PCR primers previously described (Goudeau *et al.*, 2013). Total RNA was isolated as described above using a DNase I treatment (Qiagen) to eliminate genomic DNA contamination. cDNA was synthesized from total RNA with GoScript Reverse Transcriptase (Promega, Madison, WI) using gene-specific primers. SYBR Green qPCR was performed using 20 µL reaction mixtures containing 10 µL (1X) of Platinum SYBR Green real-time PCR SuperMix-UDG (Life Technologies, Foster City, CA), 1 µL (5 µM) of each primer, 1 µL of template cDNA, and 7µL of nuclease free water. A negative control (nuclease free water) and an RNA sample without reverse transcriptase were included to detect potential genomic DNA contamination for each reaction. qRT-PCR was performed in a Rotor-Gene 6000 thermocycler (Corbett Research, Sydney, Australia) with an initial hold for 10 min at 95°C, followed by 40 cycles at 95°C for 15 sec, 60°C for 15 sec, and 72°C for 60 sec. The relative expression

fold change for each gene was calculated using a method described previously (Pfaffl, 2001) using the equation $R = E_{\text{target}}^{\Delta\text{Cp target}}/E_{\text{ref}}^{\Delta\text{Cp ref}}$, where R is the relative expression ratio, E is the qPCR efficiency for each gene, "ref" refers the gyrB reference, "target" refers to target genes, and ΔCp equals control threshold crossing point (Cp) minus treatment Cp.

Transmission electron microscopy. Transmission electron microscopy (TEM) was used to visualize untreated control and plasma-treated *Salmonella* cells to evaluate the morphological effects of the plasma treatment. A suspension of approximately 10^7 CFU/mL of attenuated *Salmonella* Typhimurium cells prepared as described above were spotted onto carbon-backed gold TEM grids placed onto sterile glass coverslips, air-dried for 60 minutes, and treated with SDBD plasma actuators for 2, 4, and 6 minutes at a distance of 1 cm as described above. The cells were then negative stained with phosphotungstic acid and visualized with a JEOL JEM-2100 Scanning Transmission Electron Microscope System.

RESULTS

Global transcriptional changes resulting from SDBD treatment.

An average of 1.12 log CFU/mL reduction was observed after a 2 min treatment for 3 replicates. The SDBD plasma treatment of dried *Salmonella* Enteritidis cells on sterile glass coverslips resulted in significant transcriptional changes within surviving cells. Among 4,631 annotated genes of *Salmonella* Typhimurium LT2, 764 (16.5%) were differentially expressed by at least 1.5-fold. Interestingly, twice as many genes were

downregulated ≤ -1.5-fold (509) than upregulated ≥ 1.5-fold (255) (Tables 3 and 4). The fold changes of downregulated genes were also noticeably higher, down to -120-fold with 65 genes expressed ≤ -5.0-fold, whereas all upregulated genes were expressed less than 5.0-fold and only 43 were expressed ≥ 2.0-fold. Compared to similar transcriptomic studies using microarrays and bacterial cells in suspension or on growth media, the relatively moderate differential gene expression observed may be a result of the potential shadowing effect of the dried cells on the coverslips in which some cells are shielded from the reactive plasma-generated species by other cells and may have had less contact with the reactive species. For this reason, genes having statistically significant expression changes (*P*-value ≤ 0.01 and FDR *P*-value ≤ 0.05) as minor as 1.5-fold were further investigated in this study. Functional annotation clustering based on known or predicted gene ontology was performed using PANTHER 10.0 (Mi *et al.,* 2016). Co-regulated genes and gene pathways were identified by the KEGG Pathway database and STRING 10.0 (Szklarczyk *et al.,* 2015). Three major KEGG pathways were differentially expressed and helped reveal the primary responses of *Salmonella* to SDBD plasma and the potential mechanisms by which inactivation of Gram-negative bacteria may occur. As identified by STRING 10.0, "bacterial secretion system" was the single upregulated KEGG pathway, while "ribosome" and "biosynthesis of siderophore group nonribosomal proteins" were the two significantly downregulated KEGG pathways. The major functional groups to which differentially expressed genes were clustered were transport and localization, metabolism, regulatory functions, and pathogenesis (Table 5).

Transport and localization. At least 8 ATP-binding cassette (ABC) transporters were differentially expressed after SDBD plasma treatment when compared to untreated

control samples. More transport associated genes were downregulated than upregulated, with upregulated genes primarily associated with histidine (*hisMPQ*), arginine (*artQ*), sulfate (*cysCUW*) or dipeptide (*dppDF, sapDF*) transport. Genes involved in phosphate transport were among the most highly downregulated (Tables 4 and 5). The Pst operon (*pstSCAB-phoU*), encoding a high-affinity phosphate-specific ABC transport complex that rapidly imports inorganic phosphate into the cell (Van Veen, 1997; Aguena *et al.*, 2002), was downregulated by -11.5- to -50-fold. PstS is a periplasmic protein that binds inorganic phosphate, PstA and PstC form a membrane channel, and PstB is an ATPase that interacts with PstC and provides the energy for phosphate translocation (Hsieh and Wanner, 2010). The Pst system is regulated by the PhoB/PhoR two component system (both downregulated) in which the histidine-kinase PhoR phosphorylates PhoB in phosphate limited conditions and inactivates the regulator of the Pst operon, PhoU (Dong and Schellhorn, 2009; Hsieh and Wanner, 2010). Phosphorylated PhoB also regulates the *ugp* operon (*ugpABCE*), which encodes an ABC transport system for glycerol-3-phosphate and glycerophosphoryl diesters (Kasahara *et al.*, 1991), and the phnR to phnX operon (*phnSTUV*), importing 2-aminoethylphosphonate (Kim *et al.*, 2002). These operons are also activated under phosphate-limited conditions but were both downregulated after plasma treatment. Since all of these phosphate transport systems are directly regulated by the intracellular availability of phosphate (Hsieh and Wanner, 2010; Kasahara *et al.*, 1991; Kim *et al.*, 2002), a significant downregulation of these genes after plasma treatment indicates an evident increase in phosphate availability. Further evidence of increased phosphate concentrations is upregulation of *ppk*, encoding a polyphosphate kinase that generates long polyphosphate chains in the presence of abundant phosphate

availability (Crooke *et al.*, 1994). Since phosphate is a major constituent of the phospholipids that make up bacterial cell membranes, the increased phosphate availability after plasma treatment may be a result of lipid peroxidation and subsequent phospholipid oxidative degradation by plasma-generated RONS. Such downregulation of phosphate import systems may be experienced either by cells with damaged outer membranes due to lipid peroxidation or by undamaged cells adjacent to damaged or possibly lysed cells.

In addition to decreased phosphate transport, multiple cation trans-membrane transport genes for magnesium (*mgtAB, corA*), zinc (*zntAB*), and potassium (*kdpBC*) were significantly downregulated after plasma treatment (Table 5). Such downregulation may indicate a reduction in osmotic stress experienced by the dried *Salmonella* cells following treatment with SDBD plasma. Expression of the *kdp* operon is one of the primary responses to osmotic stress and well-studied in *E. coli*, allowing rapid intracellular accumulation of potassium ions (Roe *et al.*, 2000). Another well-known gene induced by osmotic stress, *osmB*, encoding an osmotically induced lipoprotein precursor (Boulanger *et al.*, 2005), was also highly downregulated by more than 20-fold (Table 5). Since no additional nutrients were added to plasma treated samples, an increased availability of necessary cations and alleviated osmotic stress was not expected and might be explained by lysis of surrounding cells by the plasma treatment and extensive cytosol leakage. This would alleviate the osmotic stress and nutrient limitation of cells that might not have been exposed to a damaging dose of plasma-generated reactive species. In addition to lipid peroxidation by RONS, SDBD actuators have been found to produce high amounts of negative ions that can travel a short distance from the actuator surface when the plasma is

generated in air (Pai *et al.,* 2015) and may be responsible for a trans-membrane ionic potential that may contribute to cell lysis (Lunov *et al.,* 2016).

Metabolism. The metabolic pathways for which genes were differentially expressed as a result of plasma treatment included ethanolamine utilization, colanic acid synthesis, and enterobactin synthesis. Phosphoethanolamine is one of the most abundant phospholipids in prokaryotes and is readily broken down by phosphodiesterases into ethanolamine and glycerol (Garsin, 2010). Ethanolamine can then be utilized as a carbon and nitrogen source, particularly as a precursor of acetyl-CoA (Jones and Turner, 1984). The ethanolamine utilization process, well-undersood for *Salmonella* Typhimurium, is encoded by 17 genes on a single *eut* operon, and often takes place within a cellular microcompartment termed the carboxysome (Kofoid *et al.,* 1999). Six of the 17 *eut* genes were significantly upregulated after plasma treatment (1.85 - 2.5-fold). EutS and EutN are carboxysome structural proteins, EutT is a cobalamin adenosyltransferase, EutD is a phosphotransacetylase, and EutP and EutQ are ethanolamine utilization proteins of unknown function (Garsin, 2010; Kofoid *et al.,* 1999). Increased expression of these genes in response to plasma treatment may indicate an increased availability of ethanolamine, as would be expected by significant lipid peroxidation. Interestingly, the propanediol utilization pathway, encoded by the similarly extensive *pdu* operon, which also requires cobalamin (vitamin B_{12}) and is often expressed in conjunction with the *eut* operon under anaerobic conditions, was not differentially expressed. In fact, the negative regulator of the *pdu* operon, PrpR, was moderately upregulated (1.93-fold). Increased utilization of ethanolamine but not propanediol further indicates a potential increase in ethanolamine concentration via lipid peroxidation following plasma treatment.

While ethanolamine utilization was upregulated, colanic acid biosynthesis was significantly downregulated. Colanic acid is a major capsular polysaccharide produced by several enteric bacteria in response to desiccation, temperature, acid, osmotic, or oxidative stress (Lee and Chen, 2004; Chen *et al.*, 2004; Navasa *et al.*, 2013). Colanic acid is synthesized in the cell interior and then exported to the cell surface. Expression of the colonic acid biosynthesis (*cps*) operon is positively activated by the Rcs phosphorelay system (Clarke, 2010), primarily through the action of RcsA and RcsB (Ebel and Trempy, 1999), the genes for both of which were downregulated by -7.99 and -1.78-fold, respectively. Accordingly, at least 14 of the 21 genes in the *cps* cluster were downregulated by as much as -32-fold (ranging from -1.68 – 31.78-fold). This significant downregulation also indicates a reduced stress response by the plasma-treated *Salmonella* cells. Again, this response may be a result of lipid peroxidation and lysis of the cells surrounding those from which RNA was isolated. Lysis of some cells may have the effect of creating a nutrient-rich microenvironment for the surviving cells with prevalent cellular and extracellular components, alleviating desiccation, osmotic, or oxidative stress.

Biosynthesis of enterobactin, a high-affinity siderophore that acquires extracellular iron for intracellular transport and subsequent utilization, was also significantly downregulated. The iron uptake system via enterobactin is composed of at least 11 proteins (Fleming *et al.*, 1983). The 7 proteins encoded by *entA*-*entG* synthesize enterobactin from chorismate and serine while the proteins encoded by *fepA, fepB, tonB,* and *fes* allow reception, internalization, and release of the iron molecule bound to enterobactin (Fleming *et al.*, 1983). Nine of these 11 genes were significantly

downregulated following SDBD plasma treatment, ranging from -1.54 to -8.61-fold. However, the enterobactin transport protein FepE was moderately upregulated 1.56-fold. It is expected that the presence of free iron within cells exposed to cold plasma would be a significant liability due to rapid production of the highly reactive hydroxyl radical by the Fenton reaction (Fang, 2004). Thus, it is expected that cells exposed to plasma-generated reactive species would downregulate iron sequestration mechanisms. However, based on the widespread downregulation of nutrient uptake pathways discussed above, the observed downregulation of the enterobactin iron uptake system may be a result of indirect alleviation of nutrient limitation or desiccation stress rather than direct oxidative stress caused by the plasma treatment.

Regulatory functions. Two component systems are well-conserved sensory systems consisting of a sensor and a transcriptional regulator that allow *Salmonella* to respond to environmental signals (Capra and Laub, 2012). Several two component systems were differentially expressed following plasma treatment, indicating a coordinated response to the treatment. The TtrR/TtrS two component system, allowing *Salmonella* to use tetrathionate as a terminal respiratory electron acceptor under anaerobic conditions (Hensel *et al.,* 1999), was downregulated due to increased expression of the response sensor gene *ttrR* (1.52-fold) and the response regulator gene *ttrS* (1.76-fold). Downregulation of tetrathionate utilization may indicate a reduction of anaerobic conditions or an increase in nutrient availability. The FlhD/FlhC two component system, positively regulating flagella biosynthesis (Stafford and Hughes, 2007), was upregulated after plasma treatment (2.04-fold for flhD and 2.05-fold for flhC) but none of the flagella biosynthesis genes for which it regulates were differentially

expressed. Similarly, the gene encoding the CsgD protein, a master regulator of curli biosynthesis, was upregulated 2.59-fold but only csgE and csgF were upregulated (2.85 and 1.97-fold, respectively) from the csgDEFG and csgBA operons (Barnhart and Chapman, 2006). Thus, it is unclear whether changes in flagella or curli biosynthesis, and therefore chemotaxis, were altered by plasma treatment.

Three other systems with regulatory roles in the maintenance of transmembrane proton motive force were differentially expressed. These included the *nuo* locus, the *hyb* operon, and the Psp system, encoding a proton-translocating NADH dehydrogenase, hydrogenase 2, and phage-shock-proteins, respectively. Such systems are of interest since SDBD plasma produces a high local concentration of negative ions and potentially produces hydrogen ions through the interaction of reactive species with water molecules on cell surfaces (Pai *et al.,* 2015). The *nuo* locus is composed of 14 genes that encode structural proteins associated with a type I NADH dehydrogenase, the first enzyme complex in the prokaryotic electron transport chain, that couples the oxidation of NADH to the generation of a proton motive force. NuoE, part of the peripheral fragment of the complex and exhibiting NADH dehydrogenase activity that oxidizes NADH to NAD^+, and NuoK, part of the membrane fragment that catalyzes ubiquinone (Q) to its reduced form (QH_2) (Falk-Krzesinski *et al.,* 1998), were upregulated by 1.5 and 1.6-fold, respectively. While the *nuo* locus proteins aid proton translocation into the cytosol, hydrogenases then reduce the amount of reactive protons by converting them to hydrogen (H_2). The *hyb* operon has 7 open reading frames associated with production of hydrogenase 2, which catalyzes H_2 production under glycerol fermentation (Trchounian and Trchounian, 2009). Six of the 7 genes in the *hyb* operon (*hybB, D, E, F, and G*) were

upregulated by 1.63 to 2.12-fold after plasma treatment, along with *hypA* (by 2.05-fold), which may be essential for proper hydrogenase function (Menon *et al.*, 1994). Also associated with maintenance of proton motive force in addition to other functions (Darwin, 2005), several phage-shock-proteins were also differentially expressed, albeit downregulated in contrast to the *nuo* locus and the *hyb* operon. Phage-shock-protein genes *pspA-D* and *pspG* were downregulated by -1.94 to -3.43-fold following plasma treatment. Downregulation of these genes may indicate a reduction in proton motive force as well as alleviation of osmotic or oxidative stress by the cells from which RNA was isolated after plasma treatment (Darwin, 2005).

Regulation of gene expression on a more global level was observed after plasma treatment by significant downregulation of multiple genes associated with ribosome structure and function. Identified as one of the major KEGG pathways differentially expressed in this study by STRING 10.0, this observation may explain the imbalanced downregulation of genes compared to upregulation after plasma treatment. Ribosome synthesis has been found to be downregulated in conditions where energy yield is restricted and in cases of essential nutrient starvation (Liu *et al.*, 2005; Hayes *et al.*, 2006). A majority of genes encoding ribosomal subunit proteins (*rps*, *rpm*, and *rpl*) were significantly downregulated following plasma treatment.

One of the most unexpected findings of this study was downregulation of multiple DNA repair related genes. It was suspected that SDBD plasma treatment would induce nucleic acid strand breaks due to the generation of reactive oxygen species and that DNA repair mechanisms would be upregulated, as previously observed in other studies (references). However, 9 genes of the SOS response pathway were downregulated

following plasma treatment (Table 5), along with the SOS response activator RecA (-5.21-fold) and regulator LexA (-1.78-fold) (Kreuzer, 2013). Other downregulated constituents of the SOS response were RuvA (-2.12-fold) and RuvB (-1.5-fold), Holliday junction ATPases, UvrA (-1.9-fold) and UvrB (-2.0-fold), parts of an excision repair endonuclease complex, and SulA (-6.5-fold), which is associated with cell cycle arrest (Kreuzer, 2013). Additionally, the oxidative stress related OxyR and SoxRS regulons, which are activated by increased intracellular hydrogen peroxide and superoxide concentrations, were not differentially expressed after plasma treatment. These data indicate that DNA damage and oxidative stress via increased RONS production by SDBD actuators may not have been major contributors to bacterial inactivation in this study.

Pathogenesis. Another unexpected finding of this study was increased expression of multiple pathogenicity genes, especially those located on *Salmonella* pathogenicity island 2 (SPI2) which encodes a type 3 secretion system (T3SS) and associated effector proteins. *Salmonella* Typhimurium has as many as 5 SPIs, each with slightly different functions in pathogenesis (Marcus *et al.,* 2000). SPI1 and SPI2 are among the most well-known and encode proteins that allow entry into and survival within eukaryotic host cells (Ochman *et al.,* 1996). SPI1 is primarily associated with invasion into epithelial cells whereas SPI2 is primarily associated with macrophage infection and survival within a *Salmonella*-containing vacuole (SCV) within macrophages (Marcus *et al.,* 2000; Chakraborty *et al.,* 2015). At least 39 genes associated with SPI1 and SPI2 were upregulated after plasma treatment, with as many as 26 contained within SPI2 (Figure 6). Accordingly, the major regulators of SPI2 expression, SsrA and SsrB (Xu and Hensel, 2010), were upregulated 1.78 and 1.61-fold, respectively. However, upon closer analysis

of the upregulation of these genes among the 3 treated replicates, increased expression of SPI1 and SPI2 was inconsistent. SPI1 was more upregulated in replicate 1 whereas SPI2 was more upregulated in replicates 2 and 3 (Figure 6). Despite this inconsistency, twice as many genes from SPI2 were upregulated as from SPI1, indicating a potentially more dominant role of SPI2 in response to SDBD treatment (Figure 6). Although the precise signals that trigger SPI2 expression when *Salmonella* cells interact with macrophages is not known, acidification of the bacterial cytoplasm by macrophages is thought to be a major contributor (Chakraborty *et al.*, 2015). Phosphate and magnesium ion limitation and hydrogen peroxide stress have also been found to play a key role in inducing expression of the SPI2-encoded T3SS and the secreted effector proteins, respectively (Kroger *et al.*, 2013). Since hydrogen peroxide stress was minimal in treated cells, acidification of the bacterial cytoplasm may be the major contributor to increased SPI2 expression resulting from plasma treatment by SDBD.

qRT-PCR validation of RNA-seq gene expression.

qRT-PCR analysis of 4 downregulated genes (*pstA, phoR, phnU, fimA*) and 2 upregulated genes (*eutD, invA*) was used to validate differential gene expression identified by RNA-seq. The fold change differences for each gene were similar for the two methods despite their inherent differences in sensitivity (Figure 6). However, the 2 genes upregulated by RNA-seq (*eutD, invA*) were found to be downregulated by qRT-PCR.

Cell surface effects of SDBD treatment.

TEM of SDBD plasma-treated and untreated *Salmonella* cells revealed noticeable morphological differences in the former, their significance increasing with increasing treatment times ranging from 2 to 6 min (Figure 5). Untreated cells had distinct boundaries when clustered in groups, with multiple cells undergoing mitosis and fimbriae clearly visible using high magnification (20,000-40,000 X). After 2 min treatments cell surfaces were visually darker and cell boundaries appeared more ragged, less uniform, and less distinct between individual cells. Substantially more debris was also visible in treated samples and may be a result of membrane damage and cytosol leakage. Membrane and cell surface damage became increasingly more evident after 4 and 6 min treatments, evidenced by darker staining, less distinct cellular margins, and increasing extracellular debris (Figure 5).

DISCUSSION

Despite the recent increased interest in cold plasma-induced bacterial inactivation for surface decontamination applications, there are no known studies evaluating the transcriptomic response of bacterial cells exposed to cold plasma outside of a suspension or growth promoting medium. Since bacterial cells on contaminated surfaces are usually in a low moisture environment with limited nutritional resources, it is necessary to evaluate how bacteria in such environments respond to cold plasma if this technology is to be used for surface decontamination applications. Thus, it was the goal of this study to evaluate the morphological and transcriptional changes that are induced in air-dried

bacterial cells by exposure to cold atmospheric plasma generated by SDBD. *Salmonella* was selected for this purpose since the transcriptomic response of *Salmonella* to desiccation stress has been well studied (Deng and Zhang, 2012; Gruzdev *et al.*, 2012; Finn *et al.*, 2014), allowing potential differentiation between desiccation-related stress and plasma-induced stress. Typical desiccation stress responses, such as increased nutrient import, osmoregulation, and fatty acid metabolism (Li *et al.*, 2012), were expected to be upregulated in untreated control samples and plasma treated samples. In contrast, genes associated with oxidative stress were expected to be overexpressed only in plasma treated samples as a result of the high concentration of RONS produced by SDBD plasma actuators. However, a very different response to SDBD plasma treatment was supported by the data.

Genes associated with phosphate uptake, cation uptake, osmoregulation, tetrathionate utilization, phage-shock proteins, and DNA damage repair were significantly downregulated by surviving cells after plasma treatment, indicating a reduction of cellular stress. In contrast, as many as 21 ribosomal subunit proteins were downregulated and as many as 39 pathogenicity associated proteins were upregulated after plasma treatment, indicating an increase in cellular stress. Differentially expressed metabolic pathways included upregulation of ethanolamine utilization and downregulation of colonic acid and enterobactin biosynthesis, associated with nutrient limitation, desiccation stress, and oxidative stress, respectively. It is important to note that the RNA isolation protocol used in this study only allowed isolation of RNA from intact cells and a suboptimal SDBD plasma treatment of only 2 minutes was used to ensure enough intact bacterial cells could be recovered after treatment. This method was chosen

so that the response of potentially injured but surviving cells could be investigated. However, due to a shadowing effect of multiple layers of dried cells on coverslip surfaces, many cells might not have been exposed to a damaging dose of cold plasma. Therefore, taking these apparently conflicting results and methodological considerations into account, it became evident that the identified differential gene expression was from minimally injured cells responding to membrane damage and lysis of adjacent cells rather than injured cells responding to the cold plasma treatment *per se*. Widespread and rapid lipid peroxidation of some cells resulting in degradation of membrane phospholipids, membrane damage, and cytosol leakage helps explain the results of this study. Phospholipid and lipopolysaccharide degradation would result in increased availability of phosphate, colonic acid, and ethanolamine, resulting in downregulation of phosphate uptake and colonic acid biosynthesis along with upregulation of ethanolamine utilization pathways. Cytosolic leakage would alleviate any osmotic stress experienced by adjacent cells and would also provide ample nutrient availability, allowing downregulation of important cation translocation pathways. TEM further confirmed rapid lipid peroxidation and membrane damage. However, stress responses were not completely eliminated as evidenced by downregulation of ribosomal subunit genes and upregulation of pathogenicity islands, resulting from mild oxidative stress or cytosolic acidification. Indeed, on a global transcriptomic scale, the observed response of *Salmonella* to SDBD plasma was similar to its observed response to acidic environments (Ryan *et al.*, 2015).

Thus, lipid peroxidation rather than DNA or protein damage is supported by the results of this study as the primary means of inactivation for dried Gram-negative bacteria on an inorganic surface. Plasma generated by DBD devices has long been used

in material science applications for surface modification of carbon-based polymers through an etching mechanism caused by random ion bombardment and physical deposition of RONS (Solis-Fernandez et al., 2010). The same mechanism can cause physical damage to living cellular surface structures, leading to partial or complete cell lysis and bacterial inactivation (Joshi *et al.,* 2011; Kvam *et al.,* 2012; Han *et al.,* 2016). TEM was an ideal method to visualize the superficial effects of SDBD in this study since TEM grids can be directly inoculated with a suspension of bacteria, air-dried, treated with SDBD plasma, stained, and immediately viewed with no fixation or surface modification steps that may alter physical cellular structures. TEM revealed rapid membrane damage and apparent cytosolic leakage following plasma treatment in accordance with results from other groups using membrane adsorption techniques (Kvam *et al.,* 2012), scanning electron microscopy (Lunov *et al.,* 2016; Han *et al.,* 2016), and TEM (Ma *et al.,* 2008; Venezia *et al.,* 2008) but with different plasma generation devices.

The type of device used to generate cold plasma and the means of delivery of plasma-produced reactive species has critical effects on the rates of bacterial inactivation and potentially on the mechanisms of inactivation (Mai-Prochnow *et al.,* 2014; Kvam *et al.,* 2012; Han *et al.*, 2016). Direct plasma treatments, in which plasma directly contacts treated bacterial cells, result in more rapid inactivation rates than indirect treatments, in which only the longer-lived plasma-produced reactive species interact with treated cells (Misra *et al.,* 2011; Kong *et al.,* 2009). SDBD has been described as a semi-direct plasma treatment method since cells do not interact directly with the plasma itself, as in volumetric DBD apparatuses, but reactive species produced by SDBD are actively pushed towards cells by the locally induced airflow. The active pushing of reactive

species by SDBD is in contrast to simple diffusion alone as in indirect methods (Pai *et al.,* 2015; Chapter 3). The results of this study further substantiate SDBD as a semi-direct plasma treatment method. The bacterial inactivation rate of SDBD is comparable to indirect methods (Misra et al., 2011; Niemira, 2012; Mai-Prochnow *et al.,* 2014), while the inactivation mechanisms of rapid lipid peroxidation and ion bombardment are comparable to direct methods (Lunov *et al.,* 2016; Han *et al.,* 2016). Inactivation rates by SDBD may be less than direct methods due to a lower concentration of short-lived reactive species and ions reaching cell surfaces. An increased role of lipid peroxidation by SDBD compared to indirect methods may be a result of cellular interaction with shorter-lived RONS (such as superoxide) and ions rather than only longer-lived RONS (such as ozone and nitric oxide).

Whether or not treated bacterial cells are in a liquid suspension during plasma treatment may also affect the rate and mechanism of inactivation (Kvam *et al.*, 2010). Most of the available methods for evaluating bacterial responses to antibacterial treatments require treatment of liquid suspensions. Accordingly, a majority of studies evaluating bacterial responses to cold plasma have been done using bacterial suspensions (Kong et al., 2009; Mai-Prochnow *et al.,* 2014). However, RONS produced by plasma rapidly interact with water molecules and are potentially altered in abundance and characteristics before contacting bacterial cells in a suspension. Moreover, alteration of the properties of the liquid, such as pH reduction (Pai *et al.,* 2015), may also indirectly affect bacterial inactivation mechanisms. All other known studies evaluating the transcriptomic response of bacterial cells to cold plasma treatment have used cells in suspension and have found differing emphases of oxidative stress responses. Sharma *et*

al. (2009) found DNA damage repair mechanisms and general oxidative stress responses to be upregulated after plasma treatment in *Escherichia coli,* whereas Winter *et al.* (2010) and Mols *et al.,* (2013) found upregulation of general oxidative stress responses only after plasma treatment in *Bacillus subtillus* and *Bacillus cereus*, respectively. In contrast, the results of this study indicate a general reduction of both oxidative stress responses and DNA damage repair. However, these results were observed among surviving cells that might not have been directly exposed to reactive plasma-produced species. Significant downregulation of ribosomal subunit proteins, an indication of a reduction in metabolic activity, and upregulation of pathogenicity associated genes may have been more a result of mild cytosolic acidification rather than widespread oxidative stress (Kroger *et al.,* 2013; Ryan *et al.,* 2015; Chakraborty *et al.,* 2015). Cytosolic acidification may instead have resulted from an indirect combination of oxidative stress from plasma-produced RONS and rapid cytosolic leakage and increased nutrient availability from adjacent cells. It is suspected that the importance of the role of lipid peroxidation in bacterial inactivation may not have been identified in previous transcriptomic studies as a result of treating cells in suspensions rather than dried cells directly exposed to the treatment.

In summary, the results of this study underscore lipid peroxidation as the primary means of Gram-negative bacterial inactivation on dried surfaces. This was observed by TEM and by the transcriptomic response by RNA-seq of surviving cells adjacent to inactivated cells that were lysed or had significant cell membrane damage as a result of the plasma treatment. This is the first known report evaluating the transcriptomic response of dried bacterial cells by RNA-seq exposed to SDBD plasma treatments. The results confirm that SDBD, as a semi-direct plasma treatment device, can rapidly

inactivate bacterial pathogens via production of RONS and has potential for a variety of surface decontamination applications. DNA damage repair processes and oxidative stress responses were alleviated rather than induced after plasma treatments of *Salmonella* cells experiencing desiccation stress on dried coverslips, indicating a minimal negative response of cells not exposed to plasma generated species and rapid inactivation and lysis of those that are. Accordingly, these results further support the claims that cold plasma treatments, especially by SDBD, inactivate bacterial cells by a multimodal physical means to which the potential for developing resistance may be minimal. Based on these results, SDBD is confirmed to be an efficient cold plasma generation and RONS delivery apparatus that overcomes many of the practical limitations of more complex and resource-intensive plasma apparatuses and has immediate potential for multiple surface decontamination or sterilization applications.

LITERATURE CITED

Aguena, M., Yagil, E., & Spira, B. (2002). Transcriptional analysis of the pst operon of Escherichia coli. *Molecular Genetics and Genomics, 268*(4), 518-524.

Ahlfeld, B., Li, Y., Boulaaba, A., Binder, A., Schotte, U., Zimmermann, J. L., . . . Klein, G. (2015). Inactivation of a Foodborne Norovirus Outbreak Strain with Nonthermal Atmospheric Pressure Plasma. *mBio, 6*(1).

Alkawareek, M. Y., Gorman, S. P., Graham, W. G., & Gilmore, B. F. (2014). Potential cellular targets and antibacterial efficacy of atmospheric pressure non-thermal plasma. *International Journal of Antimicrobial Agents, 43*(2), 154-160.

Barnhart, M. M., & Chapman, M. R. (2006). Curli Biogenesis and Function. *Annual review of microbiology, 60*, 131-147.

Bhagwat, A. A., Ying, Z. I., Karns, J., & Smith, A. (2013). Determining RNA quality for NextGen sequencing: some exceptions to the gold standard rule of 23S to 16S rRNA ratio§. *Microbiology Discovery, 1*(1).

Boulanger, A., Francez-Charlot, A., Conter, A., Castanié-Cornet, M.-P., Cam, K., & Gutierrez, C. (2005). Multistress Regulation in Escherichia coli: Expression of osmB Involves Two Independent Promoters Responding either to σS or to the RcsCDB His-Asp Phosphorelay. *Journal of Bacteriology, 187*(9), 3282-3286.

Capra, E. J., & Laub, M. T. (2012). The Evolution of Two-Component Signal Transduction Systems. *Annual review of microbiology, 66*, 325-347.

Chakraborty, S., Mizusaki, H., & Kenney, L. J. (2015). A FRET-Based DNA Biosensor Tracks OmpR-Dependent Acidification of <italic>Salmonella</italic> during Macrophage Infection. *PLoS Biol, 13*(4), e1002116.

Chen, J., Lee, S. M., & Mao, Y. (2004). Protective effect of exopolysaccharide colanic acid of Escherichia coli O157:H7 to osmotic and oxidative stress. *International Journal of Food Microbiology, 93*(3), 281-286.

Clarke, D. J. (2010). The Rcs phosphorelay: more than just a two-component pathway. *Future Microbiology, 5*(8), 1173-1184.

Crooke, E., Akiyama, M., Rao, N. N., & Kornberg, A. (1994). Genetically altered levels of inorganic polyphosphate in Escherichia coli. *J Biol Chem, 269*(9), 6290-6295.

Darwin, A. J. (2005). The phage-shock-protein response. *Molecular Microbiology, 57*(3), 621-628.

Deng, X., Li, Z., & Zhang, W. (2012). Transcriptome sequencing of Salmonella enterica serovar Enteritidis under desiccation and starvation stress in peanut oil. *Food Microbiology, 30*(1), 311-315.

Dong, T., & Schellhorn, H. E. (2009). Global effect of RpoS on gene expression in pathogenic Escherichia coli O157:H7 strain EDL933. [journal article]. *BMC Genomics, 10*(1), 1-17.

Ebel, W., & Trempy, J. E. (1999). Escherichia coli RcsA, a positive activator of colanic acid capsular polysaccharide synthesis, functions To activate its own expression. *J Bacteriol, 181*(2), 577-584.

Falk-Krzesinski, H. J., & Wolfe, A. J. (1998). Genetic Analysis of the nuo Locus, Which Encodes the Proton-Translocating NADH Dehydrogenase inEscherichia coli. *Journal of Bacteriology, 180*(5), 1174-1184.

Fang, F. C. (2004). Antimicrobial reactive oxygen and nitrogen species: concepts and controversies. *Nat Rev Microbiol, 2*(10), 820-832.

Finn, S., McClure, P., Amézquita, A., & Fanning, S. (2014). Transcriptomic Responses of Salmonella Species to Desiccation and Low-Moisture Environments: Extending Our Knowledge of How Bacteria Cope with Low-Moisture Stress. In B. J. Gurtler, P. M. Doyle & L. J. Kornacki (Eds.), *The Microbiological Safety of Low Water Activity Foods and Spices* (pp. 49-66). New York, NY: Springer New York.

Fleming, T. P., Nahlik, M. S., & McIntosh, M. A. (1983). Regulation of enterobactin iron transport in Escherichia coli: characterization of ent::Mu d(Apr lac) operon fusions. *J Bacteriol, 156*(3), 1171-1177.

Garsin, D. A. (2010). Ethanolamine utilization in bacterial pathogens: roles and regulation. *Nat Rev Micro, 8*(4), 290-295.

Gruzdev, N., McClelland, M., Porwollik, S., Ofaim, S., Pinto, R., & Saldinger-Sela, S. (2012). Global Transcriptional Analysis of Dehydrated Salmonella enterica Serovar Typhimurium. *Applied and Environmental Microbiology, 78*(22), 7866-7875.

Han, L., Patil, S., Boehm, D., Milosavljević, V., Cullen, P. J., & Bourke, P. (2015). Mechanism of Inactivation by High Voltage Atmospheric Cold Plasma Differs between Escherichia coli and Staphylococcus aureus. *Applied and Environmental Microbiology*.

Hayes, E. T., Wilks, J. C., Sanfilippo, P., Yohannes, E., Tate, D. P., Jones, B. D., . . . Slonczewski, J. L. (2006). Oxygen limitation modulates pH regulation of catabolism and hydrogenases, multidrug transporters, and envelope composition in Escherichia coli K-12. *BMC Microbiology, 6*, 89-89.

Hensel, M., Hinsley, A. P., Nikolaus, T., Sawers, G., & Berks, B. C. (1999). The genetic basis of tetrathionate respiration in Salmonella typhimurium. *Mol Microbiol, 32*(2), 275-287.

Hsieh, Y.-J., & Wanner, B. L. (2010). Global regulation by the seven-component Pi signaling system. *Current Opinion in Microbiology, 13*(2), 198-203.

Huaiyu Mi, Sagar Poudel, Anushya Muruganujan John T Casagrande and Paul D. Thomas *Nucl. Acids Res. (2016)*

Illumina. (2014). Evaluating RNA Quality from FFPE Samples. Available at: http://www.illumina.com/documents/products/technotes/technote-truseq-rna-access.pdf

Jones, P. W., & Turner, J. M. (1984). Interrelationships between the enzymes of ethanolamine metabolism in Escherichia coli. *J Gen Microbiol, 130*(2), 299-308.

Joshi, S. G., Cooper, M., Yost, A., Paff, M., Ercan, U. K., Fridman, G., Brooks, A. D. (2011). Nonthermal dielectric-barrier discharge plasma-induced inactivation involves oxidative DNA damage and membrane lipid peroxidation in Escherichia coli. *Antimicrob Agents Chemother, 55*(3), 1053-1062.

Kang, D. H., & Fung, D. Y. (2000). Application of thin agar layer method for recovery of injured Salmonella typhimurium. *Int J Food Microbiol, 54*(1-2), 127-132.

Kim, A. D., Baker, A. S., Dunaway-Mariano, D., Metcalf, W. W., Wanner, B. L., & Martin, B. M. (2002). The 2-aminoethylphosphonate-specific transaminase of the 2-aminoethylphosphonate degradation pathway. *J Bacteriol, 184*(15), 4134-4140.

Klämpfl, T.G., G. Isbary, T. Shimizu, Y.F. Li, J.L. Zimmermann, W. Stolz, & J.U. Schmidt. (2012). Cold Atmospheric Air Plasma Sterilization against Spores and Other Microorganisms of Clinical Interest. *Applied and Environmental Microbiology.* 78(15):5077-5082.

Kofoid, E., Rappleye, C., Stojiljkovic, I., & Roth, J. (1999). The 17-gene ethanolamine (eut) operon of Salmonella typhimurium encodes five homologues of carboxysome shell proteins. *J Bacteriol, 181*(17), 5317-5329.

Kong, M. G., Kroesen, G., Morfill, G., Nosenko, T., Shimizu, T., Dijk, J. v., & Zimmermann, J. L. (2009). Plasma medicine: an introductory review. *New Journal of Physics, 11*(11), 115012.

Kreuzer, K. N. (2013). DNA Damage Responses in Prokaryotes: Regulating Gene Expression, Modulating Growth Patterns, and Manipulating Replication Forks. *Cold Spring Harbor Perspectives in Biology, 5*(11).

Kröger, C., Colgan, A., Srikumar, S., Händler, K., Sivasankaran, Sathesh K., Hammarlöf, Disa L., . . . Hinton, Jay C. D. An Infection-Relevant Transcriptomic Compendium for Salmonella enterica Serovar Typhimurium. *Cell Host & Microbe, 14*(6), 683-695.

Kvam, E., Davis, B., Mondello, F., & Garner, A. L. (2012). Nonthermal atmospheric plasma rapidly disinfects multidrug-resistant microbes by inducing cell surface damage. *Antimicrob Agents Chemother, 56*(4), 2028-2036.

Laroussi, M. (2005). Low Temperature Plasma-Based Sterilization: Overview and State-of-the-Art. *Plasma Processes and Polymers, 2*(5), 391-400.

Lee, S. M., & Chen, J. (2004). Survival of Escherichia coli O157:H7 in set yogurt as influenced by the production of an exopolysaccharide, colanic acid. *J Food Prot, 67*(2), 252-255.

Li, H., Bhaskara, A., Megalis, C., & Tortorello, M. L. (2012). Transcriptomic Analysis of Salmonella Desiccation Resistance. *Foodborne Pathogens and Disease, 9*(12), 1143-1151.

Li, Y.H., Y. Wu, H.M. Song, H. Liang and M. Jia . (2011). Plasma Flow control. *In* M. Mulder (Ed.). Aeronautics and Astronautics. InTech publishing, Rijeka, Croatia.

Liu, M., Durfee, T., Cabrera, J. E., Zhao, K., Jin, D. J., & Blattner, F. R. (2005). Global transcriptional programs reveal a carbon source foraging strategy by Escherichia coli. *J Biol Chem, 280*(16), 15921-15927.

Lu, H., Patil, S., Keener, K. M., Cullen, P. J., & Bourke, P. (2014). Bacterial inactivation by high-voltage atmospheric cold plasma: influence of process parameters and effects on cell leakage and DNA. *Journal of Applied Microbiology, 116*(4), 784-794.

Lunov, O., Zablotskii, V., Churpita, O., Jäger, A., Polívka, L., Syková, E., Kubinová, Š. (2016). The interplay between biological and physical scenarios of bacterial death induced by non-thermal plasma. *Biomaterials, 82*, 71-83.

Ma, Y., Zhang, G. J., Shi, X. M., Xu, G. M., & Yang, Y. (2008). Chemical Mechanisms of Bacterial Inactivation Using Dielectric Barrier Discharge Plasma in Atmospheric Air. *IEEE Transactions on Plasma Science, 36*(4), 1615-1620.

Ma, Y., Ha, C. S., Hwang, S. W., Lee, H. J., Kim, G. C., Lee, K.-W., & Song, K. (2014). Non-Thermal Atmospheric Pressure Plasma Preferentially Induces Apoptosis in p53-Mutated Cancer Cells by Activating ROS Stress-Response Pathways. *PLoS ONE, 9*(4), e91947.

Marcus, S. L., Brumell, J. H., Pfeifer, C. G., & Finlay, B. B. (2000). Salmonella pathogenicity islands: big virulence in small packages. *Microbes and Infection, 2*(2), 145-156.

Mai-Prochnow, A., A.B. Murphy, K.M. McLean, M.G. Kong, & K. Ostrikov. (2014). Atmospheric pressure plasmas: Infection control and bacterial responses. *International Journal of Antimicrobial Agents*. *43*(6), 508-517.

Menon, N. K., Chatelus, C. Y., Dervartanian, M., Wendt, J. C., Shanmugam, K. T., Peck, H. D., Jr., & Przybyla, A. E. (1994). Cloning, sequencing, and mutational analysis of the hyb operon encoding Escherichia coli hydrogenase 2. *J Bacteriol, 176*(14), 4416-4423.

Misra, N.N., B.K. Tiwari, K.S.M.S. Raghavarao, & P.J. Cullen. (2011). Nonthermal plasma inactivation of food-borne pathogens. *Food Engineering Reviews.* 3(3-4):159-170.

Mols, M., Mastwijk, H., Nierop Groot, M., & Abee, T. (2013). Physiological and transcriptional response of Bacillus cereus treated with low-temperature nitrogen gas plasma. *Journal of Applied Microbiology, 115*(3), 689-702.

Navasa, N., Rodríguez-Aparicio, L., Ferrero, Miguel Á., Monteagudo-Mera, A., & Martínez-Blanco, H. (2013). Polysialic and colanic acids metabolism in Escherichia coli K92 is regulated by RcsA and RcsB. *Bioscience Reports, 33*(3).

Niemira, B.A. (2012). Cold Plasma Decontamination of Foods. *Annual Review of Food Science and Technology.* 3(1):125-142.

Niemira, B. A., Boyd, G., & Sites, J. (2014). Cold Plasma Rapid Decontamination of Food Contact Surfaces Contaminated with Salmonella Biofilms. *Journal of Food Science, 79*(5), M917-M922.

Ochman, H., Soncini, F. C., Solomon, F., & Groisman, E. A. (1996). Identification of a pathogenicity island required for Salmonella survival in host cells. *Proc Natl Acad Sci U S A, 93*(15), 7800-7804.

Pai, K. K., Singarapu, K., Jacob, J. D., & Madihally, S. V. (2015). Dose Dependent Selectivity and Response of Different Types of Mammalian Cells to Surface Dielectric Barrier Discharge (SDBD) Plasma. *Plasma Processes and Polymers, 12*(7), 666-677.

Pfaffl, M. W. (2001). A new mathematical model for relative quantification in real-time RT–PCR. *Nucleic Acids* Research, *29*(9), e45.

Puac, Z. L. Petrovic, G. Malovic, A. Dordevic, S. Zivkovic, Z. Giba, & D. Grubisic. (2006). Measurements of voltage–current characteristics of a plasma needle and its effect on plant cells. *J. Phys. D, Appl. Phys.*, 39(16), 3514–3519.

Roe, A. J., McLaggan, D., O'Byrne, C. P., & Booth, I. R. (2000). Rapid inactivation of the Escherichia coli Kdp K+ uptake system by high potassium concentrations. *Molecular Microbiology, 35*(5), 1235-1243.

Ryan, D., Pati, N. B., Ojha, U. K., Padhi, C., Ray, S., Jaiswal, S., . . . Suar, M. (2015). Global transcriptome and mutagenic analyses of the acid tolerance response of Salmonella enterica serovar Typhimurium. *Appl Environ Microbiol, 81*(23), 8054-8065.

Solís-Fernández, P., Paredes, J. I., Cosío, A., Martínez-Alonso, A., & Tascón, J. M. D. (2010). A comparison between physically and chemically driven etching in the oxidation of graphite surfaces. *Journal of Colloid and Interface Science, 344*(2), 451-459.

Stafford, G. P., & Hughes, C. (2007). Salmonella typhimurium flhE, a conserved flagellar regulon gene required for swarming. *Microbiology, 153*(2), 541-547.

Stoffels, E., Sladek, R. E. J., Kieft, I. E., Kersten, H., & Wiese, R. (2004). Power outflux from the plasma: an important parameter in surface processing. *Plasma Physics and Controlled Fusion, 46*(12B), B167. Dec. 2004.

Szklarczyk, D., Franceschini, A., Wyder, S., Forslund, K., Heller, D., Huerta-Cepas, J., . . . von Mering, C. (2015). STRING v10: protein-protein interaction networks, integrated over the tree of life. *Nucleic Acids Res, 43*, 28.

Trchounian, K., & Trchounian, A. (2009). Hydrogenase 2 is most and hydrogenase 1 is less responsible for H2 production by Escherichia coli under glycerol fermentation at neutral and slightly alkaline pH. *International Journal of Hydrogen Energy, 34*(21), 8839-8845.

Untergasser A, Cutcutache I, Koressaar T, Ye J, Faircloth BC, Remm M, and Rozen SG. (2012). Primer3 - new capabilities and interfaces. *Nucleic Acids Research.* 40(15):e115.

*van Veen, H. W. 1997***.** Phosphate transport in prokaryotes: molecules, mediators and mechanisms. *Antonie van Leeuwenhoek 72:****299***-315.

Venezia, R., Orrico, M., Houston, E., Yin, S., & Naumova, Y. (2008). Lethal Activity of Nonthermal Plasma Sterilization Against Microorganisms. *Infection Control and Hospital Epidemiology, 29*(5), 430-436.

Wang, Z., M. Gerstein, and M. Snyder. (2009). RNA-Seq: a revolutionary tool for transcriptomics. *Nat Rev Genet.* 10(1):57-63.

Weiss, M., Gümbel, D., Hanschmann, E.-M., Mandelkow, R., Gelbrich, N., Zimmermann, U., Stope, M. B. (2015). Cold Atmospheric Plasma Treatment Induces Anti-Proliferative Effects in Prostate Cancer Cells by Redox and Apoptotic Signaling Pathways. *PLoS ONE, 10*(7), e0130350.

Winter, T., Winter, J., Polak, M., Kusch, K., Mäder, U., Sietmann, R., . . . Kusch, H. (2011). Characterization of the global impact of low temperature gas plasma on vegetative microorganisms. *Proteomics, 11*(17), 3518-3530.

Xu, X., & Hensel, M. (2010). Systematic Analysis of the SsrAB Virulon of Salmonella enterica. *Infection and Immunity, 78*(1), 49-58.

Zhang, X., Liu, D., Zhou, R., Song, Y., Sun, Y., Zhang, Q., & Yang, S.-Z. (2014). Atmospheric cold plasma jet for plant disease treatment. *Applied Physics Letters, 104*(4), 043702.

Ziuzina, D., S. Patil, P.J. Cullen, K.M. Keener, & P. Bourke. (2014). Atmospheric cold plasma inactivation of *Escherichia coli, Salmonella enterica* serovar Typhimurium *and Listeria monocytogenes* inoculated on fresh produce. *Food Microbiology.* 42(0):109-116.

Ziuzina, D., Patil, S., Cullen, P. J., Boehm, D., & Bourke, P. (2014b). Dielectric Barrier Discharge Atmospheric Cold Plasma for Inactivation of Pseudomonas aeruginosa Biofilms. *4*(1-4), 137-152.

TABLES

Table 1. Total number of cDNA sequence reads, number of mapped reads, and percentage of mapped reads for each treated and untreated control replicate.

Sample	Total number of reads	Number of mapped reads	Percentage of mapped reads
Control (1)	22,819,401	19,088,383	83.65
Control (2)	22,679,322	19,214,731	84.72
Control (3)	23,616,195	19,999,609	84.69
Treated (1)	21,718,998	17,986,809	82.82
Treated (2)	23,288,150	20,022,770	85.98
Treated (3)	22,325,699	18,933,845	84.81

Table 2. Target genes, gene function, and primer pair sequences used for qRT-PCR validation of differential gene expression observed by RNA-seq.

Gene name	Function	Primer pair (5'-3')
pstA	phosphate ABC transporter permease subunit	F: GAATCCCGTCGCAAGATG R: GGCGTCATTTCGGTAAACAG
phoR	sensory kinase	F: TCATTTGGTGCTCAATACCG R: CAATACCGTCAAGGGCGTA
phnU	2-aminoethylphosphonate ABC transporter permease	F: CTGCCGATGATGGTTTACAG R: CAGGCGATAGAGGGAGAACA
fimA	type-1 fimbrial protein subunit A	F: GCTGGCTGTCTCCTCTGC R: AGCGTATTGGTGCCTTCAAC
eutD	phosphotransacetylase	F: CGACCCACACAGCAACCT R: CCTGCGATACACACATCAGC
invA	invasion protein	F: TCCAACAATCCATCAGCAAG R: ACCGCCAGACAGTGGTAAAG
gyrB	DNA gyrase subunit B	F: CGCCGATAACTCCGTGTCCGTAAC R: CGACAGAGCGTTGACTACCGAGAC

Table 3. Functional description, fold change, and statistical significance of genes upregulated by 1.5-fold or greater after SDBD plasma treatment.

Gene name	Function[a]	Fold change	Log_2 fold change	P-value	FDR p-value
agp	glucose-1-phosphatase/inositol phosphatase	1.5	0.59	0.01	0.05
aidB	DNA alkylation damage repair protein	1.58	0.66	2.38E-03	0.02
argR	arginine repressor	1.65	0.72	1.39E-03	0.01
aroD	3-dehydroquinase	1.5	0.58	1.78E-03	0.01
aroG	3-deoxy-7-phosphoheptulonate synthase	1.77	0.82	1.73E-03	0.01
artQ	arginine ABC transporter permease ArtQ	1.5	0.58	3.37E-03	0.02
bssR	biofilm formation regulatory protein BssR	1.6	0.68	3.54E-04	3.55E-03
cafA	RNase G	1.59	0.67	1.80E-03	0.01
cbiJ	cobalt-precorrin-6x reductase	1.59	0.67	2.10E-03	0.02
cbiO	cobalt ABC transporter ATP-binding protein CbiO	1.6	0.67	2.18E-03	0.02
cbiQ	cobalt ABC transporter permease CbiQ	1.78	0.83	1.52E-06	2.88E-05
ccmA_1		1.96	0.97	4.72E-03	0.03
celA	N'-diacetylchitobiose-specific transporter subunit IIB	1.57	0.65	4.23E-04	4.18E-03
celB	N'-diacetylchitobiose-specific transporter subunit IIC	1.56	0.64	4.32E-04	4.24E-03
celD	cel operon transcriptional repressor	1.92	0.94	1.05E-06	2.07E-05
celF	6-phospho-beta-glucosidase	1.57	0.65	1.42E-03	0.01
citC	[citrate (pro-3S)-lyase] ligase	1.58	0.66	6.38E-04	5.89E-03
cobT	nicotinate-nucleotide--dimethylbenzimidazole phosphoribosyltransferase	1.55	0.63	5.17E-04	4.94E-03
cobU	adenosylcobinamide kinase/adenosylcobinamide phosphate guanyltransferase	1.52	0.6	7.25E-04	6.59E-03
csgD	DNA-binding transcriptional regulator CsgD	2.59	1.37	6.64E-11	2.29E-09
csgE	curli production assembly/transport protein CsgE	2.85	1.51	1.75E-12	7.58E-11
csgF	curli production assembly/transport protein CsgF	1.97	0.98	7.86E-07	1.60E-05
cspB	cold-shock protein	2.11	1.08	3.87E-05	5.17E-04
cspD	stress response protein	1.67	0.74	1.44E-04	1.64E-03
cysC	adenylyl-sulfate kinase	1.5	0.59	9.21E-03	0.05
cysU	sulfate/thiosulfateABC transporter permease CysU	1.58	0.66	7.43E-03	0.04
cysW	sulfate/thiosulfate ABC transporter permease CysW	1.62	0.69	5.28E-03	0.03
dcuR	transcriptional regulator	1.59	0.66	4.92E-03	0.03

dppC	dipeptide ABC transporter permease DppC	1.66	0.73	3.23E-04	3.27E-03
dppD	dipeptide ABC transporter ATP-binding subunit DppD	1.8	0.85	7.28E-04	6.60E-03
dppF	dipeptide ABC transporter ATP-binding subunit DppF	1.68	0.75	8.38E-03	0.05
eutD	phosphotransacetylase EutD	1.89	0.92	3.32E-03	0.02
eutN	microcompartment shell protein EutN	1.82	0.86	3.18E-03	0.02
eutP	ethanolamine utilization protein EutP	2.34	1.23	1.43E-07	3.29E-06
eutQ	ethanolamine utilization protein EutQ	2.03	1.02	4.91E-04	4.74E-03
eutS	carboxysome structural protein EutS	2.5	1.32	1.20E-08	3.26E-07
eutT	cobalamin adenosyltransferase EutT	2.11	1.08	1.20E-03	9.82E-03
fepE	ferric enterobactin transport protein	1.56	0.64	1.32E-04	1.53E-03
flhC	transcriptional regulator FlhC	2.05	1.04	2.35E-05	3.39E-04
flhD	transcriptional regulator FlhD	2.04	1.03	5.44E-06	8.66E-05
fliE	flagellar hook-basal body complex protein FliE	1.65	0.72	8.15E-04	7.22E-03
fliF	flagellar MS-ring protein FliF	1.73	0.79	9.80E-06	1.50E-04
fliG	flagellar motor switch protein FliG	1.56	0.64	2.12E-03	0.02
fre	NAD(P)H-flavin reductase	1.56	0.64	3.24E-04	3.27E-03
ftsW	lipid II flippase FtsW	1.5	0.59	1.24E-03	0.01
galS	HTH-type transcriptional regulator GalS	1.57	0.65	1.65E-03	0.01
gpsA	glycerol-3-phosphate dehydrogenase	1.59	0.67	9.76E-03	0.05
hilD	transcriptional regulator HilD	1.5	0.59	3.16E-03	0.02
hisM	histidine ABC transporter permease HisM	2	1	2.26E-06	4.08E-05
hisP	histidine ABC transporter ATP-binding protein HisP	1.81	0.86	1.80E-04	2.01E-03
hisQ	histidine ABC transporter permease HisQ	1.84	0.88	1.73E-03	0.01
hutC	histidine utilization repressor	1.53	0.61	8.07E-04	7.16E-03
hutG	formimidoylglutamase	1.63	0.71	7.97E-05	9.82E-04
hutI	imidazolonepropionase	1.58	0.66	3.27E-03	0.02
hybB	hydrogenase 2 b cytochrome subunit	1.63	0.71	1.08E-03	8.97E-03
hybD	hydrogenase 2 maturation endopeptidase	1.89	0.92	5.09E-05	6.60E-04
hybE	hydrogenase 2-specific chaperone	2.01	1.01	2.82E-08	7.26E-07
hybF	hydrogenase nickel incorporation protein HybF	2.04	1.03	9.53E-08	2.27E-06
hybG	hydrogenase 2 accessory protein HypG	2.12	1.08	5.17E-10	1.63E-08
hypA	hydrogenase nickel incorporation protein	2.05	1.03	1.13E-03	9.27E-03
iacP	acyl carrier protein	1.75	0.8	4.27E-05	5.64E-04
idnT	GntP family L-idonate transport protein	1.52	0.6	4.98E-04	4.79E-03
ilvL	ilvG operon leader peptide	1.72	0.78	6.31E-04	5.85E-03
invA	invasion protein InvA	1.66	0.74	1.08E-04	1.29E-03
invB	surface presentation of antigens protein SpaK	1.86	0.9	4.80E-05	6.24E-04
invE	invasion protein InvE	1.7	0.77	3.99E-05	5.31E-04
invI	surface presentation of antigens protein	1.75	0.81	1.36E-04	1.57E-03

	SpaM				
ksgA	rRNA small subunit methyltransferase A	1.51	0.59	4.56E-03	0.03
manX	PTS system mannose-specific transporter subunit IIAB	1.65	0.72	1.49E-03	0.01
mig-14	transcriptional activator	1.95	0.96	1.98E-03	0.01
napF	ferredoxin-type protein	1.5	0.59	4.51E-03	0.03
nuoE	NADH-quinone oxidoreductase subunit E	1.6	0.68	7.72E-03	0.04
nuoK	NADH-quinone oxidoreductase subunit K	1.5	0.59	1.71E-03	0.01
orfX	pathogenicity island-encoded protein	1.7	0.76	1.93E-04	2.14E-03
pgtB	phosphoglycerate transport system sensor protein PgtB	1.53	0.61	0.01	0.05
pheV		1.85	0.89	6.43E-03	0.04
pipD	dipeptidase	1.62	0.7	9.62E-03	0.05
pmrD	signal transduction protein PmrD	1.57	0.65	2.45E-04	2.59E-03
pocR	transcriptional regulator PocR	1.53	0.61	3.12E-03	0.02
ppk	polyphosphate kinase	1.6	0.68	5.55E-04	5.24E-03
ppx	exopolyphosphatase	1.55	0.63	2.92E-04	3.01E-03
pqaA	PhoPQ-regulated protein	1.64	0.71	3.63E-05	4.86E-04
prgH	secretion system protein PrgH	1.59	0.67	1.15E-03	9.39E-03
prgJ	secretion system protein PrgJ	1.61	0.69	1.03E-03	8.65E-03
prgK	secretion system lipoprotein PrgK	1.79	0.84	2.99E-04	3.06E-03
prpR	propionate catabolism operon regulatory protein	1.93	0.95	5.90E-05	7.57E-04
res	type III restriction-modification system DNA helicase	1.57	0.65	4.22E-03	0.03
rfaL	O-antigen ligase	1.75	0.8	1.07E-03	8.93E-03
rfbN	O antigen biosynthesis rhamnosyltransferase RfbN	1.5	0.59	8.98E-03	0.05
rfbU	O-antigen biosynthesis protein RfbU	1.52	0.6	6.47E-04	5.97E-03
rfbX	O-antigen transferase	2.22	1.15	3.10E-04	3.14E-03
rfc	O-antigen polymerase	1.8	0.85	3.77E-07	8.16E-06
rimJ	ribosomal-protein-S5-alanine N-acetyltransferase	1.8	0.85	3.28E-06	5.56E-05
sapD	peptide ABC transporter ATP-binding protein SapD	1.51	0.59	2.03E-04	2.22E-03
sapF	peptide ABC transporter ATP-binding protein SapF	1.55	0.63	2.74E-03	0.02
sicP	chaperone protein SicP	1.95	0.96	1.14E-06	2.23E-05
sigE	chaperone protein SigE	1.5	0.58	1.81E-03	0.01
sirB2	regulatory protein SirB2	1.53	0.62	1.35E-03	0.01
sopD	secreted effector protein SopD	1.59	0.67	4.59E-03	0.03
spaP	surface presentation of antigens protein SpaP	2.12	1.08	6.98E-10	2.13E-08
spaQ	surface presentation of antigens protein SpaQ	1.64	0.72	4.55E-04	4.45E-03
spaR	surface presentation of antigens protein	1.89	0.92	1.60E-04	1.80E-03

	SpaR				
spaS	surface presentation of antigens protein SpaS	2.28	1.19	7.91E-07	1.60E-05
ssaB	secretion system apparatus protein SsaB	2.58	1.37	5.79E-07	1.21E-05
ssaC	secretion system apparatus outer membrane protein SsaC	1.82	0.86	2.91E-05	4.03E-04
ssaD	secretion system apparatus protein SsaD	2.24	1.16	1.62E-08	4.29E-07
ssaE	secretion system effector SsaE	2.32	1.21	5.41E-07	1.14E-05
ssaG	secretion system apparatus protein SsaG	2.69	1.43	1.95E-11	7.35E-10
ssaH	secretion system apparatus protein SsaH	2.43	1.28	2.24E-12	9.35E-11
ssaI	secretion system apparatus protein SsaI	1.77	0.82	2.35E-04	2.51E-03
ssaJ	secretion system apparatus lipoprotein SsaJ	1.93	0.95	2.27E-04	2.43E-03
ssaK	secretion system apparatus protein SsaK	2.36	1.24	1.54E-10	5.09E-09
ssaL	secretion system apparatus protein SsaL	1.93	0.95	1.94E-04	2.14E-03
ssaM	secretion system apparatus protein SsaM	2.09	1.07	2.27E-04	2.43E-03
ssaN	secretion system apparatus ATP synthase SsaN	1.9	0.93	1.29E-03	0.01
ssaO	secretion system apparatus protein SsaO	3.23	1.69	0	0
ssaP	secretion system apparatus protein SsaP	3.16	1.66	1.62E-13	8.08E-12
ssaQ	secretion system apparatus protein SsaQ	2.24	1.16	5.53E-06	8.77E-05
ssaR	secretion system apparatus protein SsaR	1.93	0.95	1.08E-05	1.65E-04
ssaS	secretion system apparatus protein SsaS	3.08	1.62	6.87E-14	3.54E-12
ssaT	secretion system apparatus protein SsaT	2.01	1.01	2.80E-03	0.02
ssaV	secretion system apparatus protein SsaV	2.08	1.06	7.87E-04	7.01E-03
sscB	secretion system chaperone SscB	1.73	0.79	1.98E-03	0.01
sseD	translocation machinery protein SseD	1.5	0.58	8.16E-03	0.04
sseE	secretion system effector SseE	1.54	0.63	3.20E-03	0.02
sseF	secretion system effector SseF	2.51	1.33	1.36E-09	3.99E-08
sseG	secretion system effector SseG	2.44	1.29	1.29E-08	3.48E-07
sseI	required for maintaining a long-term systemic infection	1.87	0.9	2.65E-05	3.73E-04
sseL	deubiquitinase SseL	1.76	0.81	4.64E-05	6.08E-04
ssrA	secretion system sensor kinase SsrA	1.78	0.83	8.20E-07	1.65E-05
ssrB	secretion system transcriptonal activator SsrB	1.61	0.69	5.98E-05	7.65E-04
STM0028.1n	hypothetical protein	1.51	0.59	6.29E-03	0.04
STM0211	hypothetical protein	1.59	0.67	2.29E-03	0.02
STM0258	hypothetical protein	1.52	0.61	4.91E-04	4.74E-03
STM0327	cytoplasmic protein	1.75	0.8	3.04E-03	0.02
STM0354	transcriptional regulator	1.66	0.73	2.60E-04	2.74E-03
STM0355	copper chaperone	1.73	0.79	2.84E-03	0.02
STM0412		1.57	0.65	6.14E-03	0.04
STM0438	hypothetical protein	1.67	0.74	8.87E-04	7.75E-03
STM04630	hypothetical protein	1.53	0.61	5.12E-03	0.03

STM05020	hypothetical protein	1.59	0.67	9.06E-04	7.87E-03
STM05025	hypothetical protein	1.55	0.63	3.75E-03	0.02
STM0557	inner membrane protein	1.68	0.75	1.79E-03	0.01
STM05625	hypothetical protein	1.78	0.83	1.02E-03	8.59E-03
STM0699	cytoplasmic protein	1.78	0.83	1.76E-03	0.01
STM0763.s	LysR family transcriptional regulator	1.78	0.83	3.58E-07	7.81E-06
STM0859	LysR family transcriptional regulator	1.83	0.87	6.42E-07	1.32E-05
STM0907	prophage chitinase	2.35	1.24	1.16E-03	9.52E-03
STM0972	secreted effector protein SopD2	1.77	0.83	7.95E-03	0.04
STM1048	host specificity protein J	1.5	0.59	1.08E-03	8.97E-03
STM1052		1.83	0.87	1.03E-03	8.67E-03
STM1055	hypothetical protein	1.61	0.68	4.75E-04	4.61E-03
STM1089	pathogenicity island-encoded protein	1.86	0.89	1.52E-04	1.72E-03
STM1123	periplasmic protein	1.57	0.66	4.35E-03	0.03
STM1146	hypothetical protein	1.52	0.6	5.12E-03	0.03
STM1188	inner membrane lipoprotein	1.88	0.91	2.47E-07	5.51E-06
STM1248		1.58	0.66	1.51E-03	0.01
STM1262		1.67	0.74	1.62E-03	0.01
STM1265	response regulator	1.57	0.65	1.60E-03	0.01
STM1266	transcriptional regulator	2.03	1.02	4.56E-06	7.49E-05
STM1269	chorismate mutase	1.66	0.73	3.48E-03	0.02
STM1317	hypothetical protein	1.57	0.66	2.75E-03	0.02
STM1388	hypothetical protein	1.63	0.71	7.20E-05	9.04E-04
STM1410	cytoplasmic protein	2.5	1.32	4.25E-11	1.50E-09
STM1484	protease	1.71	0.77	3.36E-03	0.02
STM1530	outer membrane protein	2.05	1.04	3.19E-07	7.07E-06
STM1531	hydrogenase nickel incorporation protein HypA	2.05	1.03	2.21E-07	5.00E-06
STM1532	dehydrogenase protein	1.82	0.87	9.09E-07	1.82E-05
STM1533	hydrogenase	1.68	0.75	4.16E-04	4.12E-03
STM1541	GntR family regulatory protein	1.54	0.62	3.05E-04	3.11E-03
STM1542	zinc-binding dehydrogenase	1.82	0.87	1.45E-06	2.75E-05
STM1543	transporter	1.59	0.67	7.34E-03	0.04
STM1549	translation initiation inhibitor	1.59	0.67	1.26E-03	0.01
STM1613	PTS system transporter subunit IIB	1.56	0.64	0.01	0.05
STM1618	sgc operon DeoR familytranscriptional repressor	1.53	0.62	7.24E-04	6.59E-03
STM1672	cytoplasmic protein	1.58	0.66	8.85E-03	0.05
STM1697	diguanylate cyclase/phosphodiesterase domain-containing protein	1.66	0.73	1.66E-03	0.01
STM1829	cytoplasmic protein	2.05	1.04	2.96E-05	4.09E-04
STM1864	inner membrane protein	1.59	0.67	1.19E-04	1.41E-03
STM1866		1.74	0.8	2.54E-05	3.61E-04
STM1872	cytoplasmic protein	1.86	0.9	1.42E-04	1.63E-03

STM2137	cytoplasmic protein	2.13	1.09	1.82E-06	3.38E-05
STM2240	cytoplasmic protein	2.2	1.14	1.90E-06	3.51E-05
STM2288	cytoplasmic protein	2.32	1.21	8.57E-08	2.07E-06
STM2302	4-amino-4-deoxy-L-arabinose-phosphoundecaprenol flippase subunit ArnE	1.86	0.89	3.93E-06	6.52E-05
STM2303	4-amino-4-deoxy-L-arabinose-phospho-UDP flippase	1.66	0.73	5.35E-05	6.92E-04
STM2452	hypothetical protein	1.71	0.78	1.77E-03	0.01
STM2585A	PagK-like protein	1.79	0.84	1.63E-06	3.06E-05
STM2651	protein lysine acetyltransferase	1.51	0.59	8.17E-03	0.04
STM2690	outer membrane efflux protein	1.57	0.65	2.95E-04	3.03E-03
STM2704	tail fiber assembly-like protein	2.72	1.44	6.54E-09	1.80E-07
STM2705	hypothetical protein	1.57	0.66	3.02E-03	0.02
STM2938	CRISPR-associated endonuclease Cas1	1.62	0.7	1.31E-03	0.01
STM2942	transposase	1.61	0.68	3.29E-03	0.02
STM2943	cytoplasmic protein	1.55	0.63	2.23E-03	0.02
STM3096	hypothetical protein	1.5	0.59	1.77E-03	0.01
STM3124	response regulator	1.58	0.66	7.54E-04	6.77E-03
STM3369	hypothetical protein	1.56	0.64	4.15E-04	4.12E-03
STM3460		1.62	0.7	1.33E-04	1.55E-03
STM3599	anaerobic C4-dicarboxylate transporter	1.52	0.6	6.56E-03	0.04
STM3600	sugar kinase	1.73	0.79	3.08E-03	0.02
STM4155	inner membrane protein	1.54	0.63	1.08E-03	8.96E-03
STM4156	cytoplasmic protein	1.61	0.68	2.41E-03	0.02
STM4157	cytoplasmic protein	1.97	0.98	4.25E-08	1.07E-06
STM4186	cytoplasmic protein	1.53	0.61	2.64E-03	0.02
STM4262	bacteriocin/lantibiotic ABC transporter	1.81	0.85	2.65E-06	4.67E-05
STM4272	inner membrane protein	1.61	0.69	7.06E-03	0.04
STM4302	cytoplasmic protein	1.76	0.82	1.58E-04	1.79E-03
STM4504	cytoplasmic protein	1.88	0.91	6.76E-06	1.05E-04
tctD	transcriptional regulator TctD	1.98	0.99	6.55E-06	1.03E-04
tctE	tricarboxylic transport regulatory protein	1.76	0.82	2.15E-05	3.13E-04
ttrR	tetrathionate response regulator TtrR	1.52	0.6	7.69E-04	6.89E-03
ttrS	tetrathionate sensor histidine kinase TtrS	1.76	0.81	2.95E-04	3.03E-03
tus	DNA replication terminus site-binding protein	1.7	0.76	6.28E-03	0.04
tyrB	aromatic amino acid aminotransferase	1.56	0.64	7.78E-04	6.95E-03
uvrC	excinuclease ABC subunit C	1.92	0.94	6.75E-05	8.56E-04
uvrY	LuxR/UhpA family response regulator	1.69	0.76	2.93E-03	0.02
valV		1.9	0.93	2.69E-03	0.02
yaaY	cytoplasmic protein	1.87	0.91	4.60E-05	6.04E-04
yafK	periplasmic protein	1.52	0.6	2.91E-04	3.01E-03

ybdN	3'-phosphoadenosine 5'-phosphosulfate sulfotransferase	1.5	0.58	5.20E-04	4.95E-03
ybfM	required for uptake of chitin-derived oligosaccharides	1.54	0.62	2.18E-03	0.02
ybgE	inner membrane protein	1.71	0.78	2.33E-05	3.38E-04
ybgT	outer membrane lipoprotein	1.54	0.62	1.35E-03	0.01
ybhQ	inner membrane protein	1.93	0.95	7.80E-04	6.96E-03
ybhR	ABC transporter permease	1.51	0.59	1.01E-03	8.50E-03
ydcI	LysR family transcriptional regulator	1.73	0.79	2.28E-03	0.02
yeaS	leucine efflux protein	1.75	0.81	9.08E-06	1.40E-04
yfbB	4-cyclohexadiene-1-carboxylate synthase	1.5	0.58	5.89E-04	5.49E-03
yfdH	glycosyltransferase	1.54	0.63	7.51E-03	0.04
yfeC	negative regulator	1.69	0.76	3.35E-06	5.62E-05
yfeD	negative regulator	1.61	0.69	2.41E-05	3.47E-04
yfiM	outer membrane lipoprotein	1.5	0.59	1.56E-03	0.01
ygbE	inner membrane protein	1.55	0.64	4.75E-03	0.03
ygbJ	3-hydroxyisobutyrate dehydrogenase	1.73	0.79	3.29E-03	0.02
ygcB	helicase	2.04	1.03	3.86E-08	9.89E-07
ygcH	cytoplasmic protein	1.55	0.63	0.01	0.05
ygjR	dehydrogenase	1.58	0.66	1.82E-03	0.01
yheL	tRNA 2-thiouridine synthesizing protein TusB	1.6	0.68	5.68E-04	5.34E-03
yheM	tRNA 2-thiouridine synthesizing protein TusC	1.58	0.66	9.57E-04	8.19E-03
yheN	tRNA 2-thiouridine synthesizing protein TusD	1.58	0.66	1.38E-04	1.59E-03
yheO	regulatory protein	1.68	0.75	1.97E-03	0.01
yhfA	inner membrane protein	1.77	0.82	2.04E-04	2.22E-03
yhfK	inner membrane protein	1.51	0.6	5.17E-04	4.94E-03
yhjV	HAAAP family transport protein	1.85	0.89	2.20E-04	2.37E-03
yjfN	inner membrane protein	1.77	0.82	7.26E-05	9.09E-04
yjfO	biofilm peroxide resistance protein	2	1	4.86E-06	7.89E-05
yncJ	periplasmic protein	1.86	0.9	1.16E-06	2.26E-05
ynfA	membrane protein	1.54	0.62	5.44E-03	0.03
yoaE	inner membrane protein	1.53	0.61	6.54E-04	6.02E-03
yobF	cytoplasmic protein	2.38	1.25	1.90E-05	2.79E-04
yqgF	Holliday junction resolvase	1.67	0.74	4.24E-04	4.18E-03
yrfA	inner membrane protein	1.71	0.77	9.18E-03	0.05
yrfC	inner membrane protein	1.65	0.73	9.40E-04	8.08E-03
ytfP	cytoplasmic protein	1.54	0.62	4.25E-04	4.18E-03

[a] Functional annotations are from NCBI for *Salmonella* Typhimurium strain LT2 (accession number NC_003197). Gene function is unknown for blank fields.

Table 4. Functional description, fold change, and statistical significance of genes downregulated by -1.5-fold or greater after SDBD plasma treatment.

Gene name	Function[a]	Fold change	Log_2 fold change	P-value	FDR p-value
aaeX	membrane protein AaeX	-1.54	-0.63	3.05E-03	0.02
adk	adenylate kinase	-1.59	-0.67	8.44E-03	0.05
ahpF	alkyl hydroperoxide reductase subunit F	-1.82	-0.87	1.72E-03	0.01
alaT		-1.59	-0.67	6.81E-03	0.04
alaV		-1.74	-0.8	4.98E-04	4.79E-03
alaW		-2.1	-1.07	6.77E-03	0.04
amiC	N-acetylmuramoyl-L-alanine amidase	-2.24	-1.16	1.44E-07	3.29E-06
apbE	thiamine biosynthesis lipoprotein ApbE	-1.91	-0.94	4.75E-04	4.61E-03
apeE	outer membrane N-acetyl phenylalanine beta-naphthyl ester-cleaving esterase	-1.87	-0.9	2.70E-05	3.79E-04
argO	arginine exporter protein ArgO	-2.75	-1.46	9.99E-16	5.78E-14
bioA	adenosylmethionine--8-amino-7-oxononanoate aminotransferase BioA	-1.77	-0.83	4.67E-04	4.55E-03
bioB	biotin synthetase	-2.37	-1.24	1.65E-05	2.47E-04
bioF	8-amino-7-oxononanoate synthase	-1.95	-0.96	2.23E-04	2.40E-03
carA	carbamoyl phosphate synthase small subunit	-1.53	-0.61	9.33E-04	8.04E-03
chaA	calcium/sodium:proton antiporter	-2.3	-1.2	6.32E-10	1.94E-08
cigR	inner membrane protein	-3.39	-1.76	1.23E-06	2.36E-05
cirA	catecholate siderophore receptor CirA	-3.73	-1.9	0	0
cmk	cytidylate kinase	-2.03	-1.03	7.16E-08	1.75E-06
cobA	cob(I)yrinic acid a; c-diamide adenosyltransferase	-2.48	-1.31	3.35E-06	5.62E-05
corA	magnesium transport protein CorA	-2.46	-1.3	5.60E-10	1.74E-08
cpsG	phosphomannomutase	-6.76	-2.76	0	0
cpxA	sensory kinase CpxS	-1.56	-0.64	4.14E-04	4.12E-03
cpxP	cpx regulon periplasmic repressor	-2.62	-1.39	1.69E-05	2.52E-04
cpxR	response reguator CpxR	-1.63	-0.7	2.05E-04	2.23E-03
csgB	minor curlin subunit	-2.1	-1.07	1.31E-03	0.01
cueO	blue copper oxidase CueO	-1.79	-0.84	5.36E-06	8.59E-05
cutF		-1.95	-0.96	5.61E-07	1.18E-05
cvpA	colicin V production protein	-1.7	-0.76	1.22E-03	9.90E-03
cysZ	sulfate transport protein CysZ	-3.44	-1.78	0	0
dacB	D-alanyl-D-alanine carboxypeptidase	-1.54	-0.62	1.08E-03	8.97E-03
dcoB	oxaloacetate decarboxylase subunit beta	-1.59	-0.67	1.64E-03	0.01

deoA	thymidine phosphorylase	-1.54	-0.62	6.86E-03	0.04
deoC	2-deoxyribose-5-phosphate aldolase	-1.74	-0.8	1.37E-03	0.01
dinF	DNA-damage-inducible protein F	-2.7	-1.43	2.17E-11	8.10E-10
dinI	DNA damage-inducible protein I	-7.16	-2.84	0	0
dinP	DNA polymerase IV	-2.61	-1.39	1.01E-13	5.10E-12
dkgB	5-diketo-D-gluconic acid reductase B	-1.62	-0.7	1.38E-04	1.59E-03
dps	DNA starvation/stationary phase protection protein	-1.73	-0.79	2.27E-03	0.02
dsrB	protein DsrB	-3.73	-1.9	7.16E-14	3.64E-12
dxr	1-deoxy-D-xylulose 5-phosphate reductoisomerase	-1.86	-0.9	5.41E-06	8.65E-05
eco	ecotin	-3.6	-1.85	3.65E-09	1.03E-07
emrD	MFS family multidrug tranport protein	-1.99	-0.99	1.33E-07	3.11E-06
endA	DNA-specific endonuclease I	-2.1	-1.07	5.56E-07	1.17E-05
entA	3-dihydro-2-3-dihydroxybenzoate dehydrogenase	-4.99	-2.32	2.25E-14	1.21E-12
entB	3-dihydro-2-3-dihydroxybenzoate synthetase	-6.35	-2.67	0	0
entC	isochorismate synthase	-9.79	-3.29	0	0
entD	4'-phosphopantetheinyl transferase	-3.87	-1.95	0	0
entE	3-dihydroxybenzoate-AMP ligase	-8.61	-3.11	0	0
entF	enterobactin synthase subunit F	-2.31	-1.21	8.57E-07	1.72E-05
envE	lipoprotein EnvE	-2.68	-1.42	4.44E-11	1.56E-09
envF	lipoprotein EnvF	-4.52	-2.18	0	0
fbaB	fructose-bisphosphate aldolase	-2.48	-1.31	3.77E-07	8.16E-06
fepA	outer membrane porin	-5.33	-2.41	0	0
fes	enterochelin esterase	-2.84	-1.5	1.73E-09	5.03E-08
fhuE	ferric-rhodotorulic acid outer membrane transporter	-5.43	-2.44	0	0
fieF	cation-efflux pump FieF	-2.09	-1.06	2.74E-09	7.83E-08
fimA	type-1 fimbrial protein subunit A	-2.32	-1.21	9.56E-07	1.90E-05
fimC	chaperone protein FimC	-1.66	-0.73	2.27E-03	0.02
fimI	fimbrin-like protein FimI	-1.64	-0.72	1.54E-03	0.01
fis	DNA-binding protein Fis	-1.84	-0.88	5.94E-06	9.38E-05
fliR	flagellar biosynthesis protein FliR	-3.59	-1.84	0	0
folA	dihydrofolate reductase	-1.83	-0.87	1.65E-04	1.86E-03
folB	bifunctional dihydroneopterin aldolase/dihydroneopterin triphosphate 2'-epimerase	-2.15	-1.1	3.33E-05	4.54E-04
ftsE	cell division ATPase FtsE	-1.81	-0.86	2.80E-05	3.91E-04
ftsX	cell division protein FtsX	-1.6	-0.68	1.68E-04	1.88E-03
ftsY	aignal recognition particle receptor FtsY	-2.01	-1.01	1.33E-05	2.01E-04

galF	UTP--glucose-1-phosphate uridylyltransferase subunit GalF	-1.68	-0.75	2.84E-03	0.02
gidA	tRNA uridine 5-carboxymethylaminomethyl modification protein GidA	-1.72	-0.78	2.83E-05	3.94E-04
glnK	nitrogen regulatory protein P-II 2	-1.98	-0.98	7.77E-03	0.04
glnU		-1.98	-0.98	1.43E-05	2.15E-04
glnW		-2.06	-1.04	4.38E-06	7.25E-05
glnX		-1.58	-0.66	8.70E-03	0.05
glrK	sensor kinase GlrK	-1.53	-0.61	1.08E-03	8.97E-03
gltU		-2.07	-1.05	1.26E-03	0.01
gltV		-1.79	-0.84	8.96E-03	0.05
glyT		-2.8	-1.48	2.81E-11	1.01E-09
gmd	GDP-D-mannose dehydratase	-13.46	-3.75	0	0
gpt	xanthine phosphoribosyltransferase	-2.24	-1.16	5.44E-09	1.52E-07
greA	transcription elongation factor GreA	-1.64	-0.71	2.41E-03	0.02
guaB	inosine 5'-monophosphate dehydrogenase	-2.15	-1.1	7.00E-11	2.40E-09
hha	hemolysin expression-modulating protein	-1.83	-0.87	1.72E-05	2.55E-04
hisR		-2.62	-1.39	2.28E-08	5.94E-07
holB	DNA polymerase III subunit delta'	-1.63	-0.71	5.89E-05	7.57E-04
holD	DNA polymerase III subunit psi	-1.66	-0.73	7.39E-04	6.67E-03
holE	DNA polymerase III subunit theta	-1.53	-0.61	8.79E-03	0.05
hopD	leader peptidase HopD	-1.68	-0.75	2.51E-05	3.59E-04
hrpB	ATP-dependent helicase	-1.68	-0.75	9.06E-05	1.09E-03
hslJ	heat-inducible protein HslJ	-3.27	-1.71	0	0
htpX	protease HtpX	-1.95	-0.96	2.75E-06	4.83E-05
htrA	serine endoprotease	-2.01	-1.01	4.30E-03	0.03
iap	alkaline phosphatase isozyme conversion aminopeptidase	-1.62	-0.7	2.37E-03	0.02
iciA	chromosome replication initiation inhibitor protein	-2.16	-1.11	2.55E-11	9.30E-10
ileT		-2.03	-1.02	4.77E-05	6.22E-04
ileU		-2.03	-1.02	6.63E-05	8.44E-04
ileV		-2.44	-1.29	8.01E-06	1.24E-04
ilvG	acetolactate synthase 2 catalytic subunit	-1.53	-0.61	9.59E-04	8.20E-03
iroB	glycosyl transferase	-1.5	-0.59	3.13E-03	0.02
kdpB	potassium-transporting ATPase subunit B	-1.66	-0.73	5.68E-03	0.03
kdpC	potassium-transporting ATPase subunit C	-1.62	-0.7	1.33E-03	0.01
leuA	2-isopropylmalate synthase	-2.19	-1.13	2.77E-06	4.85E-05
leuB	3-isopropylmalate dehydrogenase	-1.72	-0.78	1.60E-03	0.01
leuC	3-isopropylmalate dehydratase large subunit	-1.76	-0.81	3.45E-03	0.02
leuO	HTH-type transcriptional regulator LeuO	-1.8	-0.85	2.59E-03	0.02
leuQ		-1.82	-0.86	8.57E-05	1.04E-03

leuT		-2.59	-1.37	9.00E-10	2.69E-08
leuU		-1.87	-0.9	7.39E-05	9.21E-04
leuW		-2.21	-1.15	2.70E-08	6.99E-07
leuZ		-1.61	-0.69	4.27E-03	0.03
lexA	LexA repressor	-1.75	-0.81	1.37E-03	0.01
ligT	2'-5' RNA ligase	-1.88	-0.91	3.07E-06	5.25E-05
lolA	outer-membrane lipoprotein carrier protein	-1.82	-0.86	1.70E-03	0.01
lppB	major outer membrane lipoprotein	-1.62	-0.7	6.66E-03	0.04
lysV		-2.35	-1.23	8.46E-05	1.04E-03
maa	maltose O-acetyltransferase	-1.7	-0.76	4.25E-05	5.63E-04
malE	maltose ABC transporter substrate-binding protein MalE	-2.17	-1.12	9.12E-03	0.05
manA	mannose-6-phosphate isomerase	-1.84	-0.88	1.36E-05	2.05E-04
manC	mannose-1-phosphate guanylyltransferase	-5.07	-2.34	0	0
mdoD	glucan biosynthesis protein D	-2.65	-1.4	3.31E-06	5.59E-05
metW		-1.67	-0.74	0.01	0.05
metZ		-1.69	-0.76	4.37E-03	0.03
mgtA	magnesium-transporting ATPase	-16.17	-4.02	0	0
mgtB	magnesium-transporting ATPase	-8.04	-3.01	3.12E-11	1.11E-09
mgtC	protein MgtC	-16.64	-4.06	0	0
mliC	lysozyme inhibitor	-3.11	-1.64	5.21E-10	1.63E-08
mltD	membrane-bound lytic murein transglycosylase D	-1.51	-0.6	6.91E-03	0.04
mnmA	tRNA-specific 2-thiouridylase MnmA	-1.57	-0.65	3.30E-04	3.32E-03
mntH	divalent metal cation transporter MntH	-2.29	-1.2	1.28E-12	5.63E-11
mrcB	transpeptidase/transglycosylase	-2.53	-1.34	1.03E-07	2.43E-06
msgA	virulence protein MsgA	-4.34	-2.12	0	0
murA	UDP-N-acetylglucosamine 1-carboxyvinyltransferase	-1.57	-0.65	3.10E-03	0.02
mutT	8-dihydro-8-oxoguanine-triphosphatase	-1.63	-0.7	3.29E-04	3.31E-03
mutY	A/G-specific adenine glycosylase	-2.36	-1.24	1.41E-08	3.77E-07
nadA	quinolinate synthetase	-3.3	-1.72	2.07E-12	8.73E-11
nadB	L-aspartate oxidase	-1.52	-0.6	1.17E-03	9.53E-03
ndh	respiratory NADH dehydrogenase 2	-2.37	-1.24	2.35E-11	8.63E-10
obgE	GTPase ObgE	-2.12	-1.08	3.52E-05	4.75E-04
ompX	outer membrane protease	-4.53	-2.18	2.97E-06	5.14E-05
osmB	osmotically inducible lipoprotein B	-20.71	-4.37	0	0
osmY	hyperosmotically inducible periplasmic protein	-3.72	-1.89	3.68E-13	1.75E-11
otsB	trehalose-phosphate phosphatase	-1.8	-0.85	2.99E-06	5.15E-05
panB	3-methyl-2-oxobutanoate hydroxymethyltransferase	-1.77	-0.82	6.70E-06	1.05E-04
panC	pantoate synthetase	-1.5	-0.59	2.47E-03	0.02

pdhR	pyruvate dehydrogenase complex repressor	-1.84	-0.88	6.19E-06	9.75E-05
pdxH	pyridoxamine 5'-phosphate oxidase	-1.77	-0.82	9.27E-04	8.01E-03
pdxK	pyridoxal kinase	-1.65	-0.72	9.69E-04	8.24E-03
pfkA	6-phosphofructokinase	-1.73	-0.79	5.08E-06	8.17E-05
phnS	2-aminoethylphosphonate ABC transporter substrate-binding protein PhnS	-6.36	-2.67	1.67E-15	9.41E-14
phnT	2-aminoethylphosphonate ABC transporter ATP-binding protein PhnT	-2.65	-1.41	1.44E-05	2.16E-04
phnU	2-aminoethylphosphonate ABC transporter permease PhnU	-2.43	-1.28	6.32E-09	1.75E-07
phoB	response regulato PhoB	-7.31	-2.87	0	0
phoE	outer membrane phosphoporin protein E	-3.3	-1.72	1.83E-10	6.01E-09
phoR	sensory kinase PhoR	-6.67	-2.74	0	0
phoU	transcriptional regulator PhoU	-6.88	-2.78	1.15E-09	3.40E-08
pliC	lysozyme inhibitor	-2.61	-1.38	5.71E-04	5.35E-03
potA	putrescine/spermidine ABC transporter ATP-binding protein PotA	-2.03	-1.02	2.59E-09	7.45E-08
pphA	serine/threonine-protein phosphatase 1	-1.71	-0.77	1.02E-05	1.55E-04
prfH	peptide chain release factor	-2.01	-1.01	1.19E-07	2.80E-06
priB	primosomal replication protein N	-2.67	-1.42	6.63E-04	6.09E-03
proM		-2.39	-1.26	6.44E-05	8.21E-04
pspA	phage shock protein PspA	-3.43	-1.78	5.01E-11	1.75E-09
pspB	phage shock protein PspB	-3.07	-1.62	6.25E-13	2.86E-11
pspC	DNA-binding transcriptional activator PspC	-2.8	-1.48	3.11E-13	1.52E-11
pspD	inner membrane phage-shock protein	-2.61	-1.38	1.11E-16	6.77E-15
pspG	phage shock protein G	-2.2	-1.14	8.59E-10	2.60E-08
pstA	phosphate ABC transporter permease subunit PtsA	-17.91	-4.16	0	0
pstB	phosphate ABC transporter ATP-binding protein PstB	-11.49	-3.52	7.11E-15	3.92E-13
pstC	phosphate ABC transporter permease PstC	-26.42	-4.72	0	0
pstS	phosphate ABC transporter substrate-binding protein PstS	-57.1	-5.84	0	0
ptrB	protease 2	-1.83	-0.87	9.88E-04	8.38E-03
purR	HTH-type transcriptional repressor PurR	-2.02	-1.02	3.65E-09	1.03E-07
purT	phosphoribosylglycinamide formyltransferase 2	-1.55	-0.64	2.01E-03	0.01
pyrF	OMP decarboxylase; OMPDCase; OMPdecase	-3.45	-1.79	0	0
pyrH	uridylate kinase	-1.65	-0.73	1.27E-04	1.49E-03
queA	S-adenosylmethionine--tRNA ribosyltransferase-isomerase	-1.88	-0.91	1.70E-05	2.52E-04
rapA	RNA polymerase-associated protein RapA	-1.94	-0.95	2.39E-04	2.53E-03

rcsA	transcriptional regulator RcsA	-7.99	-3	0	0
rcsB	transcriptional regulator RcsB	-1.78	-0.84	6.54E-03	0.04
recA	recombinase A	-5.21	-2.38	8.76E-10	2.63E-08
recN	DNA repair protein RecN	-6.94	-2.8	0	0
recX	recombination regulator RecX	-2.96	-1.57	1.11E-16	6.77E-15
rfbD	dTDP-4-dehydrorhamnose reductase	-1.6	-0.68	9.76E-03	0.05
rhaA	L-rhamnose isomerase	-1.72	-0.78	2.03E-04	2.22E-03
rhlE	ATP-dependent RNA helicase RhlE	-2.13	-1.09	5.51E-04	5.21E-03
rimO	ribosomal protein S12 methylthiotransferase RimO	-2.02	-1.01	1.99E-06	3.66E-05
rimP	ribosome maturation factor RimP	-2.13	-1.09	1.08E-06	2.11E-05
rlmL	bifunctional rRNA large subunit methyltransferase	-1.84	-0.88	2.02E-03	0.01
rluC	rRNA lager subunit pseudouridylate synthase C	-1.89	-0.92	1.86E-06	3.44E-05
rnc	ribonuclease III	-1.66	-0.73	8.12E-05	9.97E-04
rnpA	ribonuclease P protein	-1.6	-0.68	4.62E-03	0.03
rph	ribonuclease PH	-2.5	-1.32	2.45E-12	1.01E-10
rplA	50S ribosomal protein L1	-3.57	-1.83	4.54E-05	5.97E-04
rplB	50S ribosomal protein L2	-2.78	-1.48	1.97E-03	0.01
rplC	50S ribosomal protein L3	-3.31	-1.73	2.04E-04	2.23E-03
rplD	50S ribosomal protein L4	-3.09	-1.63	4.39E-04	4.30E-03
rplI	50S ribosomal protein L9	-2.74	-1.45	1.49E-03	0.01
rplK	50S ribosomal protein L11	-3.98	-1.99	4.76E-08	1.18E-06
rplP	50S ribosomal protein L16	-2.19	-1.13	0.01	0.05
rplS	50S ribosomal protein L19	-2.16	-1.11	2.71E-03	0.02
rplV	50S ribosomal protein L22	-2.46	-1.3	4.31E-03	0.03
rplW	50S ribosomal protein L23	-3.05	-1.61	3.32E-04	3.34E-03
rplY	50S ribosomal protein L25	-2.39	-1.26	1.54E-04	1.74E-03
rpmB	50S ribosomal protein L28	-1.85	-0.89	4.84E-03	0.03
rpmC	50S ribosomal protein L29	-2.07	-1.05	8.55E-03	0.05
rpmE	50S ribosomal protein L31	-2.22	-1.15	1.50E-03	0.01
rpmH	50S ribosomal protein L34	-1.82	-0.87	2.62E-05	3.71E-04
rpsC	30S ribosomal protein S3	-2.38	-1.25	7.88E-03	0.04
rpsF	30S ribosomal protein S6	-2.87	-1.52	5.90E-04	5.49E-03
rpsJ	30S ribosomal protein S10	-2.84	-1.51	3.89E-04	3.89E-03
rpsP	30S ribosomal protein S16	-1.94	-0.95	2.55E-03	0.02
rpsR	30S ribosomal protein S18	-2.92	-1.55	1.44E-04	1.64E-03
rpsS	30S ribosomal protein S19	-2.68	-1.42	1.30E-03	0.01
rrsA		-3.16	-1.66	1.13E-03	9.31E-03
rrsB		-3.38	-1.76	6.29E-04	5.84E-03
rrsC		-3.26	-1.7	9.70E-04	8.24E-03
rsmC	16S rRNA methyltransferase	-1.84	-0.88	1.18E-06	2.28E-05

rsuA	16S rRNA pseudouridine(516) synthase	-1.91	-0.94	3.00E-06	5.15E-05
rtcA	RNA 3'-terminal-phosphate cyclase	-15.51	-3.96	0	0
rtcB	RNA-splicing ligase RtcB	-52.11	-5.7	0	0
rumB	23S rRNA (uracil(747)-C(5))-methyltransferase RlmC	-2.53	-1.34	1.04E-12	4.67E-11
ruvA	Holliday junction ATP-dependent DNA helicase RuvA	-2.12	-1.08	1.95E-08	5.13E-07
ruvB	Holliday junction ATP-dependent DNA helicase RuvB	-1.5	-0.58	5.41E-03	0.03
sbmC	DNA gyrase inhibitor	-5.38	-2.43	4.44E-16	2.60E-14
scsA	copper sensitive suppression protein A	-2.76	-1.46	4.59E-08	1.15E-06
scsB	copper sensitive suppression protein	-2.2	-1.14	4.48E-06	7.38E-05
secG	preprotein translocase IISp family protein	-1.74	-0.8	2.90E-04	3.01E-03
serB	3-phosphoserine phosphatase	-1.59	-0.67	9.65E-04	8.23E-03
serW		-2	-1	6.89E-03	0.04
setB	sugar efflux transporter B	-1.79	-0.84	7.33E-05	9.15E-04
sinH	intimin-like protein SinH	-1.63	-0.7	1.70E-03	0.01
slrB	PTS system glucitol/sorbitol-specific transporter subunit IIA	-1.6	-0.68	5.29E-04	5.03E-03
smvA	methyl viologen resistance protein SmvA	-4.49	-2.17	0	0
spy	stress response protein	-2.59	-1.37	4.67E-12	1.88E-10
ssb	single-stranded DNA-binding protein	-1.72	-0.78	5.39E-04	5.11E-03
STM0016	hypothetical protein	-3	-1.58	2.58E-05	3.66E-04
STM0080	outer membrane lipoprotein	-17.56	-4.13	0	0
STM0100	cytoplasmic protein	-3.74	-1.9	1.63E-07	3.73E-06
STM0257	drug efflux protein	-2.2	-1.13	4.96E-07	1.06E-05
STM0289	cytoplasmic protein	-1.97	-0.98	3.29E-03	0.02
STM0314		-5.23	-2.39	0	0
STM0341	inner membrane protein	-1.97	-0.98	7.97E-05	9.82E-04
STM0342	periplasmic protein	-2.28	-1.19	7.57E-06	1.18E-04
STM0402	thiol-alkyl hydroperoxide reductase	-2.29	-1.2	1.68E-03	0.01
STM0458	cysteine synthase/cystathionine beta-synthase	-1.53	-0.61	4.04E-03	0.03
STM04610	hypothetical protein	-3.47	-1.79	1.06E-04	1.27E-03
STM0474	cytoplasmic protein	-1.79	-0.84	3.07E-03	0.02
STM0478	small-conductance mechanosensitive channel	-1.59	-0.67	1.96E-03	0.01
STM05040	hypothetical protein	-3.68	-1.88	6.60E-03	0.04
STM0551	diguanylate cyclase/phosphodiesterase domain-containing protein	-2.29	-1.2	8.65E-04	7.57E-03
STM0554	integrase	-2.6	-1.38	1.12E-04	1.34E-03
STM0555		-1.7	-0.76	1.07E-03	8.92E-03
STM0564	oxidoreductase	-1.96	-0.97	2.39E-07	5.35E-06
STM0587	cytoplasmic protein	-3.31	-1.73	9.61E-11	3.27E-09

STM0610	anaerobic dehydrogenase component	-1.9	-0.93	4.30E-03	0.03
STM0759	hypothetical protein	-8.44	-3.08	0	0
STM0770	cobalamin/Fe3+-siderophore ABC transporter permease	-1.88	-0.91	1.35E-04	1.57E-03
STM0801	hypothetical protein	-1.5	-0.59	8.60E-04	7.54E-03
STM0869	TetR/Acr family regulator	-2.06	-1.04	1.79E-07	4.06E-06
STM0950	SlsA protein	-1.83	-0.87	2.15E-04	2.33E-03
STM0951	cytoplasmic protein	-6.01	-2.59	0	0
STM0952	LysR family transcriptional regulator	-2.69	-1.43	3.33E-15	1.86E-13
STM1024	hypothetical protein	-3.11	-1.64	9.18E-04	7.94E-03
STM1025	hypothetical protein	-3.26	-1.7	2.75E-11	9.94E-10
STM1060	iron-sulfur protein	-1.51	-0.6	3.22E-03	0.02
STM1241.1		-7.82	-2.97	0	0
STM1243	cold shock-like protein CspH	-2.3	-1.2	6.32E-08	1.56E-06
STM1247		-3.44	-1.78	2.82E-10	8.95E-09
STM1254	outer membrane lipoprotein	-2.05	-1.03	7.10E-07	1.45E-05
STM1273	nitric oxide reductase	-2.93	-1.55	3.12E-12	1.28E-10
STM1309	excinuclease	-3.65	-1.87	0	0
STM1311	DNA-binding transcriptional activator	-1.99	-0.99	1.03E-04	1.23E-03
STM1472	periplasmic protein	-1.8	-0.85	8.49E-05	1.04E-03
STM1492	ABC transporter permease	-1.91	-0.94	2.26E-06	4.08E-05
STM1493	ABC transporter substrate-binding protein	-2.58	-1.37	7.38E-12	2.87E-10
STM1494	ABC transporter permease	-2.73	-1.45	1.99E-12	8.47E-11
STM1561	lipoprotein	-2	-1	3.27E-07	7.21E-06
STM1573.S	hypothetical protein	-2.44	-1.29	5.29E-12	2.11E-10
STM1585	outer membrane lipoprotein	-2.34	-1.23	7.08E-07	1.45E-05
STM1586	hypothetical protein	-1.5	-0.58	6.06E-04	5.63E-03
STM1621	periplasmic protein	-1.88	-0.91	7.60E-05	9.41E-04
STM1627	alcohol dehydrogenase class III	-1.63	-0.71	8.67E-05	1.05E-03
STM1628	cytoplasmic protein	-2.01	-1	5.04E-06	8.13E-05
STM1633	extracellular solute-binding protein	-1.77	-0.82	2.34E-03	0.02
STM1634	ABC transporter permease	-1.61	-0.68	3.16E-03	0.02
STM1649	cytoplasmic protein	-1.88	-0.91	3.10E-05	4.26E-04
STM1650	hypothetical protein	-3.61	-1.85	6.73E-12	2.66E-10
STM1665	cytoplasmic protein	-1.61	-0.69	4.35E-03	0.03
STM1670	lipoprotein	-1.79	-0.84	8.60E-03	0.05
STM1841	hypothetical protein	-2.08	-1.05	3.11E-06	5.30E-05
STM1869A	hypothetical protein	-1.98	-0.98	6.62E-03	0.04
STM1870	hypothetical protein	-1.86	-0.89	0.01	0.05
STM1881	hypothetical protein	-6.84	-2.77	0	0
STM2003		-2.27	-1.18	9.50E-05	1.14E-03
STM2126	multidrug resistance protein MdtA	-1.74	-0.8	2.45E-05	3.52E-04
STM2148	periplasmic protein	-1.59	-0.67	8.32E-03	0.05

STM2198	regulatory protein	-1.64	-0.71	9.39E-04	8.08E-03
STM2209.1	hypothetical protein	-2.43	-1.28	5.05E-03	0.03
STM2797	ArsR family regulatory protein	-1.82	-0.87	1.00E-04	1.20E-03
STM2800	L-alanine exporter AlaE	-1.83	-0.87	4.46E-07	9.57E-06
STM2803	GntR family regulatory protein	-1.73	-0.79	4.87E-06	7.89E-05
STM2821		-2	-1	3.55E-04	3.55E-03
STM2822		-2.24	-1.16	1.90E-04	2.11E-03
STM2823		-2.14	-1.1	2.33E-04	2.49E-03
STM2824		-2.17	-1.12	4.20E-04	4.15E-03
STM2825		-1.9	-0.93	1.87E-03	0.01
STM2922	3-polyprenyl-4-hydroxybenzoate decarboxylase	-1.59	-0.67	2.78E-04	2.89E-03
STM2986.S	integral membrane protein	-1.5	-0.58	8.45E-03	0.05
STM3022	transporter	-1.95	-0.96	3.02E-05	4.16E-04
STM3025.1	hypothetical protein	-1.88	-0.91	2.10E-05	3.07E-04
STM3026	outer membrane protein	-2.01	-1.01	1.55E-03	0.01
STM3085	outer membrane lipoprotein	-4.3	-2.1	0	0
STM3168	hypothetical protein	-1.74	-0.8	3.04E-03	0.02
STM3270	hypothetical protein	-1.94	-0.95	1.68E-06	3.15E-05
STM3397		-2.3	-1.2	1.88E-04	2.10E-03
STM3516	cytoplasmic protein	-2.17	-1.11	1.37E-07	3.18E-06
STM3517	DNA-damage-inducibile protein	-4.82	-2.27	0	0
STM3520		-120.67	-6.91	0	0
STM3521	ribonucleoprotein related-protein	-93.74	-6.55	0	0
STM3580	inner membrane lipoprotein	-1.86	-0.9	5.90E-03	0.03
STM3595	phosphatase	-1.56	-0.64	1.51E-03	0.01
STM3624A	cystathionine gamma-synthase	-2.01	-1.01	3.09E-04	3.14E-03
STM3632	hypothetical protein	-1.85	-0.89	1.50E-04	1.70E-03
STM3633	regulatory protein	-2.65	-1.41	1.03E-10	3.45E-09
STM3650	hypothetical protein	-1.93	-0.95	5.50E-05	7.10E-04
STM3657	lipoprotein	-3	-1.58	1.11E-16	6.77E-15
STM3663	hypothetical protein	-2.9	-1.54	1.13E-12	5.03E-11
STM3761	inner membrane protein	-1.97	-0.98	1.02E-03	8.57E-03
STM3796A.	integral membrane protein	-2.33	-1.22	2.53E-10	8.07E-09
STM3898	hypothetical protein	-2.1	-1.07	8.75E-05	1.06E-03
STM3980	outer membrane protein	-1.5	-0.59	6.77E-03	0.04
STM4032	acetyl esterase	-2.71	-1.44	1.11E-16	6.77E-15
STM4032.2	hypothetical protein	-1.79	-0.84	7.09E-05	8.93E-04
STM4041	inner membrane protein	-2.41	-1.27	2.94E-06	5.13E-05
STM4042	branched-chain amino acid permease	-2.47	-1.3	2.60E-06	4.60E-05
STM4134		-1.65	-0.73	1.11E-03	9.15E-03
STM4239	cytoplasmic protein	-1.74	-0.8	2.46E-04	2.59E-03
STM4268	hypothetical protein	-1.86	-0.89	2.60E-06	4.60E-05

STM4289	hypothetical protein	-1.83	-0.87	3.19E-05	4.38E-04
STM4309	hypothetical protein	-1.74	-0.8	1.44E-04	1.64E-03
STM4310	inner membrane protein	-1.59	-0.67	2.33E-03	0.02
STM4457	transposase	-2.12	-1.08	1.61E-06	3.03E-05
STM4509.S	hypothetical protein	-4.09	-2.03	1.99E-10	6.49E-09
STM4510	aspartate racemase	-2	-1	1.06E-06	2.08E-05
STM4552	inner membrane protein	-4.32	-2.11	1.33E-15	7.62E-14
STM4562	hypothetical protein	-2.55	-1.35	1.92E-11	7.30E-10
suhB	inositol monophosphatase	-2.41	-1.27	1.37E-08	3.67E-07
sulA	cell division inhibitor SulA	-6.5	-2.7	0	0
tbpA	thiamine ABC transporter substrate-binding protein ThiP	-3.16	-1.66	2.56E-14	1.37E-12
tgt	queuine tRNA-ribosyltransferase	-1.9	-0.93	2.20E-06	3.99E-05
thiC	phosphomethylpyrimidine synthase	-1.86	-0.89	3.41E-05	4.61E-04
thiD	hydroxymethylpyrimidine/phosphomethyl pyrimidine kinase	-1.82	-0.86	3.62E-05	4.86E-04
thiE	thiamine-phosphate synthase	-1.58	-0.66	5.03E-03	0.03
thiM	hydroxyethylthiazole kinase	-1.82	-0.86	2.36E-04	2.51E-03
thiP	thiamine ABC transporter permease ThiP	-2.08	-1.06	7.37E-08	1.79E-06
thiQ	thiamine ABC transporter ATP-binding protein	-1.64	-0.72	7.59E-05	9.41E-04
thrT		-2.95	-1.56	8.27E-12	3.19E-10
tmk	thymidylate kinase	-1.73	-0.79	4.74E-06	7.73E-05
tnpA_3	insertion sequence element IS200 transposase	-2.98	-1.58	4.43E-03	0.03
tnpA_6	insertion sequence element IS200 transposase	-2.56	-1.35	3.39E-03	0.02
tolA	cell envelope integrity inner membrane protein TolA	-1.69	-0.75	6.65E-04	6.10E-03
tolQ	colicin uptake protein TolQ	-1.82	-0.86	2.66E-04	2.80E-03
tolR	colicin uptake protein TolR	-1.64	-0.72	3.68E-03	0.02
tonB	transport protein TonB	-1.54	-0.63	1.62E-03	0.01
topA	DNA topoisomerase I	-1.57	-0.65	6.31E-03	0.04
treR	HTH-type transcriptional regulator TreR	-2.62	-1.39	4.58E-13	2.14E-11
trpE	anthranilate synthase component I	-1.56	-0.64	5.70E-04	5.35E-03
trxC	thioredoxin 2	-1.59	-0.67	2.71E-04	2.84E-03
tyrU		-2	-1	1.78E-04	1.99E-03
tyrV		-1.56	-0.65	8.34E-03	0.05
udp	uridine phosphorylase	-1.64	-0.72	5.41E-03	0.03
ugpA	glycerol-3-phosphate ABC transporter permease UdpA	-11.14	-3.48	0	0
ugpB	glycerol-3-phosphate ABC transporter substrate-binding protein UdpB	-11.45	-3.52	1.11E-16	6.77E-15

ugpC	glycerol-3-phosphate ABC transporter ATP-binding protein UgpC	-8.11	-3.02	0	0
ugpE	glycerol-3-phosphate ABC transporter permease UdpE	-13.51	-3.76	0	0
ugpQ	glycerophosphodiester phosphodiesterase	-1.98	-0.98	2.68E-04	2.81E-03
upp	uracil phosphoribosyltransferase	-2.79	-1.48	2.09E-06	3.82E-05
uraA	uracil transporter	-1.58	-0.66	2.77E-03	0.02
uup	ABC transporter ATPase	-1.66	-0.73	7.40E-04	6.67E-03
uvrA	excinuclease ABC subunit A	-1.9	-0.93	6.83E-04	6.24E-03
uvrB	excinuclease ABC subunit B	-2	-1	2.27E-06	4.08E-05
valU		-1.82	-0.86	1.00E-03	8.50E-03
valX		-1.63	-0.71	7.93E-03	0.04
valY		-1.68	-0.75	8.70E-03	0.05
wcaA	glycosyl transferase	-7.66	-2.94	0	0
wcaB	colanic acid biosynthesis acetyltransferase WcaB	-4.41	-2.14	4.57E-14	2.38E-12
wcaC	glycosyl transferase	-5.53	-2.47	8.60E-12	3.29E-10
wcaD	colanic acid polymerase	-8.69	-3.12	0	0
wcaE	glycosyl transferase family protein	-25.76	-4.69	0	0
wcaF	colanic acid biosynthesis acetyltransferase WcaF	-26.86	-4.75	0	0
wcaG	GDP-fucose synthetase	-12.91	-3.69	0	0
wcaH	GDP-mannose mannosyl hydrolase	-10.3	-3.36	0	0
wcaI	glycosyl transferase	-7.82	-2.97	0	0
wcaJ	UDP-glucose lipid carrier transferase	-2.14	-1.1	2.36E-06	4.22E-05
wza	polysaccharide export protein	-28.28	-4.82	0	0
wzb	protein-tyrosine-phosphatase	-31.78	-4.99	0	0
wzc	tyrosine-protein kinase	-14.72	-3.88	0	0
wzxC	colanic acid exporter	-1.75	-0.81	9.51E-04	8.15E-03
xylA	xylose isomerase	-1.68	-0.75	4.05E-05	5.38E-04
yabI	DedA family membrane protein	-1.85	-0.89	3.32E-05	4.53E-04
yadI	PTS system transporter subunit IIA	-1.7	-0.77	2.64E-03	0.02
yaeJ	hydrolase domain-containing protein	-1.58	-0.66	6.97E-04	6.35E-03
yaiW	outer membrane lipoprotein	-1.86	-0.9	5.95E-07	1.24E-05
yaiY	inner membrane protein	-4.94	-2.31	0	0
yajG	lipoprotein	-1.65	-0.72	1.16E-04	1.37E-03
yajI	outer membrane lipoprotein	-11.29	-3.5	0	0
ybbA	ABC transporter ATP-binding protein	-1.67	-0.74	2.65E-05	3.73E-04
ybcI	membrane-bound metal-dependent hydrolase	-1.84	-0.88	2.76E-04	2.88E-03
ybdA	enterobactin exporter EntS	-2.26	-1.18	2.21E-11	8.18E-10
ybdB	proofreading thioesterase EntH	-3.64	-1.87	3.59E-13	1.73E-11
ybdR	dehydrogenase	-1.59	-0.67	1.31E-04	1.53E-03
ybgC	acyl-CoA thioester hydrolase	-1.85	-0.89	9.11E-04	7.90E-03

ybgR	zinc transporter ZitB	-2.06	-1.04	4.06E-08	1.03E-06
ybhO	cardiolipin synthase	-1.81	-0.85	2.18E-06	3.98E-05
ybhP	cytoplasmic protein	-1.85	-0.88	3.00E-06	5.15E-05
ybiJ	periplasmic protein	-1.54	-0.63	9.24E-03	0.05
ybiS	periplasmic protein	-2.42	-1.27	7.69E-09	2.11E-07
ybjO	inner membrane protein	-1.79	-0.84	1.54E-06	2.91E-05
ycaD	MFS family transporter protein	-2.96	-1.57	2.22E-16	1.32E-14
ycaO	cytoplasmic protein	-1.75	-0.81	2.79E-04	2.90E-03
ycaP	inner membrane protein	-1.6	-0.68	2.45E-03	0.02
yceG	septation protein	-2.05	-1.03	1.04E-06	2.06E-05
ycfJ	outer membrane lipoprotein	-11.22	-3.49	0	0
ycfR	outer membrane protein	-2.68	-1.42	6.87E-05	8.67E-04
ycfS	periplasmic protein	-2.71	-1.44	5.44E-13	2.52E-11
yciA	acyl-CoA thioesterase	-1.94	-0.95	3.28E-07	7.21E-06
yciH	translation initiation factor Sui1	-8.92	-3.16	0	0
yciK	oxoacyl-ACP reductase	-3.34	-1.74	1.58E-14	8.59E-13
yciL	23S rRNA pseudouridylate synthase B	-2.91	-1.54	3.97E-13	1.88E-11
ydaO	tRNA 2-thiocytidine biosynthesis protein TtcA	-1.7	-0.77	1.30E-03	0.01
yddX	biofilm-dependent modulation protein	-3.16	-1.66	1.01E-10	3.43E-09
ydeA	sugar efflux transporter	-1.65	-0.72	3.02E-04	3.09E-03
ydeI	periplasmic protein	-1.77	-0.82	8.41E-06	1.30E-04
ydeJ	competence damage-inducible protein A	-2.18	-1.12	3.66E-09	1.03E-07
ydgC	inner membrane protein	-1.83	-0.87	1.24E-04	1.46E-03
ydgF	spermidine export protein MdtJ	-1.92	-0.94	2.18E-04	2.36E-03
ydgI	amino acid transporter	-2.52	-1.33	6.99E-12	2.74E-10
ydhB	LysR family transcriptional regulator	-1.62	-0.69	6.80E-05	8.60E-04
ydhC	MFS family transport protein	-2.07	-1.05	2.00E-10	6.49E-09
ydiL	cytoplasmic protein	-1.96	-0.97	3.61E-03	0.02
ydiN	MFS family transport protein	-1.88	-0.91	0.01	0.05
ydjM	LexA-regulated protein	-1.8	-0.85	5.73E-04	5.36E-03
ydjN	kinase-like protein	-1.77	-0.82	1.97E-04	2.16E-03
yebE	inner membrane protein	-4.04	-2.01	1.13E-09	3.35E-08
yebG	DNA damage-inducible protein	-10.6	-3.41	0	0
yeeA	inner membrane protein	-3.45	-1.79	1.02E-10	3.43E-09
yeeF	amino acid transport protein	-3.34	-1.74	3.80E-06	6.33E-05
yegD	chaperone	-2.42	-1.28	4.70E-06	7.69E-05
yegQ	protease	-1.93	-0.95	9.17E-08	2.20E-06
yegS	lipid kinase	-2.51	-1.33	1.84E-09	5.34E-08
yehE	outer membrane protein	-3.79	-1.92	2.22E-16	1.32E-14
yfaZ	inner membrane protein	-1.93	-0.95	4.32E-07	9.30E-06
yfcB	50S ribosomal protein L3 glutamine methyltransferase	-1.85	-0.88	8.71E-05	1.06E-03

yfdC	inner membrane protein	-1.55	-0.64	8.99E-04	7.84E-03
yfgB	dual-specificity RNA methyltransferase RlmN	-1.8	-0.85	1.57E-03	0.01
yfiF	tRNA/rRNA methyltransferase	-1.98	-0.99	2.35E-05	3.39E-04
ygaC	cytoplasmic protein	-5.28	-2.4	0	0
ygaM	inner membrane protein	-1.88	-0.91	1.24E-08	3.35E-07
ygdR	POT family peptide transport protein	-2.6	-1.38	2.06E-08	5.40E-07
yggE	oxidative stress defense protein	-4.97	-2.31	2.10E-13	1.04E-11
yggG	Zn-dependent protease	-1.82	-0.86	1.04E-05	1.58E-04
yggX	Fe(2+)-trafficking protein	-1.88	-0.91	3.54E-06	5.91E-05
ygjT	inner membrane protein	-2.03	-1.02	2.24E-07	5.03E-06
yhbE		-3.04	-1.6	0	0
yhbO	intracellular proteinase	-2.44	-1.29	6.39E-13	2.90E-11
yhdG	tRNA-dihydrouridine synthase B	-2.41	-1.27	2.36E-10	7.59E-09
yhdV	outer membrane lipoprotein	-5.83	-2.54	1.85E-12	7.95E-11
yhfC	transporter	-2.14	-1.1	1.38E-07	3.19E-06
yhgF	RNase R	-1.88	-0.91	2.25E-03	0.02
yhjB	transcriptional regulator	-1.64	-0.71	1.69E-03	0.01
yhjK	diguanylate cyclase/phosphodiesterase	-1.83	-0.87	6.42E-07	1.32E-05
yiaD	outer membrane lipoprotein	-9.03	-3.18	1.11E-16	6.77E-15
yiaE	glyoxylate/hydroxypyruvate reductase B	-1.74	-0.8	2.84E-05	3.96E-04
yiaJ	IclR family transcriptional repressor	-1.52	-0.6	3.27E-03	0.02
yibD	glycosyl transferase	-2.15	-1.1	4.24E-08	1.07E-06
yidY	multidrug resistance protein MdtL	-1.81	-0.85	2.39E-04	2.53E-03
yieH	bifunctional phosphoenolpyruvate/6-phosphogluconate phosphatase	-2.32	-1.21	5.55E-08	1.37E-06
yigM	membrane protein	-1.67	-0.74	1.18E-04	1.39E-03
yiiU	cell division protein ZapB	-1.61	-0.69	8.86E-03	0.05
yjaB	N-acetyltransferase	-1.59	-0.67	1.93E-04	2.14E-03
yjbE	outer membrane protein	-10.27	-3.36	0	0
yjbF	outer membrane lipoprotein	-25.86	-4.69	0	0
yjbG	periplasmic protein	-19.47	-4.28	0	0
yjbH	outer membrane lipoprotein	-2.63	-1.39	1.86E-05	2.74E-04
yjbJ	stress-response protein	-2.67	-1.42	6.43E-08	1.58E-06
yjcB	inner membrane protein	-3.21	-1.68	1.55E-12	6.79E-11
yjeA	elongation factor P--(R)-beta-lysine ligase	-1.63	-0.71	3.55E-03	0.02
yjeM	inner membrane transporter	-1.73	-0.79	1.04E-03	8.73E-03
yjiO	multidrug resistance protein MdtM	-1.7	-0.77	7.90E-04	7.02E-03
yjjQ	LuxR/UhpA family transcriptional regulator	-1.78	-0.83	7.45E-03	0.04
yjjU	phosphoesterase	-1.78	-0.83	1.44E-06	2.75E-05
yncB	NADP-dependent oxidoreductase	-1.5	-0.59	8.60E-04	7.54E-03
yneH	glutaminase	-1.51	-0.59	8.50E-04	7.49E-03
yohL	transcriptional repressor RcnR	-3.59	-1.85	4.10E-14	2.16E-12

yohM	nickel/cobalt efflux protein RcnA	-2.38	-1.25	1.02E-07	2.43E-06
yojI	multidrug transporter permease/ATP-binding protein	-1.56	-0.64	7.51E-04	6.75E-03
ypeC	periplasmic protein	-6.49	-2.7	3.18E-12	1.29E-10
ypfG	periplasmic protein	-9.47	-3.24	0	0
yqcC	cytoplasmic protein	-1.57	-0.65	5.87E-03	0.03
yqjH	transporter	-1.69	-0.75	3.39E-05	4.61E-04
yrbA	BolA family transcriptional regulator	-1.69	-0.76	1.99E-05	2.91E-04
yrbB	STAS domain-containing protein	-2.13	-1.09	5.22E-07	1.11E-05
yrbC	ABC transporter substrate-binding protein	-2.33	-1.22	3.61E-05	4.86E-04
yrbE	ABC transporter permease	-1.64	-0.71	1.64E-03	0.01
yrbF	ABC transporter ATP-binding protein	-1.62	-0.69	5.07E-04	4.86E-03
yrfH	ribosome-associated heat shock protein Hsp15	-1.55	-0.63	8.20E-04	7.24E-03
ysdA		-5.05	-2.34	0	0
ysdB		-4.39	-2.14	0	0
zntA	zinc/cadmium/mercury/lead-transporting ATPase	-8.91	-3.16	0	0
zntB	zinc transport protein ZntB	-1.93	-0.95	2.47E-06	4.41E-05
zur	zinc uptake transcriptional repressor	-2.15	-1.1	5.62E-10	1.74E-08

[a] Functional annotations are from NCBI for *Salmonella* Typhimurium strain LT2 (accession number NC_003197). Gene function is unknown for blank fields.

Table 5. Differentially expressed genes of interest associated with transport, metabolism, regulatory, and pathogenesis functions.

Gene name	Function[a]	Fold change	Log_2 fold change	P-value	FDR p-value
Transport and localization					
artQ	arginine ABC transporter permease ArtQ	1.5	0.58	3.37E-03	0.02
cysU	sulfate/thiosulfateABC transporter permease CysU	1.58	0.66	7.43E-03	0.04
cysW	sulfate/thiosulfate ABC transporter permease CysW	1.62	0.69	5.28E-03	0.03
dppC	dipeptide ABC transporter permease DppC	1.66	0.73	3.23E-04	3.27E-03
dppD	dipeptide ABC transporter ATP-binding subunit DppD	1.8	0.85	7.28E-04	6.60E-03
dppF	dipeptide ABC transporter ATP-binding subunit DppF	1.68	0.75	8.38E-03	0.05
hisM	histidine ABC transporter permease HisM	2	1	2.26E-06	4.08E-05
hisP	histidine ABC transporter ATP-binding protein HisP	1.81	0.86	1.80E-04	2.01E-03
hisQ	histidine ABC transporter permease HisQ	1.84	0.88	1.73E-03	0.01
kdpB	potassium-transporting ATPase subunit B	-1.66	-0.73	5.68E-03	0.03
kdpC	potassium-transporting ATPase subunit C	-1.62	-0.7	1.33E-03	0.01
mgtA	magnesium-transporting ATPase	-16.17	-4.02	0	0
mgtB	magnesium-transporting ATPase	-8.04	-3.01	3.12E-11	1.11E-09
mgtC	protein MgtC	-16.64	-4.06	0	0
osmB	osmotically inducible lipoprotein B	-20.71	-4.37	0	0
phnS	2-aminoethylphosphonate ABC transporter substrate-binding protein PhnS	-6.36	-2.67	1.67E-15	9.41E-14
phnT	2-aminoethylphosphonate ABC transporter ATP-binding protein PhnT	-2.65	-1.41	1.44E-05	2.16E-04
phnU	2-aminoethylphosphonate ABC transporter permease PhnU	-2.43	-1.28	6.32E-09	1.75E-07
phoB	response regulato PhoB	-7.31	-2.87	0	0
phoE	outer membrane phosphoporin protein E	-3.3	-1.72	1.83E-10	6.01E-09
phoR	sensory kinase PhoR	-6.67	-2.74	0	0
phoU	transcriptional regulator PhoU	-6.88	-2.78	1.15E-09	3.40E-08
ppk	polyphosphate kinase	1.6	0.68	5.55E-04	5.24E-03
pstA	phosphate ABC transporter permease subunit PtsA	-17.91	-4.16	0	0
pstB	phosphate ABC transporter ATP-binding protein PstB	-11.49	-3.52	7.11E-15	3.92E-13
pstC	phosphate ABC transporter permease PstC	-26.42	-4.72	0	0
pstS	phosphate ABC transporter substrate-binding protein PstS	-57.1	-5.84	0	0
sapD	peptide ABC transporter ATP-binding	1.51	0.59	2.03E-04	2.22E-03

	protein SapD				
sapF	peptide ABC transporter ATP-binding protein SapF	1.55	0.63	2.74E-03	0.02
ugpA	glycerol-3-phosphate ABC transporter permease UdpA	-11.14	-3.48	0	0
ugpB	glycerol-3-phosphate ABC transporter substrate-binding protein UdpB	-11.45	-3.52	1.11E-16	6.77E-15
ugpC	glycerol-3-phosphate ABC transporter ATP-binding protein UgpC	-8.11	-3.02	0	0
ugpE	glycerol-3-phosphate ABC transporter permease UdpE	-13.51	-3.76	0	0
ugpQ	glycerophosphodiester phosphodiesterase	-1.98	-0.98	2.68E-04	2.81E-03
zntA	zinc/cadmium/mercury/lead-transporting ATPase	-8.91	-3.16	0	0
zntB	zinc transport protein ZntB	-1.93	-0.95	2.47E-06	4.41E-05
zur	zinc uptake transcriptional repressor	-2.15	-1.1	5.62E-10	1.74E-08
Metabolism					
entA	3-dihydro-2-3-dihydroxybenzoate dehydrogenase	-4.99	-2.32	2.25E-14	1.21E-12
entB	3-dihydro-2-3-dihydroxybenzoate synthetase	-6.35	-2.67	0	0
entC	isochorismate synthase	-9.79	-3.29	0	0
entD	4'-phosphopantetheinyl transferase	-3.87	-1.95	0	0
entE	3-dihydroxybenzoate-AMP ligase	-8.61	-3.11	0	0
entF	enterobactin synthase subunit F	-2.31	-1.21	8.57E-07	1.72E-05
eutD	phosphotransacetylase EutD	1.89	0.92	3.32E-03	0.02
eutN	microcompartment shell protein EutN	1.82	0.86	3.18E-03	0.02
eutP	ethanolamine utilization protein EutP	2.34	1.23	1.43E-07	3.29E-06
eutQ	ethanolamine utilization protein EutQ	2.03	1.02	4.91E-04	4.74E-03
eutS	carboxysome structural protein EutS	2.5	1.32	1.20E-08	3.26E-07
eutT	cobalamin adenosyltransferase EutT	2.11	1.08	1.20E-03	9.82E-03
fepA	outer membrane porin	-5.33	-2.41	0	0
fepE	ferric enterobactin transport protein	1.56	0.64	1.32E-04	1.53E-03
fes	enterochelin esterase	-2.84	-1.5	1.73E-09	5.03E-08
prpR	propionate catabolism operon regulatory protein	1.93	0.95	5.90E-05	7.57E-04
rcsA	transcriptional regulator RcsA	-7.99	-3	0	0
rcsB	transcriptional regulator RcsB	-1.78	-0.84	6.54E-03	0.04
tonB	transport protein TonB	-1.54	-0.63	1.62E-03	0.01
wcaA	glycosyl transferase	-7.66	-2.94	0	0
wcaB	colanic acid biosynthesis acetyltransferase WcaB	-4.41	-2.14	4.57E-14	2.38E-12
wcaC	glycosyl transferase	-5.53	-2.47	8.60E-12	3.29E-10
wcaD	colanic acid polymerase	-8.69	-3.12	0	0
wcaE	glycosyl transferase family protein	-25.76	-4.69	0	0

wcaF	colanic acid biosynthesis acetyltransferase WcaF	-26.86	-4.75	0	0
wcaG	GDP-fucose synthetase	-12.91	-3.69	0	0
wcaH	GDP-mannose mannosyl hydrolase	-10.3	-3.36	0	0
wcaI	glycosyl transferase	-7.82	-2.97	0	0
wcaJ	UDP-glucose lipid carrier transferase	-2.14	-1.1	2.36E-06	4.22E-05
wza	polysaccharide export protein	-28.28	-4.82	0	0
wzb	protein-tyrosine-phosphatase	-31.78	-4.99	0	0
wzc	tyrosine-protein kinase	-14.72	-3.88	0	0
wzxC	colanic acid exporter	-1.75	-0.81	9.51E-04	8.15E-03
Regulatory					
csgD	DNA-binding transcriptional regulator CsgD	2.59	1.37	6.64E-11	2.29E-09
csgE	curli production assembly/transport protein CsgE	2.85	1.51	1.75E-12	7.58E-11
csgF	curli production assembly/transport protein CsgF	1.97	0.98	7.86E-07	1.60E-05
flhC	transcriptional regulator FlhC	2.05	1.04	2.35E-05	3.39E-04
flhD	transcriptional regulator FlhD	2.04	1.03	5.44E-06	8.66E-05
hybB	hydrogenase 2 b cytochrome subunit	1.63	0.71	1.08E-03	8.97E-03
hybD	hydrogenase 2 maturation endopeptidase	1.89	0.92	5.09E-05	6.60E-04
hybE	hydrogenase 2-specific chaperone	2.01	1.01	2.82E-08	7.26E-07
hybF	hydrogenase nickel incorporation protein HybF	2.04	1.03	9.53E-08	2.27E-06
hybG	hydrogenase 2 accessory protein HypG	2.12	1.08	5.17E-10	1.63E-08
hypA	hydrogenase nickel incorporation protein	2.05	1.03	1.13E-03	9.27E-03
lexA	LexA repressor	-1.75	-0.81	1.37E-03	0.01
nuoE	NADH-quinone oxidoreductase subunit E	1.6	0.68	7.72E-03	0.04
nuoK	NADH-quinone oxidoreductase subunit K	1.5	0.59	1.71E-03	0.01
pspA	phage shock protein PspA	-3.43	-1.78	5.01E-11	1.75E-09
pspB	phage shock protein PspB	-3.07	-1.62	6.25E-13	2.86E-11
pspC	DNA-binding transcriptional activator PspC	-2.8	-1.48	3.11E-13	1.52E-11
pspD	inner membrane phage-shock protein	-2.61	-1.38	1.11E-16	6.77E-15
pspG	phage shock protein G	-2.2	-1.14	8.59E-10	2.60E-08
recA	recombinase A	-5.21	-2.38	8.76E-10	2.63E-08
rplA	50S ribosomal protein L1	-3.57	-1.83	4.54E-05	5.97E-04
rplB	50S ribosomal protein L2	-2.78	-1.48	1.97E-03	0.01
rplC	50S ribosomal protein L3	-3.31	-1.73	2.04E-04	2.23E-03
rplD	50S ribosomal protein L4	-3.09	-1.63	4.39E-04	4.30E-03
rplI	50S ribosomal protein L9	-2.74	-1.45	1.49E-03	0.01
rplK	50S ribosomal protein L11	-3.98	-1.99	4.76E-08	1.18E-06
rplP	50S ribosomal protein L16	-2.19	-1.13	0.01	0.05
rplS	50S ribosomal protein L19	-2.16	-1.11	2.71E-03	0.02
rplV	50S ribosomal protein L22	-2.46	-1.3	4.31E-03	0.03

rplW	50S ribosomal protein L23	-3.05	-1.61	3.32E-04	3.34E-03
rplY	50S ribosomal protein L25	-2.39	-1.26	1.54E-04	1.74E-03
rpmB	50S ribosomal protein L28	-1.85	-0.89	4.84E-03	0.03
rpmC	50S ribosomal protein L29	-2.07	-1.05	8.55E-03	0.05
rpmE	50S ribosomal protein L31	-2.22	-1.15	1.50E-03	0.01
rpmH	50S ribosomal protein L34	-1.82	-0.87	2.62E-05	3.71E-04
rpsC	30S ribosomal protein S3	-2.38	-1.25	7.88E-03	0.04
rpsF	30S ribosomal protein S6	-2.87	-1.52	5.90E-04	5.49E-03
rpsJ	30S ribosomal protein S10	-2.84	-1.51	3.89E-04	3.89E-03
rpsP	30S ribosomal protein S16	-1.94	-0.95	2.55E-03	0.02
rpsR	30S ribosomal protein S18	-2.92	-1.55	1.44E-04	1.64E-03
rpsS	30S ribosomal protein S19	-2.68	-1.42	1.30E-03	0.01
ruvA	Holliday junction ATP-dependent DNA helicase RuvA	-2.12	-1.08	1.95E-08	5.13E-07
ruvB	Holliday junction ATP-dependent DNA helicase RuvB	-1.5	-0.58	5.41E-03	0.03
sulA	cell division inhibitor SulA	-6.5	-2.7	0	0
ttrR	tetrathionate response regulator TtrR	1.52	0.6	7.69E-04	6.89E-03
ttrS	tetrathionate sensor histidine kinase TtrS	1.76	0.81	2.95E-04	3.03E-03
uvrA	excinuclease ABC subunit A	-1.9	-0.93	6.83E-04	6.24E-03
uvrB	excinuclease ABC subunit B	-2	-1	2.27E-06	4.08E-05
Pathogenesis					
hilD	transcriptional regulator HilD	1.5	0.59	3.16E-03	0.02
invA	invasion protein InvA	1.66	0.74	1.08E-04	1.29E-03
invB	surface presentation of antigens protein SpaK	1.86	0.9	4.80E-05	6.24E-04
invE	invasion protein InvE	1.7	0.77	3.99E-05	5.31E-04
invI	surface presentation of antigens protein SpaM	1.75	0.81	1.36E-04	1.57E-03
prgH	secretion system protein PrgH	1.59	0.67	1.15E-03	9.39E-03
prgJ	secretion system protein PrgJ	1.61	0.69	1.03E-03	8.65E-03
prgK	secretion system lipoprotein PrgK	1.79	0.84	2.99E-04	3.06E-03
sopD	secreted effector protein SopD	1.59	0.67	4.59E-03	0.03
spaP	surface presentation of antigens protein SpaP	2.12	1.08	6.98E-10	2.13E-08
spaQ	surface presentation of antigens protein SpaQ	1.64	0.72	4.55E-04	4.45E-03
spaR	surface presentation of antigens protein SpaR	1.89	0.92	1.60E-04	1.80E-03
spaS	surface presentation of antigens protein SpaS	2.28	1.19	7.91E-07	1.60E-05
ssaB	secretion system apparatus protein SsaB	2.58	1.37	5.79E-07	1.21E-05
ssaC	secretion system apparatus outer membrane protein SsaC	1.82	0.86	2.91E-05	4.03E-04
ssaD	secretion system apparatus protein SsaD	2.24	1.16	1.62E-08	4.29E-07
ssaE	secretion system effector SsaE	2.32	1.21	5.41E-07	1.14E-05

ssaG	secretion system apparatus protein SsaG	2.69	1.43	1.95E-11	7.35E-10
ssaH	secretion system apparatus protein SsaH	2.43	1.28	2.24E-12	9.35E-11
ssaI	secretion system apparatus protein SsaI	1.77	0.82	2.35E-04	2.51E-03
ssaJ	secretion system apparatus lipoprotein SsaJ	1.93	0.95	2.27E-04	2.43E-03
ssaK	secretion system apparatus protein SsaK	2.36	1.24	1.54E-10	5.09E-09
ssaL	secretion system apparatus protein SsaL	1.93	0.95	1.94E-04	2.14E-03
ssaM	secretion system apparatus protein SsaM	2.09	1.07	2.27E-04	2.43E-03
ssaN	secretion system apparatus ATP synthase SsaN	1.9	0.93	1.29E-03	0.01
ssaO	secretion system apparatus protein SsaO	3.23	1.69	0	0
ssaP	secretion system apparatus protein SsaP	3.16	1.66	1.62E-13	8.08E-12
ssaQ	secretion system apparatus protein SsaQ	2.24	1.16	5.53E-06	8.77E-05
ssaR	secretion system apparatus protein SsaR	1.93	0.95	1.08E-05	1.65E-04
ssaS	secretion system apparatus protein SsaS	3.08	1.62	6.87E-14	3.54E-12
ssaT	secretion system apparatus protein SsaT	2.01	1.01	2.80E-03	0.02
ssaV	secretion system apparatus protein SsaV	2.08	1.06	7.87E-04	7.01E-03
sscB	secretion system chaperone SscB	1.73	0.79	1.98E-03	0.01
sseD	translocation machinery protein SseD	1.5	0.58	8.16E-03	0.04
sseE	secretion system effector SseE	1.54	0.63	3.20E-03	0.02
sseF	secretion system effector SseF	2.51	1.33	1.36E-09	3.99E-08
sseG	secretion system effector SseG	2.44	1.29	1.29E-08	3.48E-07
sseI	required for maintaining a long-term systemic infection	1.87	0.9	2.65E-05	3.73E-04
sseL	deubiquitinase SseL	1.76	0.81	4.64E-05	6.08E-04
ssrA	secretion system sensor kinase SsrA	1.78	0.83	8.20E-07	1.65E-05
ssrB	secretion system transcriptonal activator SsrB	1.61	0.69	5.98E-05	7.65E-04

[a] Functional annotations are from NCBI for *Salmonella* Typhimurium strain LT2 (accession number NC_003197).

FIGURES

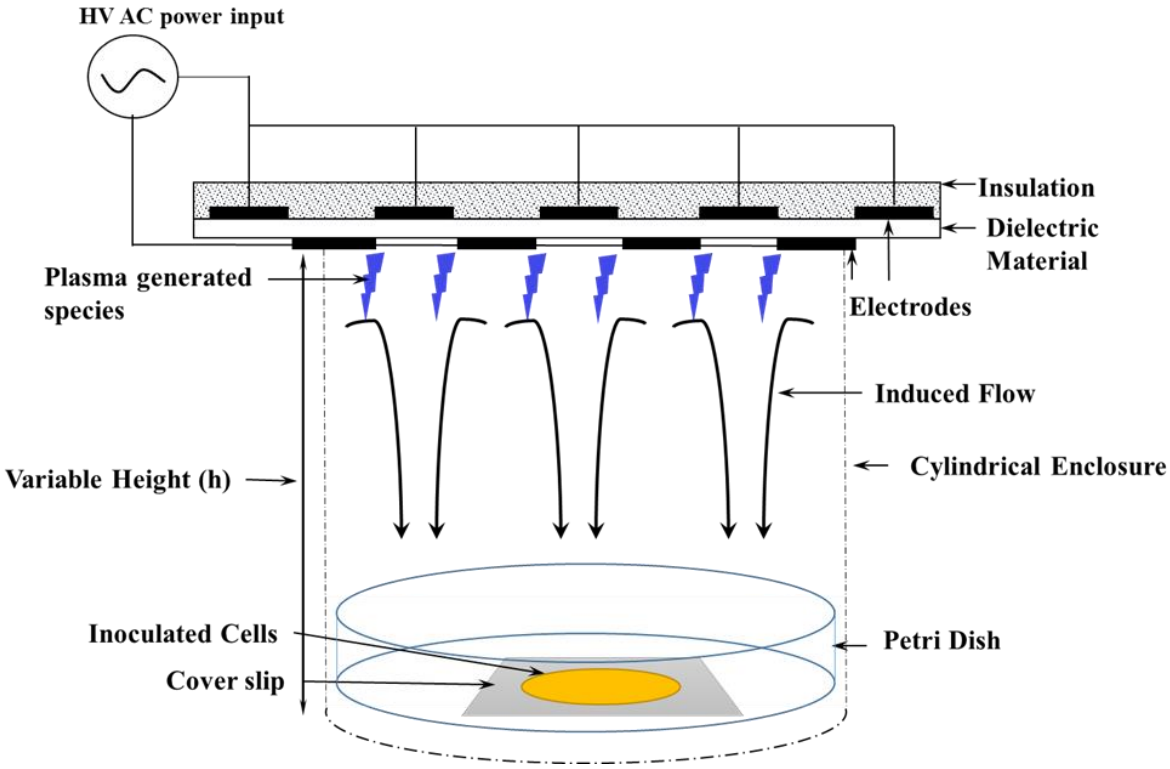

Figure 1. Schematic representation of the asymmetric SDBD set up for treating pathogen-inoculated coverslips,

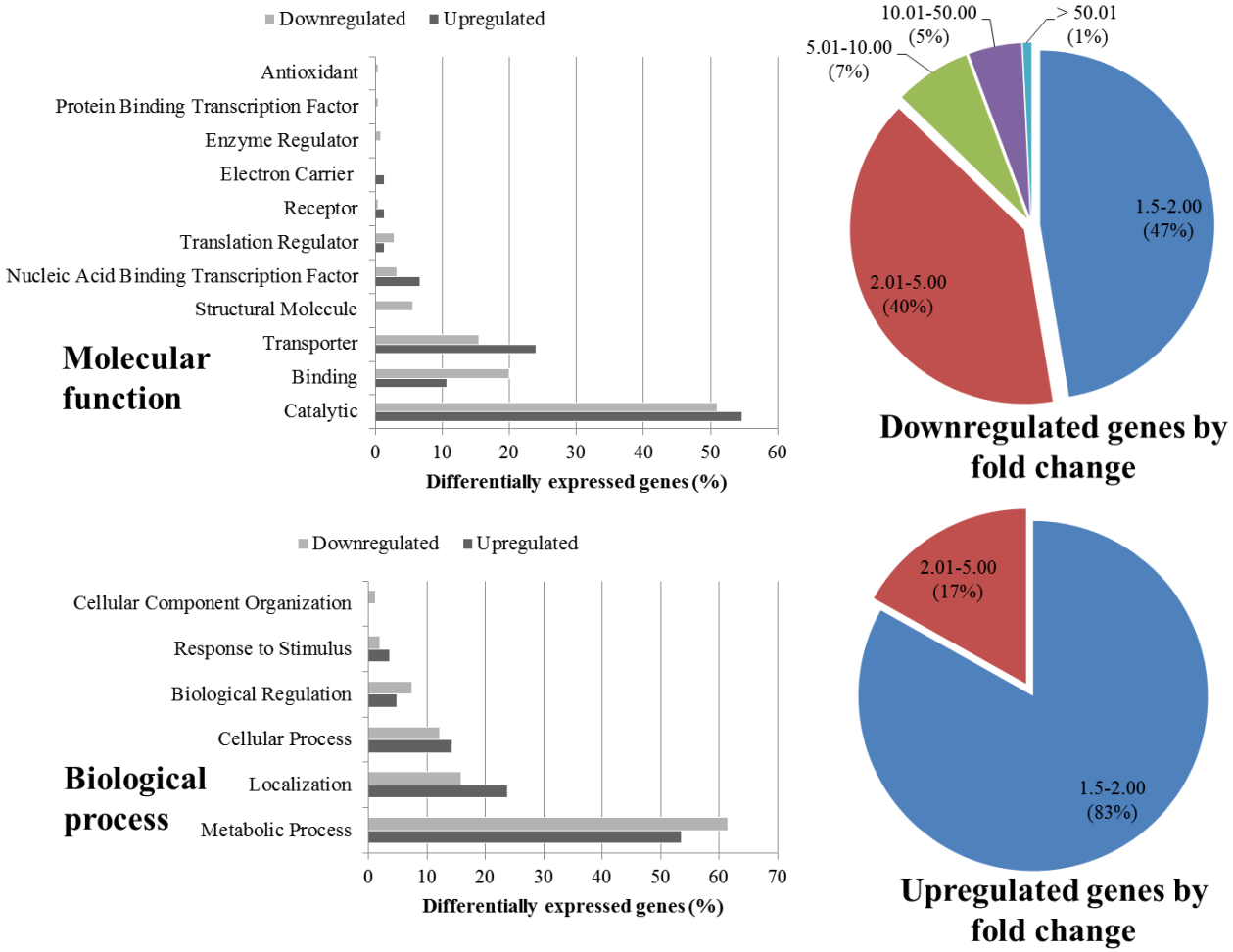

Figure 2. Number of differentially expressed genes with known molecular function and biological processes, as reported by PANTHER, and number of upregulated and downregulated genes by fold change.

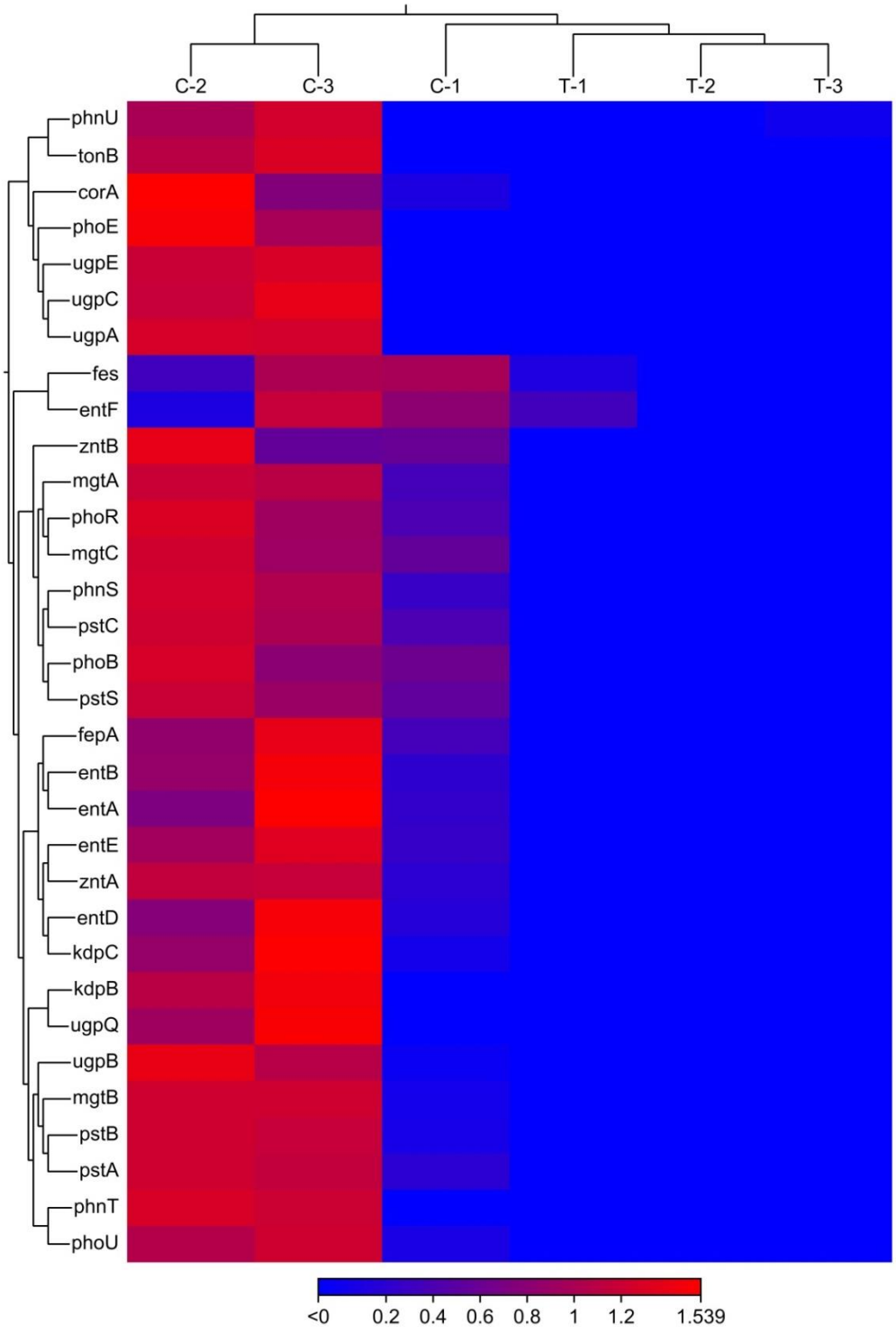

Figure 3. Hierarchical clustering of major downregulated genes involved in phosphate and cation transport and ethanolamine biosynthesis, showing correlation between treated and control samples replicates. Treated sample replicates are designated T-1-T-3 and untreated control sample replicates are designated C-1-C-3.

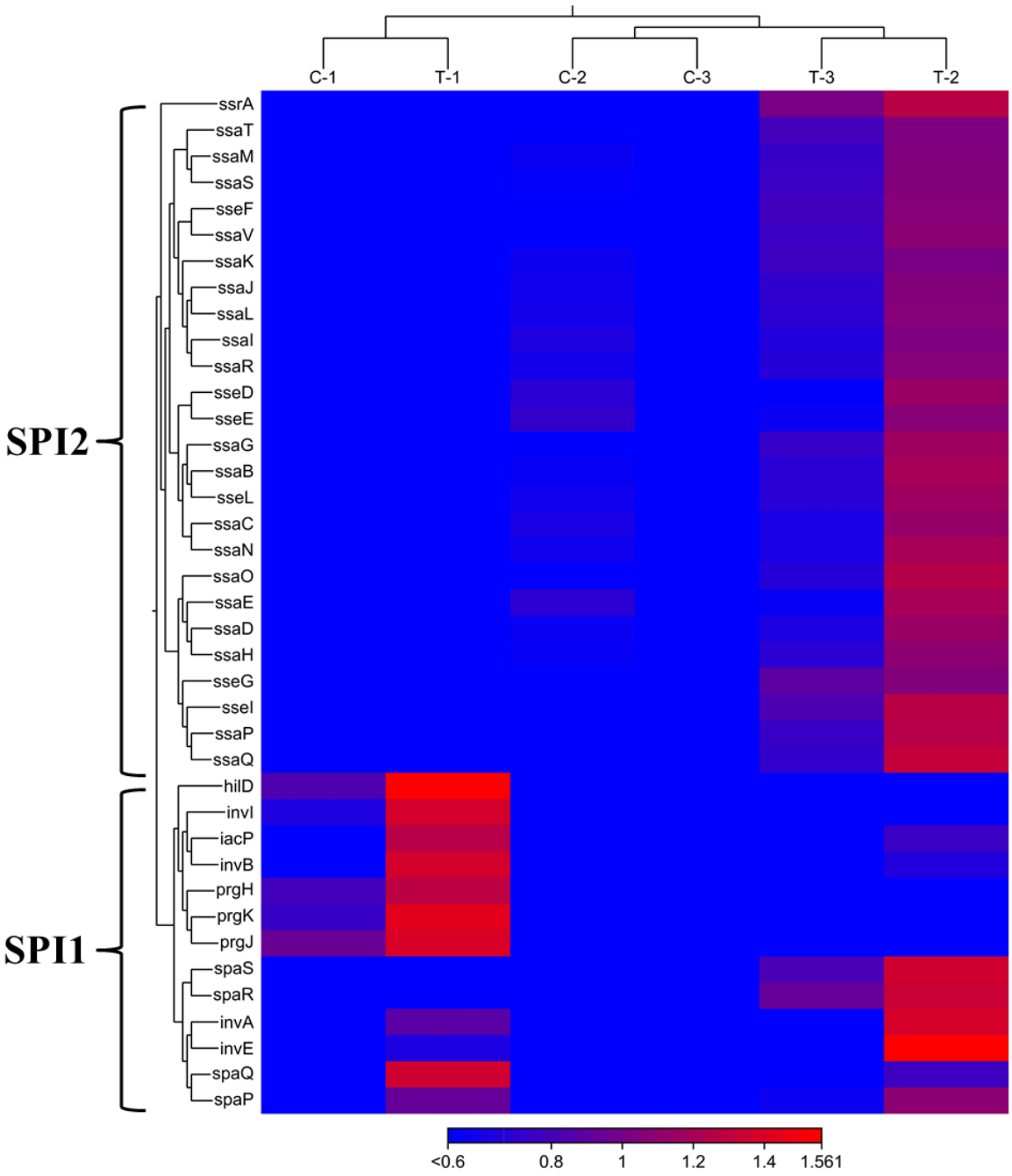

Figure 4. Hierarchical clustering of upregulated genes by pathogenicity island, showing uncorrelated clustering due to inconsistent expression between replicates. Treated sample replicates are designated T-1-T-3 and untreated control sample replicates are designated C-1-C-3. SPI2 was upregulated in treated replicates T-2 and T-3 while SPI1 was upregulated in treated replicate T-1.

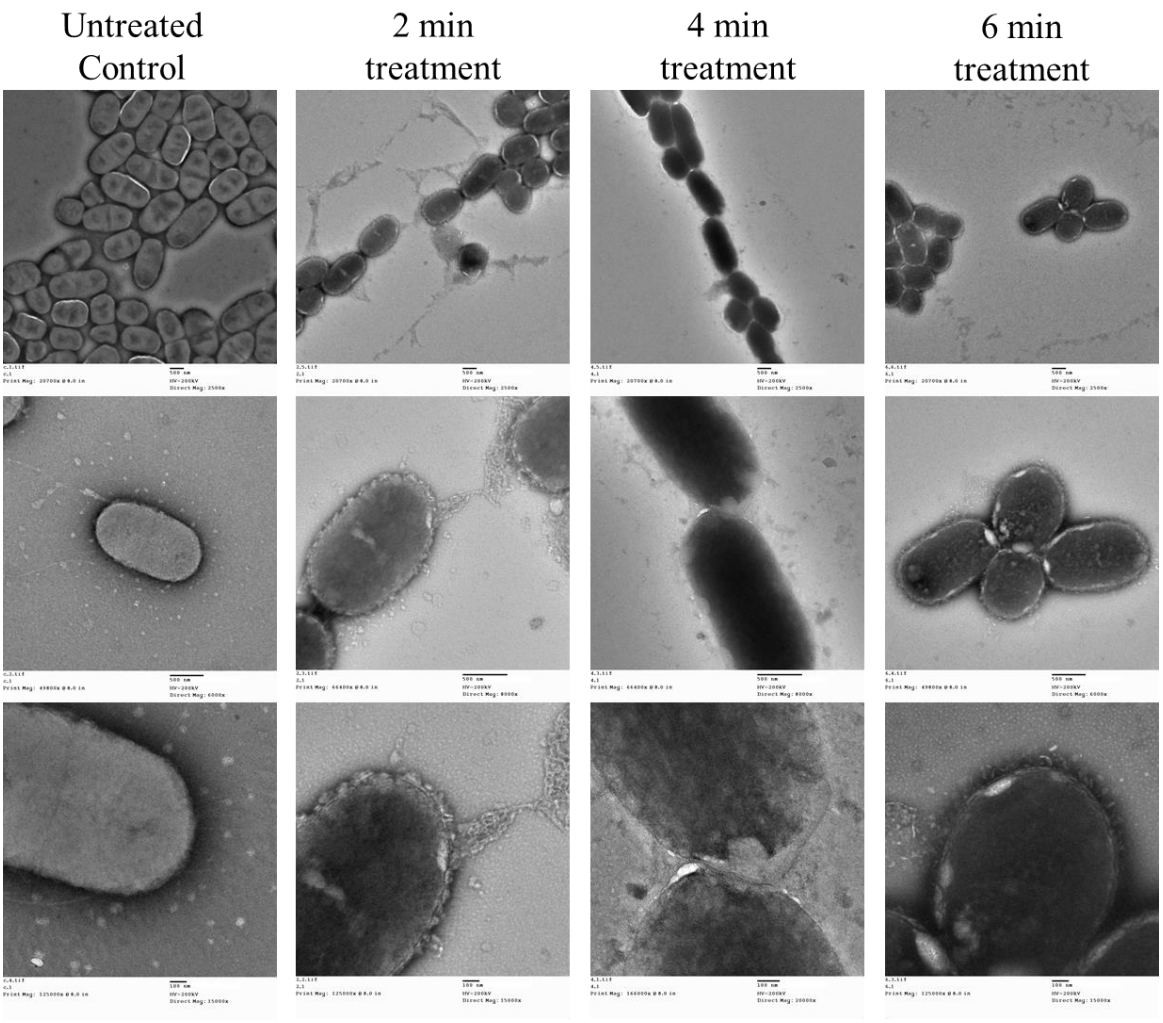

Figure 5. TEM of *Salmonella* Typhimurium treated with SDBD cold plasma for 2, 4, and 6 min, compared with an untreated control.

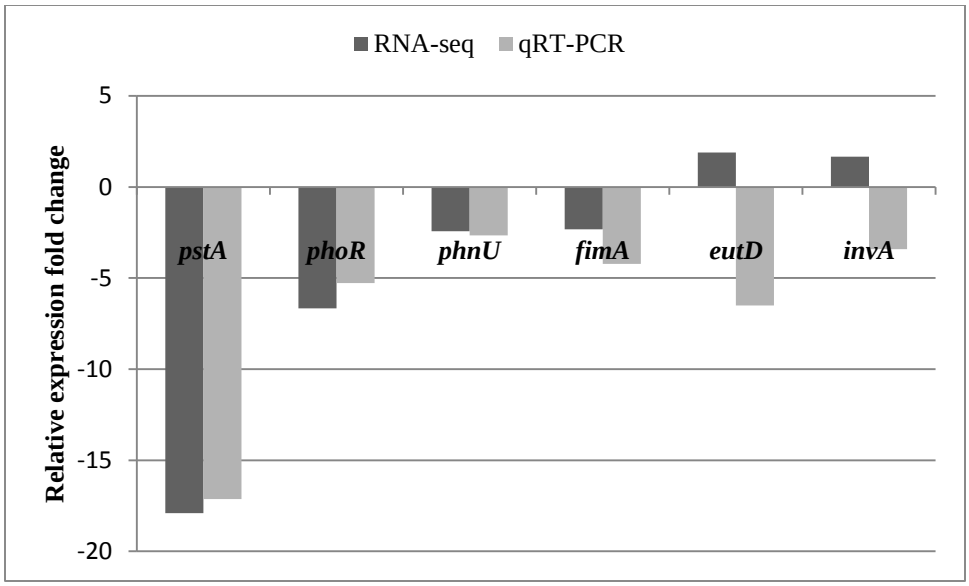

Figure 6. Comparison of average relative gene expression fold changes identified by RNA-seq and qRT-PCR. *gyrB* was not differentially expressed and used as a control for data normalization.

CHAPTER V

EVALUATION OF THE POTENTIAL DEVELOPMENT OF RESISTANCE TO COLD PLASMA TREATMENT BY *SALMONELLA* ENTERITIDIS THROUGH TRANSCRIPTOMIC ANALYSIS

ABSTRACT

Cold atmospheric plasma treatment is emerging as a surface sterilization or food decontamination alternative that inactivates bacterial pathogens through a multi-modal mechanism of physical damage to cellular macromolecules by charged particles and reactive oxygen and nitrogen species (RONS). Due to the indiscriminate, physical damage caused by RONS on bacterial cells, one of the major potential benefits of cold plasma treatments is a potentially limited ability for bacteria to develop resistance to the treatment. To preliminarily evaluate this potential, the purpose of this study was to compare the transcriptomic response of dried *Salmonella* cells before and after 5 successive rounds of plasma treatment with surface dielectric barrier discharge (SDBD) actuators. Bacterial inactivation was not significantly different ($P \leq 0.01$) for all 5 treatments. Among 1,136 differentially expressed genes having fold changes greater than 1.50 ($P \leq 0.01$, FDR ≤ 0.05), 492 were up-regulated (1.50 to 6.06-fold) and 644 were downregulated (-1.50 top -241.14-fold) after plasma treatment with 533 genes differentially expressed in common before and after 5 rounds of plasma treatment.

Downregulated genes were associated with nutrient uptake, osmoregulation, alternative carbon and nitrogen source utilization, transcription, translation, and DNA damage repair. The major upregulated genes included those encoding pathogenicity associated proteins, especially those from *Salmonella* pathogenicity island 2 (SPI2). A reduction in overall cellular stress, observed before and after 5 rounds of plasma treatment, is thought to be caused by cytosol leakage and cell lysis via lipid peroxidation, alleviating nutrient, osmotic, and desiccation stress. Differentially gene expression unique to treatment after the 5 rounds was associated with the same or similar pathways as prior to the 5 rounds, except that more genes within the pathways were differentially expressed. No significant differences in bacterial inactivation rates or differential gene expression that could potentially lead to resistance development were identified. To our knowledge, this is the first known study evaluating the potential of bacterial pathogens to develop resistance to cold plasma treatment and further confirms the role of cellular structural damage contributing to inactivation of Gram-negative bacteria. Following further optimization and delineation of plasma generation apparatuses and treatment parameters, cold plasma may be a viable alternative to help alleviate the global burden of continued antibiotic resistance development among bacterial pathogens.

INTRODUCTION

Cold atmospheric plasma is a versatile emerging technology that has multiple potential applications ranging from surface sterilization to food decontamination (Kong *et al.,* 2009; Misra *et al.,* 2011). Consisting of ionized air generated at ambient temperature and atmospheric pressure, cold plasma is composed of UV light, charged particles, and

reactive oxygen and nitrogen species (RONS) that can have damaging effects on prokaryotic and eukaryotic cells in a dose-dependent manner (Mai-Prochnow *et al.,* 2014; Pai *et al.,* 2015). RONS are emerging as the primary plasma-produced products that damage living cells through oxidative stress. More specifically, lipid peroxidation, DNA damage, and protein damage can accumulate rapidly in plasma treated cells resulting in cell lysis, necrosis, and/or apoptosis (Han *et al.,* 2016). Bacteria are among the organisms most sensitive to cold plasma-induced damage and are rapidly inactivated via lipid peroxidation and DNA damage (Joshi *et al.,* 2011; Han *et al.,* 2016; Kvam *et al.,* 2016). Gram-negative bacteria in particular are rapidly inactivated with cold plasma through membrane damage resulting in cytosol leakage and cell lysis (Kvam *et al.,* 2016; Lunov *et al.,* 2016). Since Gram-negative bacteria are among the most important foodborne and hospital acquired pathogens, with increasing reports of multiple-drug resistance development (Chang *et al.,* 2015), cold plasma has gained intense recent interest as a surface sterilization or decontamination method (Kong *et al.,* 2009; Mai-Prochnow *et al.,* 2014).

One of the most promising features of cold plasma treatment is that the multi-modal effects of RONS and charged particles on lipids, nucleic acids, and peptides may result in limited potential for bacteria to develop resistance to this method (Alkawareek *et al.,* 2014). With an ever increasing number of multiple drug resistant bacterial strains (Chang *et al.,* 2015) and growing worldwide concern about widespread antibiotic use (Littmann *et al.,* 2015), there is a great need for antibiotic treatments having minimal risks for additional antibiotic resistance development (Spellberg and Shlaes, 2014). Although limited to surface sterilization or decontamination applications, cold plasma

treatments have great potential applications in this area due to the unique combination and interplay between biological and physical scenarios of bacterial inactivation (Lunov *et al.*, 2016). However, no known studies have been published investigating the potential for resistance development by treating a surviving population of plasma-exposed cells multiple times and comparing the genotypic and phenotypic characteristics. Additionally, although most practical applications of cold plasma treatment are for surface decontamination applications, almost all studies investigating the mechanistic effects of cold plasma treatment on bacteria have been evaluated using bacterial suspensions and bacteria growing on agar or growth-supporting membrane filters rather than dried cells on a given substrate, as would be more representative of real-world applications.

Therefore, the goal of this study was to evaluate the transcriptomic responses of dried *Salmonella* cells to surface dielectric barrier discharge (SDBD) cold plasma treatment using RNA sequencing (RNA-seq) after five rounds of successive cold plasma treatment of plasma-injured cells. RNA-seq is ideally suited for this purpose due to its high resolution with limited background noise and high dynamic range, allowing identification of even relatively subtle differential gene expression changes resulting from the treatment (Wang *et al.*, 2009). *Salmonella*, a robust and common bacterial foodborne pathogen that has a high tolerance to desiccation stress, was used in this study (Li *et al.*, 2012). Compared with a previous study evaluating the morphological and transcriptomic response of *Salmonella* to SDBD cold plasma treatment (Chapter 4), this study allowed for a preliminary evaluation of the potential for bacterial development of resistance to cold plasma treatment.

MATERIALS AND METHODS

Bacterial strain and culture conditions. *Salmonella enterica* subspecies *enterica* serovar Enteritidis strain H4639 was used in this study. For all experiments the strains were grown aerobically for 18-20 hours with shaking (250 rpm) at 37°C in 5 mL tryptic soy broth (TSB, Difco, Sparks, MD). The bacterial concentration of each liquid culture was determined by serially diluting the culture in 0.1% (w/v) sterile peptone (Difco, Sparks, MD) and plating in duplicate on tryptic soy agar (TSA, Difco, Sparks, MD), incubated overnight at 37°C.

Plasma actuator construction. Surface dielectric barrier discharge (SDBD) actuators were constructed using 3.6 cm x 0.5 cm x 0.5 mm (*l* x *w* x *h*) copper electrodes (McMaster-Carr Supply Company, GA, USA) placed on both sides of 5 cm^2 x 0.127 mm Teflon dielectric barrier sheets (McMaster-Carr Supply Company, GA). Electrodes were staggered in relation to the dielectric material and grounded electrodes were insulated to prevent plasma ignition (Figure 1). SDBD actuators were operated with an input power of 13.5 V with a 50% duty cycle using a high voltage transformer (Information Unlimited, NH) and pulse width modulation (PWM) with an Arduino Uno microcontroller setup (Arduino LLC, Italy) was used to allow actuators to be on for 800 ms and off for 300 ms.

Selection of plasma-injured cells for successive plasma treatments and potential resistance development analysis. To help determine if *Salmonella* has the potential of developing resistance to cold plasma treatments, *Salmonella* cells that were injured but not inactivated by cold plasma were needed for successive treatments. However, it is difficult to determine if surviving cells were actually exposed to the plasma species because of a suspected shadowing effect in which some cells within a

population are shielded from the reactive species by other cells. To overcome this difficulty and to select potentially injured cells, treated coverslip wash fluids were plated onto xylose lysine deoxycholate (XLD, Difco, Sparks, MD) agar with a TSA overlay (Kang and Fung, 2000). XLD agar, a selective medium for *Salmonella,* can inhibit injured cells from growing (particularly heat-injured cells), whereas TSA, a non-selective medium, is nutrient rich and supports the growth of injured *Salmonella* cells. Therefore, by plating on XLD with a TSA overlay, injured *Salmonella* cells can resuscitate on the TSA overlay while the selective agents of the XLD agar diffuse into the TSA overlay (Kang and Fung, 2000). This process allows the injured and resuscitated *Salmonella* cells to produce a typical black colony color reaction to XLD while not inhibiting colony growth completely.

In this study, since not all of the *Salmonella* cells plated onto the XLD with TSA overlay medium were injured, after 24 hours of incubation at 37 °C the colony numbers were counted and noticeably smaller colonies were marked. Smaller colonies were suspected to have arisen from injured cells that were resuscitated on the TSA but prolific growth was inhibited by the selective XLD agents. In contrast, larger colonies were assumed to be uninjured cells that may not have been exposed to the plasma generated reactive species. In contrast, colony sizes from untreated control samples plated onto XLD with TSA overlay were uniform in size. After 48 hours of incubation at 37 °C, the marked small colonies or colonies newly emerged within the second 24 hours of incubation were selected for successive cold plasma treatments. These colonies were then grown aerobically for 18-20 hours with shaking (250 rpm) at 37°C in 5 mL TSB and spot inoculated onto sterile glass coverslips and treated with cold plasma as described below.

After the fifth successive SDBD cold plasma treatment of *Salmonella* Enteritidis, each for 4 minutes at 1 cm, 3 replicates of 10 coverslips each were inoculated with plasma-injured *Salmonella* cells and treated for 2 minutes at 1 cm for subsequent RNA isolation and RNA-seq analysis.

Plasma treatment conditions for RNA-seq analysis. *Salmonella* Enteritidis culture suspensions were spot inoculated onto sterile glass coverslips and air dried, uncovered, for 60 minutes in a biosafety cabinet prior to cold plasma treatment. To prepare the inocula, 1 mL of liquid culture was centrifuged at 9,000 x g for 3 minutes and re-suspended in 1 mL of 0.1% (w/v) sterile peptone. One hundred µL of the bacterial suspensions were used as inocula, spotted in 20-25 evenly spaced spots onto sterile 22 x 22 mm glass coverslips (approximately 10^8 CFU/coverslip, between 10^6 and 10^7 CFU/spot). Three replicates, each consisting of 10 inoculated coverslips placed in sterile 35 mm petri dishes, were treated with SDBD cold plasma for 2 minutes at a distance of 1 cm from the actuators at room temperature (~25°C) and atmospheric pressure (Figure 1). The sub-optimal treatment time of 2 minutes, correlating to an approximately 1 log reduction (Figure 2), and 10 coverslips per replicate were used so that a sufficient bacterial concentration (approximately 10^8 CFU) could be recovered for RNA isolation.

Plasma-treated and untreated control cell-inoculated coverslips were washed by vortexing for 30 s in 10 mL 0.1% (w/v) sterile peptone in 50 mL conical tubes. The 10 coverslips of each replicate were washed individually in the same wash fluid in immediate succession following treatment of all coverslips for each replicate. The 10 untreated control coverslips for each of 3 replicates were washed in the same way after drying for 60 minutes. Wash fluids were 10-fold serially diluted in 0.1% peptone for

enumeration, for which 100 µL of each dilution was plated in duplicate on TSA and incubated overnight at 37 °C. Bacterial inactivation due to cold plasma treatment was assessed by comparing the bacterial recovery from plasma-treated samples to that from untreated controls.

Isolation of bacterial RNA. Bacterial RNA was isolated from the 10 mL of 0.1% peptone used to wash the 10 coverslips of each of 3 replicates of plasma-treated and untreated control samples (12 total samples, 6 prior to successive treatments, 6 after successive treatments). Wash fluids for each replicate were centrifuged at 9,000 x g for 3 minutes and the pellet was re-suspended in 400 µL of 0.1% peptone and then added to 800 µL of Qiagen RNA Protect Bacteria Reagent according to the manufacturer's protocol. RNA was then isolated using the Qiagen RNeasy minikit with an on-column RNase-free DNase treatment according to the manufacturer's protocol. The quantity and quality of isolated RNA was assessed using a NanoDrop ND-2000 spectrophotometer (Thermo Fisher Scientific) and an Agilent 2100 Bioanalyzer (Agilent Technologies). Since fragmented 23S rRNA is characteristically high in Enterobacteriaceae (Bhagwat *et al.*, 2013) and since the plasma treatment itself was suspected to contribute further to RNA degradation (Joshi *et al.*, 2011), DV_{200} values were used as a measure of RNA quality rather than the traditional RNA integrity number (RIN). The DV_{200} value, a metric developed by Illumina that correlates to the percentage of RNA transcripts of at least 200 nucleotides in length, was found to be more reliable than RIN for high quality RNA-sequencing (Illumina, 2014). Only samples with a DV_{200} value of 40 or higher were used for cDNA library preparation and sequencing.

Library preparation and sequencing. Enrichment of mRNA by rRNA depletion, fragmentation of mRNA, cDNA synthesis, and cDNA library preparation were done using the ScriptSeq Complete Kit (Bacteria) (Illumina). This kit is specifically designed for low input and partially degraded RNA samples. Some RNA degradation was expected as a result of the plasma treatment and was confirmed by the relatively low RIN numbers. Library quality was assessed using an Agilent 2100 Bioanalyzer and subsequently normalized and diluted according to Illumina protocols. All sample libraries were sequenced in a multiplexed manner on an Illumina HiSeq flow cell. Library preparation and sequencing was performed by Cofactor Genomics (St. Louis, MO).

Read mapping and differential gene expression analysis. Mapping and analysis of FastQ-files were performed using the CLC Genomics Workbench version 9 (Qiagen) using default mapping parameters. Although *Salmonella* Enteritidis strain H4639 was used in this study, sequence reads were mapped against *Salmonella enterica* subspecies *enterica* serovar Typhimurium strain LT2 (accession number NC_003197) rather than *Salmonella enterica* subspecies *enterica* serovar Enteritidis strain P125109 (accession number NC_011294) since strain LT2 is more fully annotated than strain P125109. When comparing read mapping against LTS and P125109, mapping was almost identical for the annotations in common (data not shown). The average percentage of reads mapped to the reference sequence was 84.49% (Table 1). Reproducibility of the read mapping was confirmed by comparing 3 replicates of each treatment and untreated control. Average gene fold changes were calculated from the combined replicates of each condition and genes were considered to be differentially expressed if the average fold change was greater than 1.5 or less than -1.5 with a false discovery rate (FDR) ≤ 0.05 and

P value ≤ 0.01. Functional annotation clustering based on known or predicted gene ontology was performed using PANTHER 10.0 (Mi *et al.,* 2016). Co-regulated genes and gene pathways were identified by the KEGG Pathway database and STRING 10.0 (Szklarczyk *et al.,* 2015).

qRT-PCR analysis. Six differentially expressed ($P < 0.01$) genes (*pstA, phoR, phnU, fimA, eutD, invA*) by RNA-seq were selected for analysis by quantitative real-time reverse transcriptase-PCR (qRT-PCR). Primer3 software (Untergasser *et al.,* 2012) was used to design PCR primers, producing amplicon sizes between 100 and 200 bp (Table 2). The gene encoding GyrB was used as a reference for relative expression normalization using PCR primers previously described (Goudeau *et al.,* 2013). Total RNA was isolated as described above using a DNase I treatment (Qiagen) to eliminate genomic DNA contamination. cDNA was synthesized from total RNA with GoScript Reverse Transcriptase (Promega, Madison, WI) using gene-specific primers. SYBR Green qPCR was performed using 20 µL reaction mixtures containing 10 µL (1X) of Platinum SYBR Green real-time PCR SuperMix-UDG (Life Technologies, Foster City, CA), 1 µL (5 µM) of each primer, 1 µL of template cDNA, and 7µL of nuclease free water. A negative control (nuclease free water) and an RNA sample without reverse transcriptase were included to detect potential genomic DNA contamination for each reaction. qRT-PCR was performed in a Rotor-Gene 6000 thermocycler (Corbett Research, Sydney, Australia) with an initial hold for 10 min at 95°C, followed by 40 cycles at 95°C for 15 sec, 60°C for 15 sec, and 72°C for 60 sec. The relative expression fold change for each gene was calculated using a method described previously (Pfaffl, 2001) using the equation $R = E_{\text{target}}^{\Delta\text{Cp target}}/E_{\text{ref}}^{\Delta\text{Cp ref}}$, where *R* is the relative expression

ratio, *E* is the qPCR efficiency for each gene, "ref" refers the gyrB reference, "target" refers to target genes, and ΔCp equals control threshold crossing point (Cp) minus treatment Cp.

Statistical analysis. Three biological replicates of each treatment were conducted. The plate counts of recovered cells from wash fluids for each replicate were transformed to log CFU/mL. Log reductions due to plasma treatment were calculated by comparing the numbers of recovered cells from treated samples to untreated controls. Analysis of variance (ANOVA) was used to calculate statistical differences between samples from plate counts using SAS (Statistical Analysis System. Inst. Inc., Cary, NC, USA). Significant difference was defined at $P \leq 0.01$.

RESULTS

Inactivation of *Salmonella* Enteritidis by SDBD.

Rates of inactivation of *Salmonella* Enteritidis by SDBD treatments of 2 and 4 min at 1 cm were similar to those of a 5-strain mixture of *Salmonella* serovars in a previous study (Chapter 3). An approximately 1 log CFU/mL reduction was observed after 2 min treatments and an approximately 2.5 log CFU/mL reduction was observed after 4 min treatments (Figures 2 and 3). Average log CFU/mL reductions of treated samples used for RNA-seq analysis after 1 treatment (1x) and 5 successive treatments (5x) were not significantly different ($P \leq 0.01$) at 1.14 and 1.44 CFU/mL, respectively (Figure 2). Five successive plasma treatments for 4 min also were not significantly different ($P \leq 0.01$) from each other with average log CFU/mL reductions ranging from 2.22 to 2.76 (Figure 3).

Global transcriptional changes resulting from SDBD treatment.

The SDBD plasma treatment of dried *Salmonella* Enteritidis cells on sterile glass coverslips after 5 successive treatments resulted in significant transcriptional changes within surviving cells. Among 4,631 annotated genes of *Salmonella* Typhimurium LT2, 1,136 (24.5%) were expressed differentially by at least 1.5-fold (*P*-value ≤ 0.01 and FDR *P*-value ≤ 0.05) when compared to the untreated controls. A total of 644 genes were downregulated from -1.5-fold to -241.14-fold and 492 genes were upregulated from 1.5-fold to 6.06-fold. More genes were downregulated than upregulated (644 vs. 492) the former had a significantly higher range of fold change (-241.14 vs. 6.06). Compared to a previous study evaluating the transcriptomic response of *Salmonella* to SDBD plasma prior to successive treatments of injured cells (Chapter 4), similar general patterns of differential expression were observed (Figure 4). The same three major KEGG pathways of "bacterial secretion system" (upregulated), "ribosome" (downregulated), and "biosynthesis of siderophore group nonribosomal proteins" (downregulated) were differentially expressed (Chapter 4). Heat map comparisons of differentially expressed genes after the 5 successive plasma treatments revealed high correlation between treated and control replicates, with treated samples clustering together and control samples clustering separately (Figure 5). The high reproducibility observed between replicates in this study was in contrast to the results of the previous study, in which one control replicate (C1) and one treated replicate (T1) were more similar to each other than to the other two control or treated replicates (Figure 5). When all 6 samples from both studies were compared in a single heat map of 1,340 differentially expressed genes (Figure 5), all

treated replicates clustered together, separate from control replicates. However, the 3 treated and 3 control replicates after 5 successive plasma treatments clustered together while only 2 of the treated and 2 of the control replicates from the previous study clustered together (Figure 5).

A total of 533 genes were expressed differentially in both studies by $\leq$ -1.5-fold or $\geq$ 1.5-fold with a FDR P value $\leq$ 0.05, both prior to and after 5 successive plasma treatments (Figure 4B). Two hundred and nine genes were differentially expressed only in the first study while 598 genes were differentially expressed in the second study (Figure 4B). The 533 genes expressed differentially in common included downregulation of genes associated with phosphate uptake, cation uptake, osmoregulation, tetrathionate utilization, phage-shock proteins, ribosomal subunit proteins, and DNA damage repair. The major upregulated genes included those encoding pathogenicity associated proteins, especially those from *Salmonella* pathogenicity island 2 (SPI2). Differentially expressed metabolic pathways common to both studies included upregulation of ethanolamine utilization and downregulation of colonic acid and enterobactin biosynthesis, associated with nutrient limitation, desiccation stress, and oxidative stress, respectively. Among the 209 genes differentially expressed only prior to the 5 successive treatments, 149 were downregulated and 60 were upregulated. No significant functional enrichments were observed using STRING 10 for either downregulated or upregulated genes. Among the 598 genes differentially expressed only after 5 successive plasma treatments, 287 were downregulated and 311 were upregulated. The major functional groups to which genes clustered were transport, metabolism, regulatory functions, and pathogenesis.

Transport and localization. Genes expressed differentially after plasma treatment having transmembrane transport functions were associated with ribose transport and diffusion of small molecules, all of which were downregulated. The *rbsABCD* operon encodes an ATP-binding cassette (ABC) transport system that actively transports ribose, which is passively transported across the outer membrane, across the cytoplasmic membrane into the cell (Barroga *et al.,* 1996). *rbsA*, *B*, *C*, and *D* were downregulated between -2.34 and -3.49-fold. Outer membrane porin proteins OmpA, OmpC, and OmpF, each associated with passive diffusion of small molecules and solutes across the outer membrane (Wang, 2002; Martínez-Flores *et al.,* 1999), also were downregulated. Expression of OmpC and OmpF in *Salmonella* is regulated in response to changes in osmolarity by OmpR (Martínez-Flores *et al.,* 1999), which was also downregulated. Decreased expression of the ribose transport system and small molecule diffusion porins may indicate increased availability of ribose and vital small molecules with a decrease in osmotic stress.

Metabolism. Multiple metabolic pathways were significantly differentially expressed after 5 successive plasma treatments but were not after only a single treatment. As reported by STRING 10, as many as 69 downregulated genes were associated with known metabolic processes. At least 21 downregulated genes were associated with amino acid biosynthesis and 16 with purine and pyrimidine metabolism (Table 3). While biosynthesis of glycine, serine, threonine, histidine, valine, leucine, and isoleucine were downregulated, cysteine biosynthesis genes within the *cysCDHIJ* regulon (Tei *et al.,* 1990) were upregulated (Table 3). Other downregulated genes with metabolic processes included those with riboflavin, carboxcylic acid, and propanediol metabolism functions

(Table 3). Propanediol metabolic proteins, encoded within the extensive *pdu* operon, are often expressed in conjunction with ethanolamine utilization proteins, encoded within the equally extensive *eut* operon (Goudeau *et al.,* 2013). While 4 propanediol utilization genes (*pduC, E, N, P*) were downregulated, 6 ethanolamine utilization genes (*eutA, E, G, H, J, R*) were upregulated. These 6 upregulated genes are in addition to another 6 *eut* genes (*eutD, N, P, Q, S, T*) upregulated in common to this study and the previous study prior to 5 successive plasma treatments. These results confirm the increased role of ethanolamine utilization but not propanediol utilization after plasma treatment, possibly as a result of increased availability of ethanolamine, a major constituent of phospholipid membranes. Also upregulated were 4 genes within the *citCDEFXGT* operon (*citD, G, F,* and *X*), which allows *E. coli* to use citrate as a sole energy and carbon source in anaerobic conditions (Pos *et al.*, 1998). Since anaerobic conditions were not expected on the plasma treated coverslips, increased expression of these genes may be due to increased availability of acetyl CoA, which is a byproduct of EutE within the ethenaolamine utilization process and is a precursor to citrate (Goudeau *et al.,* 2013). Other upregulated metabolism related genes of interest included several lipid (*lpxB, D, rfaJ, L, Y, rfbP, rfe,* and *wzxE*) and cell wall component biosynthesis genes (*mraY, murD, F*) (Table 3). Additionally, a superoxide dismutatse gene, *sodA*, which would be expected to be upregulated in response to plasma treatment and potentially increased intracellular superoxide concentrations, was downregulated -1.80-fold.

Regulatory functions. Already mentioned for its role in osmoregulation, OmpR is also an important transcription factor that regulates expression of several key pathways (Cai and Inouye, 2002). Overexpression of OmpR represses flagellar filament expression

while promoting expression of curli synthesis genes (Shin and Park, 1995; Prigent-Combaret *et al.,* 2001). Thus, downregulation of OmpR, as observed in this study by -1.72-fold, would result in increased expression of the flagellar gene regulators FlhC/D and downregulation of the curli synthesis regulator CsgD (Gutenplan and Kearns, 2013). However, the genes for all 3 of these proteins were upregulated after plasma treatment. Increased expression of the FlhC/D two component system would be expected to result in increased expression of flagellar genes, but no such increase was observed. In fact, 9 genes within the *flg* operon, encoding flagellar basal body structural genes (Glutenplan and Kearns, 2013), were significantly downregulated from -1.53 to -2.74-fold. Similarly, increased expression of CsgD would be expected to result in increased expression of curli synthesis genes within the *csgDEFG* and *csgBA* operons (Barnhart and Chapman, 2006). However, only *csgE* and *csgF* were upregulated by 2.85 and 1.97-fold, respectively. Thus, the role of motility and chemotaxis is again unclear after plasma treatment with SDBD.

The importance of the maintenance of a transmembrane proton motive force in response to plasma treatment was confirmed after 5 successive plasma treatments. While only two genes (*nuoE* and *nuoK*) within the *nuo* locus, composed of 14 genes that encode structural proteins associated with a type I NADH dehydrogenase in the prokaryotic electron transport chain (Falk-Krzesinski *et al.,* 1998), were upregulated in response to plasma treatment in the previous study, an additional 6 *nuo* genes (*nuoH, I, J, L, M, N*) were upregulated, in this study, from 1.53 to 1.76-fold. Additionally, *proP* and *proV,* genes encoding proteins that serve as proton symporters, sensing and responding to osmotic shift by importing osmolytes (Culham *et al.,* 2003), were also upregulated by

2.16 and 1.7-fold. Since SDBD plasma produces a high local concentration of negative ions and potentially produces hydrogen ions through the interaction of reactive species with water molecules on cell surfaces (Pai *et al.,* 2015), it is expected that ion accumulation at the cell surface may contribute to bacterial death (Lunov *et al.,* 2016). Upregulation of such osmotic regulators may also be in response to the changing osmotic conditions experienced by surviving cells in response to cytosolic leakage and lysis of surrounding cells.

A more general global downregulation of gene expression observed previously in response to plasma treatment, as evidenced by downregulation of genes encoding ribosomal structural proteins, was confirmed in this study. While at least 21 ribosomal structural proteins were downregulated in the previous study, an additional 27 were downregulated after 5 successive plasma treatments (Table 3). Additionally, *rpoA, rpoB,* and *rpoC,* encoding the α-, β-, and β'-subunits of RNA polymerase (Zalenskaya *et al.,* 1990), were also significantly downregulated by -1.50 to -1.65-fold. Decreased expression of at least 38 ribosomal structural proteins and the 3 subunits of RNA polymerase underscore decreased transcription and translation as an important response of *Salmonella* to SDBD plasma treatment. Decreased translation via downregulation of ribosomal genes is a general response to cellular stress (Starosta *et al.,* 2014), indicating a potential stress response by *Salmonella* resulting from plasma treatment.

Pathogenesis. In the previous study evaluating the transcriptomic response of *Salmonella* after a single plasma treatment, at least 39 genes associated with SPI1 and SPI2 were upregulated after plasma treatment, with as many as 26 of these contained within SPI2. Thirty five of those 39 genes were upregulated after 5 successive treatments

in addition to 7 more (*ssaU, sseC, D, J, sifA, B, pipA, B, STM1638*), 6 of which are secreted effector proteins located within SPI2 (*ssaU* is a T3SS structural apparatus protein). The 4 genes not upregulated after 5 successive plasma treatments (*prgH, J, K, hilD*) were all located within SPI1. In contrast to the previous study, differential expression of genes within SPI1 and SPI2 were expressed more consistently among the 3 replicates (Figure 6). These results confirm the increased expression of genes located within SPI2 in contrast to SPI1 (Figure 6). *In vivo,* SPI1 is associated primarily with invasion into epithelial cells and SPI2 is primarily associated with macrophage infection and survival within macrophages (Marcus *et al.,* 2000; Chakraborty *et al.,* 2015). As noted previously, acidification of the cellular cytoplasm by macrophage attack is a major contributor to induced expression of SPI2-encoded proteins (Chakraborty *et al.*,2015), with phosphate and magnesium ion limitation and hydrogen peroxide and nitric oxide stress also playing a role (Kroger *et al.,* 2013). It is suspected that the changing osmotic conditions resulting from lysis of adjacent cells by the plasma treatment and an increased proton motive force may contribute to an acidification of the cytoplasm of surviving cells, thus inducing increased expression of SPI2-located genes.

qRT-PCR validation of RNA-seq gene expression.

qRT-PCR analysis of 4 downregulated genes (*pstA, phoR, phnU, fimA*) and 2 upregulated genes (*eutD, invA*) was used to validate differential gene expression identified by RNA-seq. The fold change differences for each gene were similar for the two methods despite their inherent differences in sensitivity (Figure 6). However, the 2

genes shown to be upregulated when analyzed by RNA-seq (*eutD, invA*) were shown to be downregulated when analyzed by qRT-PCR.

DISCUSSION

One of the most attractive aspects of cold atmospheric plasma treatments for surface sterilization or decontamination applications is the limited potential for development of resistance in bacteria (Alkawareek *et al.,* 2014). Multiple recent studies have highlighted the interplay between both physical and biological mechanisms leading to bacterial inactivation resulting from exposure to plasma-produced reactive species (Lunov *et al.,* 2016; Han *et al.,* 2016; Kvam *et al.,* 2016). The multi-modal nature of plasma-induced bacterial inactivation is caused by RONS and charged particles that damage lipids, nucleic acids, and proteins in a non-discriminate manner (Kong *et al.,* 2009; Mai-Prochnow *et al.,* 2014). Accordingly, unlike most antibiotic drugs, bacterial inactivation by cold plasma does not target a single cell product or process but damages cellular macromolecules to a point beyond which cells are not able to recover (Mai-Prochnow *et al.,* 2014).

When comparing the potential for development of resistance to cold plasma treatment with that to antibiotic drugs, there are 2 main features in common; 1) bacterial inactivation occurs through damage or inhibition of key cellular processes and 2) bacterial inactivation is dose-dependent on the length or intensity of cold plasma treatment and the amount or concentration of antibiotic applied (Levy and Marshall, 2004; Mai-Prochnow *et al.,* 2014). In general, the dosage used for each method must be high enough that cellular repair mechanisms or normal cellular processes are not able to

recover from the damage imposed (Hughes and Andersson, 2012; Alkawareek *et al.*, 2014). However, in the case of antibiotics, some bacterial cells within a population have been able to survive due to some phenotypic or genotypic variation that reduces their susceptibility to the antibiotic (Levy and Marshall, 2004; Hughes and Andersson, 2012). As a result, these cells are able to proliferate, affected very little or not at all by a single (or multiple) antibiotic(s). This process is more likely to occur when a single antibiotic drug is used to target a single protein or enzyme than when antibiotic cocktails are used (Allen *et al.*, 2010). Bacterial resistance to the major classes of antibiotics has largely been a result of expression of only one or a few enzymes that negate the effects of the antibiotic (Hughes and Andersson, 2012). Specific identification of the mechanisms by which cold plasma inactivates cells is still not well understood and may be elusive due to the more general cellular damage that it causes, acting not on a single cellular process but on many, in addition to purely physical damage. Despite interest in the possibly limited potential for bacterial cells to develop resistance to plasma treatments, no known studies to evaluate this potential have been reported.

It was the goal of this study to evaluate the transcriptomic response of dried *Salmonella* cells to 5 successive SDBD cold plasma treatments and to compare the results to those of a previous study evaluating the transcriptomic response occurring prior to the 5 treatments (Chapter 4). The objective of this work was to preliminarily evaluate the potential for resistance development to cold plasma by Gram-negative bacterial pathogens. Bacterial inactivation rates following SDBD plasma treatment were not statistically different prior to and after the treatments or throughout the 5 treatments (Figures 2 and 3). The transcriptomic response after the 5 successive treatments was also

strikingly similar to the transcriptomic response prior to the 5 treatments (Figure 5). Significantly downregulated genes included those associated with phosphate uptake, cation uptake, osmoregulation, tetrathionate utilization, phage-shock proteins, DNA damage repair, colonic acid biosynthesis, propanediol utilization, and enterobactin biosynthesis. Significantly upregulated genes coded for multiple ribosomal subunit proteins, pathogenicity associate proteins, and ethanolamine utilization proteins. While a general decreased stress response was observed, as evidenced by downregulation of nutrient and cation import, DNA damage repair, osmoregulation, and capsule compound forming genes, downregulation of ribosomal subunit and upregulation of pathogenicity associated genes indicated the accumulation of some cellular stress. Upregulation of pathogenicity associated genes in response to plasma treatment is a potential concern. However, a majority of the pathogenicity associated genes expressed were associated with macrophage attack and would not necessary increase the virulence of *Salmonella* when treated on an external surface. Cellular invasion, facilitated by proteins encoded within a different pathogenicity island, would be required prior to functional use of those associated with survival within macrophages (Marcus *et al.*, 2000; Chakraborty *et al.*, 2015).

Based on the results of this study, no significant differences in bacterial inactivation rates or differential gene expression were identified that could potentially lead to resistance development. However, it should be noted that the observed transcriptomic response was an indirect response since RNA was isolated only from intact, surviving cells that might not have been exposed to plasma produced species directly. Yet, the number and pattern of differentially expressed genes indicated a distinct

response to the treatment that is thought to be caused primarily by lysis of cells adjacent to those from which RNA was isolated, creating a nutrient rich, osmotically balanced microenvironment. Accordingly, the results of this study suggest cell membrane damage via lipid peroxidation to be the primary means of bacterial inactivation for Gram-negative bacteria, in accordance other studies (Lunov *et al.,* 2016; Han *et al.,* 2016; Kvam *et al.,* 2016; Joshi *et al.,* 2011). Since lipid peroxidation by RONS is primarily a physical process depending upon the ability of RONS to interact with lipids, the potential for resistance development may be minimal (Alkawareek *et al.*, 2014). Surface structure modifications such as capsule formation, biofilm formation, or thicker cell walls may provide an adaptive advantage to sub-lethally treated bacteria and should be investigated further. Indeed, Gram-positive bacteria having thicker cell walls than Gram-negative bacteria were more resistant to plasma treatments (Lunov *et al.,* 2016), and oxidative DNA damage may have a more prominent role in inactivation than lipid peroxidation. For Gram-negative bacteria, this study confirms the importance of lipid peroxidation and cell membrane damage as major contributors to cellular inactivation and is the first known study evaluating the potential for resistance development by successively treating plasma-injured cells. No adaptive response was observed after successive treatments, suggesting that *Salmonella* has limited potential to develop resistance to cold plasma treatments. Furthermore, SDBD is confirmed as an effective plasma generation and treatment method that has multiple potential applications for surface sterilization and decontamination.

LITERATURE CITED

Alkawareek, M. Y., Gorman, S. P., Graham, W. G., & Gilmore, B. F. (2014). Potential cellular targets and antibacterial efficacy of atmospheric pressure non-thermal plasma. *International Journal of Antimicrobial Agents, 43*(2), 154-160.

Allen, H. K., Donato, J., Wang, H. H., Cloud-Hansen, K. A., Davies, J., & Handelsman, J. (2010). Call of the wild: antibiotic resistance genes in natural environments. [10.1038/nrmicro2312]. *Nat Rev Micro, 8*(4), 251-259.

Barnhart, M. M., & Chapman, M. R. (2006). Curli Biogenesis and Function. *Annual review of microbiology, 60*, 131-147.

Barroga, C. F., Zhang, H., Wajih, N., Bouyer, J. H., & Hermodson, M. A. (1996). The proteins encoded by the rbs operon of escherichia coli: I. Overproduction, purification, characterization, and functional analysis of RbsA. *Protein Science, 5*(6), 1093-1099.

Belas, R. (2014). Biofilms, flagella, and mechanosensing of surfaces by bacteria. *Trends in Microbiology, 22*(9), 517-527.

Cai, S. J., & Inouye, M. (2002). EnvZ-OmpR interaction and osmoregulation in Escherichia coli. *J Biol Chem, 277*(27), 24155-24161.

Chakraborty, S., Mizusaki, H., & Kenney, L. J. (2015). A FRET-Based DNA Biosensor Tracks OmpR-Dependent Acidification of <italic>Salmonella</italic> during Macrophage Infection. *PLoS Biol, 13*(4), e1002116.

Chang, H.-H., Cohen, T., Grad, Y. H., Hanage, W. P., O'Brien, T. F., & Lipsitch, M. (2015). Origin and Proliferation of Multiple-Drug Resistance in Bacterial Pathogens. *Microbiology and Molecular Biology Reviews, 79*(1), 101-116. doi: 10.1128/mmbr.00039-14

Culham, D. E., Henderson, J., Crane, R. A., & Wood, J. M. (2003). Osmosensor ProP of Escherichia coli responds to the concentration, chemistry, and molecular size of osmolytes in the proteoliposome lumen. *Biochemistry, 42*(2), 410-420.

Falk-Krzesinski, H. J., & Wolfe, A. J. (1998). Genetic Analysis of the nuo Locus, Which Encodes the Proton-Translocating NADH Dehydrogenase inEscherichia coli. *Journal of Bacteriology, 180*(5), 1174-1184.

Goudeau, D. M., Parker, C. T., Zhou, Y., Sela, S., Kroupitski, Y., & Brandl, M. T. (2013). The salmonella transcriptome in lettuce and cilantro soft rot reveals a niche overlap with the animal host intestine. *Appl Environ Microbiol, 79*(1), 250-262.

Han, L., Patil, S., Boehm, D., Milosavljević, V., Cullen, P. J., & Bourke, P. (2015). Mechanism of Inactivation by High Voltage Atmospheric Cold Plasma Differs between Escherichia coli and Staphylococcus aureus. *Applied and Environmental Microbiology*.

Hughes, D., & Andersson, D. I. (2012). Selection of resistance at lethal and non-lethal antibiotic concentrations. *Current Opinion in Microbiology, 15*(5), 555-560.

Illumina. (2014). Evaluating RNA Quality from FFPE Samples. Available at: http://www.illumina.com/documents/products/technotes/technote-truseq-rna-access.pdf

Joshi, S. G., Cooper, M., Yost, A., Paff, M., Ercan, U. K., Fridman, G., Brooks, A. D. (2011). Nonthermal dielectric-barrier discharge plasma-induced inactivation involves oxidative DNA damage and membrane lipid peroxidation in Escherichia coli. *Antimicrob Agents Chemother, 55*(3), 1053-1062.

Kang, D. H., & Fung, D. Y. (2000). Application of thin agar layer method for recovery of injured Salmonella typhimurium. *Int J Food Microbiol, 54*(1-2), 127-132.

Kong, M. G., Kroesen, G., Morfill, G., Nosenko, T., Shimizu, T., Dijk, J. v., & Zimmermann, J. L. (2009). Plasma medicine: an introductory review. *New Journal of Physics, 11*(11), 115012.

Kröger, C., Colgan, A., Srikumar, S., Händler, K., Sivasankaran, Sathesh K., Hammarlöf, Disa L., . . . Hinton, Jay C. D. An Infection-Relevant Transcriptomic Compendium for Salmonella enterica Serovar Typhimurium. *Cell Host & Microbe, 14*(6), 683-695.

Kvam, E., Davis, B., Mondello, F., & Garner, A. L. (2012). Nonthermal atmospheric plasma rapidly disinfects multidrug-resistant microbes by inducing cell surface damage. *Antimicrob Agents Chemother, 56*(4), 2028-2036.

Levy, S. B., & Marshall, B. (2004). Antibacterial resistance worldwide: causes, challenges and responses. *Nat Med, 10*(12 Suppl), S122-129.

Li, H., Bhaskara, A., Megalis, C., & Tortorello, M. L. (2012). Transcriptomic Analysis of Salmonella Desiccation Resistance. *Foodborne Pathogens and Disease, 9*(12), 1143-1151.

Littmann, J., Buyx, A., & Cars, O. (2015). Antibiotic resistance: An ethical challenge. *International Journal of Antimicrobial Agents, 46*(4), 359-361.

Lunov, O., Zablotskii, V., Churpita, O., Jäger, A., Polívka, L., Syková, E., . . . Kubinová, Š. (2016). The interplay between biological and physical scenarios of bacterial death induced by non-thermal plasma. *Biomaterials, 82*, 71-83.

Mai-Prochnow, A., A.B. Murphy, K.M. McLean, M.G. Kong, & K. Ostrikov. (2014). Atmospheric pressure plasmas: Infection control and bacterial responses. *International Journal of Antimicrobial Agents*. *43*(6), 508-517.

Marcus, S. L., Brumell, J. H., Pfeifer, C. G., & Finlay, B. B. (2000). Salmonella pathogenicity islands: big virulence in small packages. *Microbes and Infection, 2*(2), 145-156.

Martínez-Flores, I., Cano, R., Bustamante, V. H., Calva, E., & Puente, J. (1999). The ompB Operon Partially Determines Differential Expression of OmpC in Salmonella typhi andEscherichia coli. *Journal of Bacteriology, 181*(2), 556-562.

Misra, N.N., B.K. Tiwari, K.S.M.S. Raghavarao, & P.J. Cullen. (2011). Nonthermal plasma inactivation of food-borne pathogens. *Food Engineering Reviews.* 3(3-4):159-170.

Pai, K. K., Singarapu, K., Jacob, J. D., & Madihally, S. V. (2015). Dose Dependent Selectivity and Response of Different Types of Mammalian Cells to Surface Dielectric Barrier Discharge (SDBD) Plasma. *Plasma Processes and Polymers, 12*(7), 666-677.

Pfaffl, M. W. (2001). A new mathematical model for relative quantification in real-time RT–PCR. *Nucleic Acids* Research, *29*(9), e45.

Prigent-Combaret, C., Brombacher, E., Vidal, O., Ambert, A., Lejeune, P., Landini, P., & Dorel, C. (2001). Complex Regulatory Network Controls Initial Adhesion and Biofilm Formation in Escherichia coli via Regulation of thecsgD Gene. *Journal of Bacteriology, 183*(24), 7213-7223. doi: 10.1128/jb.183.24.7213-7223.2001

Pos, K. M., Dimroth, P., & Bott, M. (1998). The Escherichia coli citrate carrier CitT: a member of a novel eubacterial transporter family related to the 2-oxoglutarate/malate translocator from spinach chloroplasts. *J Bacteriol, 180*(16), 4160-4165.

Shin, S., & Park, C. (1995). Modulation of flagellar expression in Escherichia coli by acetyl phosphate and the osmoregulator OmpR. *Journal of Bacteriology, 177*(16), 4696-4702.

Spellberg, B. & Shlaes, D. Prioritized current unmet needs for antibacterial therapies. Clin. Pharmacol. Ther. 96, 151–153 (2014)

Starosta, A. L., Lassak, J., Jung, K., & Wilson, D. N. (2014). The bacterial translation stress response. *FEMS Microbiology Reviews, 38*(6), 1172-1201.

Tei, H., Murata, K., & Kimura, A. (1990). Molecular cloning of the cys genes (cysC, cysD, cysH, cysI, cysJ, and cysG) responsible for cysteine biosynthesis in Escherichia coli K-12. *Biotechnology and Applied Biochemistry, 12*(2), 212-216.

Untergasser A, Cutcutache I, Koressaar T, Ye J, Faircloth BC, Remm M, and Rozen SG. (2012). Primer3 - new capabilities and interfaces. *Nucleic Acids Research.* 40(15):e115.

Wang, Y. (2002). The Function of OmpA in Escherichia coli. *Biochemical and Biophysical Research Communications, 292*(2), 396-401.

Zalenskaya, K., Lee, J., Gujuluva, C. N., Shin, Y. K., Slutsky, M., & Goldfarb, A. (1990). Recombinant RNA polymerase: inducible overexpression, purification and assembly of Escherichia coli rpo gene products. *Gene, 89*(1), 7-12.

TABLES

Table 1. Total number of cDNA sequence reads, number of mapped reads, and percentage of mapped reads for each treated and untreated control replicate.

Sample (replicate)	Total number of reads	Number of mapped reads	Percentage of mapped reads
Control (5)	23,858,277	20,236,146	84.82
Control (6)	24,839,493	20,927,265	84.25
Control (7)	24,413,742	20,522,761	84.06
Treated (5)	26,926,561	22,981,911	85.35
Treated (6)	28,461,837	23,956,746	84.17
Treated (7)	23,707,975	19,985,835	84.30

Table 2. Target genes, gene function, and primer pair sequences used for qRT-PCR validation of differential gene expression observed by RNA-seq.

Gene name	Function	Primer pair (5'-3')
pstA	phosphate ABC transporter permease subunit	F: GAATCCCGTCGCAAGATG R: GGCGTCATTTCGGTAAACAG
phoR	sensory kinase	F: TCATTTGGTGCTCAATACCG R: CAATACCGTCAAGGGCGTA
phnU	2-aminoethylphosphonate ABC transporter permease	F: CTGCCGATGATGGTTTACAG R: CAGGCGATAGAGGGAGAACA
fimA	type-1 fimbrial protein subunit A	F: GCTGGCTGTCTCCTCTGC R: AGCGTATTGGTGCCTTCAAC
eutD	phosphotransacetylase	F: CGACCCACACAGCAACCT R: CCTGCGATACACACATCAGC
invA	invasion protein	F: TCCAACAATCCATCAGCAAG R: ACCGCCAGACAGTGGTAAAG
gyrB	DNA gyrase subunit B	F: CGCCGATAACTCCGTGTCCGTAAC R: CGACAGAGCGTTGACTACCGAGAC

Table 3. Differentially expressed genes of interest associated with transport, metabolism, regulatory, and pathogenesis functions.

Gene name	Function[a]	Fold change	Log_2 fold change	P-value	FDR p-value
Transport and localization					
cysU	sulfate/thiosulfateABC transporter permease	1.9	0.92	0	0
cysW	sulfate/thiosulfate ABC transporter permease	2.23	1.16	0	0
hisJ	histidine ABC transporter substrate-binding protein	1.5	0.59	0	0
hisM	histidine ABC transporter permease	2.49	1.32	0	0
hisP	histidine ABC transporter ATP-binding protein	1.86	0.9	0	0
hisQ	histidine ABC transporter permease	2.08	1.06	0	0
kdpA	potassium-transporting ATPase subunit A	-1.57	-0.65	3.82E-03	7.13E-03
kdpB	potassium-transporting ATPase subunit B	-1.56	-0.64	4.83E-05	1.16E-04
kdpC	potassium-transporting ATPase subunit C	-1.56	-0.64	1.45E-06	4.06E-06
mgtA	magnesium-transporting ATPase	-26.48	-4.73	0	0
mgtB	magnesium-transporting ATPase	-15.07	-3.91	0	0
mgtC	protein MgtC	-19.62	-4.29	0	0
ompA	outer membrane protein A	-2.21	-1.14	0	0
ompC	outer membrane porin protein C	-2.08	-1.06	0	0
ompF	outer membrane protein F	-1.56	-0.64	0	0
ompR	osmolarity response regulator OmpR	-1.72	-0.78	0	0
ompX	outer membrane protease	-8.43	-3.08	0	0
osmB	osmotically inducible lipoprotein B	-23.39	-4.55	0	0
osmY	hyperosmotically inducible periplasmic protein	-3.11	-1.64	0	0
phnS	2-aminoethylphosphonate ABC transporter substrate-binding protein PhnS	-6.34	-2.66	0	0
phnT	2-aminoethylphosphonate ABC transporter ATP-binding protein PhnT	-2.57	-1.36	0	0
phnU	2-aminoethylphosphonate ABC transporter permease PhnU	-2.21	-1.14	0	0
phnW	2-aminoethylphosphonate--pyruvate transaminase	-1.72	-0.78	5.47E-08	1.73E-07
phoB	response regulato PhoB	-8.52	-3.09	0	0
phoE	outer membrane phosphoporin protein E	-2.95	-1.56	0	0
phoN	non-specific acid phosphatase	-2.24	-1.16	0	0
phoP	virulence transcriptional regulator PhoP	-1.55	-0.63	0	0
phoR	sensory kinase PhoR	-5.63	-2.49	0	0
phoU	transcriptional regulator PhoU	-17.24	-4.11	0	0
ppk	polyphosphate kinase	1.56	0.65	0	0
pstA	phosphate ABC transporter permease subunit PtsA	-20.52	-4.36	0	0
pstB	phosphate ABC transporter ATP-binding protein PstB	-22.95	-4.52	0	0
pstC	phosphate ABC transporter permease PstC	-38.03	-5.25	0	0

pstS	phosphate ABC transporter substrate-binding protein PstS	-136.53	-7.09	0	0
rbsA	D-ribose ABC transporter ATP-binding protein RbsA	-2.34	-1.23	0	0
rbsB	D-ribose ABC transporter substrate-binding protein RbsB	-3.49	-1.8	0	0
rbsC	ribose ABC transporter permease RbsC	-2.76	-1.47	0	0
rbsD	D-ribose pyranase	-2.34	-1.23	0	0
rbsK	ribokinase	-2.31	-1.21	0	0
rbsR	transcriptional repressor RbsR	-1.8	-0.85	0	0
rcsA	transcriptional regulator RcsA	-2.96	-1.56	0	0
rcsB	transcriptional regulator RcsB	-2.02	-1.02	0	0
ugpA	glycerol-3-phosphate ABC transporter permease UdpA	-4.18	-2.06	0	0
ugpB	glycerol-3-phosphate ABC transporter substrate-binding protein UdpB	-4.61	-2.2	0	0
ugpC	glycerol-3-phosphate ABC transporter ATP-binding protein UgpC	-3.84	-1.94	0	0
ugpE	glycerol-3-phosphate ABC transporter permease UdpE	-3.54	-1.82	0	0
uhpT	hexose phosphate transport protein	-6.31	-2.66	0	0
zntA	zinc/cadmium/mercury/lead-transporting ATPase	-13.79	-3.79	0	0
zntB	zinc transport protein ZntB	-1.58	-0.66	2.79E-10	1.10E-09
zur	zinc uptake transcriptional repressor	-2.18	-1.12	0	0
Metabolism					
argB	acetylglutamate kinase	-1.66	-0.73	1.91E-10	7.61E-10
argH	argininosuccinate lyase	-1.73	-0.79	0	0
argO	arginine exporter protein ArgO	-2.42	-1.27	0	0
aroC	chorismate synthase	-1.64	-0.72	0	0
asnA	aspartate--ammonia ligase	-1.71	-0.77	1.12E-14	5.74E-14
cdd	cytidine deaminase	-2.67	-1.42	0	0
citC	[citrate (pro-3S)-lyase] ligase	1.96	0.97	1.11E-16	6.34E-16
citD	citrate lyase subunit gamma	1.68	0.75	2.35E-07	7.04E-07
citF	citrate lyase subunit alpha/citrate-ACP transferase	1.58	0.66	4.44E-16	2.48E-15
citG	2-(5''-triphosphoribosyl)-3'-dephosphocoenzyme-A synthase	1.55	0.63	8.13E-08	2.54E-07
citX	apo-citrate lyase phosphoribosyl-dephospho-CoA transferase	1.92	0.94	3.62E-13	1.70E-12
cysC	adenylyl-sulfate kinase	2.01	1.01	5.52E-14	2.70E-13
cysD	sulfate adenylyltransferase subunit 2	1.81	0.85	0	0
cysH	phosphoadenosine phosphosulfate reductase	2.24	1.17	2.20E-13	1.05E-12
cysI	sulfite reductase hemoprotein subunit beta	1.74	0.8	4.46E-09	1.57E-08
cysJ	sulfite reductase flavoprotein subunit alpha	1.83	0.87	0	0
cysN	sulfate adenylyltransferase subunit 1	1.62	0.7	8.42E-09	2.89E-08
deoA	thymidine phosphorylase	-2.62	-1.39	0	0

deoB	phosphopentomutase	-2.69	-1.43	0	0
deoC	2-deoxyribose-5-phosphate aldolase	-3.01	-1.59	0	0
deoD	purine nucleoside phosphorylase	-2.75	-1.46	0	0
entA	3-dihydro-2-3-dihydroxybenzoate dehydrogenase	-3.71	-1.89	0	0
entB	3-dihydro-2-3-dihydroxybenzoate synthetase	-4.6	-2.2	0	0
entC	isochorismate synthase	-3.67	-1.88	0	0
entD	4'-phosphopantetheinyl transferase	-2.27	-1.19	2.83E-14	1.41E-13
entE	3-dihydroxybenzoate-AMP ligase	-4.39	-2.13	0	0
entF	enterobactin synthase subunit F	-2.91	-1.54	0	0
eutA	ethanolamine utilization protein EutA	1.87	0.91	0	0
eutD	phosphotransacetylase EutD	1.92	0.94	0	0
eutE	aldehyde oxidoreductase EutE	1.98	0.99	0	0
eutG	ethanol dehydrogenase EutG	2.09	1.07	0	0
eutH	ethanolamine transporter EutH	1.77	0.83	0	0
eutJ	ethanolamine utilization protein EutJ	2.21	1.14	0	0
eutN	microcompartment shell protein EutN	2.41	1.27	0	0
eutP	ethanolamine utilization protein EutP	2.53	1.34	0	0
eutQ	ethanolamine utilization protein EutQ	2.2	1.14	0	0
eutR	HTH-type transcriptional regulator EutR	2.12	1.08	0	0
eutS	carboxysome structural protein EutS	2.84	1.51	0	0
eutT	cobalamin adenosyltransferase EutT	2.11	1.08	0	0
fepA	outer membrane porin	-4.55	-2.19	0	0
fepB	ferric-enterobactin ABC transporter substrate-binding protein FepB	-1.62	-0.7	2.03E-11	8.59E-11
fepE	ferric enterobactin transport protein	1.72	0.78	0	0
gpmA	3-bisphosphoglycerate-dependent phosphoglycerate mutase	-1.51	-0.59	0	0
hisB	bifunctional imidazole glycerol-phosphate dehydratase/histidinol phosphatase	-1.51	-0.6	0	0
hisC	histidinol-phosphate aminotransferase	-2.12	-1.08	0	0
hisD	histidinol dehydrogenase	-2.06	-1.04	0	0
hisG	ATP phosphoribosyltransferase	-2.21	-1.14	0	0
ilvE	branched-chain amino acid aminotransferase	-2.33	-1.22	0	0
ilvG	acetolactate synthase 2 catalytic subunit	-1.87	-0.9	0	0
ilvM	acetolactate synthase 2 regulatory subunit	-2.09	-1.06	0	0
ilvN	acetolactate synthase 1 regulatory subunit	-1.55	-0.63	5.55E-16	3.09E-15
lpxB	lipid-A-disaccharide synthase	1.76	0.81	0	0
lpxD	UDP-3-O-[3-hydroxymyristoyl] glucosamine N-acyltransferase	1.64	0.71	0	0
lysC	aspartokinase	-1.69	-0.76	4.90E-13	2.27E-12
mraY	phospho-N-acetylmuramoyl-pentapeptide-transferase	1.51	0.6	0	0
murD	UDP-N-acetylmuramoylalanine--D-glutamate ligase	1.55	0.63	0	0
murF	UDP-N-acetylmuramoyl-tripeptide--D-alanyl-	1.58	0.66	0	0

	D-alanine ligase				
ndk	nucleoside diphosphate kinase	-2.84	-1.51	0	0
nrdA	ribonucleotide-diphosphate reductase subunit alpha	-1.81	-0.85	0	0
nrdB	ribonucleotide-diphosphate reductase subunit beta	-1.75	-0.81	0	0
nrdE	ribonucleotide-diphosphate reductase subunit alpha	-2.25	-1.17	0	0
nrdF	ribonucleotide-diphosphate reductase subunit beta	-1.84	-0.88	6.55E-15	3.39E-14
nrdH	glutaredoxin-like protein	-3.09	-1.63	0	0
nrdI	ribonucleotide reductase stimulatory protein	-2.73	-1.45	0	0
pduC	propanediol dehydratase large subunit	-1.74	-0.8	1.02E-05	2.62E-05
pduE	propanediol dehydratase small subunit	-1.77	-0.82	4.14E-03	7.68E-03
pduN	propanediol utilization polyhedral body protein PduN	-1.91	-0.94	1.97E-03	3.83E-03
pduP	CoA-dependent propionaldehyde dehydrogenase	-1.62	-0.69	1.57E-06	4.38E-06
pfs	5'-methylthioadenosine/S-adenosylhomocysteine nucleosidase	-2.44	-1.29	0	0
purB	adenylosuccinate lyase	-1.7	-0.77	0	0
purG	phosphoribosylformylglycinamidine synthase	-1.57	-0.65	0	0
rcsA	transcriptional regulator RcsA	-2.96	-1.56	0	0
rcsB	transcriptional regulator RcsB	-2.02	-1.02	0	0
rfaJ	2-glucosyltransferase	2.05	1.03	0	0
rfaL	O-antigen ligase	2.53	1.34	0	0
rfaY	lipopolysaccharide core heptose(II) kinase RfaY	1.55	0.64	3.04E-08	9.88E-08
rfbN	O antigen biosynthesis rhamnosyltransferase RfbN	1.99	0.99	0	0
rfbP	undecaprenyl-phosphate galactose phosphotransferase	1.5	0.59	3.25E-08	1.05E-07
rfbU	O-antigen biosynthesis protein RfbU	2.97	1.57	0	0
rfbX	O-antigen transferase	3.15	1.66	0.01	0.02
rfc	O-antigen polymerase	3.07	1.62	0	0
rfe	undecaprenyl-phosphate alpha-N-acetylglucosaminyl 1-phosphate transferase	1.57	0.65	0	0
sdaA	L-serine deaminase I/L-threonine deaminase I	-1.67	-0.74	0	0
sdaC	HAAAP family serine transport protein	-1.94	-0.96	0	0
sodA	superoxide dismutase	-1.8	-0.85	0	0
STM2341	transketolase	-1.55	-0.63	1.84E-07	5.55E-07
STM3334	cytosine deaminase	-1.6	-0.68	0	0
tktA	transketolase	-2.29	-1.2	0	0
tonB	transport protein TonB	-1.81	-0.85	0	0
trpA	tryptophan synthase subunit alpha	-1.51	-0.6	0	0
trpD	bifunctional glutamine amidotransferase/anthranilate phosphoribosyltransferase	-1.81	-0.86	0	0
trxB	thioredoxin reductase	-1.62	-0.7	0	0

wcaA	glycosyl transferase	-4.49	-2.17	0	0
wcaB	colanic acid biosynthesis acetyltransferase WcaB	-3.22	-1.69	0	0
wcaC	glycosyl transferase	-2.59	-1.37	0	0
wcaD	colanic acid polymerase	-2.98	-1.57	1.22E-15	6.62E-15
wcaE	glycosyl transferase family protein	-12.22	-3.61	0	0
wcaF	colanic acid biosynthesis acetyltransferase WcaF	-13.78	-3.78	0	0
wcaG	GDP-fucose synthetase	-11.92	-3.58	0	0
wcaH	GDP-mannose mannosyl hydrolase	-8.03	-3.01	0	0
wcaI	glycosyl transferase	-5.88	-2.56	0	0
wcaJ	UDP-glucose lipid carrier transferase	-1.6	-0.68	9.98E-05	2.31E-04
wza	polysaccharide export protein	-11.79	-3.56	0	0
wzb	protein-tyrosine-phosphatase	-15.55	-3.96	0	0
wzc	tyrosine-protein kinase	-6.29	-2.65	0	0
wzxC	colanic acid exporter	-1.76	-0.82	1.43E-04	3.25E-04
wzxE	O-antigen translocase	1.64	0.72	0	0
Regulatory					
csgD	DNA-binding transcriptional regulator CsgD	3.38	1.76	0	0
csgE	curli production assembly/transport protein CsgE	2.58	1.37	0	0
csgF	curli production assembly/transport protein CsgF	1.76	0.82	0	0
flgA	flagellar basal body P-ring formation protein FlgA	-2.29	-1.19	0	0
flgB	flagellar basal body rod protein FlgB	-2.72	-1.44	0	0
flgC	flagellar basal body rod protein FlgC	-2.63	-1.4	0	0
flgD	flagellar basal body rod modification protein FlgD	-2.33	-1.22	0	0
flgE	flagellar hook protein FlgE	-2.74	-1.45	0	0
flgF	flagellar basal body rod protein FlgF	-2.04	-1.03	0	0
flgG	flagellar basal body rod protein FlgG	-2.1	-1.07	0	0
flgM	anti-sigma-28 factor FlgM	-1.69	-0.75	3.48E-13	1.64E-12
flgN	FlgK/FlgL export chaperone	-1.53	-0.61	0	0
flhC	transcriptional regulator FlhC	2.05	1.04	0	0
flhD	transcriptional regulator FlhD	2.01	1.01	0	0
fliR	flagellar biosynthesis protein FliR	-5.57	-2.48	0	0
hybD	hydrogenase 2 maturation endopeptidase	1.53	0.61	0	0
hybE	hydrogenase 2-specific chaperone	1.74	0.8	0	0
hybF	hydrogenase nickel incorporation protein HybF	1.81	0.85	0	0
hybG	hydrogenase 2 accessory protein HypG	2.09	1.06	0	0
hycB	hydrogenase-3 iron-sulfur subunit	1.76	0.81	0.01	0.02
hypA	hydrogenase nickel incorporation protein	2.15	1.1	3.27E-06	8.82E-06
lexA	LexA repressor	-3.06	-1.61	0	0
nuoH	NADH-quinone oxidoreductase subunit H	1.71	0.77	0	0

nuoI	NADH-quinone oxidoreductase subunit I	1.67	0.74	0	0
nuoJ	NADH-quinone oxidoreductase subunit J	1.72	0.78	0	0
nuoK	NADH-quinone oxidoreductase subunit K	1.69	0.76	0	0
nuoL	NADH-quinone oxidoreductase subunit L	1.61	0.69	0	0
nuoM	NADH-quinone oxidoreductase subunit M	1.64	0.71	0	0
nuoN	NADH-quinone oxidoreductase subunit N	1.53	0.61	0	0
proP	proline/betaine transporter	2.16	1.11	0	0
proV	glycine betaine ABC transporter ATP-binding protein ProV	1.7	0.76	2.09E-04	4.63E-04
pspA	phage shock protein PspA	-3.69	-1.88	0	0
pspB	phage shock protein PspB	-2.92	-1.54	0	0
pspC	DNA-binding transcriptional activator PspC	-2.54	-1.34	0	0
pspD	inner membrane phage-shock protein	-2.53	-1.34	0	0
pspG	phage shock protein G	-2.18	-1.12	0	0
recA	recombinase A	-8.96	-3.16	0	0
rplA	50S ribosomal protein L1	-5.19	-2.38	0	0
rplB	50S ribosomal protein L2	-5.88	-2.56	0	0
rplC	50S ribosomal protein L3	-5.91	-2.56	0	0
rplD	50S ribosomal protein L4	-5.83	-2.54	0	0
rplE	50S ribosomal protein L5	-2.65	-1.41	0	0
rplF	50S ribosomal protein L6	-2.61	-1.38	0	0
rplI	50S ribosomal protein L9	-6.16	-2.62	0	0
rplJ	50S ribosomal protein L10	-2.07	-1.05	0	0
rplK	50S ribosomal protein L11	-5.87	-2.55	0	0
rplL	50S ribosomal protein L7/L12	-2.17	-1.12	0	0
rplM	50S ribosomal protein L13	-1.53	-0.61	0	0
rplN	50S ribosomal protein L14	-2.28	-1.19	0	0
rplO	50S ribosomal protein L15	-1.97	-0.98	0	0
rplP	50S ribosomal protein L16	-5.4	-2.43	0	0
rplQ	50S ribosomal protein L17	-1.78	-0.83	0	0
rplR	50S ribosomal protein L18	-2.84	-1.5	0	0
rplS	50S ribosomal protein L19	-4.29	-2.1	0	0
rplU	50S ribosomal protein L21	-1.65	-0.72	0	0
rplV	50S ribosomal protein L22	-5.6	-2.49	0	0
rplW	50S ribosomal protein L23	-6	-2.59	0	0
rplX	50S ribosomal protein L24	-2.33	-1.22	0	0
rplY	50S ribosomal protein L25	-3.81	-1.93	0	0
rpmA	50S ribosomal protein L27	-1.9	-0.92	0	0
rpmB	50S ribosomal protein L28	-2.45	-1.3	0	0
rpmC	50S ribosomal protein L29	-5.39	-2.43	0	0
rpmD	50S ribosomal protein L30	-2.62	-1.39	0	0
rpmE	50S ribosomal protein L31	-5.24	-2.39	0	0
rpmF	50S ribosomal protein L32	-4.29	-2.1	0	0

rpmG	50S ribosomal protein L33	-2.13	-1.09	0	0
rpmH	50S ribosomal protein L34	-1.79	-0.84	0	0
rpoA	DNA-directed RNA polymerase subunit alpha	-1.61	-0.68	0	0
rpoB	DNA-directed RNA polymerase subunit beta	-1.65	-0.73	3.44E-13	1.62E-12
rpoC	DNA-directed RNA polymerase subunit beta'	-1.5	-0.59	0	0
rpoZ	DNA-directed RNA polymerase subunit omega	-1.61	-0.69	0	0
rpsB	30S ribosomal protein S2	-2.27	-1.18	0	0
rpsC	30S ribosomal protein S3	-5.53	-2.47	0	0
rpsD	30S ribosomal protein S4	-1.85	-0.89	0	0
rpsE	30S ribosomal protein S5	-2.77	-1.47	0	0
rpsF	30S ribosomal protein S6	-6.23	-2.64	0	0
rpsG	30S ribosomal protein S7	-2.58	-1.37	0	0
rpsH	30S ribosomal protein S8	-2.65	-1.41	0	0
rpsI	30S ribosomal protein S9	-1.8	-0.85	0	0
rpsJ	30S ribosomal protein S10	-4.48	-2.16	0	0
rpsK	30S ribosomal protein S11	-1.81	-0.86	0	0
rpsL	30S ribosomal protein S12	-2.21	-1.14	0	0
rpsM	30S ribosomal protein S13	-1.72	-0.78	0	0
rpsN	30S ribosomal protein S14	-2.85	-1.51	0	0
rpsP	30S ribosomal protein S16	-3.45	-1.79	0	0
rpsQ	30S ribosomal protein S17	-4.8	-2.26	0	0
rpsR	30S ribosomal protein S18	-6.91	-2.79	0	0
rpsS	30S ribosomal protein S19	-6.22	-2.64	0	0
rpsV	30S ribosomal subunit S22	-1.89	-0.92	0	0
ruvA	Holliday junction ATP-dependent DNA helicase RuvA	-2.79	-1.48	0	0
ruvB	Holliday junction ATP-dependent DNA helicase RuvB	-2.1	-1.07	0	0
sulA	cell division inhibitor SulA	-10.22	-3.35	0	0
uvrA	excinuclease ABC subunit A	-3.01	-1.59	0	0
uvrB	excinuclease ABC subunit B	-3.24	-1.69	0	0
Pathogenesis					
invA	invasion protein InvA	1.69	0.76	0	0
invB	surface presentation of antigens protein SpaK	1.8	0.85	8.90E-10	3.34E-09
invE	invasion protein InvE	1.64	0.71	0	0
invI	surface presentation of antigens protein SpaM	1.94	0.96	0	0
pipA	pathogenicity island-encoded protein A	1.55	0.63	0	0
pipB	pathogenicity island-encoded protein B	1.57	0.65	8.52E-10	3.20E-09
sifA	secreted effector protein SifA	1.71	0.77	1.09E-12	4.95E-12
sifB	secreted effector protein SifB	3.72	1.9	0	0
sopD	secreted effector protein SopD	1.92	0.94	1.23E-09	4.53E-09
spaP	surface presentation of antigens protein SpaP	2.52	1.34	0	0
spaQ	surface presentation of antigens protein SpaQ	2.86	1.51	0	0

spaR	surface presentation of antigens protein SpaR	2.45	1.29	0	0
spaS	surface presentation of antigens protein SpaS	2.89	1.53	0	0
ssaB	secretion system apparatus protein SsaB	3.31	1.73	0	0
ssaC	secretion system apparatus outer membrane protein SsaC	3.3	1.72	0	0
ssaD	secretion system apparatus protein SsaD	3.15	1.65	0	0
ssaE	secretion system effector SsaE	2.74	1.45	0	0
ssaG	secretion system apparatus protein SsaG	3.64	1.86	0	0
ssaH	secretion system apparatus protein SsaH	2.77	1.47	0	0
ssaI	secretion system apparatus protein SsaI	2.01	1.01	0	0
ssaJ	secretion system apparatus lipoprotein SsaJ	2.65	1.41	0	0
ssaK	secretion system apparatus protein SsaK	3.52	1.82	0	0
ssaL	secretion system apparatus protein SsaL	2.56	1.35	0	0
ssaM	secretion system apparatus protein SsaM	3.39	1.76	0	0
ssaN	secretion system apparatus ATP synthase SsaN	2.35	1.23	0	0
ssaO	secretion system apparatus protein SsaO	3.05	1.61	0	0
ssaP	secretion system apparatus protein SsaP	2.76	1.46	0	0
ssaQ	secretion system apparatus protein SsaQ	2.8	1.49	0	0
ssaR	secretion system apparatus protein SsaR	3.09	1.63	0	0
ssaS	secretion system apparatus protein SsaS	4.36	2.12	0	0
ssaT	secretion system apparatus protein SsaT	4.69	2.23	0	0
ssaU	secretion system apparatus protein SsaU	2.32	1.21	0	0
ssaV	secretion system apparatus protein SsaV	3.55	1.83	0	0
sscB	secretion system chaperone SscB	2.53	1.34	0	0
sseC	secreted effector protein SseC	1.8	0.85	0	0
sseD	translocation machinery protein SseD	1.98	0.99	0	0
sseE	secretion system effector SseE	2.03	1.02	0	0
sseF	secretion system effector SseF	2.8	1.49	0	0
sseG	secretion system effector SseG	2.52	1.33	0	0
sseI	required for maintaining a long-term systemic infection	1.79	0.84	2.58E-14	1.28E-13
sseJ	deacylase activity	1.74	0.8	3.04E-06	8.24E-06
sseL	deubiquitinase SseL	2.31	1.21	0	0
ssrA	secretion system sensor kinase SsrA	1.81	0.85	0	0
STM1698	secreted effector kinase SteC	2.55	1.35	0	0

[a] Functional annotations are from NCBI for *Salmonella* Typhimurium strain LT2 (accession number NC_003197).

FIGURES

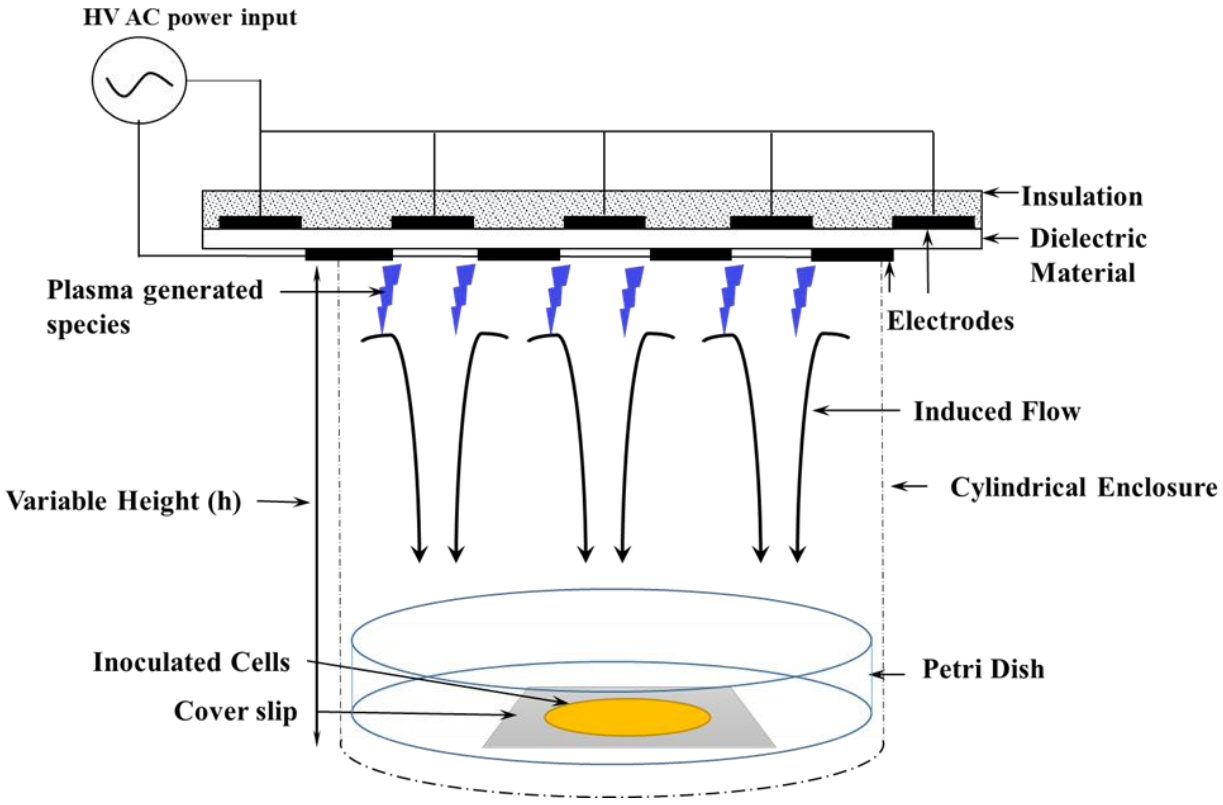

Figure 1. Schematic representation of the asymmetric SDBD set up for treating pathogen-inoculated coverslips.

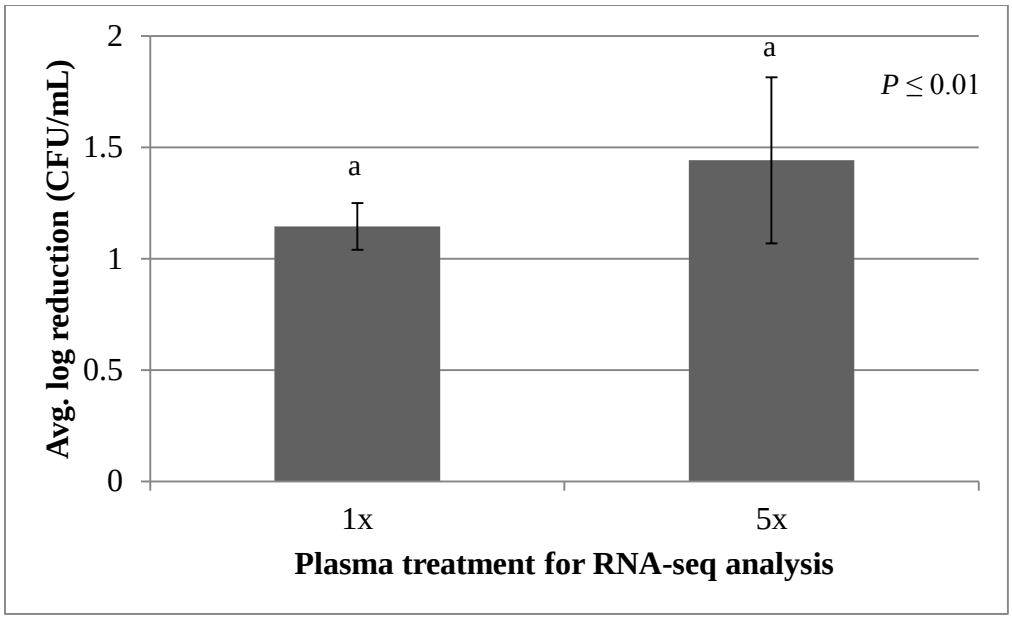

Figure 2. Average $\log_{10}$ reductions in CFU/mL for 2 min SDBD plasma treatments of dried *Salmonella* cells on sterile glass coverslips before (1x) and after (5x) 5 rounds of successive treatments. Error bars represent standard deviation from the mean.

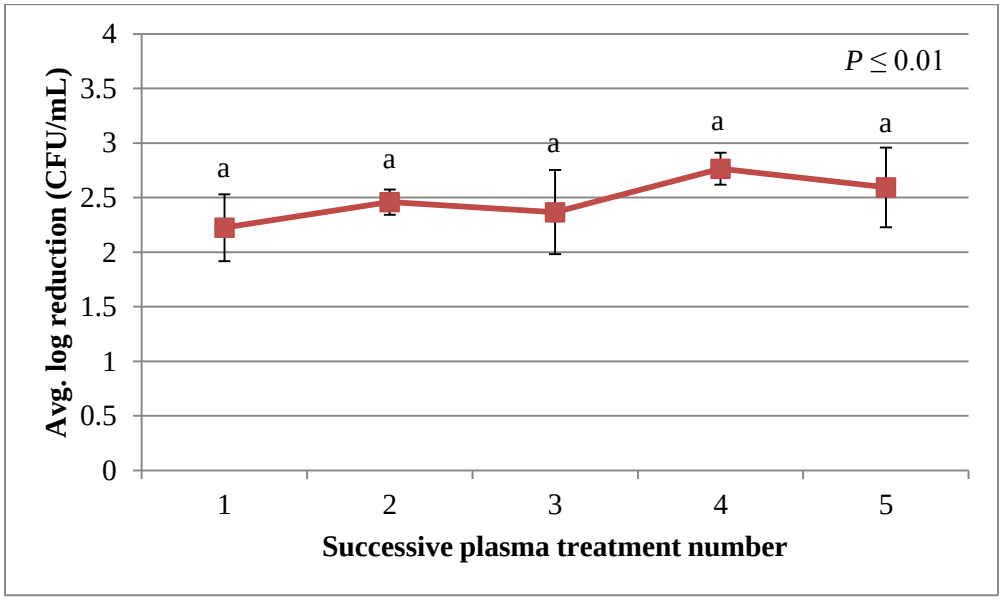

Figure 3. Average $\log_{10}$ reductions in CFU/mL for 5 successive plasma treatments using SDBD for 4 minutes. Error bars represent standard deviation from the mean.

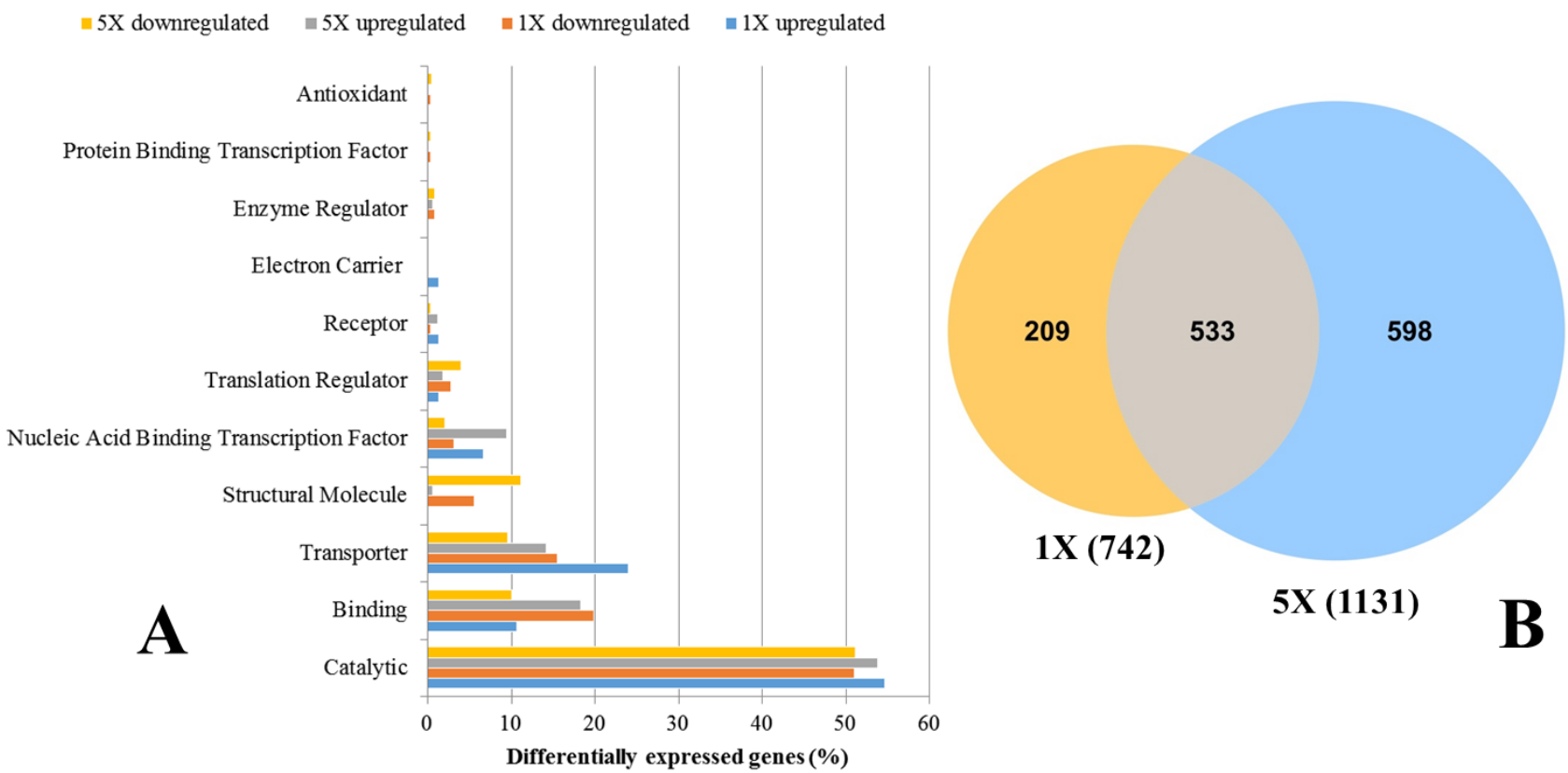

Figure 4. (A) Percentage of differentially expressed genes (≥ 1.5-fold or ≤ -1.5-fold) belonging to metabolic process categories as reported by PANTHER 10 before (1X) and after (5X) 5 rounds of successive plasma treatments of *Salmonella* Enteritidis. (B) Venn diagram representing the number of differentially expressed (≥ 1.5-fold or ≤ -1.5-fold) genes in common, before (1X), and after (5X) 5 rounds of successive plasma treatments.

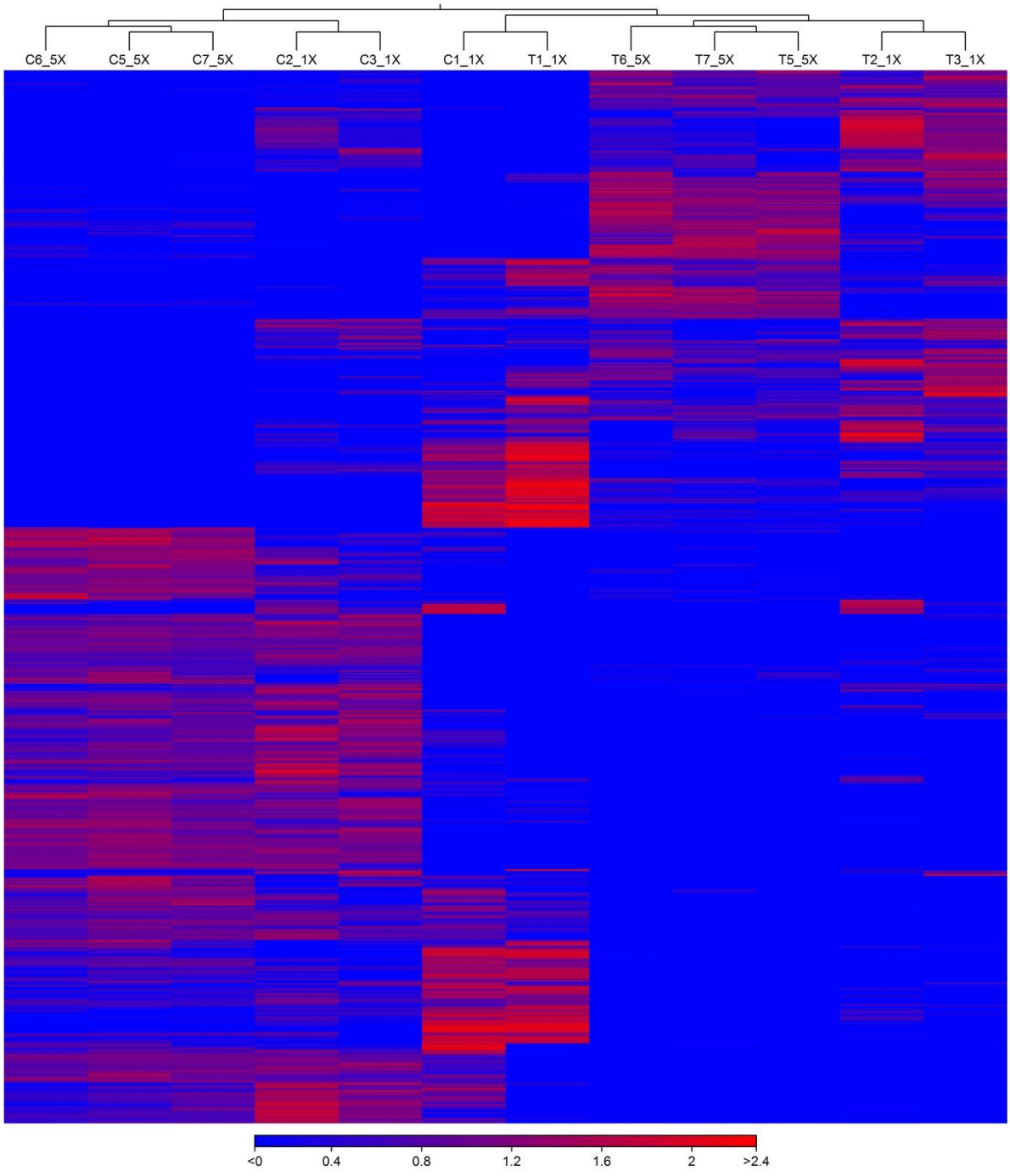

Figure 5. Hierarchical clustering of 533 differentially expressed genes in common within *Salmonella* Typhimurium LT2 cells before (1X) and after (5X) 5 rounds of successive plasma treatments showing clustering of treatment and control replicates. Treated samples prior to 5 successive treatments are designated T1-T3 and corresponding controls are designated C1-C3. Treated samples after 5 successive treatments are designated T5-T7 and corresponding controls are designated C5-C7.

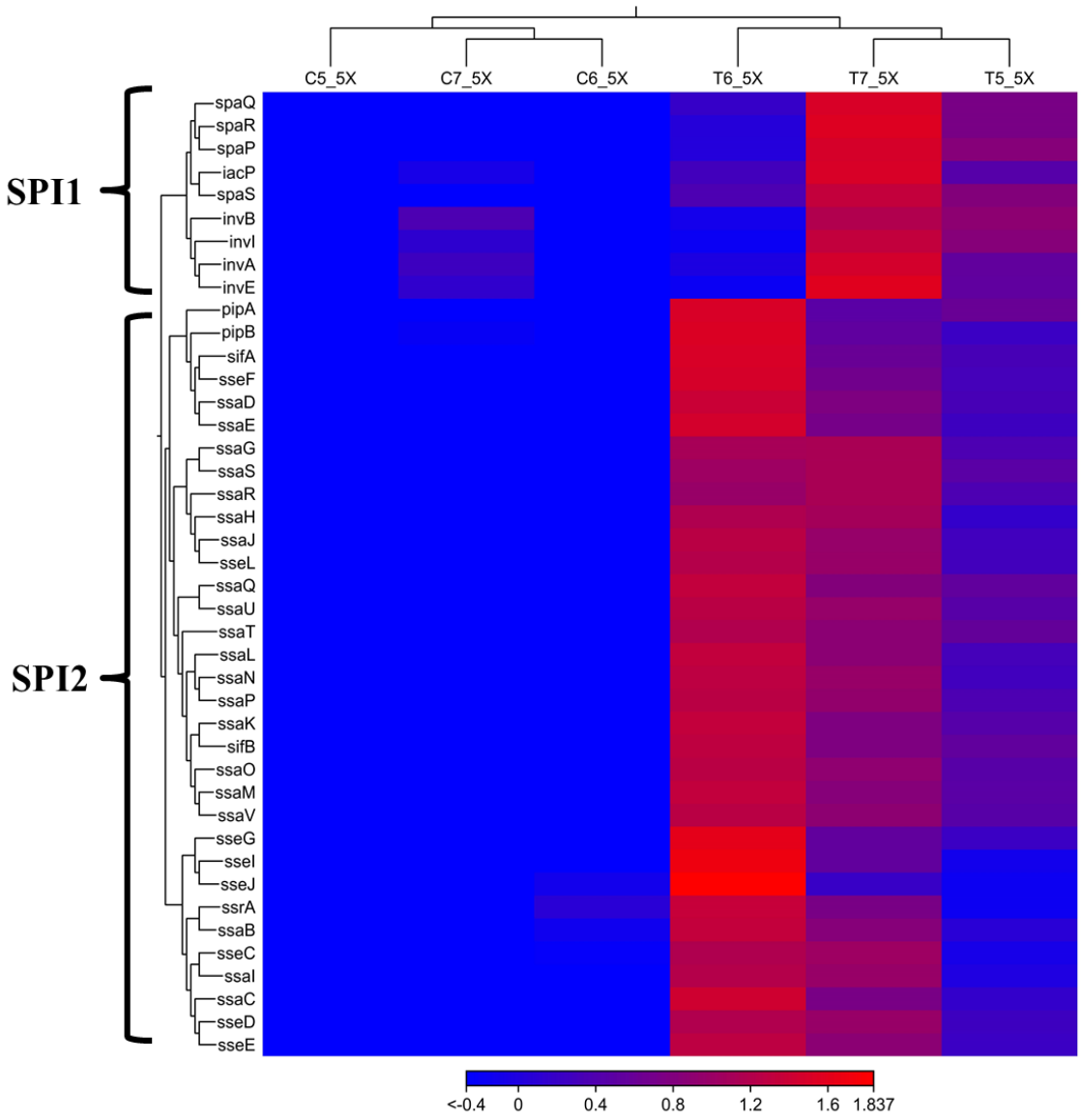

Figure 6. Hierarchical clustering of differentially expressed pathogenicity associated genes after 5 rounds of successive plasma treatment showing high correlation between treated (T5-T7) and control (C5-C7) replicates and the predominance of SPI2 expression over SPI1.

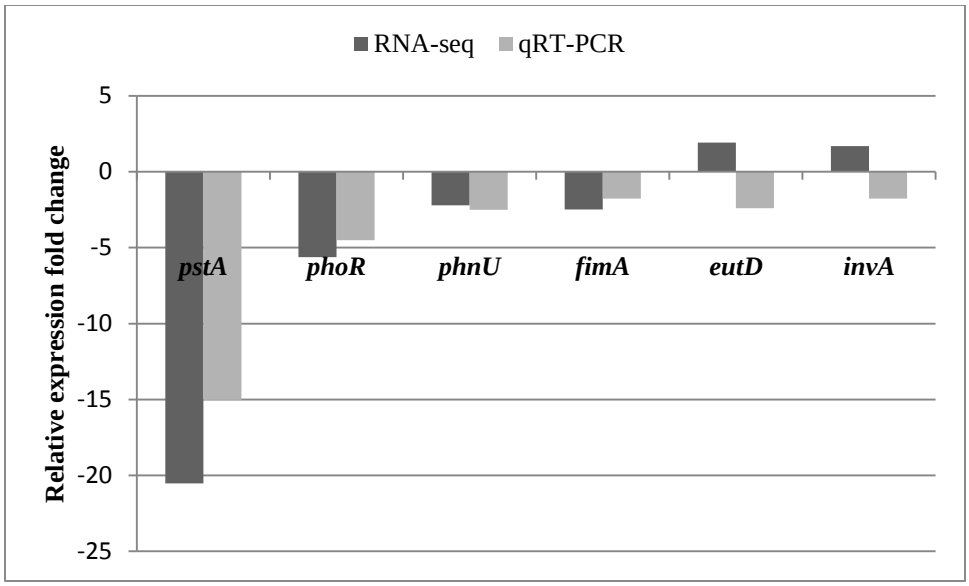

Figure 7. Comparison of average relative gene expression fold changes identified by RNA-seq and qRT-PCR. *gyrB* was not differentially expressed and used as a control for data normalization.

APPENDIX

The following manuscript was modified from a chapter in the dissertation of Kedar Pai, submitted to the the Faculty of the Graduate College of Oklahoma State University in partial fulfillment of the requirements for the Degree of Doctor of Philosophy in Mechanical and Aerospace Engineering, December, 2015. The second author has made significant contributions to the manuscript and it is included here in modified form as an appendix.

INVESTIGATION OF THE ROLES OF PLASMA SPECIES GENERATED BY SURFACE DIELECTRIC BARRIER DISCHARGE

Kedar Pai[1], Chris Timmons[2], Kevin Reohm[3], Jamey D. Jacob[1], Li Maria Ma[2], and Sundararajan V. Madihally[3]

[1]School of Mechanical and Aerospace Engineering, Oklahoma State University, Stillwater OK 74078

[2] Department of Entomology and Plant Pathology, Oklahoma State University, Stillwater OK 74078

[3] School of Chemical Engineering, Oklahoma State University, Stillwater OK 74078

ABSTRACT

As an emerging sterilization technology, cold atmospheric plasma, offers a dry, non-thermal, rapid process that is minimally damaging to a majority of substrates. However, despite intensive research in recent years, the mechanisms by which plasma interacts with living cells are poorly understood and the plasma generation apparatuses are complex and resource-intensive. Surface dielectric barrier discharge (SDBD) is a cold plasma generation technology that is more flexible, portable, scalable, and requires less input power than current cold plasma generation methods. In this study, the roles of reactive oxygen species (ROS), nitric oxide (NO), and charged particles (ions) produced by SDBD plasma on prokaryotic (5 strain mixture of *Listeria monocytogenes* (*Lm*)) and eukaryotic (human umbilical vein endothelial cells (HUVEC)) cellular function were evaluated. Oxidative stress responses, the accumulation of nitrite in aqueous media, ion

density, and bacterial inactivation at various distances from SDBD actuators were evaluated. SDBD actuator designs were also varied in terms of electrode number and length to evaluate the cellular effects of plasma volume and power distribution. NO and ions were found to contribute minimally to the observed cellular effects, whereas ROS were found to cause rapid bacterial inactivation, induce eukaryotic oxidative stress, and result in rapid oxidation of bovine muscle tissue. The results of this study underscore the dominance of ROS as the major plasma generated species responsible for prokaryotic and eukaryotic cellular effects. Furthermore, SDBD actuator designs can be optimized to maximize treatment effectiveness for flexible, non-strain-specific antibacterial therapies with potentially minimal bacterial resistance development.

SIGNIFICANCE STATEMENT

Despite the well documented bactericidal effects of atmospheric cold plasma, limited understanding of its effects on cellular function and complex plasma generation apparatuses have limited the practical applications of this technology. This study revealed that reactive oxygen species (ROS), rather than nitric oxide and ions, were the major contributors to bacterial inactivation, eukaryotic oxidative stress induction, and muscle tissue oxidation. Additionally, the effects of plasma volume and power distribution among surface dielectric barrier discharge (SBDB) actuators were found to impact ROS production efficiency. Since ROS cause physical damage to lipids, proteins, and nucleic acids, optimization of versatile and flexible SDBD actuators may provide a foundation for developing antibacterial therapies to which bacterial pathogens have a limited ability to develop resistance.

INTRODUCTION

The development of antibiotic resistance among pathogens, such as Methicillin-resistant *Staphylococcus aureus* (MRSA) [1] and carbapenem-resistant *Enterobacteriaceae* (CRE) [2, 3], has become a major health concern in recent decades. In many cases of such infections, treatment options are limited to the use of relatively toxic drugs, such as colistin, which has become a last-resort choice [4]. Currently, high-frequency monitoring and patient isolation, both of which have limited effectiveness, may be the only treatment options for some infections. Pathogen-specific drugs for multi-drug resistant bacteria are continually under development but often have limited usefulness due to the rapid development of resistance of the pathogens to new drugs. As a result, new types of drug- and non-drug-based therapies and treatment options are being investigated that could allow an increased or indefinite usable lifespan before resistance develops. A key consideration when developing such novel therapies is that they must display selectivity between eukaryotic and prokaryotic cells. Some antibacterial antibiotic-enhancing alkaloids, for example, are highly toxic to eukaryotic cells and may have negative side effects, such as immunosuppression [5]. The development of novel approaches, either those that block or circumvent resistance mechanisms or those that attack new targets, is essential. Cold plasmas, or nonthermal plasmas, have been heavily investigated in recent years due to their many potential benefits in the field of healthcare, mainly for applications in disinfection and sterilization [6-10], wound healing [11-13], and cancer treatment [14-18]. Various cold plasma technologies have shown effectiveness against drug-resistant bacteria and are currently being reviewed for clinical applications [19-21]. However, the current designs rely on close proximity [21] and

require an external gas flow for distribution of plasma-generated species to treatment sites [17,18]. Surface dielectric barrier discharge (SDBD), a novel method of nonthermal plasma generation, as previously described [6, 22], overcomes these drawbacks by having low power requirements, more treatment flexibility, and an increased effective treatment range. Because SDBD plasma generation, a semi-direct method of exposure to plasma species, does not require the substrate to complete the electric circuit, potential negative effects such as burning and tissue desiccation can be mitigated. SDBD exposure has shown a dose-based differential response in eukaryotic cells [22] and lethal effects on prokaryotic cells [6]. It was observed that prokaryotic cells have a lower tolerance to plasma-generated species than eukaryotic cells and therefore surface decontamination of eukaryotic tissues may be possible without adverse effects on the treated tissue. SDBD, being a surface treatment, may provide an alternative for precision surface treatments in hospitals, medical facilities, and dermatological applications.

Although investigated for many years, the specific mechanisms of cold plasma interaction with prokaryotic and eukaryotic cells are poorly understood. To gain a better understanding of the cellular mechanisms associated with SDBD-induced plasma species, the roles of ROS, RNS, and ions on prokaryotic and eukaryotic cells were investigated in this study. *Listeria monocytogenes* was used as a representative prokaryote and human umbilical and venous endothelial cells (HUVECs) were used to represent eukaryotic cells. Reactive oxygen species (ROS) were found to be the predominant component of the plasma species produced by SDBD that influenced prokaryotic and eukaryotic cells. Furthermore, it was shown that SDBD actuator design optimization can help lower the power requirements and increase treatment effectiveness.

MATERIALS AND METHODS

Plasma Actuator Arrangement. Plasma actuators were constructed using 0.0254-cm thick copper clad Teflon sheets (McMaster-Carr Supply Company, USA) as a dielectric medium, to which 0.2 cm wide copper tape (McMaster-Carr Supply Company, USA) was attached asymmetrically on either side to serve as electrodes (Figure 1). All experiments were carried out with identical actuators operating at 13.5 W and 50% duty cycle (effective power of 6.75 W). Different configurations of electrodes were used, as described below.

(i) To test the effects of power density on nitrite production, three different actuators were developed with electrodes of length 3.6 cm, 5.4 cm, and 11 cm. Power per unit length of the electrode was calculated for each configuration using the equation:

$$Power\ per\ unit\ length\ \left(\frac{W}{m}\right) = \frac{Input\ Power\ (W)}{Total\ length\ of\ plasma\ (m)}$$

where the total length of plasma is measured by multiplying the number of edges on which the plasma is generated by the length of the electrodes. Accordingly, power densities per unit length of 93.75 W/m, 62.5 W/m and 30.68 W/m were observed for electrode lengths of 3.6 cm, 5.4 cm, and 11 cm, respectively.

(ii) To understand the effect of number of electrodes, three actuators were prepared using 3.6 cm long electrodes on a dielectric of area 5 cm × 4 cm. The numbers of electrodes placed on the dielectric were 2, 4, and 7 with the same power input as above. Samples were exposed to plasma at 1 cm from the actuator. However, to test the effect of change in distance between the actuator and the sample, the 4-electrode configuration was used at distances of 1, 3, 5, and 7 cm from the sample.

(iii) For mammalian cell culture experiments, the actuator size had to be adjusted to fit the culture plates, according to the description in a previous study [22]. In brief, parallel electrodes of 11 cm × 0.5 cm were placed on the Teflon sheets on the side exposed to the sample being treated, with a total actuator size of 12.5 cm × 3 cm. A common ground electrode in the form of a rectangle of 11 cm × 0.5 cm was used on the opposing side (**Figure 1**). The actuator was placed at ~1 cm from the surface of the cell monolayer formed on the bottom of the petri dish. In accordance with previous work [22], all cells were treated with plasma for 4 min.

Air Ion Production due to Plasma Exposure. The density of ions generated due to SDBD cold plasma exposure were measured with an air ion counter modle AIC (AlphaLab, Inc., Salt Lake City, UT), which measures separately the number of positive and negative ions per cm^3 of air. This air ion meter is based on a Gerdien Tube (Gerdien Condenser) design and contains a fan that pulls air through the meter at a calibrated rate. The density of ions resulting from plasma exposure was measured at 1, 3, 5, and 7 cm from the actuator surface with and without turning on the fan. The air ion density resulting from plasma generation was compared to the ambient air to determine the relative increase in ion density. All measurements were done in triplicate and with the fan off to prevent any bias due to induced convection. Ion density was measured once a steady state reading was observed by the air ion counter.

Microbial Inoculation and Sample Preparation. Five strains of *Listeria monocytogenes* (F6854, 12433, G3982, J0161 and, Scott A) were cultured for 24 hours at

37°C in tryptic soy broth (TSB, Difco). After incubation, 1 mL of each culture was centrifuged at 9,000 x g for 3 minutes. Pellets were re-suspended in 1 mL of 0.1% (w/v) sterile peptone water (Difco) and combined to obtain a 5-strain mixture (5 mL total). The mixture was then diluted 10-fold to produce the desired inoculum concentration of 10^6 CFU/mL, and was uniformly distributed in 20-25 spots on sterile glass coverslips (22 mm x 22 mm). Inoculated coverslips were air dried in a biosafety cabinet for approximately 60 min prior to plasma treatment.

Electrical Conductivity of Plasma Treated Water and Media. Ten mL of water or growth medium used for HUVEC culture were treated with plasma for 2 and 4 minutes. The electrical conductivity of the treated water and growth medium was measured with a portable pH/EC/TDS meter model MW802 (Milwaukee Instruments, Inc., Rocky Mt, NC) at 30 min, 1 hr, 12 hr, and 24 hr after plasma treatment.

Endothelial Cell Culture. Human umbilical vein endothelial cells (HUVEC-2, derived from single donors, Life Technologies) cells were cultured in Medium 200 phenol red free (PRF), supplemented with low serum growth supplement (LSGS, containing 2% v/v fetal bovine serum, 1 µg/mL hydrocortisone, 10 ng/mL human epidermal growth factor, 3 ng/mL basic fibroblast growth factor, and 10 µg/mL heparin) following the manufacturer's instructions, as described previously [22]. HUVECs were maintained at 37°C, 5% CO_2/95% air, in a humidified cell culture incubator and fed with fresh medium every 36 hours. When confluent, cells were dissociated with 0.025% trypsin and 0.01% EDTA in PBS and neutralized with trypsin neutralizer solution

(phosphate-buffered saline (PBS) containing calf serum as a trypsin inhibitor), centrifuged at 125×g for 5 minutes and resuspended in growth medium. Viable cells were counted using trypan blue and seeded into various culture plates, as required. Based on viability analysis [22], cells were exposed to plasma for 4 minutes at a distance of approximately 1 cm.

Extracellular Nitrite Detection. Cells were seeded into a 24 well plate at 12,000 cells per well and incubated with 500 µL medium. After 24 hours, cells were pretreated with carboxy-PTIO (100 µM), which scavenges NO stoichiometrically, and incubated for 45 minutes before they were exposed to plasma. Untreated samples with and without the NO scavenger were used as controls. Culture medium was retrieved at 30 min, 1 hour, 12 hours, and 24 hours for nitrite analysis and mixed with an equal volume of Griess Reagent Kit (for nitrite detection) as specified by the vendor (Molecular Probes, Life Technologies, USA), then incubated at room temperature for 20 min. The absorbance was measured at 490 nm with an Emax precision microplate reader using the software SoftMax Pro 4.3 (Molecular Devices, Sunnyvale, CA), using a calibration curve with a range of 0–100 µM concentrations of $NaNO_2$.

Fresh medium was used to measure nitrite production induced by plasma to establish a baseline nitrite concentration attributable to plasma exposure to discount nitric oxide synthase (NOS) activity. For measuring the effects of power density and number of electrodes, tests were conducted using 1 mL of medium in a 6-well plate and nitrite concentrations were measured 1 hour after exposure.

Intracellular ROS Detection. Cells were seeded in a 96 well plate at a density of 7,000 cells per well and incubated with 200 µL medium. Caboxy-H_2DCF-DA was added to all cultures at 50µM following the vendor's protocol. Four different conditions were created: (a) Control with NAC (5mM, based on ref [23]) but not exposed to plasma; (b) Plasma treated cells without NAC; (c) Plasma treated cells with NAC; (d) H_2O_2 (200µM) as a positive control. For conditions containing NAC, the scavenger was added 45 minutes prior to plasma treatment. Intracellular ROS levels were assessed using the Image-IT LIVE Green Reactive Oxygen Species Detection Kit (Molecular Probes, Life Technologies, USA) according to the manufacturer's protocol. Fluorescence intensity was measured in a microplate reader, SpectraMAX GEMINI XS, using the software SoftMax Pro 4.3 (Molecular Devices, Sunnyvale, CA) at 495/529 nm. Fluorescence intensity was recorded at 30 min, 1 hour, 12 hours, and 24 hours after plasma treatment using an inverted microscope (Nikon Eclipse TE 2000-U, Melville, NY).

Evaluation of ROS and Plasma Effects on Bovine Muscle Tissue. Two separate sets of experiments were designed to evaluate the role of plasma generated ROS on muscle tissue. First, the tissue was inoculated with pathogens (5 strain cocktail of *Listeria monocytogenes*) and exposed to plasma for 4 minutes with a 4 electrode configuration at 1 cm from the sample. In the second experiment, the muscle tissue was coated with 1 ml of 5 mM NAC prepared in PBS to observe if the effects of plasma were due predominately to ROS. Samples that did not have NAC were coated with PBS alone so as to prevent desiccation. Treatment conditions were the same as those for the first experiment.

Transmission electron microscopy. Transmission electron microscopy (TEM) was used to visualize untreated control and plasma-treated *Escherichia coli* K12 cells to evaluate the morphological effects of the plasma treatment. A suspension of approximately 10^7 CFU/mL of *E. coli* K12 cells, prepared as described above, were spotted onto carbon-backed gold TEM grids placed onto sterile glass coverslips, air-dried for 60 minutes, and treated with SDBD plasma actuators for 2 and 4 minutes at a distance of 1 cm, as described above. The cells were then negative stained with phosphotungstic acid and visualized with a JEOL JEM-2100 Scanning Transmission Electron Microscope System

Statistical Analysis. All the experiments were conducted in triplicate. Reported values were represented as mean ± SD. Significant difference between two groups was analyzed using a paired sample t-test with a 95% confidence interval. Differences in the results were considered statistically significant when $p < 0.05$.

RESULTS AND DISCUSSION

Correlation of Nitrite Production and Power Distribution

Nitric oxide (NO) is an important intracellular and intercellular signaling molecule involved in regulation of cardiovascular, nervous, and immunological function [24]. NO regulates vascular tone, endothelial permeability, smooth muscle cell proliferation, platelet aggregation, and other functions [24, 25]. It is synthesized intracellularly during the conversion of L-arginine into L-citrulline in the presence of oxygen (O_2), a reaction catalyzed by nitric oxide synthase (NOS). Nitrites (NO_2^-) are

generated readily in aqueous solutions by oxidation of NO [26] by O_3 or O_2^-. For this reason, the production of extracellular NO following exposure to cold plasma was determined by measuring the accumulation of NO_2^-, the stable metabolite of NO secreted into the culture medium to provide evidence of reactive nitrogen species (RNS) produced by the plasma source [27, 28].

To evaluate the correlation of nitrite formation with power consumption, a two-electrode configuration was used, wherein the actuator consisted of two exposed electrodes with a single encapsulated electrode on the opposite side of the dielectric. The plasma was generated between the two exposed electrodes. HUVEC media (without cells) in a 6-well plate was exposed to plasma at approximately 1 cm from the actuator for a treatment time of 2 minutes. The power per unit length was varied by altering the length of the electrodes. Three different actuators with different power densities were tested. It was observed (**Figure 2a)** that the nitrite concentration increased with the increase in the power per unit length. This result suggested a direct correlation of power with nitrite generation, and hence suggests that higher NO concentrations can be generated with a higher power input. These results agree with the findings of Pavlovich *et al.,* who suggested a transition to higher NOx phase with increased power density [29].

Correlation of Nitrite Production and Bacterial Inactivation

The correlation of nitrite generation and bacterial inactivation was evaluated using a five strain mixture of *Listeria monocytogenes*. Additionally, the effect of increased plasma volume was investigated by varying the number of electrodes between 2, 4, and 7. Since all tests were carried out after sufficient drying of bacterial suspensions on glass

coverslips, the observed results were on a dry surface. However, the presence of moisture and humidity on the cellular level cannot be ruled out completely and further analysis is required to quantify the effect of moisture on bacterial inactivation with plasma treatment. A higher concentration of OH radicals were observed through optical emission spectroscopy in moist environments in a previous study [22].

Listeria cells were exposed to plasma for a period of 2 minutes at 1 cm from the samples. Nitrite concentration decreased with increasing electrode numbers from two to four and remain relatively the same between 4 and 7 (**Figure 2b**). Since the same net power was applied to all configurations, by increasing the number of electrodes, the volume of plasma produced increased, while the power per unit length decreased. Therefore, an increased electrode number increased the plasma volume, albeit at lower power per unit length. The 2-electrode configuration had a power per unit length of 93.75 W/cm, as compared to the 15.63 W/cm in the 7 electrode configuration.

Bacterial inactivation showed an opposite trend, increasing with an increase in electrode number at the same power input (decrease in power per unit length). A complete inactivation of the bacterial cells inoculated on glass coverslips (10^6 CFU/mL) was observed with the 4 and 7 electrode configurations after 2 minutes of treatment. The increased bacterial inactivation associated with increased plasma volume suggests no clear correlation between nitrite production and bacterial inactivation. A lower power per unit length still produced a high reduction of *L. monocytogenes,* in contrast to what was observed by others [30] and suggests that device design may be a major contributing factor to bacterial inactivation [29, 31-33]. The increase in decontamination effects with increase in the number of electrodes may be a consequence of overall increase in the

relative densities of different plasma species as a result of increased plasma volume. The results do suggest that the low power, large plasma volume regime may be a better approach for sterilization and decontamination, thus making possible development of low power plasma devices for decontamination applications.

Correlation of Ion Density and Bacterial Inactivation

To investigate the role of ions in the plasma decontamination process, ion density was correlated with bacterial inactivation using a 4-electrode plasma actuator with treatment distances between 1 and 7 cm (**Figure 1**). The 4-electrode configuration was selected since a substantially higher bacterial reduction was observed as compared to that measured with the 2-electrode configuration. Ions are produced by the plasma process from secondary electrons near the actuator [34]. Measurements from the air ion counter indicated that the ion densities at the treated surface were correlated with distances from the actuator, at approximately 2200 ions/cm^3 and 400 ions/cm^3 at 1 and 7 cm, respectively. The technique reported here prevented a biased extraction of ions from the surface of the plasma actuator and results revealed that ion density decreases with increased distance from the plasma generation source. These ions and electrons transfer energy to radicals and metastables, which are responsible for microbial inactivation and other cellular effects. Ozone, one of the primary metastables produced, increased to more than 0.14 ppm within 10 seconds (data not shown).

Bacterial inactivation decreased with increased plasma treatment distance from 1-7 cm, correlating with the decreased ion flux (**Figure 3a**). Alternatively, bacterial inactivation increased with increasing electrode numbers for the same power input.

Antibacterial activities were measured at 1 cm from the actuators, where the ion densities are at the highest. Complete inactivation was observed within 2 minutes of treatment with the 7-electrode arrangement (**Figure 2b**). However, the magnitude of ions produced (~ 10^3 -10^4) was the same for the 2, 4 and 7 electrode configurations, demonstrating that increased net ion density does not correlate with the increased bacterial inactivation observed with increased electrode numbers. This finding may suggest that ions have a synergistic effect close to the actuators, but their effects decrease with distance from the actuators.

Ion Accumulation in Aqueous Media

In addition to actuator distance, duration of exposure to ions is also a factor in plasma effects on cells, particularly in aqueous environments. To understand this factor, the lifespan of ions was measured in deionized (DI) water and untreated medium by observing the change in conductivity over time after different durations of plasma exposure (**Figure 3b**). The conductivity in the untreated medium was significantly higher than that in DI water, probably due to the presence of electrolytes and proteins in the medium. Hence, conductivity changes in the medium could not be measured. The ionic perturbations observed in DI water after plasma treatments were negligible. Untreated DI water retained a conductivity of 0 mS/cm^3, even after 24 hours. The absence of change in the perturbations introduced in the conductivity of DI water post treatment showed that the conductivity created is a consequence of oxygen and nitrogen species rather than ions, which have a life span on the order of nanoseconds to milliseconds [31, 37]. Therefore,

the effects of ions in aqueous environments may be discounted as playing an important role.

Another possible explanation for these results is the generation of acidic H_3O^+ ions by reactions of the water molecules with H_2O_2 [36]. Other researchers have noted an increase in acidity and formation of nitrous (HNO_2) and nitric (HNO_3) acid, along with H_2O_2, in unbuffered water [33, 38]. A similar decrease in pH was observed in previous work [22] and was attributed to formation of HNO_2 and HNO_3, along with carbonic acid (H_2CO_3). Increased conductivity may be a result of dissociation of these acids since acidified aqueous nitrate and nitrite anions have been shown to form when water is exposed to atmospheric plasmas [33, 39].

No substantial increase in ionic perturbations (conductivity) with increased electrode numbers was observed, further suggesting that ions may not contribute to the cellular effects of plasma treatment but rather to the formation of nitrites and increase in the oxidative species, also contributing to increased acidity. The pH ranged from 7 to 3.6, 3.6, and 3.4 and remained constant over a period of 24 hours when exposed to plasma with the 2, 4, and 7 electrode configurations, respectively, for 2 minute treatments at 1 cm. These results corroborate the theory of Kono *et al*. that a synergystic antimicrobial effect occurs as a result of NO_2^-, H_2O_2, and low pH [39, 40]. This is another example of how device design affects device performance, evident from the difference in trends of pH change observed here and that observed by Kojtari *et al* [41]. A time course analysis is required for each of the electrode arrangements to ascertain the full effect on change in pH. Hence, in an aqueous medium the ions do not contribute to observed cellular effects

due to their short lifespans (on the order of nanoseconds) and to their inability to travel across the cell membrane due to the presence of charge (e.g., O_2^-).

Eukaryotic Cellular Responses to RNS

To evaluate the cellular effects of RNS, HUVEC cells were treated with SDBD cold plasma with and without the presence of a water-soluble NO scavenger, cPTIO. The resulting concentration of nitrites in the most stable configuration, the metabolite form of NO, in aqueous media, was then measured via the Griess assay [28, 44, 45] (**Figure 4**). One hundred µM of c-PTIO was used since this concentration was effective at mitigating the effects of both extracellular and intracellular NO with no observable effects on the cells themselves [14, 23]. In plasma, NO_2 produced from NO and ozone (O_3) reacts with H_2O to form NO_2^- and NO_3^- [43].

$NO + O_3 \rightarrow NO_2 + O_2$

$2NO_2 + H_2O \rightarrow HNO_2(aq) + HNO_3(aq)$

Nitrite concentrations in plasma treated samples containing HUVEC cells without the c-PTIO scavenger were nearly 10 fold higher than in samples containing both HUVEC cells and the scavenger (**Figure 5A**), indicating that increased nitrite concentration is due to NO conversion to nitrite. Thirty minutes after plasma exposure of samples without the scavenger, nitrite concentrations were observed to be as high as 195 µM, decreased to approximately 130 µM after one hour, and stabilized to approximately 105 µM after 24 hours. HUVEC cell-containing control samples (no plasma exposure) with and without the scavenger had negligible nitrite concentrations at all time points. These results confirm that the increased nitrite concentration was not produced solely by

the enzyme NOS in HUVEC cells, but rather was a result of the plasma treatment. This finding corroborates those of another study in which high HUVEC cell viability was measured after a 4 min plasma treatment [22].

When evaluating nitrite concentrations in HUVEC medium devoid of cells, a similar trend was observed. Nitrite concentrations in HUVEC medium without the scavenger were highest 30 minutes after plasma exposure, with an average of 70 µM, and then decreased to18 µM over a period of 24 hours. This finding suggests that the increased concentration of nitrites was a result of oxidative stress caused by ROS rather than RNS. ROS can also interact with NO to produce other reactive species that may contribute to the reduced pH. Acids such as nitric acid may also be significant contributors to the increased NOS activity, as indicated by the decrease in pH [22, 32, 46]. In acidic environments, NO_2^- and O_2^- can react to form peroxynitrous acid (ONOOH) and nitrous acid (HNO_2) [46].

Eukaryotic Cellular Responses to ROS

The cellular effects of ROS produced by SDBD plasma were also evaluated using HUVEC cells, but with the addition of a ROS scavenger (NAC) and a ROS indicator (carboxy-H_2DCF-DA) (**Figure 4**). NAC readily binds with all ROS, including those that contain nitrogen [48], both intracellularly and extracellularly [49]. At the intracellular level, NAC is rapidly hydrolyzed to L-cysteine, allowing increased production of glutathione (GSH), a powerful antioxidant. In the presence of glutathione peroxidase (GSH-Px), GSH and H_2O_2 react to form disulfide (GS-SG) and water [49, 50-52] **(Figure 4)**. At the extracellular level, NAC simply acts as a nucleophile, donating an electron to

ROS introduced by the plasma treatment [49]. Five mM of NAC was used in this study since this concentration was found to provide effective cyto-protective properties while also not having toxic effects on the cells [23, 53]. Carboxy-H_2DCF-DA is an acetylated form of fluorescin that is deacytelated by ROS, causing it to fluoresce. Thus, relative fluorescence intensity can be correlated to the relative intracellular accumulation of ROS.

The extent of oxidative stress experienced by a cell depends on the concentration of ROS within a cell and the rate at which the ROS can be reduced. O_2^- and H_2O_2 are produced during normal cellular respiration but are rapidly and efficiently reduced by several enzymes [47]. Oxidative stress occurs when these enzymes are not able to reduce ROS rapidly enough, causing an increase in ROS concentration and the potential for oxidative damage to DNA, lipids, and proteins. O_2^- and H_2O_2, although having the potential to cause oxidative damage themselves, can serve as precursors to the more potent hydroxyl radical (OH^*) through pathways such as the Fenton reaction [47]. OH^* is the most reactive ROS and rapidly causes oxidative damage to cellular components.

The effect of ROS generated by plasma treatment on HUVEC cells was observed by using carboxy-H_2DCF-DA, with and without the presence of NAC (**Figure 5B**). Positive control samples without NAC, containing 200 µM H_2O_2 (**Figure 5C(c)**), had a fluorescence intensity similar to that of the plasma treated samples without NAC (**Figure 5C(a)**). Fluorescent micrographs showed the highest fluorescence intensity for the plasma treated samples without NAC (**Figure 5C(a)**) and the lowest for the untreated control samples with NAC (**Figure 5C(d)**). Plasma treated samples with NAC (**Figure 5C(b)**) showed a lower intensity than those without, indicating that NAC was able to neutralize the plasma generated ROS and reduce the level of oxidative stress experienced

by the cells. Additionally, fluorescence intensity increased over time after plasma treatment and was highest after 24 hours, indicating the occurrence of oxidative stress within the cells. No significant ROS related stress was observed in any of the untreated control samples, with or without NAC.

Taken together, these results suggest three major conclusions. First, production of a relatively high concentration of ROS by SDBD plasma was confirmed, with the relative concentration (and therefore cellular effects) negatively correlated with increased distance from the actuators. Second, ROS produced by SDBD plasma was found to cause oxidative stress in HUVEC cells that continued to increase after plasma treatment was stopped. Third, compared with ROS, NO and ions play a minor role in the eukaryotic and prokaryotic cellular response to cold plasma treatment.

Extracellular ROS generation by SDBD plasma actuators was assessed using optical emission spectroscopy in a previous work, wherein the major oxidative species were found to be O_3, OH*, NO, and O_2^+ [22]. These ROS can serve as precursors to other ROS, such as H_2O_2 and HNO_2, in an aqueous medium [54]. Several authors have attempted to validate the dominance of HNO_3 and H_2O_2 in the plasma interaction with cells, especially in the generation of plasma activated water (PAW) [38]. However, the general conclusion was that these agents, alone [55] or in combination, did not give the same response as observed with plasma treatment [33, 41, 56], thus indicating a multicomponent chemical dynamic.

ROS and Plasma Effects on Bovine Muscle Tissue

The dominance of the role of ROS rather than RNS in the plasma treatment process was further confirmed by assessing the effects of plasm treatment on pathogen-inoculated bovine muscle tissue. Interestingly, negligible bacterial inactivation was observed on muscle tissue samples surface inoculated with *L. monocytogenes*. This observation may be partly attributed to the surface roughness and porosity of the muscle tissue [57], providing more shelter for the bacteria, or a shadowing effect, from the plasma generated species. Alternatively, this observation may be a result of the high concentration of myoglobin and other components having high affinities for oxidation by ROS. Pavlovich *et al.* observed similar results using pig skin, in which a slight reduction in *E. coli* concentration was observed after plasma treatment as compared to other substrates [29]. The presence of such compounds may reduce the concentration of ROS able to interact with and damage bacterial cells.

Although limited bacterial inactivation was observed, the texture and color of the muscle tissue noticeably changed from smooth to wrinkled and from bright red to a rustic brown. This texture and color change may be characteristic evidence of oxymyoglobin (OxyMb) oxidation to form methemoglobin (MetHb) by ROS [26]. The high concentration of iron in oxymyoglobin (or oxyhemoglobin) may contribute to the high affinity of ROS to oxymyoglobin [58]. Tang *et al* [59] reported a similar observation in which the addition of glutathione to bovine muscle cytosol improved oxymyoglobin redox stability. Further investigation of this observation was carried out by treating the muscle tissue samples, with and without NAC, an ROS scavenger, prior to plasma treatment. Plasma treated samples with NAC showed no observable color or texture changes, whereas those without NAC exhibited the characteristic color change from

bright red to rustic brown (**Figure 6)**. NAC produced no visibly detrimental effects on untreated muscle tissue control samples (**Figure 6(a)**). These results confirm that SDBD produces a relatively high concentration of ROS, even beyond the plasma region itself, and is a major contributing factor to the cellular effects of plasma treatment. Further histological analysis of the tissue samples is required to better characterize the observed effects of cells subjected to plasma treatment.

Cell Surface Effects of SDBD Treatment.

TEM of SDBD plasma-treated *E. coli* cells compared to untreated controls revealed noticeable morphological differences with increasing treatment times ranging from 2 to 4 min (Figure 7). Untreated cells had distinct boundaries when clustered in groups, with multiple cells undergoing mitosis and clearly visible fimbriae under high magnification. After 2 min treatments cell surfaces were visually darker and cell boundaries appeared more ragged, less uniform, and less distinct between individual cells. Substantially more debris, also visible only in treated samples, may be a result of membrane damage and cytosol leakage. Membrane and cell surface damage became increasingly more evident after 4 min treatments, evidenced by darker staining, less distinct cellular margins, and greater amounts of extracellular debris (Figure 7).

Summary and Conclusions

A differential response to plasma treatment between prokaryotic and eukaryotic cells has been observed by several resarchers [9, 66 ,22]. Compared to eukaryotes, prokaryotic cells are much more sensitive to oxidative stress [64]. A similar differential

response has been observed between normally functioning eukaryotic cells and cancer cells [67], attributed to the Warburg effect, by which cancer cells are damaged more readily by ROS due to their increased reliance on aerobic metabolism [68, 69]. Based on this characteristic, a selective treatment of cancer cells among healthy mammalian cells may be possible [67, 70]. The rate of cellular inactivation by plasma generated in air or oxygen was several times faster than when it is generated in noble gases, further corroborating the dominant role of ROS on cellular effects [65]. Identifying and quantifying the specific ROS produced will aid in further tuning of the system for higher precision and effective applications. Since nonthermal plasmas allow a surface treatment effect rather than a bulk effect, it will be beneficial to tune the system for etching-like capabilities, providing an exact treatment approach. Furthermore, an increased understanding of the utilization of the flow induction capabilities of SDBD for long range applications should be investigated further and be more fully characterized.

To summarize, these results provide evidence that ROS, rather than NO and ions, are the primary contributors to plasma-induced bacterial inactivation, eukaryotic oxidative stress, and muscle tissue oxidation. Maximal cellular effects were observed when samples were placed in close proximity to plasma actuators, possibly the result of a synergistic effect of ROS, NO, and ions that decreased with increasing distance from the actuators, as was also observed by Kono *et al.* [40]. The observed ion density was highest immediately adjacent to the plasma region and decreased rapidly with increased distance from the actuators. In aqueous medium, ROS, NO, and ions contributed to a decrease in pH, adding to the synergistic effects. At increased distances from plasma actuators, ROS were the major plasma generated species interacting with treated cells.

Nitrites may be beneficial in higher concentrations for wound care applications such as in acidified nitrite creams for topical NO donating wound healing agents [71] and surface disinfection of robust, difficult to inactivate bacterial strains [72]. Direct plasma exposure methods such as volumetric DBD, although sometimes more efficient at bacterial inactivation, have been observed to cause tissue damage and often provides a non-uniform treatment [29]. Hence, the semidirect method of plasma exposure used in this work (SDBD) is a good alternative with capabilities of flow control to push the generated plasma species to the surface being treated. SDBD actuator designs also allow manipulation of the species being generated by changing the plasma parameters and electrode configurations, thus providing a specific desired effect (i.e. sterilization vs. wound healing). The selectivity and tuning capabilities offered by this technology can help in our efforts to resolve major global public health issues such as the development of bacterial antimicrobial resistance, chronic wound infections, and sterilization of a variety of both organis and inorganic surfaces. Optimized SDBD actuators are viable candidate for numerous applications in the healthcare industry, especially for sterilization and wound healing.

Acknowledgements: Financial support for this work was provided by Plasma Bionics LLC.

LITERATURE CITED

1. Grundmann, H., et al., *Emergence and resurgence of meticillin-resistant Staphylococcus aureus as a public-health threat.* The Lancet, 2006. **368**(9538): p. 874-885.

2. Carbapenemases, C.A., *Global spread of carbapenemase-producing Enterobacteriaceae.* 2011.

3. Levy, S.B. and B. Marshall, *Antibacterial resistance worldwide: causes, challenges and responses.* Nature medicine, 2004. **10**: p. S122-S129.

4. Markou, N., et al., *Intravenous colistin in the treatment of sepsis from multiresistant Gram-negative bacilli in critically ill patients.* Critical Care, 2003. **7**(5): p. R78.

5. Cushnie, T.P.T., B. Cushnie, and A.J. Lamb, *Alkaloids: An overview of their antibacterial, antibiotic-enhancing and antivirulence activities.* International Journal of Antimicrobial Agents, 2014. **44**(5): p. 377-386.

6. Pai, K. and J. Jacob. *Evaluation of Dielectric Barrier Discharge Configurations for Biological Decontamination*. in *in Proc. 51st AIAA Aerosp. Sci. Meeting* 2013. Dallas, Texas: American Institute of Aeronautics and Astronautics.

7. Maisch, T., et al., *Decolonisation of MRSA, S. aureus and E. coli by cold-atmospheric plasma using a porcine skin model in vitro.* PloS one, 2012. **7**(4): p. e34610.

8. Machala, Z., L. Chládeková, and M. Pelach, *Plasma agents in bio-decontamination by dc discharges in atmospheric air.* Journal of Physics D: Applied Physics, 2010. **43**(22): p. 222001.

9. Brun, P., et al., *Disinfection of ocular cells and tissues by atmospheric-pressure cold plasma.* PloS one, 2012. **7**(3): p. e33245.

10. Sung, S.-J., et al., *Sterilization effect of atmospheric pressure non-thermal air plasma on dental instruments.* The journal of advanced prosthodontics, 2013. **5**(1): p. 2-8.

11. Julák, J. and V. Scholtz, *Decontamination of human skin by low-temperature plasma produced by cometary discharge.* Clinical Plasma Medicine, 2013. **1**(2): p. 31-34.

12. Isbary, G., et al., *Successful and safe use of 2 min cold atmospheric argon plasma in chronic wounds: results of a randomized controlled trial.* British Journal of Dermatology, 2012. **167**(2): p. 404-410.

13. Ermolaeva, S.A., et al., *Comparative Study of Three Nonthermal Plasma Sources against Causative Agents of Nosocomial Infections.* Plasma Medicine, 2012. **2**(1-3).

14. Ahn, H.J., et al., *Targeting cancer cells with reactive oxygen and nitrogen species generated by atmospheric-pressure air plasma.* PloS one, 2014. **9**(1).

15. Lee, H., et al., *Degradation of adhesion molecules of G361 melanoma cells by a non-thermal atmospheric pressure microplasma.* New J. Phys, 2009. **11**(11): p. 115026.

16. Volotskova, O., et al., *Targeting the cancer cell cycle by cold atmospheric plasma.* Scientific Reports, 2012. **2**: p. 636.

17. Kong, M.G., et al., *Plasma medicine: an introductory review.* New Journal of Physics, 2009. **11**(11): p. 115012.

18. Fridman, G., et al., *Applied plasma medicine.* Plasma Processes and Polymers, 2008. **5**(6): p. 503-533.

19. Daeschlein, G., et al., *Cold plasma–a new antimicrobial treatment tool against multidrug resistant pathogens.* Worldwide Research Efforts in the Fighting Against Microbial Pathogens–From Basic Research to Technological Developments. Ed. Mendez-Vilas. Brown Walker Press Boca Raton, Florida, USA, 2013: p. 110-113.

20. Kvam, E., et al., *Nonthermal atmospheric plasma rapidly disinfects multidrug-resistant microbes by inducing cell surface damage.* Antimicrobial agents and chemotherapy, 2012. **56**(4): p. 2028-2036.

21. Isbary, G., et al., *Non-thermal plasma—More than five years of clinical experience.* Clinical Plasma Medicine, 2013. **1**(1): p. 19-23.

22. Pai, K.K., et al., *Dose Dependent Selectivity and Response of Different Types of Mammalian Cells to Surface Dielectric Barrier Discharge (SDBD) Plasma.* Plasma Processes and Polymers, 2015: p. DOI:10.1002/ppap.201400134.

23. Ma, Y., et al., *Non-thermal atmospheric pressure plasma preferentially induces apoptosis in p53-mutated cancer cells by activating ROS stress-response pathways.* PloS one, 2014. **9**(4): p. e91947.

24. Aktan, F., *iNOS-mediated nitric oxide production and its regulation.* Life sciences, 2004. **75**(6): p. 639-653.

25. Kojda, G. and D. Harrison, *Interactions between NO and reactive oxygen species: pathophysiological importance in atherosclerosis, hypertension, diabetes and heart failure.* Cardiovascular research, 1999. **43**(3): p. 652-671.

26. Ignarro, L.J., *Biosynthesis and metabolism of endothelium-derived nitric oxide.* Annual review of pharmacology and toxicology, 1990. **30**(1): p. 535-560.

27. Amano, F. and T. Noda, *Improved detection of nitric oxide radical (NO•) production in an activated macrophage culture with a radical scavenger, car□y PTIO, and Griess reagent.* FEBS Letters, 1995. **368**(3): p. 425-428.

28. Sherman, M.P., et al., *Pyrrolidine Dithiocarbamate Inhibits Induction of Nitric Oxide Synthase Activity in Rat Alveolar Macrophages.* Biochemical and Biophysical Research Communications, 1993. **191**(3): p. 1301-1308.

29. Pavlovich, M.J., et al., *Effect of Discharge Parameters and Surface Characteristics on Ambient-Gas Plasma Disinfection.* Plasma Processes and Polymers, 2013. **10**(1): p. 69-76.

30. Pavlovich, M.J., D.S. Clark, and D.B. Graves, *Quantification of air plasma chemistry for surface disinfection.* Plasma Sources Science and Technology, 2014. **23**(6): p. 065036.

31. Sysolyatina, E., et al., *Role of the charged particles in bacteria inactivation by plasma of a positive and negative corona in ambient air.* Plasma Processes and Polymers, 2014. **11**(4): p. 315-334.

32. Schwabedissen, A., et al., *PlasmaLabel–a new method to disinfect goods inside a closed package using dielectric barrier discharges.* Contributions to Plasma Physics, 2007. **47**(7): p. 551-558.

33. Oehmigen, K., et al., *The role of acidification for antimicrobial activity of atmospheric pressure plasma in liquids.* Plasma Processes and Polymers, 2010. **7**(3-4): p. 250-257.
34. Likhanskii, A., et al., *Modeling of interaction between weakly ionized near-surface plasmas and gas flow.* AIAA Paper, 2006. **1204**: p. 2006.

35. Müller, S., R.-J. Zahn, and J. Grundmann, *Extraction of Ions from Dielectric Barrier Discharge Configurations.* Plasma Processes and Polymers, 2007. **4**(S1): p. S1004-S1008.

36. Chih Wei, C., L. How-Ming, and C. Moo Been, *Inactivation of Aquatic Microorganisms by Low-Frequency AC Discharges.* Plasma Science, IEEE Transactions on, 2008. **36**(1): p. 215-219.

37. Sysolyatina, E.V., et al., *Experimental Evidences on Synergy of Gas Discharge Agents in Bactericidal Activity of Nonthermal Plasma.* 2013. **3**(1-2): p. 137-152.

38. Traylor, M.J., et al., *Long-term antibacterial efficacy of air plasma-activated water.* Journal of Physics D: Applied Physics, 2011. **44**(47): p. 472001.

39. Naïtali, M., et al., *Combined effects of long-living chemical species during microbial inactivation using atmospheric plasma-treated water.* Applied and environmental microbiology, 2010. **76**(22): p. 7662-7664.

40. Kono, Y., et al., *Lactate-dependent killing of Escherichia coli by nitrite plus hydrogen-peroxide: A possible role of nitrogen dioxide.* Archives of biochemistry and biophysics, 1994. **311**(1): p. 153-159.

41. Kojtari, A., et al., *Chemistry for antimicrobial properties of water treated with non-equilibrium plasma.* J. Nanomed. Biotherapeutic Discovery, 2013. **4**: p. 120.

42. Bir, S.C., et al., *Hydrogen sulfide stimulates ischemic vascular remodeling through nitric oxide synthase and nitrite reduction activity regulating hypoxia-inducible factor-1alpha and vascular endothelial growth factor-dependent angiogenesis.* J Am Heart Assoc, 2012. **1**(5): p. e004093.

43. Arjunan, K.P., *Plasma Produced Reactive Oxygen and Nitrogen Species in Angiogenesis*. 2011, Drexel University.

44. Sun, J., et al., *Measurement of nitric oxide production in biological systems by using Griess reaction assay.* Sensors, 2003. **3**(8): p. 276-284.

45. Wimalawansa, S.J., *Nitric oxide and bone.* Annals of the New York Academy of Sciences, 2010. **1192**(1): p. 391-403.

46. Graves, D.B., *The emerging role of reactive oxygen and nitrogen species in redox biology and some implications for plasma applications to medicine and biology.* Journal of Physics D: Applied Physics, 2012. **45**(26): p. 263001.

47. Imlay, J.A., *Pathways of oxidative damage.* Annual Reviews in Microbiology, 2003. **57**(1): p. 395-418.

48. Zafarullah, M., et al., *Molecular mechanisms of N-acetylcysteine actions.* Cellular and Molecular Life Sciences CMLS, 2003. **60**(1): p. 6-20.

49. De Vries, N. and S. De Flora, *N-acetyl-l-cysteine.* Journal of Cellular Biochemistry, 1993. **53**(S17F): p. 270-277.

50. Nitescu, N., et al., *N-acetylcysteine attenuates kidney injury in rats subjected to renal ischaemia-reperfusion.* Nephrology Dialysis Transplantation, 2006. **21**(5): p. 1240-1247.

51. Zhang, F., S.S. Lau, and T.J. Monks, *The Cytoprotective Effect of N-acetyl-L-cysteine against ROS-Induced Cytotoxicity Is Independent of Its Ability to Enhance Glutathione Synthesis.* Toxicological Sciences, 2011. **120**(1): p. 87-97.

52. Kim, J.H., et al., *N-acetylcysteine attenuates glycerol-induced acute kidney injury by regulating MAPKs and Bcl-2 family proteins.* Nephrology Dialysis Transplantation, 2010. **25**(5): p. 1435-1443.

53. Lunov, O., et al., *Cell death induced by ozone and various non-thermal plasmas: therapeutic perspectives and limitations.* Scientific reports, 2014. **4**.

54. Lukes, P., et al., *Aqueous-phase chemistry and bactericidal effects from an air discharge plasma in contact with water: evidence for the formation of peroxynitrite through a pseudo-second-order post-discharge reaction of H2O2 and HNO2.* Plasma Sources Science and Technology, 2014. **23**(1): p. 015019.

55. Vandamme, M., et al., *ROS implication in a new antitumor strategy based on non-thermal plasma.* International Journal of Cancer, 2012. **130**(9): p. 2185-2194.

56. Ercan, U.K., et al., *Nonequilibrium Plasma-Activated Antimicrobial Solutions are Broad-Spectrum and Retain their Efficacies for Extended Period of Time.* Plasma Processes and Polymers, 2013. **10**(6): p. 544-555.

57. Kholodnykh, A.I., et al., *Precision of measurement of tissue optical properties with optical coherence tomography.* Applied Optics, 2003. **42**(16): p. 3027-3037.

58. Ignarro, L.J., et al., *Oxidation of Nitric Oxide in Aqueous Solution to Nitrite but not Nitrate: Comparison with Enzymatically Formed Nitric Oxide From L-Arginine.* Proceedings of the National Academy of Sciences of the United States of America, 1993. **90**(17): p. 8103-8107.

59. Tang, J., et al., *Effect of Glutathione on Oxymyoglobin Oxidation.* Journal of Agricultural and Food Chemistry, 2003. **51**(6): p. 1691-1695.

60. Gaunt, L.F., C.B. Beggs, and G.E. Georghiou, *Bactericidal Action of the Reactive Species Produced by Gas-Discharge Nonthermal Plasma at Atmospheric Pressure: A Review.* Plasma Science, IEEE Transactions on, 2006. **34**(4): p. 1257-1269.

61. Ikawa, S., K. Kitano, and S. Hamaguchi, *Effects of pH on Bacterial Inactivation in Aqueous Solutions due to Low-Temperature Atmospheric Pressure Plasma Application.* Plasma Processes and Polymers, 2010. **7**(1): p. 33-42.

62. Kröncke, K.-D., K. Fehsel, and V. Kolb-Bachofen, *Nitric Oxide: Cytotoxicity versus Cytoprotection— How, Why, When, and Where?* Nitric Oxide, 1997. **1**(2): p. 107-120.

63. Wink, D.A. and J.B. Mitchell, *Chemical biology of nitric oxide: insights into regulatory, cytotoxic, and cytoprotective mechanisms of nitric oxide.* Free Radical Biology and Medicine, 1998. **25**(4–5): p. 434-456.

64. Stoffels, E., Y. Sakiyama, and D.B. Graves, *Cold Atmospheric Plasma: Charged Species and Their Interactions With Cells and Tissues.* Plasma Science, IEEE Transactions on, 2008. **36**(4): p. 1441-1457.

65. Laroussi, M. and F. Leipold, *Evaluation of the roles of reactive species, heat, and UV radiation in the inactivation of bacterial cells by air plasmas at atmospheric pressure.* Int. J. Mass Spectrom, 2004. **233**(1): p. 81-86.

66. Wende, K., et al., *Distinctive activity of a nonthermal atmospheric-pressure plasma jet on eukaryotic and prokaryotic cells in a cocultivation approach of keratinocytes and microorganisms.* IEEE Trans. Plasma Sci, 2010. **38**(9): p. 2479-2485.

67. Siu, A., et al., *Differential effects of cold atmospheric plasma in the treatment of malignant glioma.* PloS one, 2015. **10**(6).

68. Vander Heiden, M.G., L.C. Cantley, and C.B. Thompson, *Understanding the Warburg effect: the metabolic requirements of cell proliferation.* science, 2009. **324**(5930): p. 1029-1033.

69. Engel, R.H. and A.M. Evens, *Oxidative stress and apoptosis: a new treatment paradigm in cancer.* Frontiers in bioscience: a journal and virtual library, 2005. **11**: p. 300-312.

70. Heinlin, J., et al., *Plasma applications in medicine with a special focus on dermatology.* Journal of the European Academy of Dermatology and Venereology, 2011. **25**(1): p. 1-11.

71. Weller, R. and M.J. Finnen, *The effects of topical treatment with acidified nitrite on wound healing in normal and diabetic mice.* Nitric Oxide, 2006. **15**(4): p. 395-399.

72. Wullt, M., I. Odenholt, and M. Walder, *Activity of three disinfectants and acidified nitrite against Clostridium difficile spores.* Infection Control, 2003. **24**(10): p. 765-768.

FIGURES

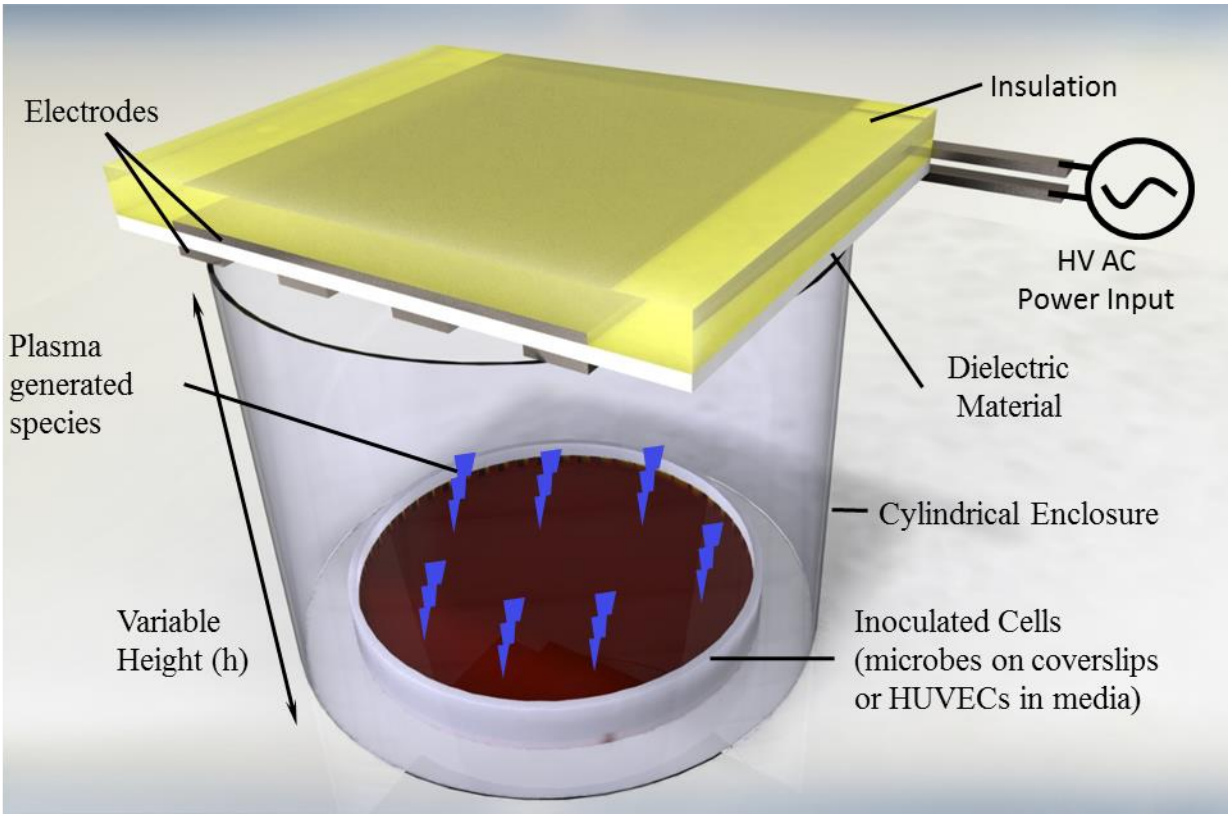

Figure 1. Schematic showing differential height treatment for the prokaryotic and eukaryotic cells.

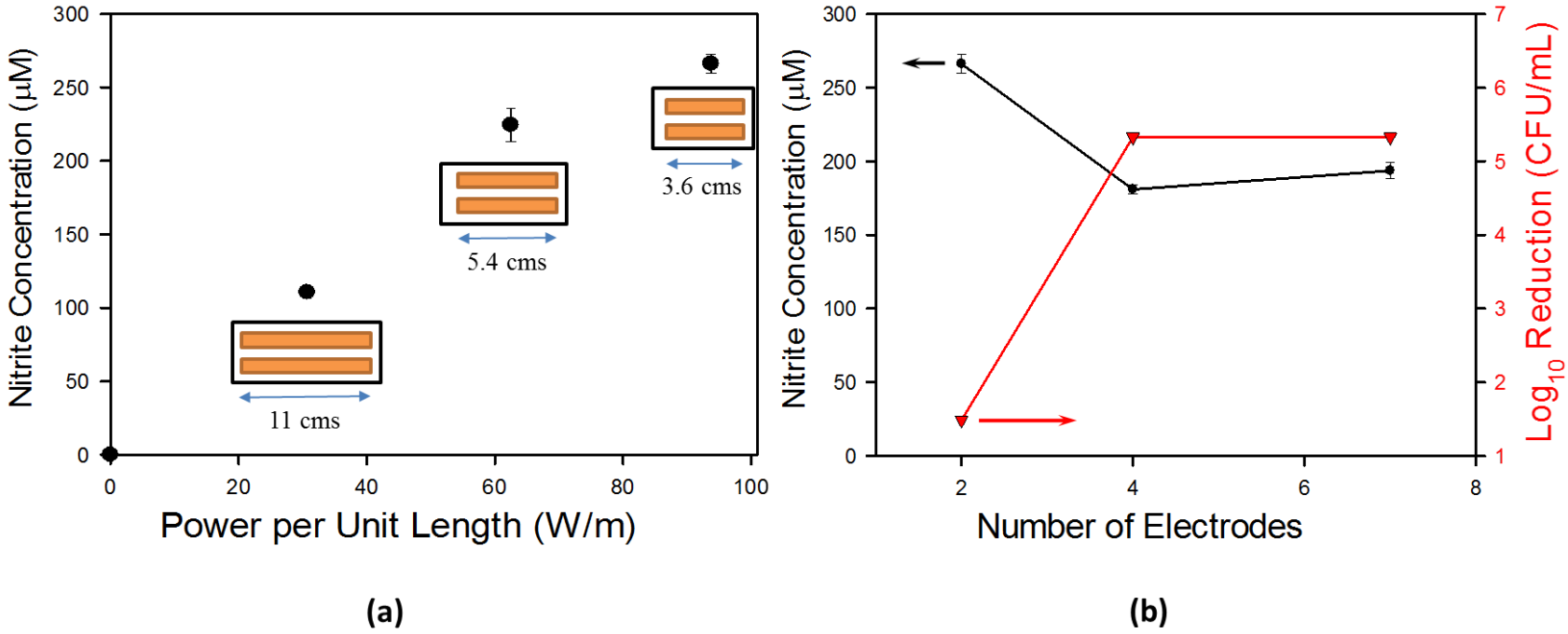

Figure 2. (a) Correlation of power density per unit length of electrode to nitrite production using a two electrode configuration by changing the electrode length; (b) Correlation of reduction in *Listeria monocytogenes* (5 strain mixture) with increase in number of electrodes for the same power density, with production of nitrites.

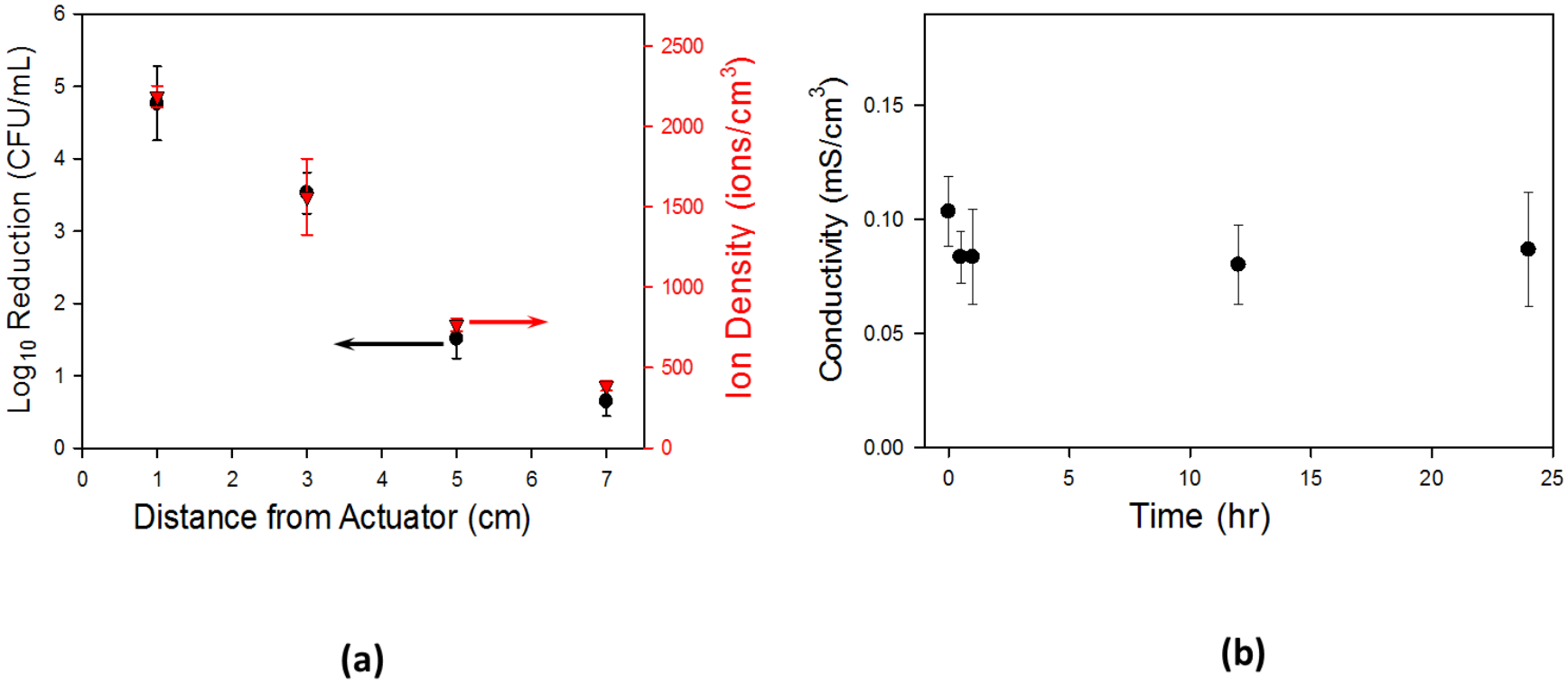

Figure 3. (a) Correlation of change in ion density and reduction in concentration of *Listeria monocytogenes* (5 strain mixture), with distance from plasma actuators using a four electrode configuration; (b) Change in conductivity of deionized water over 24 hours after a 4 minute treatment with plasma actuator using a two electrode configuration.

.

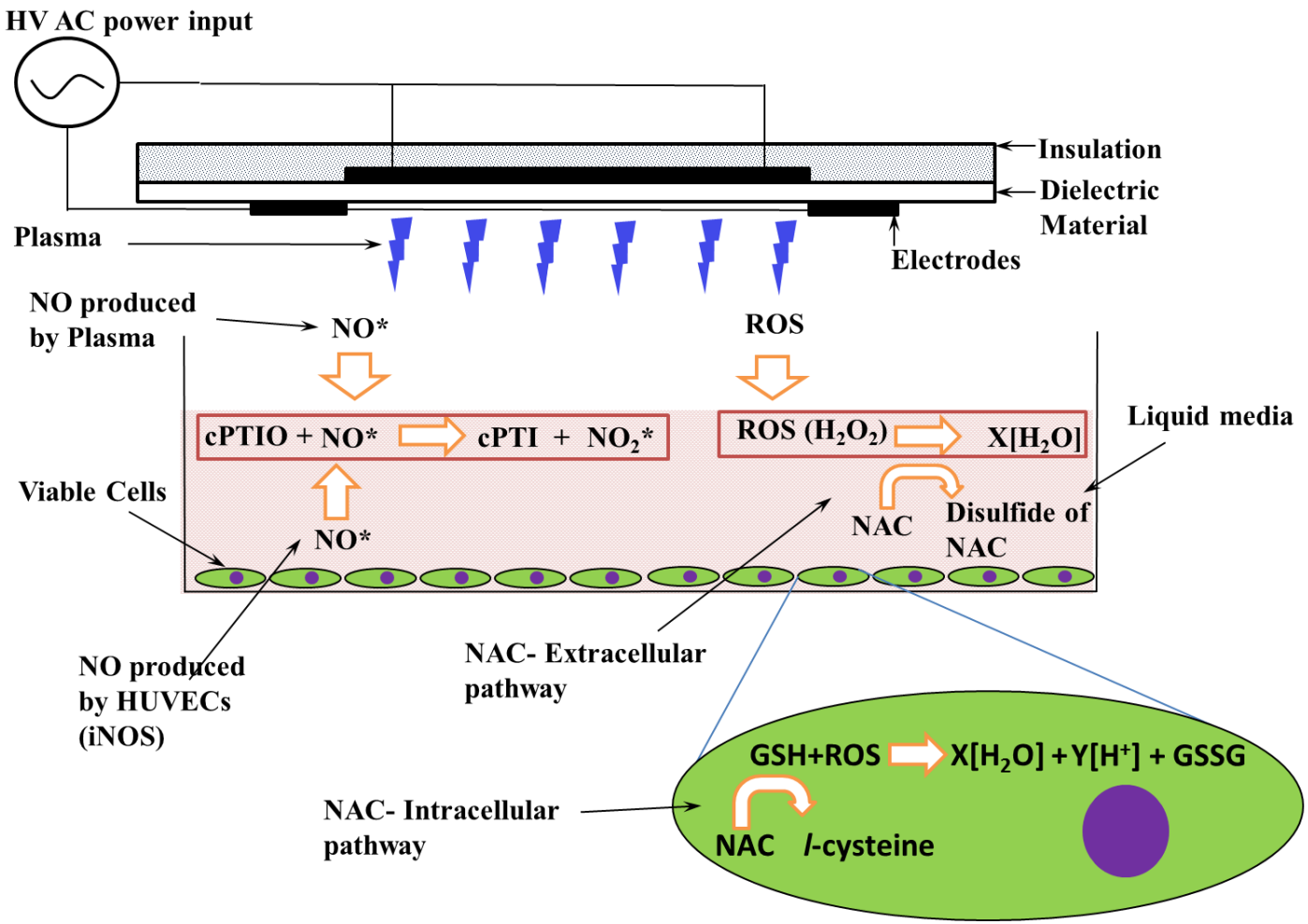

Figure 4. Schematic showing the cytoprotective interactions of ROS scavenger NAC (5mM) with different ROS species (both intracellular and extracellular mechanisms) and NO with NO scavenger cPTIO (100 µM), respectively.

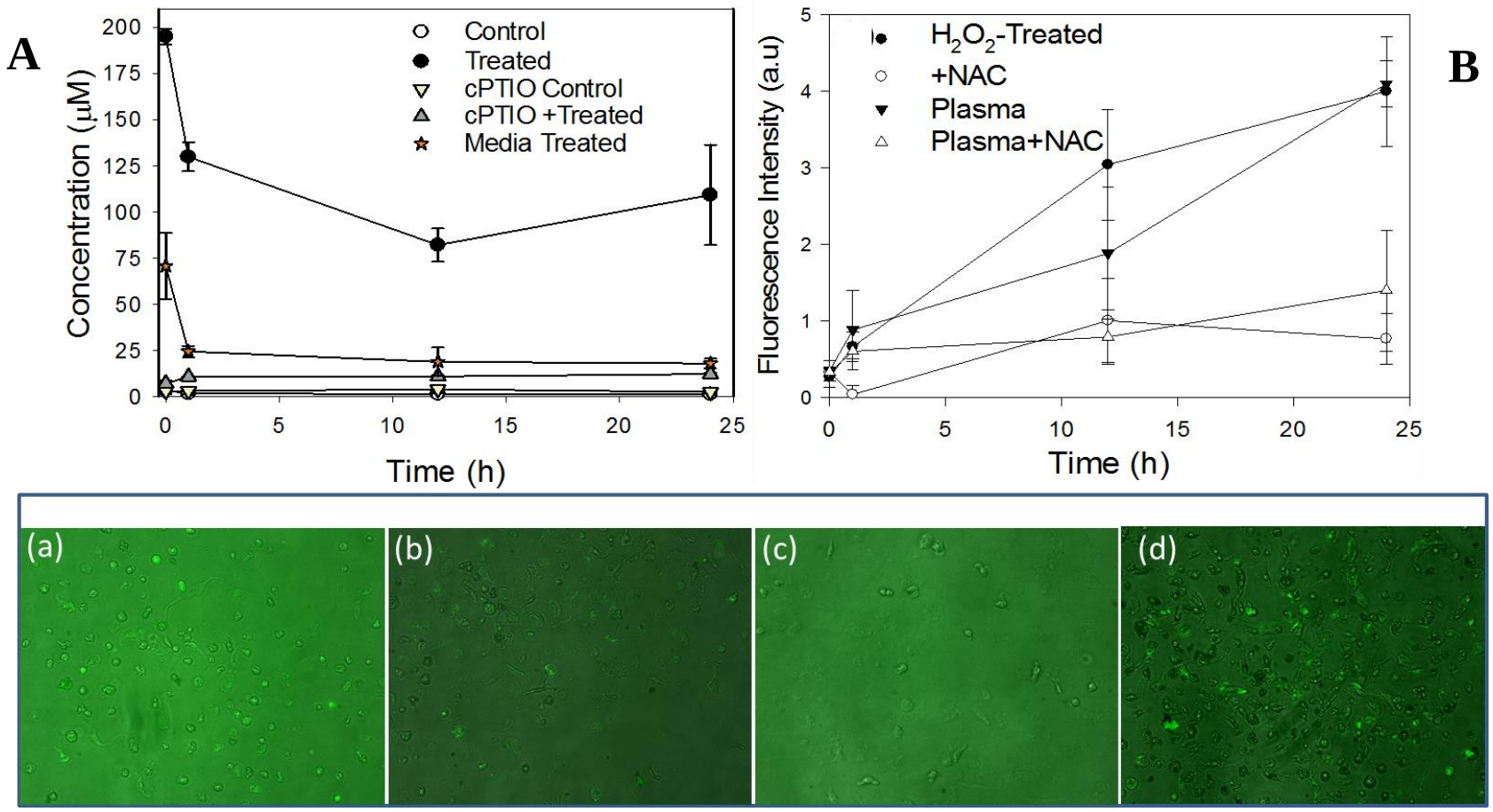

Figure 5. (**A**) Analysis of plasma induced nitrite concentration as a indicator for NO generation, with and without NO scavenger cPTIO; (**B**)Analysis of plasma induced intracellular ROS (Oxidative stress response) as a indicator for ROS generation, with and without ROS scavenger NAC (5mM); (**C**) Fluorescent micrographs of HUVECs representing oxidative stress response to plasma with and without ROS scavenger NAC (5mM). (a) Plasma treated HUVECs; (b) Plasma treated HUVECs with NAC (5mM); (c) Positive control (200 μM H_2O_2); (d) untreated control with NAC (5mM)..

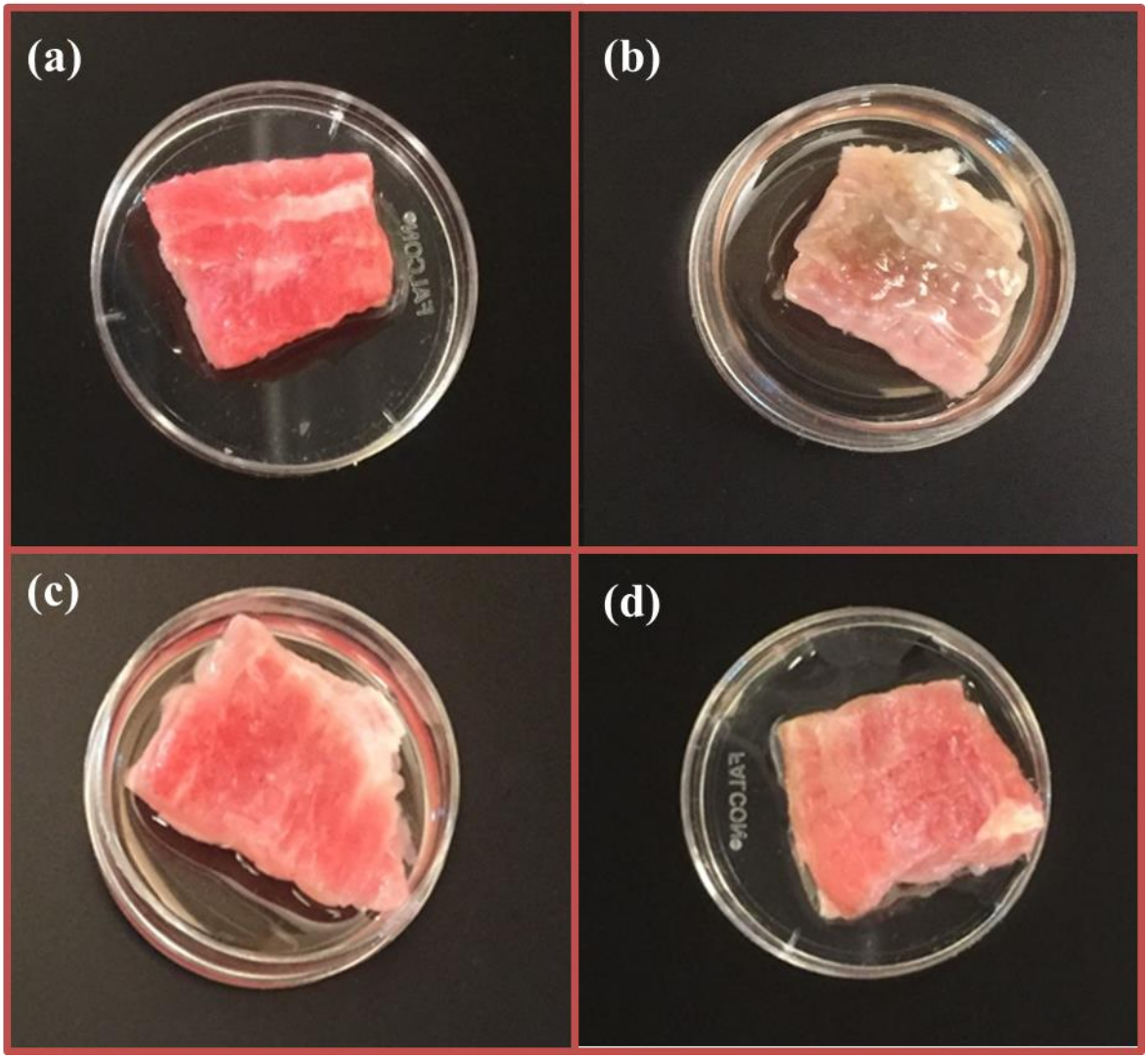

Figure 6. Effects of plasma exposure on bovine muscle tissue; (a) control (no NAC); (b) plasma treated (no NAC); (c) control (with 5mM NAC); (d) plasma treated sample (with 5mM NAC.

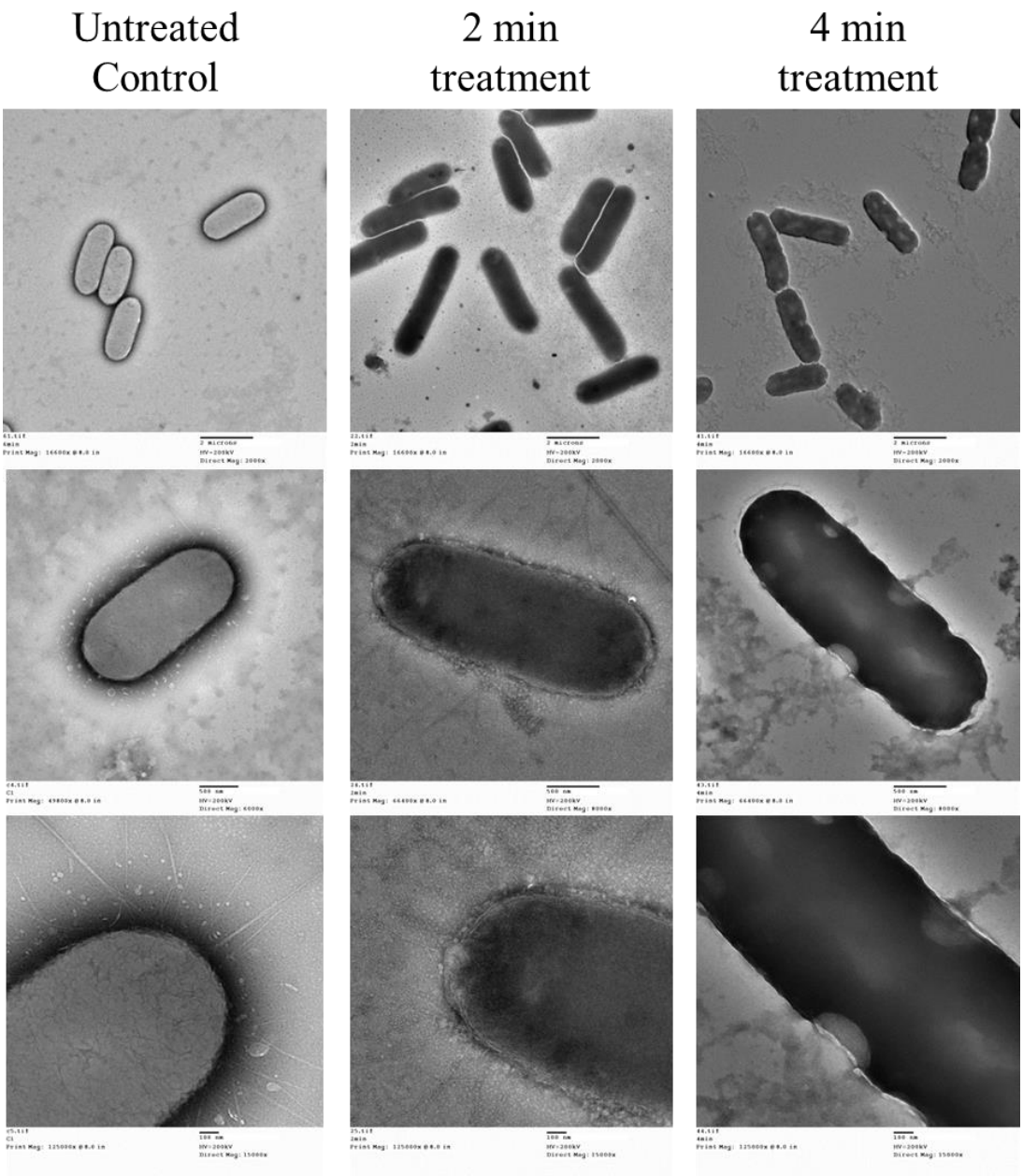

Figure 7. TEM of *Escherichia coli* K12 treated with SDBD cold plasma for 2 and 4 min, compared with an untreated control.

VITA

Christopher Timmons

Candidate for the Degree of

Doctor of Philosophy

Thesis: ELUCIDATION OF THE MOLECULAR MECHANISMS OF FOODBORNE HUMAN PATHOGEN INACTIVATION BY COLD ATMOSPHERIC PLASMA THROUGH RNA-SEQ ANALYSIS

Major Field: Plant Pathology

Biographical:

Education:

Completed the requirements for the Doctor of Philosophy in Plant Pathology at Oklahoma State University, Stillwater, Oklahoma in July, 2016.

Completed the requirements for the Master of Science in Entomology and Plant Pathology at Oklahoma State University, Stillwater, Oklahoma in 2012.

Completed the requirements for the Bachelor of Science in Biology at the University of Texas at Tyler, Tyler, Texas in 2010.

Experience:

Graduate Research Assistant. National Institute for Microbial Forensics and Food and Agricultural Biosecurity (NIMFFAB), Henry Bellmon Research Center, Oklahoma State University, Stillwater, Oklahoma, August 2010 to July 2016.

Undergraduate Research Assistant. Department of Biology, University of Texas at Tyler, Tyler, Texas, May 2008 to August 2010.

Professional Memberships:

American Phytopathological Society
International Society of Food Protection
Entomological Society of America